A Three Dimensional Spatial Reconstruction of the Left Ventricle and Analysis of Ventricular Geometry.

by

Mr. Nicola L. Fazzalari

B.App.Sc. B.Sc(Hons.) Dip.Ed.

University of Adelaide

Thesis submitted for the degree of

Doctor of Philosophy

in the Department of Pathology

University of Adelaide

September, 1986

CONTENTS

ABSTRACT

This thesis has applied a relatively new technology, that of echocardiography, and attempted to optimise both the technical and anatomical constraints on effective cardiac imaging to study left ventricular geometry. A theoretical study of the various tomographic slices available for left ventricular imaging showed that rotational apical views about the long axis optimise the spatial data available for both qualitative and quantitative analysis. From four anatomically defined apical views a 3D reconstruction of the left ventricle was generated by computer. Polar integration, which minimised geometric assumptions about the left ventricle, gave reliable volume estimates for ellipsoidal vessels, post mortem human hearts and in vivo studies with respect to a cineangiographic reference.

Left ventricular shape analysis at end diastole and end systole has for the first time described global fluctuations and region variation in ventricular geometry. The proportion of global geometric fluctuation is greatest for normal patients but the magnitude of the fluctuation is greatest for the pathological groups. The regional surface and volume proportions for the segmented ventricle in a normal population were described. The changes

which occurred in 13 patients with ischemic heart disease were then quantified and compared to the normal data. In all instances change in left ventricular shape was detected in at least one region. This confirms that ischemic heart disease is closely linked with ventricular shape change and that this change is closely linked with ventricular dysfunction.

A 3D spatial reconstruction can be performed in a clinical setting which enhances the qualitative evaluation of global and regional ventricular shape. This, in combination with quantitative data has the potential to improve patient assessment, and the understanding of cardiac function and performance.

SIGNED STATEMENT

The contents of this thesis have not been submitted to any university for the purpose of obtaining any other degree or diploma, and to the best of my knowledge, it contains no material previously published by any other person, except where due reference is made in the text.

The author consents to the thesis being made available for photocopying and loan if applicable if accepted for the award of the degree.

N. L. FAZZALARI

ACKNOWLEDGEMENTS

I am greatly in debt to my supervisior, Professor B. Vernon Roberts not only for his supervision but also for the advice and support he provided throughout this project. In the initial period of this project supervision was also provided by Dr. J. Mazumdar of Applied Mathematics.

Thanks are extended to the Cardio-Vascular Investigation Unit of the Royal Adelaide Hospital in particular to Mr. J. Davidson, for his generous co-operation, capable advice and assistance in the echocardiographic data acquisition.

In addition, I am grateful that the Institute of Medical and Veterinary Science has given me the opportunity to undertake this project.

I extend my gratitude to my friend and colleague Dr. Robert Conyers for his continuous encouragement and support particularly when the objectives of the project could have become secondary to political considerations.

I wish to thank the staff of the photographic unit, Mr M Fitzgerald for his advice on the preparation of the illustrations and, in particular, Miss Peta Grant for her effort in the production of the final prints.

There are of course may other individuals, to numerous to mention, who have in some way helped me, for their assistance I am thankful.

Finally, I wish to express my deepest gratitude to my wife, Louise, for her support in countless ways during my writing of this thesis.

PUBLICATIONS

The following publications were prepared by the author of this thesis during the course of this study. The work reported is primarily his work with assistance for echocardiographic and ventriculographic imaging and patient data provided by Mr. J. Davidson, Dr. L. Mahar, Dr. E. Goldblatt and Dr. P. Adams. Mr. E. DeNardi provided assistance with post mortem hearts and Dr. J. Mazumdar advice on the integration algorithms reported.

Fazzalari NL, Davidson JA, Mazumdar J, Mahar LJ, DeNardi E. (1984)

Three dimensional reconstruction of the left ventricle from four anatomically defined apical two-dimensional echocardiographic views.

Acta Cardiologica. 39: 409-436

Fazzalari NL, Goldblatt E, Adams APS.

A composite three dimensional echocardiographic technique for left ventricular volume estimation in children: Comparison with angiography and established echographic methods.

J. Clinical Ultrasound. (In press).

CHAPTER 1

INTRODUCTION

1.1 General Introduction

The function of the heart is to maintain an adequate circulation of blood volume through the body. This is achieved by the heart's muscular contraction causing a change in ventricular shape which is translated into the ejection of blood. The measurement of heart volume and heart geometry at end diastole and end systole is the subject of this study.

In each cardiac cycle the left and right ventricles are first filled with blood from the left and right atria respectively, in the diastolic phase of the cycle. The deceleration of the blood stream as the ventricles fill closes the valves between the atria and the ventricles (Bellhouse and Talbot, 1969). Then contraction of the heart muscle begins and the pressure in the ventricles rises. When the pressure in the left ventricle exceeds that in the aorta and the pressure in the right ventricle exceeds that in the pulmonary artery, the aortic valve in the left and the pulmonary valve in the right are pushed open and blood is ejected into the aorta and the lung. This is the systolic phase. The ejection continues until the deceleration of the blood stream closes the valves. The muscle relaxes, the pressures decrease and the diastolic phase begins.

The development of methods that allow quantitation of the state of cardiac function is linked to the measurement of cardiac volume. The methods currently in use to estimate volume make assumptions about heart geometry in relation to shape and symmetry or use empirical formulae which may not have a sound scientific or physiological basis (Lalani and Lee, 1976). These methods contribute to systematic errors which are errors introduced by inherent inaccuracies in the measurements.

Assessment of left ventricular performance is a most important investigative procedure for the diagnosis and prognosis of heart disease. The information gained from such studies often determines the course of medical and/or surgical treatment. From volume estimates at end diastole and end systole a number of derived numerical parameters can be calculated, such as stroke volume, ejection fraction, cardiac output and cardiac index (Feigenbaum, 1976). The problem of cardiac function is more complex than the simplistic concept that a big heart is a bad heart, for a big heart may have excellent or markedly reduced myocardial function. For instance, heart size may be increased in a case of excellent contractile function by excessive preload (end diastolic volume) or normal preload and poor contractile function. Hence, an index of function related to volume which discriminates between these two classes is necessary. In the first instance the heart is large but associated with greater than normal pressure. In the second instance, an index of function should show impairment.

Most studies that are concerned with the relation between cardiac performance and various physiological conditions consider the functioning of the heart as a whole. However, there is an increasing amount of evidence that regional differences occur in the functioning of the ventricles. These differences are attributed to local variations in wall shape, myocardial fibre orientation, contraction activation sequence, contractile and viscoelastic properties of the myocardial tissue. A regional assessment of ventricular function with respect to global ventricular geometry is required for an accurate description and analysis of cardiac performance. Patients with coronary heart disease will exhibit regional abnormalities of wall motion. These areas include scar tissue following myocardial infarction, aneurysmal scars or regions of ischaemic but still living myocardium. Cardiac dysfunction can, of course, be global or segmental depending on the degree of disease.

Techniques for measuring ventricular volume and geometry have been developed and are appplied for the clinical diagnosis of cardiac dysfunction, these include radionuclide and x-ray ventriculography. The advantages of such methods are that they provide an image of the heart which can be used for quantitative clinical diagnosis. They enable the estimation of volume and related parameters to evaluate global and regional cardiac dysfunction. X-ray ventriculography also allows the evaluation of heamodynamic parameters to investigate the relationships between pressure measurements and spatial measurements, volume and length changes. The main dis-advantages of these methods are such that their resolution would be of clinical significance. For instance the patients who undergo investigation are exposed to some risk due to radiation hazard and the invasive nature of the methods. The procedures are not suitable to use for repeated investigation in longitudinal studies. Study of normal individuals at random is not possible. The images of the heart chambers are projected images and, hence, some of the image information is lost and cannot be utilised. Consequently, evaluation of global and regional dysfunction is confounded in instances where the dysfunction cannot be projected as a boundary anomaly. Therefore, the measurement of shape and volume in an intact heart remains a challenging problem.

Ultrasound imaging of the heart or ultrasound echocardiography has provided new data not available by other means, more complete or more accurate data than invasive methods, together with less risk and inconvenience to the patient. Echocardiography provides high repetition rate one-dimensional data or unique spatial information in tomographic views previously unavailable. The high sampling frequency of M-mode (about 1KHz) compared with two-dimensional (2-D) echocardiographic images (about 30 Hz) means that very fast cardiac movements are tracked better with M-mode. For example, high frequency vibrations of valve structures indicating abnormal flow are usually discernable. On the other hand, the enhanced anatomical information of 2-D echocardiography has made significant contributions to the diagnosis of congenital heart disease and the relative size of the heart chambers. The alteration in cardiac wall motion relative to more normal motion among segments of the heat is used to recognise and quantify the effect of coronary artery disease.

Modelling of the left ventricle for effective volume estimation has presented problems for both invasive and non-invasive investigative methodologies. Ventricular geometry does not conform to any single geometric shape nor is there any constancy of shape during the cardiac cycle, particularly for various pathological conditions (Dumesnil and Shoucri, 1982). Consequently, models based on a particular geometric shape have involved invalid assumptions about left ventricular shape. Various geometric models better suit left ventricular shape at different phases of the cardiac cycle and in different pathological states. In invasive cardiac catheterisation the recognised comparative standard for volume estimation is the area-length method of Dodge and Sandler (1960). However, there are at least eight mathematical models applicable to ventriculograms for left ventricular volume estimations (Davila and Sanmarco, 1966). The non-invasive methods developed initially utilised M-mode ultrasound which provides a single ray view of cardiac structures over time (Feigenbaum, 1976). This imaging mode provides minimal spatial information and, hence, resulted in the most simple of ventricular models. A major assumption is that the ventricular shape is that of a prolate ellipsoid with an aspect ratio (major/minor axis) of 2:1 for all stages of the cardiac cycle, irrespective of pathology. Nevertheless, M-mode echocardiography has provided useful information, supported empirically, where there is no left ventricular segmental wall motion abnormalities (Murray, Johnston, Reid, 1972; Teichholz, Kreulen, Herman et al, 1976; Kronik, Slany, Mosslacher, 1979).

Two-dimension echocardiography permits unique visualisation of the heart in vivo (Tajik, Seward, Hagler et al, 1978) and provides spatial information in tomographic views previously unavailable. The availability of this spatial information has led to the development of more sophisticated models of the left ventricle, many of which still require some basic assumptions about shape and geometry (Folland, Parisi, Moynihan et al, 1979; Alpert, Bloom, Gilday et al, 1979; Schiller, Acquatella, Ponts et al, 1979; Silverman, Ports, Snider et al, 1980). The complexity of the models is often reflected in the difficulty of data acquisition and analysis.

Few studies have been reported which obviate geometric assumptions, particularly with respect to symmetry. To overcome the limitations of geometric mathematical models it is necessary to consider the spatial arrangement of the ventricle in three dimensions. The ability to represent or display a 3-D object is fundamental to the understanding of the shape of the object. Furthermore the ability to rotate translate and project views of the object is also, in many cases, fundamental to the understanding of its shape. This is easily demonstrated by picking up a relatively complex unfamiliar object. Immediately one rotates it, holds it at arms length, stands back from it, in order to obtain an understanding of its shape.

An analysis of ventricular geometry is central to a thorough description of regional and global left ventricular function. It is the changes in heart geometry which accompany a change in the enclosed chamber volumes that determine the heart's pumping performance. Therefore, geometry of the heart chambers, with changing volume from end diastole to end systole, require three spatial dimensions for both a proper qualitative and quantitative assessment of changes. Though numerous studies have been carried out on global heart geometry and regional or segmental geometric aspects for various pathologies all have been either one or two-dimensional studies. These have involved the use of invasive techniques such as X-ray ventriculography, radio nuclide or fluoroscopic methods. M-mode and 2-D echocardiography have been used for mainly qualitative non-invasive investigations (Naggar, 1981; Foale, Stefanini, Richards, 1982; Tei, Shah, Ormiston, 1982.). Quantitative ventriculograph analysis of cases with coronary heart disease and cardiomyopathies have demonstrated that quantitative methods appear to be essential to the proper interpretation of left ventricular regional geometric changes (Leighton, Wilt, Lewis, 1974; St. John Sutton, Tajik, Gibson et al, 1978). However, there is still a substantial lack of information on the global and regional heart geometry in relation to heart performance. One of the principle reasons for this is that one or 2-D images are inadequate for a complete description of geometric changes and their relationships to chamber volumes.

The purpose of this study is to provide new information about cardiac performance from the point of view of a 3-D left ventricular reconstruction. To overcome the limitations of one or 2-D regular geometrical mathematical models which assume rotational symmetry it is necessary to consider the spatial arrangement of the ventricle in 3-D. This thesis will present the description of a 3-D reconstruction method based on anatomically defined echocardiographic apical views. An analysis of the accuracy of the method together with clinical applications. Study groups will include isolated post-mortem hearts, patients referred for investigation on clinical grounds and normal healthy volunteers. Volume estimates at end diastole and end systole together with global and regional or segmental analysis of 3-D ventricular geometry are studied with respect to normal and pathological conditions.

1.2 References

Alpert BS, Bloom KR, Gilday D, Olley PM (1979)
The comparison between non-invasive and invasive methods of stroke volume determination in children
Am. Heart J. 98: 763-766

Bellhouse BJ, Talbot L (1969)
The fluid mechanics of the aortic valve
J. Fluid Mech. 35: 721-735

Davila JC, Sanmarco ME (1966)
An analysis of the fit of mathematical models applicable to the measurement of ventricular volume
Am. J. Cardiol. 18: 31-43

Dodge HT, Sandler H, Ballew DW, Lord JD (1960)
The use of biplane angiocardiography for the measurement of left ventricular volume in man.
Am. Heart J. 60: 766-776

Dumesnil JG, Shoucri RM (1982)
Effect of the geometry of the left ventricle on the calculation of ejection fraction.

Circulation. 65: 91-98

Feigenbaum H (1976)
Echocardiography. 2nd ed. Lea and Febiger, Philadelphia.

Foal R, Stefanini L, Richards A, Somerville J (1982)
Left and right ventricular morphology in complex congenital heart disease defined by two-dimensional echocardiography.
Am. J. Cardiol. 49: 93-99

Folland ED, Parisi AF, Moynihan PF, Jones MS, Feldman CL, Tow DE (1979)
Assessment of left ventricular ejection fraction and volumes by real-time, two-dimensional echocardiography. A comparison of cineangiographic and radionuclide techniques.
Circulation. 60: 760-766

Kronik G, Slany J, Mosslacher H (1979)
Comparative value of eight M-mode echocardiographic formulas for determining left ventricular stroke volume. A correlative study with thermodilution and left ventricular single-plane cineangiography.

Circulation. 60: 1308-1316

Lalani A, Lee SJK (1976)
Echocardiographic measurement of cardiac output using the mitral valve and aortic root echo.
Circulation. 54: 738-743

Leighton RF, Wilt SM, Lewis RP (1974)
Detection of hypokinesis by a quantitative analysis of left ventricular cineangiograms.
Circulation. 50: 121-127

Murray JA, Johnston W, Reid JM (1972)
Echocardiographic determination of left ventricular dimensions, volume and performance.
Am. J. Cardiol. 30: 252-257

Naggar CZ (1981)
Ultrasound studies of cardiac Motion. Clinical application of two-dimensional echocardiography.
Lahey Clinic Foundation Bulletin. 30: 133-166

Schiller NB, Acquatella H, Ports TA, Drew D, Goerke J, Ringertz H, Silverman NH, Brundage B, Botvinick EH, Boswell R, Carlsson E, Parmley WW (1979)
Left ventricular volume from paired biplane two-dimensional echocardiography.
Circulation. 60: 547-555

Silverman NH, Ports TA, Snider RA, Schiller NB, Carlsson E, Heilbron DC (1980)
Determination of left ventricular volume in children: Echocardiographic and angiographic comparisons.
Circulation. 62: 548-557

St. John Sutton MG, Tajik AJ, Gibson DG, Brown DJ, Seward JB, Giuliani ER (1978)
Echocardiographic assessment of left ventricular filling and septal and posterior wall dynamics in idiopathic hypertrophic subaortic stenosis.
Circulation. 57: 512-520

Tajik AJ, Seward JB, Hangler DJ, Mair DD, Lie JT (1978)
Two-dimensional real-time ultrasonic imaging of the heart and great vessels. Technique, image orientation, structure identification and validation.
Mayo Clinic Proc. 53: 271-303

Tei C, Shah PM, Cherian G, Wong M, Ormiston JK (1982)
The correlates of an abnormal first heart sound in mitral valve prolapse syndromes.
New England J. Medicine. August. 5: 334-339

Teichholz LE, Kreulen T, Herman MV, Gorlin R (1976)
Problems in echocardiographic volume determinations: echocardiographic angiographic correlations in the presence or absence of asynergy.
Am. J. Cardiol. 37: 7-11

CHAPTER 2

THE MEASUREMENT OF CARDIAC VOLUME AND GEOMETRY AND IT'S RELATION TO HEART FUNCTION

2.1 Introduction

The heart is perhaps unique in the body as an example of the interrelationship between its anatomical geometric structure, biochemical activity and physiological performance. These interrelationships are critical in determining volume and flow throughout the vascular system.

The heart is composed of four cavities, surrounded by muscle walls. It is regarded as a combination of two halves, a left side and a right side, each consisting of an atrium and a ventricle. Valves which allow flow in one direction separate the atria and ventricles and are also present between the ventricles and arterial blood vessels (Fig. 2.1).

The heart fulfills its pump function by the contraction and relaxation of the muscle fibres in its walls. This causes a cyclic change in the

Figure 2.1 A schematic diagram of the heart showing the directions of blood flow in response to the pump action of the heart as it cycles between end diastole and end systole.

SVC	Superior Vena Cava
IVC	Inferior Vena Cava
RA	Right Atrium
T	Tricuspid Valve
P	Pulmonary Valve
PA	Pulmonary Artery
RV	Right Ventricle
LV	Left Ventricle
Ao	Aortic Valve
M	Mitral Valve
LA	Left Atrium

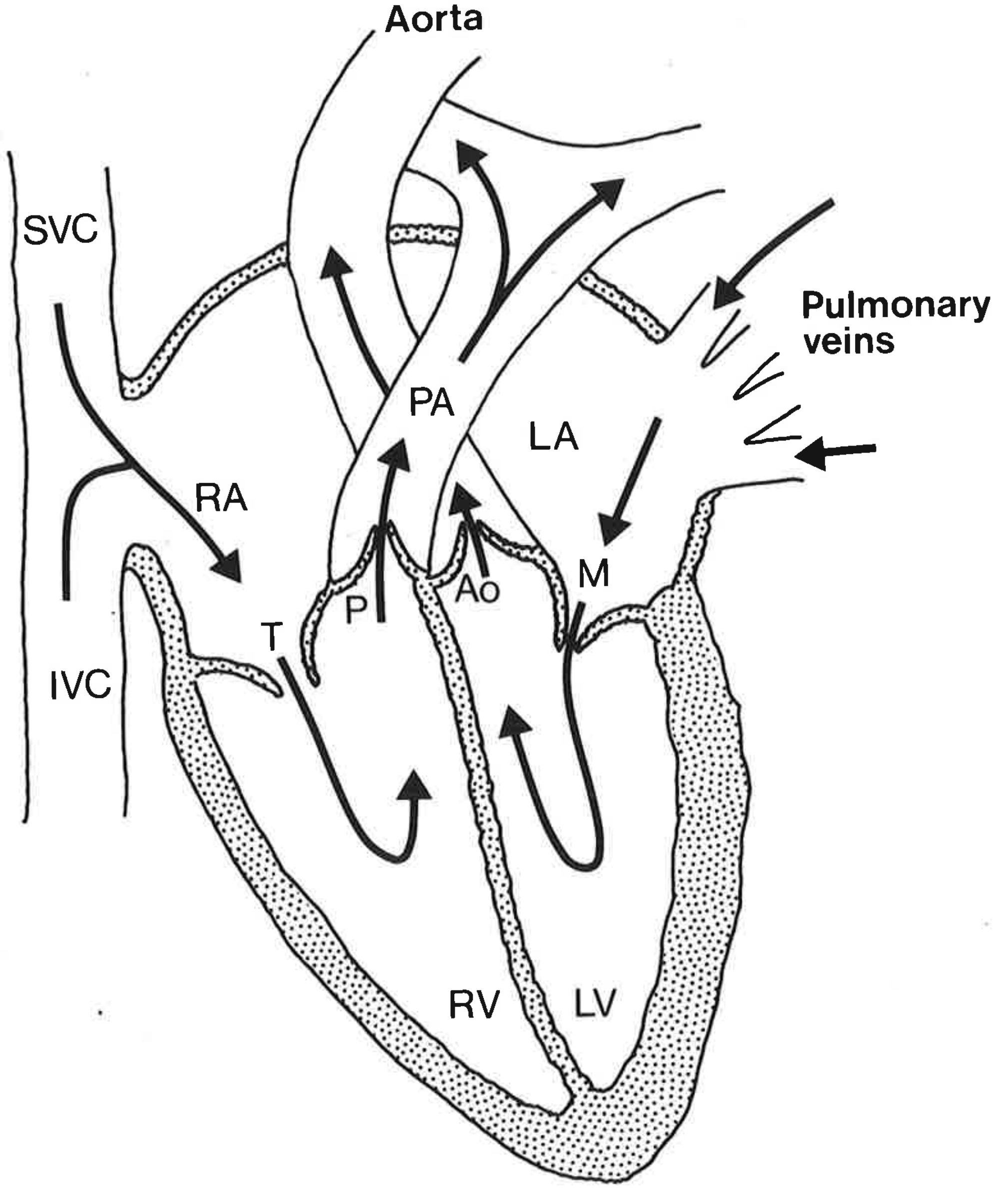
Aorta
SVC
Pulmonary
veins
PA
LA
RA
M
Ao
P
T
IVC
RV
LV

volume of the cavities and hence a transport of blood from the veins into the arteries. The amount of blood that is pumped during a cardiac cycle depends on the filling of ventricles before contraction and the impedance that the ejected blood experiences during muscular contraction. These two conditions are referred to as the preload and afterload respectively. Both contractility and the response of the heart to different loading conditions are a function of the myocardial muscle fibres. The fibre adaptation to changes in diastolic fibre length by varying preload is called the Frank-Starling Law. The greater the stretch of the fibre up to a maximum, the greater the degree of fibre shortening during contraction. Starling demonstrated this by varying the volume of venous return to the heart. The larger the preload the greater the stretching of the ventricular walls and the volume of blood ejected during the next systole.

Clinically the role of diastolic fibre length can be seen in the patient with complete heart block who is unable to develop heart rate faster than about 40 beats per minute. Nevertheless, it is possible to maintain a normal volume of blood flow. This is because of a prolonged diastolic filling period and an increased end diastolic volume. The stroke ejection volume is increased to a level adequate for resting output levels. In congestive heart failure diastolic fibre length increase aids in compensating for the pathology. The increased stretch in failing heart muscle provides a heart response comparable to non-failing muscle up to a maximal stretch threshold. The response to change in contractility by varying afterload is seen in cardiac muscle velocity of shortening which is inversely proportional to the magnitude of the load. If there is no load at all, there is a maximum velocity of shortening whereas if the load is such that the muscle cannot shorten, velocity is zero. The estimation of the shortening velocity can provide clinically useful information about the inotropic state of the heart in any patient. However, it is uncommon in the clinical situation for one isolated factor to change while others remain constant. In practice, change in end diastolic fibre length is measured as change in ventricular end diastolic volume. Similarly by the ejection fraction, but it has been demonstrated the ejection fraction is determined not only by the extent of fibre shortening within the ventricular wall, but also by the specific shape of the ventricle (Dumesnil, Shoucri, 1982).

Although beat-to-beat variation in end diastolic fibre length occurs the overall size of the ventricular chamber is kept relatively constant at any particular level of cardiac function, such as rest or exercise. Dilatation of the ventricle which occurs as a clinical condition is primarily due to a marked increase in the residual volume of the ventricle because of the rearrangement of the muscle fibres. Dilatation occurs early in all volume overload syndromes, such as those caused by valvular insuffiency or intracardiac shunts. There is an improvement in the ability of the heart to eject a volume from the dilated ventricle. If each cardiac muscle fibre shortens as much as before dilation the increase in surface area causes a proportionate increase in the volume of blood ejected with each stroke, regardless of the amount of residual blood in the ventricle at end systole. However, when the cause of the dilation is related to coronary arterial occlusion and myocardial ischaemia, the dilatation and related increased demand may lead to acute myocardial insufficiency or infarction. This in turn may lead to congestive heart failure or angina pectoris.

The relationship between individual muscle fibres and the functioning of the heart as a pump is a fundamental problem in the understanding of cardiac mechanics. The properties of muscle fibres, localisation and orientation in the myocardium, the sequence of their activation and the loading conditions of the heart are all important in the modelling of heart performance (Van der Brock and Van der Brock, 1980). Clinical measurements of myocardial volume and chamber size have demonstrated that cardiac geometry is closely related to pathology (Mirsky 1976; Kronik, Slany, Mosslacher, 1979; Bassotti, Morotti, Balbarini et al, 1980; Graham, Parrish, Boucek et al, 1983). However, all these clinical studies have failed to adequately describe cardiac volume and geometry. This situation has arisen because of the absence of any effective technique of collecting adequate 3-D spatial data. Furthermore, animal experiments where it may have been possible to collect such data have not presented numerical 3-D data analysis.

The 3-D spatial study of cardiac geometry is relevant in the provision of detailed geometric information for a more rigorous analysis of cardiac physiology. Knowledge of geometry would enable a more critical evaluation of models of the heart independant of simplifying assumptions. Moreover, for clinical diagnosis it is necessary to establish the relation between cardiac geometry and different types of functioning and malfunctioning of the heart.

2.2 Literature Survey

A number of methods of measuring global cardiac volume and/or geometry are commonly used depending on the accessibility of the heart under study. In patient studies data can be obtained in vivo by the use of invasive or non-invasive methods. That is by the use of cineangiography or echocardiography respectively. In some special instances surgically inserted epicardial markers may be used (Schnittger, Fitzgerald, Daughter et al, 1982). In animal studies measurements have been made on open and closed chests or isolated hearts which allow greater control over the operating conditions for the invasive techniques. Consequently estimates of ventricular volume are more reliable. Furthermore studies have been carried out on postmortem hearts, both fixed and unfixed which demonstrates the accuracy of various mathematical models.

2.2.1 Cineangiography

In patient studies dimensional data can be obtained in vivo by the use of cineangiography as described by Dodge and Sandler and others that use either biplane (Dodge, Sandler, Ballew et al, 1960; Wynne, Green, Mann et al, 1978) or single plane (Sandler, Hawley, Dodge et al, 1965; Dodge, Sandler, Baxley et al, 1966; Green, Carlisle, Grant et al, 1967; Sandler and Dodge, 1968) projections of the heart. These methods revolve around the use of a number of standard projections. Biplane techniques rely on lateral (L) and anteriorposterior (AP) or right anterior oblique (RAO) together with the left anterior oblique (LAO). The single plane techniques use either the AP or RAO projections.

The mathematical models used for the measurement of the left ventricular volume utilizing biplane cineangiography assume that the ventricular cavity is ellipsoid with its cross-sectional outline as elliptical or circular. The basic assumption with single-plane methods is that the unprojected orthogonal minor axis equals the measured minor axis. The left ventricle is then considered a solid of revolution, that is prolate ellipsoid where the cross section outline is circular. However there are numerous mathematical models which may be used other than ellipsoid models which have been described for volume estimation from angiocardiograms. These include cylindrical or composite cyclindical models, Simpson's rule methods which assume axial symmetry and variations on the Dodge and Sandler area-length method (Davila and Sanmarco, 1966).

2.2.2 One Dimensional Echocardiography

The emergence of echocardiography lead to the introduction of M-mode (Motion mode) in the first instance. Quantitive methods which used simplistic geometrics for the left ventricle emerged secondary to extensive qualitative applications. Empirically derived expressions for the estimation of ventricular volume which could not be scientifically justified were also used. M-mode provides only one dimensional data by allowing a "torch light" view of cardiac structures of time (Feigenbaum, 1976). This imaging mode provides minimal spatial information and hence resulted in the most simple ventricular model. A major assumption is that the ventricular shape is that of a prolate ellipsoid with an aspect ratio (major/mirror axis) of 2:1 for all stages of the cardiac cycle, irrespective of pathology. Nevertheless M-mode echocardiography has provided useful information, supported empirically, where there is no left ventricular segmental wall motion abnormalities (Murray, Johnston, Reid, 1972; Teichholz, Kreulen, Herman et al, 1976; Kronik, Slany, Mosslacher, 1979). Empirical methods which lack a scientific basis have been developed by various authors. These methods of left ventricular volume estimation rely on the combination of various dimensions such as aortic root diameter, aortic leaflet separation, duration of mitral opening and others to derive estimates (Yeh, Winsberg, Mercer, 1973; Lalani, Lee, 1976; Resmussen, Corya, Feigenbaum et al, 1978; Kronik, Slany, Mosslacher, 1979). It maybe that the variables measured are related to the ultimate diastolic and systolic volumes the ventricle achieves but no rational scientific formulation of some of these empirical expressions has been presented. Their only justification for application is that they have been shown to give good comparative results with either established invasive methods or post mortem studies in some instances.

2.2.3 Two Dimensional Echocardiography

Two dimensional echocardiagraphy on the other hand permits unique visualisation of the heart in vivo and provides spatial information in tomographic views previously unavailable (Tajik, Seward, Hagler, 1978). The availability of this spatial information has led to the development of more sophisticated models of the left ventricle, many of which still require some basic assumptions about shape and geometry (Folland, Parisi, Moynihan et al, 1979; Alpert, Bloom, Gilday et al, 1979; Schiller, Acaquetella, Ports et al, 1979;

Silverman, Ports,Snider et al, 1980). The complexity of the models is often reflected in the difficulty of data acquisition and analysis. Single plane methods are used which utilise a number of views, parasternal long axis views, apical four chamber views, apical two chamber views or apical long axis views to estimate ventricular volumes. In addition biplane methods are used by the combination of orthogonal apical views (Schiller, Acquatella, Port et al, 1979; Silverman, Ports, Snider et al., 1980; Edelman, Rowe, Pechacek et al, 1981). Again the ventricular models of the ventricle are principally ellipsoidal in nature but with some variations on the theme. In addition there are bullet and conical models (Wyatt, Heng, Meerbaum et al, 1979; Folland Parisi, Moynihan et al, 1979).

In animal studies measurements have been made of ventricular volume which because of greater scope to optimise the imaging and data collection have shown reliable results. Postmortem studies to validate invasive and non invasive methods have been performed on both human and animal hearts, the latter generally of dogs. (Dodge, Sandler, Ballew et al 1960; Dodge, Sandler, Baxley et al, 1966; Wynne, Green, Mann et al, 1978; Eaton, Maughan, Shoukas et al, 1979; Wyatt, Heng, Meerbaum et al, 1980).

2.2.4 Regional Wall Motion

Regional abnormalities of left ventricular wall motion were first described by Tennant and Wiggers (1935); when they occluded a coronary artery of a dog, the area which it supplied began to move paradoxically. It was not until some thirty years later and the advent of techniques such as cardiac catheterisation and cineventriculography that such abnormalities were studied in man. Collectively they became known as asynergy which may be divided into four categories; Dyskinesis; where a region of the ventricular wall will bulge out during systole, Akinesis; where there is a total lack of movement in a region of the wall during systole, Hypokinesis; considered to have occurred when a region does not contract to its full extent and Hyperkinesis; considered to have occurred when a region contracts beyond its normal extent. Asynergy has been most widely studied amongst patients suffering from coronary heart disease.

This has highlighted the importance of local and global geometric influences on cardiac performance. Geometry, both local and global, influences stroke volume and ejection fraction because they are determined not only by the extent of muscle shortening within the ventricular wall but also by the specific shape change of the region under contraction (Dumesnil, Shoucri, 1982).

It has been estimated that 65% of all patients with coronary heart disease (CHD) will exhibit regional abnormalities of wall motion (Gorlin, 1976). The areas to exhibit such abnormalities include scar tissue following myocardial infarction, aneurysmal sacs or regions of ischaemic but still living myocardium (Basley, Reeves, 1971). Cardiac dysfunction can of course be global or segmental since CHD is of a segmental nature and it is not surprising that abnormalities of contraction are in turn segmental. It is thus to be expected that the greater the number of coronary arteries affected by atherosclerosis, the greater the degree of observed asynergy. Asynergy will adversely affect cardiac function, as a result of either decreased or ineffectual contraction. Some haemodynamic results of regional abnormalities in wall motion include decreased stroke and cardiac output (Massie, Botvinick, Brundage et al, 1978), as well as decreases in the mean rate of rise of left ventricular pressure, cardiac index and ejection rate (Baxley, Reeves, 1971). A rise in left ventricular end diastolic pressure has also been noted in asynergic hearts (Gorlin, 1976).

The presence of asynergy does not always result in decreased cardiac efficiency, since if the area of asynergy is small and the remaining myocardium not compromised in any way, compensation for the decreased contribution of the asynergic area may take place, with little change in haemodynamic parameters (Gorlin, 1976). Compensation will not occur where the remaining myocardium is impaired by diffuse ischaemia or fibrosis. The effect of a region of abnormal ventricular wall motion on cardiac function will also depend on the load imposed on the ventricle. Asynergy may eventually lead to congestive cardiac failure where a local area of dysfunction rather than a generalised disorder of the myocardium results in ineffective cardiac contractibility (Herman, Heinle, Klein et al, 1967).

The belief that asynergy in CHD is a result of myocardial ischaemia is supported by a number of studies (Sniderman, Marpole, Fallen, 1973; Massie, Botvinick, Brundage et al, 1978; Bodenheimer, Banka, Fooshee et al, 1978). Asynergy is most frequently found in the distribution of the most severely stenosed coronary artery patients without a previous documented myocardial infarction (Massie, Botvinick, Brundage et al 1978). Massie et al, (1978) concluded that coronary anatomy as shown by arteriography can be misleading, two regions supplied by apparently equally occluded arteries may have widely different patterns of contraction. They found that regional wall motion correlates better with myocardial perfusion than with coronary anatomy. Bodenheimer et al (1978) also found that areas of perfusion abnormalities were frequently areas of asynergic wall movement. Those abnormalities of perfusion that were induced by exercise and improved by rest were considered reversible and more probably made up of ischaemic, yet viable myocardium as opposed to avascular fibrous scar tissue which one would expect to demonstrate irreversible asynergy. Sniderman and his colleages (1973) found an association between the sites of major coronary occlusions and areas of asynergy. For example, in cases of occlusion of the right coronary artery, akinesis or dyskinesis of the posterior ventricular wall was a common finding. In patients who suffered from occlusion of the left coronary artery circulation, akineses was a more frequent finding. They concluded that 'there appears to be a distinctive pattern of regional abnormalities associated with the site of occlusion" (Sniderman, Marpole, Fallen 1973).

Banka and co-workers (1977) found experimentally in dogs that a 25% reduction in blood flow through a coronary artery did not result in asynergy in the region of the myocardium that it supplied. A reduction of 50% of blood flow through the artery resulted in a decreased rate of myofibril shortening. Reduction of blood flow by 75% or more accentuated the regional abnormality seen at 50% reduction of coronary blood flow, resulting in systolic akinesis and diastolic dyskinesis.

Regional abnormalities of left ventricular wall motion are frequently observed in relation to CHD and are seen as an important outcome of myocardial ischaemia. Initially description of wall motion abnormalities was by catheterisation leading to ventriculography by the injection of radioapaque dyes. Single plane left ventriculography in the right anterior oblique projection (RAO) is most commonly used for evaluating the left ventricular contraction pattern qualitatively. It displays the motion of three zones of the left ventricular inner wall, the anterior, inferior and apical. The anterior zone corresponds to the distribution of the left anterior descending artery, while the inferior zone is supplied by the right coronary artery and the apical zone by the left anterior descending artery anteriorly and left circumflex artery inferiorly. Asynergy in these zones correlates well with occlusive lesions in the corresponding arteries in patients with coronary artery disease (Herman, Heinle, Klein et al, 1967). Asnergy in the septal and posterior zones cannot be appreciated in the RAO view. Although the left anterior oblique view (LAO) provides information on the wall motion of these two zones, its addition does not improve the overall detection of asynergy (Cohn, Gorlin, Adams et al, 1974).

Quantitative methods currently employed for the analysis of the left ventriclar contraction pattern are rather approximate and their geometric basis arbitrary. The methods assess the endocardial silhouette in terms of extent of shortening or lengthening. The end diastolic frame has been taken in most studies as the intial condition (Leighton, Wilt, Lewis, 1974). For comparison, the endocardial silhouette must be properly superimposed. This is necessary because the spatial position of any point on the endocaridal silhouette is affected not only by the cardiac contraction itself but also by:-

(1) positional changes of the heart;
(2) systolic descent of the aortic and mitral valves;
(3) translation of the heart with motion of the ribs and diaphragm during breathing.

In superimposing the cardiac silhouettes a long axis is drawn through the aortic valve centre and apex. The axis is then aligned and the endocardial silhouettes superimposed either at the midpoint or at the aortic valve (Daughters, Schwarzkopf, Mead et al, 1980). The midpoint superimposition exaggerates the apical shortening by neglecting the downward displacement of the valve. Apical and inferior wall asynergy is therefore minimised. The implicit assumption made in drawing the long axis of the left ventricle is that it represents the axis of revolution of the left ventricular ellipsoid, toward which the endocardium moves during systole (Sapoznikov, Halon, Lewis et al, 1981). Various techniques are then used to quantify the asynergy that may be present in CHD. The long axis may be partitioned with chords perpendicular to the axis and their length measured. If the half chords are measured and averaged the method may fail to detect minor abnormalities of contraction involving only one wall (Gelberg, Brundage, Glantz et al, 1979; Daughters Schwarzkopf, Mead et al, 1980; Rein, Sapoznikov, Lewis et al, 1982). Radial axes have also been employed. The disadvantage with this method is that the basal and apical portions escape analysis in elongated left ventricles (Gelberg, Brundage, Glantz et al, 1979). Another approach to the characterisation of the segmental contraction patterns of the left ventricle is to calculate the percentage change in area of regions of the ventricle. The area method however suffers from the arbitary location of the long axis bisector (Gelberg, Brundage, Glantz et al, 1979; Sasayama, Nonogi, Kawai 1982). The evaluation of the above methods by using myocardial markers as a standard, has demonstrated that radial measurements provide optimal results (Ingels, Daughters, Stinson et al, 1980). The direction of ventricular wall motion is much closer to the behaviour of all the endocardium if it is expressed along radial lines. Furthermore, radionuclide studies utilise methods which are analogous to those applied to ventriculograms or variations which measure radioactivity in different regions (Maddox, Wynne, Uren et al, 1979; Vos, Vossepoel, Pauwels 1983; Wasserman, Johnston, Katz et al, 1984; Imai, Suzuki, 1984).

M-Mode and 2-D echocardiographic evaluation of segmental wall motion has provided some scope for alternatives which are not available to ventriculography or radionuclide techniques. This is because ultrasound permits the unique visualisation of the heart in vivo and provides spatial information in one dimensional and tomographic views previously unavailable (Edwards, Tajik, Seward, 1981). The mode of imaging emphasises the cross sectional anatomy of the heart as against the projection or silhouette of cineventriculography. Tomographic analysis allows the assessment of infarct location and the study of ischemic heart disease. Furthermore, the approach allows the assessments of intracardiac relationships. Tomographic sections are ideal for demonstrating not only the primary pathologic lesion but also the secondary cardiac effect of that lesion. A number of cross sectional echocardiagraphic analyses of left ventricular asynergy have been reported. The qualitative methods take the approach of dividing the ventricle into segments identified by their location on the cross sectional image. The studies have focused on the analysis of the extent of asynergy (Kisslo, Robertson, Gilbert et al, 1977; Heger, Weyman, Wann et al, 1979; Heger, Weyman, Wann et al, 1980), evaluation of coronary artery bypass surgery (Rubenson, Tucker, London et al, 1982), the detection of aneurysms and evaluation of aneurysmectomy (Weyman, Peskoe, Williams et al, 1976; Gehl, Depace, Katler et al, 1982). The interpretive techniques utilized for these studies were purely subjective and demonstrated that methods for quantitative assessment of left ventricular regional wall motion are required (Kisslo, Robertson, Gilbert et al, 1977).

Quantitative methods have focused on the analysis of parasternal short axis views and the apical four chamber view. (Moynihan, Parisi, Feldman, 1981; Schnittger, Fitzgerald, Gordon et al, 1984). The parasternal views have been either at the level of the mitral valve and/or papillary muscle. These studies have described percentage radii or area changes as indicators of asynergy. Such methods require appropriate reference axes though the tomographic views provide views which directly reflect cardiac anatomy.

None of the techniques, invasive and non invasive, have described the changes which may occur in the myocardial surface or the regional volume changes during systole. The lack of an adequate 3-D spatial reconstruction of the left ventricle has not enabled such analyses to be undertaken effectively. An angiographic study has considered the regional ejection fraction of the normal left ventricle but by rotation of a single plane (RAO) ventriculogram (Sapoznikov, Halon, Lewis et al, 1981).

2.2.5 Three Dimensional Echocardiography

There remains in both clinical and experimental cardiology then a need for an accurate, non-invasive method to comprehensively evaluate cardiac performance. It is apparent at this point that ventricular volume estimations and derived parameters are insufficient to adequately describe ventricular function. Chamber geometry has a significant effect on performance, in particular if shape changes are associated with any heart pathology. Despite the numerous attempts at the quantitation of global shape using ultrasound it remains largely qualitative. In the process of interpreting a clinical echocardiographic study, the cardiologist evaluates numerous M-mode or 2-D sequential views of the ventricle and mentally reconstructs these in 3-D. In this way, he develops a subjective opinion of the extent of an area of hypokinesis, the size of an aneurysm or an estimate of overall contraction (Edwards, Tajik, Seward 1981; Geiser, Ariet, Conetta et al, 1982; Gehl, Depace, Kotter et al, 1982).

The quantitative evaluation of regional function, hypo and hyperkinetic regions and delayed contraction have been studied by both invasive and non-invasive techniques. That is ventriculography, radioisotope studies M-mode and 2-D echocardiography. Again these studies have relied on simplisitic models of ventricular geometry to describe complex 3-D geometry not only of the "normal" ventricular shape but also in instances where geometric changes are closely associated with pathological disorders. The precise identification of regional contraction abnormalities depends on the use of a method which will separate normal motion from abnormal left ventricular wall motion more reliably than does the subjective or semi quantitative interpretation of left ventricular projections or tomograms (Rubenson, Tucker, Landon et al, 1982). The method of choice in a particular context, clinical or experimental, may be determined by local factors but nevertheless no method is generally available which describes geometric changes in a global 3-D manner. However, the use of a quantitative method appears to be essential to the proper interpretation of left ventricular wall motion. Quantitative methods used to describe wall motion can be generally classed as area, chord and radial methods with variations within each category depending on the choice of axes reference points. Numerous studies have been done to determine the most effective method but the debate continues (Leighton, Wilt, Lewis, 1974; Gelberg, Brundage, Glantz et al, 1979; Daughters, Schwarzkopf, Mead et al, 1980). The evaluation of performance at a regional level of the ventricle has been investigated by studies which have examined regional ejection fraction. These studies have attempted to determine the impact of muscle fibrosis, ischemia or myocardial infarction on the global and regional function of the ventricle (Maddox, Wynne, Uren et al, 1979; Sapoznikov, Halon, Lewis et al, 1981; Imai, Suzuki, 1984).

The 3-D architecture of the heart must be known to understand its primary mechanical function of maintaining the body's blood circulation. The techniques referred to above cannot give 3-D structural information and its relationship to functional performance because they reduce the heart to a single dimension (M-mode ultrasound) or two-dimensional structure either by radiographic project (ventriculography) or ultrasound tomography (2-D echocardiography) before measurements are made. Alterations in the functional architecture of the heart have been described in association with certain clinical features of heart disease. Grant (1953) in his paper on heart architectonics was one of the first to describe in detail the 3-D architecture of formalin fixed hearts taken at autopsy. He presented details of changes which take place in the left ventricle with mitral valve disease, hypertrophy and dilatation. More recently the significance of chamber curvature for efficient normal ventricular function and its role in the development of idiopathic hypertrophic subaortic stenosis and contribution to post infarction cardiac dysfunction has been reported (Hutchin, Bulkley, Moore et al, 1978; Hutchins, Bulkley, 1978; Hutchins, Moore, Skooge, 1985). The effects of ischemia on 3-D left ventricular mechanics in dogs has been studied to identify the alterations in regional mechanics. The studies demonstrated that regional mechanics is a result of interactions between ischemic and non-ischemic myocardium but the direct result of ischemia or myocardial infarction (Kerber, Abboud, 1973; Visner, Arentzen, O'Connor et al, 1981).

This treatment of the literature is not exhaustive though it does develop the context which illustrates the importance of an adequate description of the 3-D geometry of the heart to analyse its function and condition.

2.3 Proposed Study

The thesis will present the details of a method of 3-D recontruction of the left ventricle of the heart based on anatomically defined apical views using 2-D echocardiography. A theoretical basis for the selection of this method will be presented together with an analysis of defined geometrical shapes and post-mortem hearts. This will be followed by the presentation of a study which analyses 56 patients using the 3-D reconstruction technique to analyse left ventricular function and condition.

2.4 References

Alpert BS, Bloom KR, Gilday D, Olley PM (1979)
The comparison between non-invasive and invasive methods of stroke volume determination in children.
Am. Heart J. 98: 763-766

Banka VS, Bodenheimer MM, Helfant RH (1977)
Relation between progressive decreases in regional coronary perfusion and contractile abnormalities.
Am. J. Cardiol. 40: 200-205

Bassotti A, Morotti R, Balbarini A, Mariani M (1980)
Quantitative evaluation of the regional left ventricular function in normal subjects by means of cineangiography.
Cardiovascular Research. 14: 30-40

Baxley WA, Reeves TJ (1971)
Abnormal regional myocardial performance in CAD disease.
Progress In Cardiovascular Disease. 8: 405-421

Bodenheimer MM, Banka VS, Fooshee C, Hermann GA, Helfant RH (1978)
Relationship between the regional myocardial perfusion and the presence, severity and reversibility of asynergy in patients with CHD.
Circulation. 58: 789-795

Cohn PF, Gorlin R, Adams DF (1974)
Comparison of biplane and single plane left ventriculograms in patients with coronary artery disease.
Am. J. Cardiol. 33: 1-6

Daughters GT, Schwarzkopf A, Mead CW, Stinson EB, Alderman EL, Ingels NB (1980)
A clinical evaluation of five techniques for left ventricular wall motion assessment.
Computers in Cardiology IEEE. 249-252

Davila JC, Sanmarco ME (1966)
An analysis of the fit of mathematical models applicable to the measurement of left ventricular volume.
Am. J. Cardiol. 18: 31-43

Dodge HT, Sandler H, Ballew DW, Lord JD (1980)
The use of biplane angiocardiography for the measurement of left ventricular volume in man.
Am. Heart J. 60: 766-776

Dodge HT, Sandler H, Baxley WA, Hawley RR (1966)
Usefulness and limitations of radiographic methods for determining left ventricular volume.
Am. J. Cardiol. 18: 10-24

Dumesnil JG, Shoucri RM (1982)
Effect of the geometry of the left ventricle on the calculation of ejection fraction.
Circulation. 65: 91-98

Eaton LW, Maughan WL, Shoukas AA, Weiss JL (1979)
Accurate volume determination in the isolated ejecting canine left ventricle by two dimensional echocardiography.
Circulation. 60: 320-326

Edelman SR, Rowe DW, Pechacek LW, Garcia E (1981)
Left ventricular volumes and ejection fraction derived from apical two dimensional echocardiography
Bulletin Texas Heart Institute. 8: 344-354

Edwards WD, Tajik AJ, Seward JB (1981)
Standardised nomenclature and anatomic basis for regional tomographic analysis of the heart.
Mayo Clin. Proc. 56: 479-497

Feigenbaum (1976)
Echocardiography 2nd ed.
Lea and Febiger, Philadelphia.

Folland ED, Parisi AF, Moynihan PF, Jones MS, Feldman CL, Tow DE (1979)
Assessment of left ventricular ejection fraction and volumes by real-time, two dimensional echocardiography. A comparison of cineangiographic and radionuclide techniques.
Circulation. 60: 760-766

Gehl LG, DePace NL, Kotter MN, Haaz W, Mintz GS, Mundth E (1982)
Pre and Post ventricular aneurysmectomy: Two-dimensional echocardiographic evaluation of segmental wall motion.
J. Cardiovascular Ultrasonography. 1: 211-215

Geiser EA, Ariet M, Conetta DA, Lupkiewiez SM, Christie LG, Conti CR (1982)
Dynamic three dimensional echocardiographic reconstruction of the intact human left ventricle: Technique and initial observations in patients.
Am. Heart J. 103: 1056-1065

Gelberg HJ, Brundage BH, Glantz S, Parmley WW (1979)
Quantitative left ventricular wall motion analysis: A comparison of area, chord and radial methods.
Circulation. 59: 991-1000

Gorlin R (1976)
Coronary Artery Disease.
Vol. XI, Major Problems in Internal Medicine, Ed Smith LH,
WB Saunders Co. Philadelphia.

Graham TP, Parrish MD, Boucek RJ, Boerth RC, Breitweser JA, Thompson S, Robertson RM, Morgan JR, Friesinger GC (1983)
Assessment of ventricular size and function in congenitally corrected transposition of the great arteries.Am. J. Cardiol. 51: 244-251

Grant RP (1953)
Architectonics of the heart
Am. Heart J. 46: 404-431

Green DG, Carlisle R, Grant C (1967)
Estimation of left ventricular volume by one-plane cineangiography.
Circulation. 35: 61-65

Heger JJ, Weyman AE, Wann LS, Dillon JC, Feigenbaum H (1979)
Cross-sectional echocardiography in acute myocardial infarction: Detection and localisation of regional left ventricular asynergy.
Circulation. 60: 531-538

Heger JJ, Weyman AE, Wann LS, Rogers EW, Dillon JC, Feigenbaum H (1980)
Cross-sectional echocardiographic analysis of the extent of left ventricular asynergy in acute myocardial infarction.
Circulation. 61: 1113-1118

Herman MV, Heinle RA, Klein MD, Gorlin R (1967)
Localised disorders in myocardial contraction: Asynergy and its role in congestive heart failure.
New England Journal Medicine. 277: 222-232

Hutchins GM, Bulkley BH (1978)
Catenoid shape of the interventricular septum: Possible cause of idiopathic hypertrophic subaortic stenosis.
Circulation 58:392-397

Hutchins GM, Moore GW, Skoog DK (1985)
Catenoid shape of the interventricular septum acquired secondary to myocardial infarction.
Am. J. Clinical Path. 83: 53-58

Hutchins GM, Bulkley BH, Moore GW, Piasio MA, Lohr FT (1978)
Shape of the human cardiac ventricles.
Am. J. Cardial. 41: 646-654

Imai S, Suguki T (1984)
Differences of global and regional left ventricular function in anterior and inferior myocardial infarction: Assessment by the use of a regional ejection fraction.

Japanese Circulation Journal. 48: 1175-1183

Ingels NB, Daughters GT, Stinson EB, Alderman EL (1980)
Evaluation of methods for quantitating left ventricular segmental wall motion in man using myocardial markers as a standard.
Circulation. 61: 966-972

Kerber RE, Abboud FM (1973)
Echocardiographic detection of regional myocardial infarction An experimental study.
Circulation. 47: 997-1005

Kisslo JA, Robertson D, Gilbert BW, Von Ramm O, Behar VS (1977)
A comparison of real-time two dimensional echocardiography and cineangiography in detecting left ventricular asynergy.
Circulation. 55: 134-141

Kronik G, Slany J, Mosslacher H (1979)
Comparative value of eight M-mode echocardiographic formulas for determining left ventricular stroke volume. A correlative study with thermodilution and left ventricular single-plane cineangiography.
Circulation. 60: 1308-1316

Lalani A, Lee SJK (1976)
Echocardiographic measurement of cardiac output using the mitral valve and aortic root echo.
Circulation. 54: 738-743

Leighton RF, Wilt SM, Lewis RP (1974)
Detection of hypokinesis by a quantitative analysis of left ventricular cineangiograms.
Circulation. 50: 121-127

Maddox DE, Wynne J, Uren R, Parker JA, Idoine J, Siegel LC, Neill JM, Cohn PF, Holman BL (1979)
Regional ejection fraction: A quantitative radionuclide index of regional left ventricular performance.
Circulation. 59: 1001-1009

Massie BM, Botvinick EH, Brundage BH, Greenberg B, Shames D, Gelberg H (1978)
Relationship of regional myocardial perfusion to segmental wall motion - A physiologic basis for understanding the presence and reversibility of asynergy.
Circulation. 58: 1154-1163

Mirsky (1976)
Assessment of passive elastic stiffness of cardiac muscle: Mathematical concepts physiologic and clinical considerations, directions of future research.
Progress of Cardiovascular Diseases. 18: 277-308

Murray JA, Johnston W, Reid JM (1972)
Echocardiographic determination of left ventricular dimensions, volume and performance.
Am. J. Cardiol. 30: 252-257

O'Boyle JE, Parisi AF, Nieminen M, Kloner RA, Khuri S (1983)

Quantitative detection of regional left ventricular contraction abnormalities by two dimensional echo cardiography. Comparison of myocardial thickening and thinning and endocardial motion in a canine model.
Am. J. Cardiol. 51: 1732-1738

Rasmussen S, Corya BC, Feigenbaum H, Black MJ, Lovelace E, Phillips JF, Noble RJ, Knoebel SB (1978)
Stroke volume calculated from the mitral valve echogram in patients with and without ventricular dyssynergy.
Circulation. 58: 125-133

Rein AJJT, Sapoznikov D, Lewis N, Halon DA, Gotsman MS, Lewis BS (1982)
Regional left ventricular ejection fraction from real-time two dimensional echocardiography.
Int J. Cardiol. 2: 61-70

Rubenson DS, Tucker CR, Landon E, Miller DC, Stinson EB, Popp RL (1982)

Two dimensional echocardiographic analysis of segmental left ventricular wall motion before and after coronary artery bypass surgery.
Circulation. 66: 1025-1033

Sandler H, Dodge HT (1968)
The use of single plane angiocardiograms for the calculation of left ventricular volume in man.
Am. Heart J. 75: 325-334

Sandler H, Hawley RR, Dodge HT, Baxley WA (1965)
Calculation of left ventricular volume from single plane (A-P) angiograms.
J. Clin, Invest. 44: 1094-1095

Sapoznikov D, Halon DA, Gotsman MS (1981)
Regional ejection fraction of the normal left ventricle.
Israel J. Medical Sciences. 17: 1027-1034

Sasayama S, Nonogi H, Kawai C (1982)
Assessment of left ventricular function using an angiographic method.
Japanese Circulation Journal. 46: 1127-1137

Schiller NB, Acquatella H, Ports TA, Drew D, Goerke J, Ringertz H, Silverman NH, Brundage B, Botvinick EH, Boswell R, Carlsson E, Parmely WW (1979)
Left ventricular volume from paired biplane two dimensional echocardiography.
Circulation. 60: 547-555

Schnittger I, Fitzgerald PJ, Daughters GT, Ingels NB, Kantrowitz NE, Schwarzkopf A, Mead CW, Popp RL (1982)
Limitations of comparing left ventricular volumes by two dimensional echocardiography, myocardial markers and cineangiography.
Am. J. Cardiol. 50: 512-519

Schnittger I, Fitzgerald PJ, Gordon EP, Alderman EL, Popp RL (1984).
Computerised quantitative analysis of left ventricular wall motion by two dimensional echocardiography.
Circulation. 70: 242-254

Silverman NH, Ports TA, Snider RA, Schiller NB, Carlsson E, Heilbron DC (1980)

Determination of left ventricular volume in children: Echocardiographic and angiographic comparisons.
Circulation. 62: 548-557

Sniderman AD, Marpole D, Fallen EL (1973)
Regional contraction patterns in the normal and ischaemic left ventricle in man.
Am. J. Cardiol. 31: 484-489

Tajik AJ, Seward JB, Hagler DJ, Mair DD, Lie JT (1978)
Two-dimensional real-time ultrasonic imaging of the heart and great vessels. Technique, image orientation, structure identification and validation.
Mayo Clinic Proc. 53: 271-303

Teichholz LE, Kreulen T, Herman MV, Gorlin R (1976)
Problems in echocardiographic volume determinations: Echocardiographic angiographic correlations in the presence or absence of asynergy.
Am. J. Cardiol. 37: 7-11

Tennant R, Wiggers CJ (1935)
Effect of coronary occlusion on myocardial contraction.
Am. J. Physiol. 112: 351-361

Van der Brock JHJM, Van der Brock MHLM (1980)
Application of an ellipsoidal heart model in studying left ventricular contractions.
J. Biomechanics. 13: 493-503

Visner MS, Arentzen CE, O'Connor MJ, Crumbley AJ, Anderson RW (1981)
Effects of global ischemia on three dimensional left ventricular diastolic mechanics in the conscious dog.
Surgical Forum. 981: 263-265

Vos PH, Vossepoel AM, Pauwels EKJ (1983)
Quantitative assessment of wall motion in multiple gated studies using temporal fourier analysis.
J. of Nuclear Medicine. 24: 389-396

Wasserman AG, Johnson RA, Katz RJ, Leiboff RH, Bren GB, Varghese PJ, Ross AM (1984)

Detection of left ventricular wall motion abnormalities for the diagnosis of coronary artery disease: A comparison of exercise radionuclide and pacing intravenous digital ventriculography.
Am. J. Cardio. 54: 497-501

Weyman AE, Peskoe SM, Williams ES, Dillon JC, Feigenbaum H (1976)
Detection of left ventricular aneurysms by cross-sectional echocardiography.
Circulation. 54: 936-944

Wyatt HL, Heng MK, Meerbaum S, Gueret P, Hesteness JD, Dula E, Corday E (1980)
Cross-sectional echocardiography II Analysis of mathematic models for quantifying volume of the formalin-fixed left ventricle.
Circulation. 61: 1119-1125

Wyatt HL, Heng MK, Meerbaum S, Hesteness JD, Cobo JM, Davidson RM, Corday E (1979)
Cross-sectional echocardiography I Analysis of mathematic models for quantifying mass of the left ventricle in dogs.
Circulation. 60: 1104-1113

Wynne J, Green LH, Mann T, Levin D, Grossman W (1978)
Estimation of left ventricular volumes in man from biplane cineangiograms filmed in oblique projections.
Am. J. Cardiol. 41: 726-732

Yeh H, Winsberg F, Mercer EN (1973)
Echographic aortic valve oriface dimension: Its use in evaluating aortic stenosis and cardiac output.
J. of Clinical Ultrasound. 1: 182-189

CHAPTER 3

ECHOCARDIOGRAPHY - AN IMAGING METHOD

3.1 Introduction

Ultrasonic imaging of the human anatomy is established as a valuable diagnostic facility in medicine. The most common mode of ultrasound imaging is the pulse-echo mode. That is, a short burst of acoustic energy is directed into the body and the reflected energy is received at a later time. It has the advantage over other commonly used medical imaging methods of being non-invasive, non ionising, of not requiring a contrast medium for boundary delineation and has yet to be shown to be hazardous at the power levels required to obtain an image. The major advantage of this is the ability to permit repeated investigations and screening. There are some basic limitations to the clinical use of ultrasound tomography (2-D ultrasound). These are due to the relatively low penetration of ultrasound in bone and air. Hence, there is a relatively high attenuation of ultrasound in bone and lung compared with soft tissue. Moreover a high proportion of ultrasound is reflected at boundaries between soft tissue structures and bone or gas so ultrasound imaging is almost exclusively confined to soft tissue structures. In particular, those which are not obscured by bone or gas-filled structures. The abundance of bone and air in the human body therefore excludes many parts of the body from 2-D ultrasound imaging. However ultrasound brings several capabilities to medical imaging. An ultrasound image represents the mechanical properties of the tissue (i.e. parameters such as density and elasticity) and most people can recognise common anatomical structures in an ultrasound image since the organ boundaries and fluid-to-tissue interfaces are easily distinguished. Furthermore, the ultrasound imaging process can be done in real time. This means that the viewer can follow rapidly moving structures such as the heart without distortion. Also, it allows the operator to move the small hand held transducer over the surface of the patient's body to select the proper view in an interactive way.

3.2 Ultrasound Imaging

3.2.1 Instrumentation

The imaging process consists of two parts. First is the illumination of the objects to be imaged by the ultrasound radiation. This radiation interacts with the object by means of reflection, absorption or scattering. The second step is a reconstruction of the energy received from these interactions to form an image of the object. The most commonly used medical ultrasonic imaging method employs the pulse-echo principle with B or brightness mode scanning. A B-scan is a view of a cross-sectional slice through an object. A narrow pencil beam of ultrasound is swept through a sector to define the scan plan. The beam is formed from bursts of ultrasound such that the repetition rate of the ultrasound pulse allows the transmitted pulse time to travel to the deepest target and back before the next pulse is emitted. The pulse is assumed to travel in a straight line at a constant velocity. As the pulse propagates into the body along any scan line, echoes are generated which travel back to the receiver. These echoes vary in intensity according to the type of tissue or body structure causing them. This data is presented on a cathode-ray-tube display in which the brightness (hence the term B-mode) depends on the echo strength.

Resolution is the ability to separate small objects in the scan plane visually. It has three components, range resolution (along a scan line), azimuth resolution (perpendicular to a scan line within the plane of the sector scan) and elevation resolution (the thickness of the sector scan slice) Fig. 3.1. The range resolution is determined by the ultrasound pulse length. A shorter pulse gives higher resolution. Two targets 0.75mm apart in range can be resolved with a 1μs ultrasound pulse.

The resolution in the azimuth direction depends on the array aperture (length of the ultrasound transducer array) and the acoustic wavelength. The principles are the same as for an optical telescope. High azimuth resolution is achieved with a large aperture and a short wavelength (Joynt, Popp, 1982).

Figure 3.1 An ultrasound image is obtained by scanning a beam of ultrasound in an azimuth direction. The image quality is a function of the beams azimuth, elevation and radial resolutions.

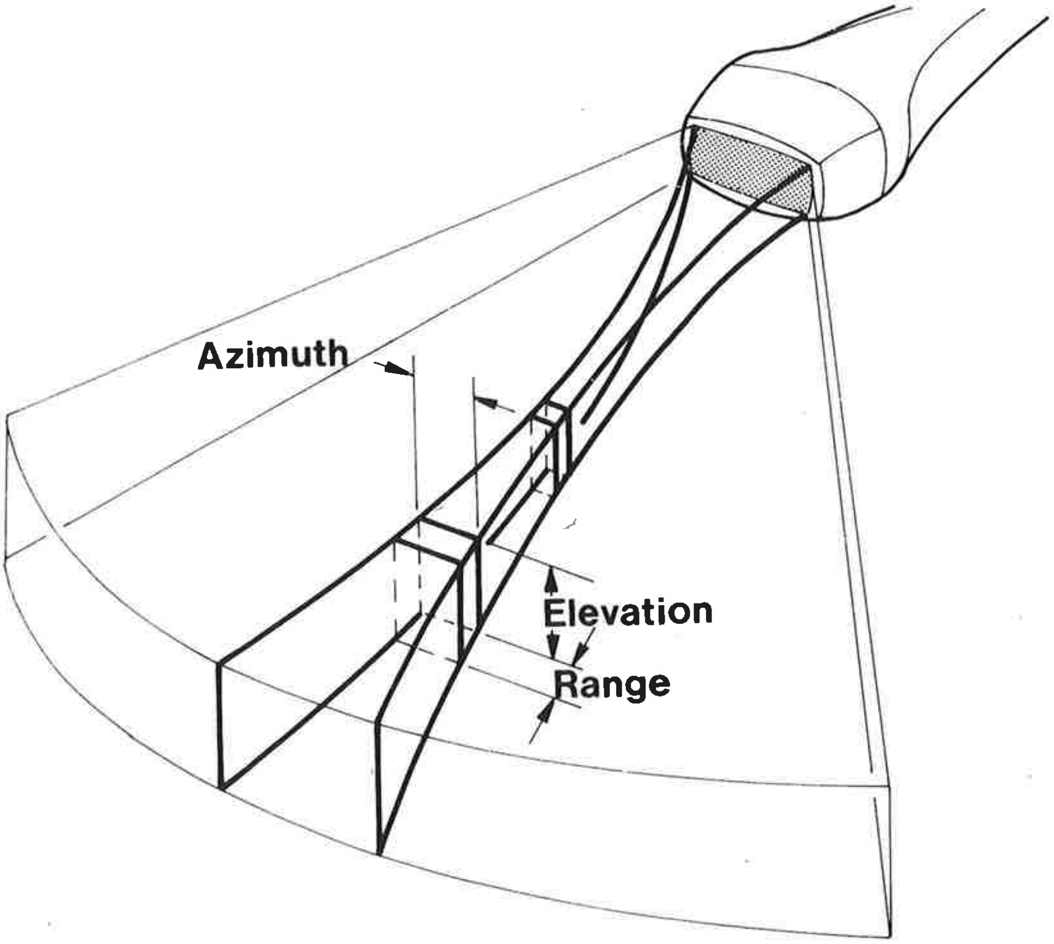
Azimuth
Elevation
Range

A block diagram for a general ultrasound imaging system is shown in Fig. 3.2. The transmitter excites the transducer elements with short electric pulses so that a burst of ultrasound is generated. The returning echoes are applied to a variable gain stage in the receiver called a time gain compensation (TGC) amplifier. This amplifier increases its gain with time, thus compensating for tissue attentuation as echoes come from deeper regions of the body. In a phased array system, each element of the transducer has its own TGC amplifier. The beam former combines the output of the individual receiver channels by using variable time delay and phase adjustment to bring the received signals into coincidence and hence bring an object into focus. Since the received echoes have a very wide dynamic range, the signal processing stage uses signal level compression. The compressed signal is then converted from analog to digital form so that an entire image frame can be stored in the memory of the digital scan converter. The digital scan converter changes the scan format from a sector display to a conventional television raster scan. It also permits digital postprocessing of the images. These various

Figure 3.2 Block diagram of a basic ultrasound imaging system using a phased-array transducer.

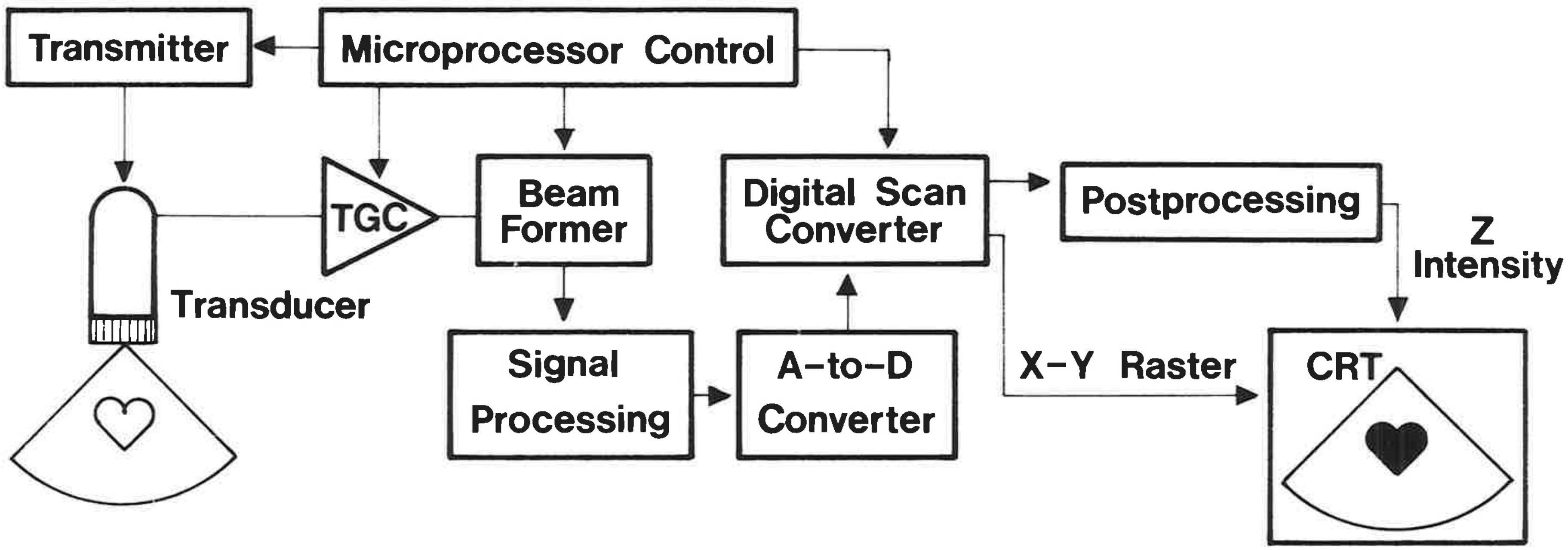
Transmitter
Microprocessor Control
TGC
Beam Former
Digital Scan Converter
Postprocessing
Z Intensity
Transducer
Signal Processing
A-to-D Converter
X-Y Raster
CRT

activities - the transmitter, TGC amplifier, beam former, scan converter, and display - are co-ordinated under microprocessor control (Gore, Leeman, 1977; Wilkinson, 1981; Chivers, 1981).

Echocardiagraphy is ultimately linked with developments in biomedical engineering. Therefore, both engineering and clinical developments determine the current and future applications of this imaging mode.

3.2.2 Ultrasound Tomography and Cardiac Anatomy

The evaluation of ventricular function and performance is fundamental in assessing the significance of certain kinds of heart disease (Feigenbaum, Henry, Pearlman et al, 1981). The availability of 2 -D echocardiagraphy has the major advantage that it can display an entire cross-sectional slice of the ventricle as opposed to a single linear dimension by M-mode echocardiographic or radioisotope methods. The tomographic view of the 2-D real time ultrasound image has a direct correspondence to cardiac anatomy. Both one dimensional M-mode and projection techniques contain less available information for evaluation. Various tomographic sections can be obtained from different positions along the long and short axes of the heart. A variety of planes have been described for 2-D imaging. Short axes tomographic sections of the left ventricle allow views of the ventricular apex, papillary muscles, mitral leaflets and ventricular outflow. Long axis or apical sections allow views of the left ventricle.

Parasternal views are classic, initially derived for M-mode echocardiography. The parasternal long axis view reveals the septal-aortic and mitral-aortic relationships. This view is essentially parallel to the long axis of the left ventricle and therefore does not show the full cardiac apex, and usually ends just below the papillary muscles. The parasternal short axis planes of the left ventricle are imaged by angulating or moving the transducer between the ribs. Below the great vessels the mitral valve is imaged. At this point the left ventricle may achieve its round contour. Further down towards the apex the image plane passes through the papillary muscles.

For the apical views, the transducer is placed at the palpable cardiac apex and aimed toward the suprasternal notch to obtain the apical four chambered view. Imaging the mitral and tricuspid valves simultaneously achieves this four chambered view. Often significant rotational adjustment of the transducer is required.

Most real time echocardiographic systems have an ECG gated raster which allows capture of a single image still frame. For instance, if one wishes to catch end diastole one can find the QRS complex and use it to set up a 2-D strobe frame. Also gated frames are often recorded.

3.3 References

Chivers RC (1981)
Tissue characterisation - Review paper.
Ultrasound in Med. and Biol. 7: 1-20

Feigenbaum H, Henry WL, Pearlman AS, Popp RL (1982)
Introduction: Echocardiographic evaluation of ventricular function: An overview.
Am J. Cardiol. 49: 1311-1318

Gore J C, Leemans S (1977)
Echo structure in medical ultrasonic pulse echo scanning.
Physics in Med. and Biol. 22: 431-443

Joynt L, Popp RL (1982)
The concept of three dimensional resolution in echocardiagraphic imaging.
Ultrasound in Med. and Biol. 8: 237-247

Wilkinson R.W. (1981)
Principles of real-time two dimensional B-scan ultrasonic imaging.
J. Medical Engineering and Technology. 5: 21-29

CHAPTER 4

A THEORETICAL BASIS FOR A LEFT VENTRICULAR THREE DIMENSIONAL RECONSTRUCTION TECHNIQUE

4.1 Introduction

Echocardiographic 3-D images have been obtained by a number of different methods. Dekker et al (1974) proposed a short axis system for imaging the heart to allow for a 3-D reconstruction. However, no attempt at reconstruction or volume estimation was reported. In 1976 Smith reported a technique for visualizing 3-D images based on viewing sequential parallel tomographic sections which had been recorded as negatives and placed in a mechanical holder in a position corresponding to their location in the patient. The technique allowed a 3-D view of an organ. Matsumato et al (1977) developed a computerised technique using recorded 2-D echograms in parallel planes along the long axis of the heart to obtain a 3-D echocardiographic display. Two cases were described initally, a healthy normal 34 year old man and a 6 year old girl with an atrial septal defect of the ostium secundum type. No quantitation was reported.

Subsequently these two cases with a further subject, a 22 year old women with an atrial septal defect, were presented in a quantitative study of volume estimates of cardiac structures (Matsumato, Inoue, Taumra et al, 1981). The investigators state that the limitation of their study was in the recording of 2-D echocardiograms in parallel planes. Similarly to Smith (1976), Greenleaf (1982) has described a method of 3-D reconstruction ultrasound which uses "stacking" of tomograms by a computer algorithm for subsequent perspective or sectional display.

Long axis reconstruction of the left ventricle has also been reported using multiple 2-D sector scan echocardiograms of apical long axis views. A system for a computer based reconstruction and analysis has been published with the results of one patient study (Eiho, Kuwahara, Asada et al, 1981). About the same time another group reported what they termed the rotation method which recorded evenly spaced rotational apical views with the ultrasound transducer placed at the apex of the heart. They reported volumetric data and ejection fraction for two patients (Ghosh, Nanda, Maurer, 1982). The rational for the method being the quality and ease of imaging the cardiac boundaries without interference of ribs or lungs.

The most extensively applied approaches to reconstruction involve the use of short axis views matched to one or more orthogonal long axis views. A detailed framework has been presented for reconstruction performed by alignment of five cross sections close to perpendicular to the long axis where the transducer has been moved in a plane nearly parallel to the long axis (Geiser, Lupkiewicz, Christie et al, 1980). The authors report that the choice to proceed in this way was arbitrary. It was based on their observation that cardiac boundries were best seen in parasternal short and long axis tomograms. A feasibility study in which four patients are reported indicates the need for further developmental and experimental studies (Geiser, Ariet, Conetta et al, 1982). A number of other quantitative investigations which used short axis views have been reported involving both patient or in vitro studies (Skorton, Chandra, Nikravesh et al, 1983; Nixon, Saffer, Lipscomb et al, 1983; Sawada, Fujii, Kato et al, 1983). A variation on the method of matching short axis views to a long axis for reconstruction is the approach of reconstruction from arbitrarily collected tomographic views of the left ventricle. As a rule more short axis views are recorded than long axis views and the complexity of the reconstruction is increased (Moritz, Pearlman, McCabe et al, 1983; Stickels, Wann, 1984).

The most recent innovation in 3-D reconstruction of the left ventricle has been the use of a miniature compound transducer which has two phased arrays mounted on the tip of a gastroscope (Tamura, Nakaro, Matsumoto et al, 1985). This enables the collection of high resolution echocardiograms but at the expense of pain to the patient because of the transesophageal approach.

Computerised techniques for implementation in catheterisation laboratories have been proposed. These techniques for left ventricular 3-D reconstruction use either single plane (30^{o} RAO) or biplane views (30^{o} RAO and 60^{o} LAO) (Zanuttini, Nicolosi, Marino et al, 1981; Yettram, Vinson, Gibson, 1982; Sjolander, Matts, Jang, 1982). They have been developed for the analysis of stress levels generated by the myocardium and assessment of their significance for cardiac performance. A summary of the reconstruction studies using x-rays to generate models of the heart both of humans and animals is provided by Yettram and Vinson (1979) and Pao (1980). The most recent development in the application of x-rays is the dynamic spatial reconstructor, a high speed imaging x-rays scanner based on computer tomographic principles. A preliminary report using this device has presented information from three patients (Sinak, Hoffman, Schwartz et al, 1985). The capital cost of this equipment and the computing facilities required are orders of magnitude higher than for the ultrasonic procedure described in this thesis.

Ultrasound tomography applied to imaging of the heart has seen the emergence of standard tomographic views in the first instance for qualitative investigation of cardiac function. The methods of quantitation for estimation of ventricular volumes or description of regional wall abnormalities have been developed around these views and the imposed symmetrical geometrical models. In the development and implementation of the various published 3-D left ventricular reconstruction techniques the tomographic slices used are abitrary. They may have been based on observations such as myocardial boundary definition or view obtained with the least interference from the presence of obstructions to the ultrasound beam such as ribs or lung. The question that needs to be addressed is; of views that can be obtained using 2-D echocardiography which will optimise the information most relevant to the 3-D reconstruction and the subsequent quantitative study of ventricular function and performance.

4.2 Problem Definition

To address the question above it is necessary to divide the problem into a number of individual questions which can be mathematically formulated and solved analytically or empirically. A number of matters need to be resolved before an analysis can be developed. They are, what type of geometric model should be selected to best represent the left ventricle and which parameters should be selected for optimisation in the context of quantitative studies of ventricular function and performance.

The objective of a complete and thorough 2-D echocardiographic left ventricular examination is to view as much of the ventricular cavity and myocardial surface that is practically possible. With the tomographic imaging mode of ultrasound this translates in a maximisation of cavity area and perimeter of myocardium that is imaged. These conditions apply for both qualitative and quantitative assessments. Qualitative assessments because they provide the operator with maximal visual information on which to base the perception of ventricular cavity volume and myocardial dynamics. Quantitative assessment to enable the measurement of ventricular function and performance. Furthermore, in the context of 3-D left ventricular reconstruction optimised data acquisition is important for the development of the computerised algorithm and ultimate "quality" of the reconstruction.

The most accepted and reported geometric model of the left ventricle is that of a spheriod either prolate, spherical or an ellipsoid of rotation (Yettram, Vinson, 1979; Wyatt, Heng, Meerbaum et al, 1980). Although there are weaknesses in the model, optimisation of data collection in the context described above is still applicable for minor deviations from spheroid geometry. Consideration is therefore given to the sectioning, of a defined class of spheroids, complementary to tomographic views of the left ventricle. Three modes of sectioning will be considered which correspond to echographic views used in 3-D reconstruction of the left ventricle. These are echocardiographic views which are parallel to the ventricular long axis, the parasternal short axis views perpendicular to the long axis and the apical views obtained by transducer rotation at the ventricular apex along the line of the long axis. For a spheroid these views translate into parallel slices along the major axis, along the minor axis and axial slices at different degrees of rotation along the major axis respectively.

4.3 Analysis

4.3.1 Parallel slices

Approximate the left ventricle by the spheroid

$$\frac{x^2}{a^2} + \frac{y^2+z^2}{b^2} = 1 \qquad (1)$$

which represents an ellipsoid of rotation. Then in terms of section area, determine the most efficient method, of slicing the ellipsoid. For a given slice thickness compare the area generated by slicing parallel to the y-z plane with the area generated by slicing parallel to the x-y plane (Fig. 4.1).

Without loss of generality assume, $a,b>0$ and define $k=\frac{a}{b}$, thus $k>0$.

If $k=1$ then $a=b$ and we have a sphere.

If $0<k<1$ then we have an oblate ellipsoid.

If $k>1$ then we have a prolate ellipsoid.

Figure 4.1 An ellipsoid of rotation with arbitrary major to minor axis ratio, k, sliced parallel to the minor and major axes generating circular and elliptical slices respectively.

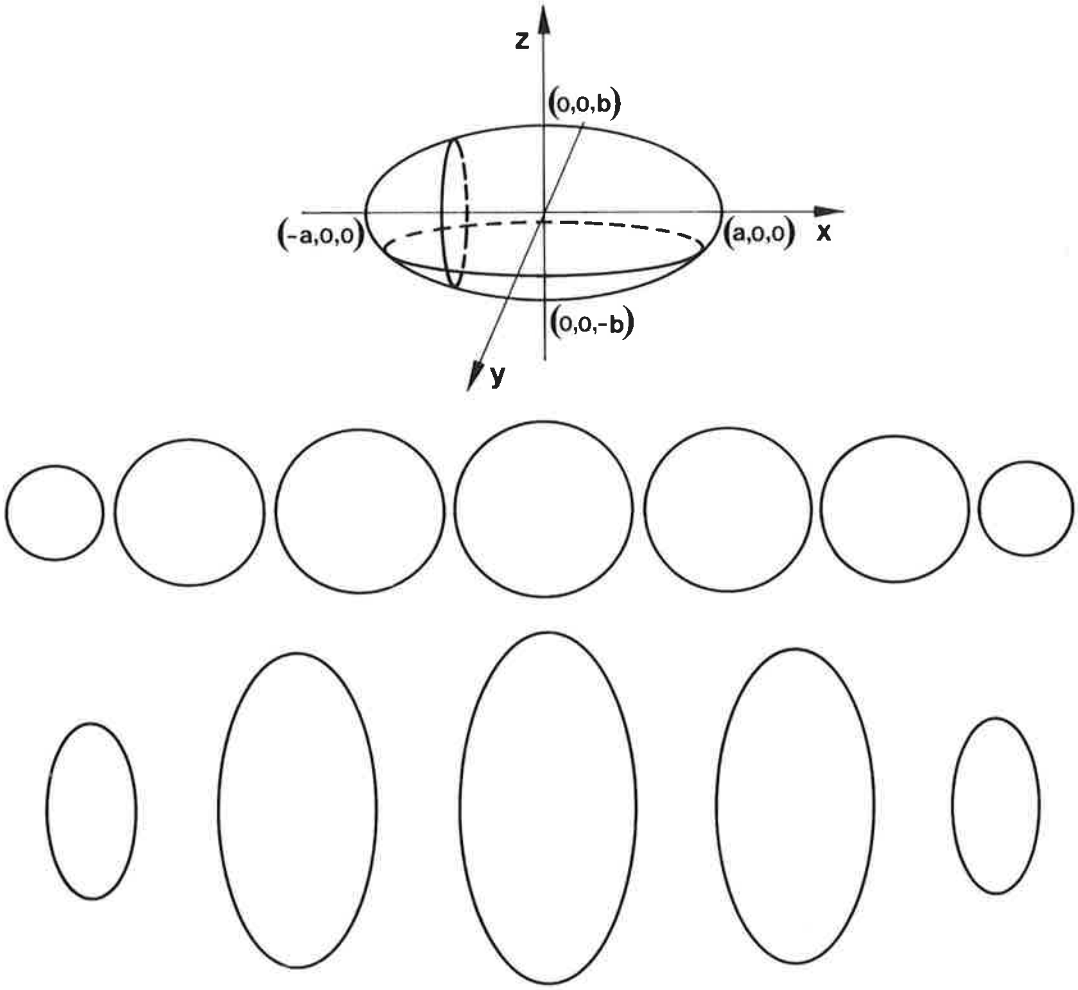
z
(0,0,b)
(-a,0,0)
(a,0,0)
x
(0,0,-b)
y

The analysis for an oblate ellipsoid is not discussed because such geometry is generally accepted does not occur for the left ventricle.

When slicing in the y-z plane we get a series of circular sections, say n of them. We note that the ellipsoid is of width 2a and begin the slicing at the left hand end (-a, 0,0) (Fig. 4.1).

If the slice thickness is t, consider only $t \geqslant 0$. The number of circular slices is then $n < 2a \leqslant n+1$. These slices are generated by putting x in equation (1) equal to a constant (r).

Thus we have n slices produced at $x=-a+t$, $-a+2t, \ldots\ldots, -a+nt$ and the plane $x=r$ intersects the ellipsoid when

$$\frac{r^2}{a^2} + \frac{y^2 + z^2}{b^2} = 1$$

rearranging $$\frac{y^2 + z^2}{b^2} = \frac{-r^2 + a^2}{a^2}$$

$$y^2+z^2 = \frac{b^2}{a^2} (a^2 - r^2) \qquad (2)$$

Equation (2) defines a circle of radius $\sqrt{\frac{b^2}{a^2} (a^2 - r^2)}$

Thus the area of the circle is $\pi \frac{b^2}{a^2} (a^2 - r^2)$

So for slices at x= $-a+t$, $-a+2t$, ... , $-a+nt$

and counting each face of the slice twice

$$\text{Total area} = 2 \sum_{i=1}^{n} \frac{\pi b^2}{a^2} (a^2-(-a+it)^2)$$

$$= 2 \sum_{i=1}^{n} \frac{\pi b^2}{a^2} (a^2-i^2t^2+2ait-a^2)$$

$$= 2 \frac{\pi b^2}{a^2} \sum_{i=1}^{n} (2ait-i^2t^2)$$

$$= \frac{2\pi b^2}{a^2}\left(2at\sum_{i=1}^{n} i - t^2\sum_{i=1}^{n} i^2\right)$$

$$= \frac{2\pi b^2}{a^2}\left(2at\frac{n(n+1)}{2} - t^2\frac{n(n+1)(2n+1)}{6}\right)$$

$$= \frac{\pi b^2 tn(n+1)(6a-t(2n+1))}{3a^2}$$

Hence $f(t)$ = Total area of circular sections

$$= \frac{\pi b^2 tn(n+1)(6a-t(2n+1)}{3a^2}$$

When slicing parallel to the x-y plane we get a series of elliptic sections, say m of them. Note that the ellipsoid is of height 2b and begin the slicing at the bottom (0,0,-b) (Fig. 4.1).

Again, if the slice thickness is t, such that $t \geqslant 0$, then the number of elliptic sections is $m < \frac{2b}{t} \leqslant m+1$.

These slices are generated by putting z in equation (1) equal to a constant (s).

Thus we have m slices produced at $z = -b+t,\ -b+2t,\ \ldots\ldots\ldots,\ -b+mt$ and the plane $z=s$ intersects the ellipsoid

when $$\frac{x^2}{a^2} + \frac{y^2+s^2}{b^2} = 1$$

rearranging $$\frac{x^2}{a^2} + \frac{y^2}{b^2} = \frac{b^2-s^2}{b^2}$$

$$\frac{x^2}{a^2\frac{(b^2-s^2)}{b^2}} + \frac{y^2}{(b^2-s^2)} = 1 \qquad (3)$$

Equation (3) defines an ellipse with semi axis $\sqrt{\frac{a^2(b^2-s^2)}{b^2}}$ and $\sqrt{(b^2-s^2)}$.

Thus the area of the ellipse is $\frac{\pi a}{b}(b^2-s^2)$.

So for slices at $z= -b+t,\ -b+2t,\ \ldots\ldots\ldots,\ -b+mt$ and counting each face of the slice twice.

$$\text{Total area} = 2\sum_{i=1}^{m} \frac{\pi a}{b}(b^2-(-b+it)^2)$$

$$= 2\frac{\pi a}{b}\sum_{i=1}^{m}(b^2 - i^2t^2 + 2itb - b^2)$$

$$= 2\frac{\pi a}{b}\sum_{i=1}^{m}(2bit - i^2t^2)$$

$$= 2\frac{\pi a}{b}\left(2bt\sum_{i=1}^{m} i - t^2\sum_{i=1}^{m} i^2\right)$$

$$= 2\frac{\pi a}{b}\left(2bt\frac{m(m+1)}{2} - t^2\frac{m(m+1)(2m+1)}{6}\right)$$

$$= \frac{\pi a}{b}tm(m+1)(6b - t(2m+1))$$

Hence $\quad g(t) =$ Total area of elliptic sections

$$= \frac{\pi a}{b}tm(m+1)(6b - t(2m+1))$$

By the definition of the problem f(t) and g(t) are continuous though n and m, the number of sections are "discontinuous" as they jump from one integer to the next depending on the value of thickness t.

Therefore, to this point of the analysis given an ellipsoid of revolution where major and minor axes a and $b>0$, with $k=\frac{a}{b}$, and slice thickness $t\geqslant 0$ we wish to compare $f(t)$, the area of n circular sections, with $g(t)$, the area of m elliptical sections. That is, given $a,b>0$ where $k=\frac{a}{b}$ and $t\geqslant 0$.

compare $$f(t) = \frac{\pi b^2}{3a^2} tn(n+1)(6a-t(2n+1))$$

with $$g(t) = \frac{\pi a}{3b} tm(m+1)(6b-t(2m+1))$$

where $$n<\frac{2a}{t} \leqslant n+1 \text{ and}$$

$$m<\frac{2b}{t} \leqslant m+1.$$

I intend to show that for $t>0$

$k\geqslant 2$, $f(t) \geqslant g(t)$ if $t < 2a$

$k=1$, $f(t) = g(t)$

Case $k=1$, show $f(t) = g(t)$

$$k = \frac{a}{b} \text{ so}$$

if $k=1$, $a=b$ thus the ellipsoid is a sphere and $n=m$

$$f(t) = \frac{\pi t}{3} n(n+1)(6a-t(2n+1)) = g(t)$$

$$f(t) = g(t)$$

For a sphere slicing parallel to all planes is the same because of symmetry.

Case k=2, show $f(t) \geqslant g(t)$

$$k=\frac{a}{b}\ ,\quad n<\frac{2a}{t}\leqslant n+1 \text{ and } m<\frac{2b}{t}\leqslant m+1$$

if k=2, a=2b

then $$m<\frac{a}{t}\leqslant m+1$$

or $$2m<\frac{2a}{t}\leqslant 2m+2$$

but $$n<\frac{2a}{t} \text{ so } n<2m+2$$

and $$\frac{2a}{t}<n+1 \text{ so } 2m<n+1$$

thus $$2m-1<n<2m+2$$

Now n and m are integers so either n=2m or n=2m+1.

For n=2m show $f(t) \geqslant g(t)$

$$\frac{\pi b^2}{3a^2}tn(n+1)(6a-t(2n+1))\geqslant\frac{\pi a}{3b}tm(m+1)(6b-t(2m+1))$$

substitute n=2m and a=2b,

the above reduces to $3t(2m+1) \geqslant 12b$

that is $3t(n+1) \geqslant 6a$

$$n+1 \geqslant \frac{2a}{t}$$

This is true by definition of n.

For n=2m+1 show $f(t) \geqslant g(t)$

$$\frac{\pi b^2}{3a^2} tn(n+1)(6a-t(2n+1)) \geqslant \frac{\pi a}{3b} tm(m+1)(6b-t(2m+1)$$

substitute n=2m+1 and a=2b,

the above reduces to $\quad 12b \geqslant 3t(2m+1)$

that is $\quad 6a \geqslant 3tn$

$$\frac{2a}{t} \geqslant n$$

This is true be definition of n.

Similarly for k=p where p=2,3,4 ... P

4.3.2 Parallel versus axially rotated slices.

Approximate the left ventricle by the spheroid which represents an ellipsoid of rotation.

$$\frac{x^2}{a^2} + \frac{y^2+z^2}{b^2} = 1$$

Determine the most efficient method, in terms of section area, of slicing the ellipsoid. The two methods are slicing parallel to the y-z plane and slicing with planes containing the x-axis at equal angles of axial rotation - axial slices (Fig. 4.2).

Figure 4.2 An ellipsoid of rotation with arbitrary major to minor axis ratio, k, sliced parallel to the minor axis and through the major axis generating circular and elliptical slices respectively.

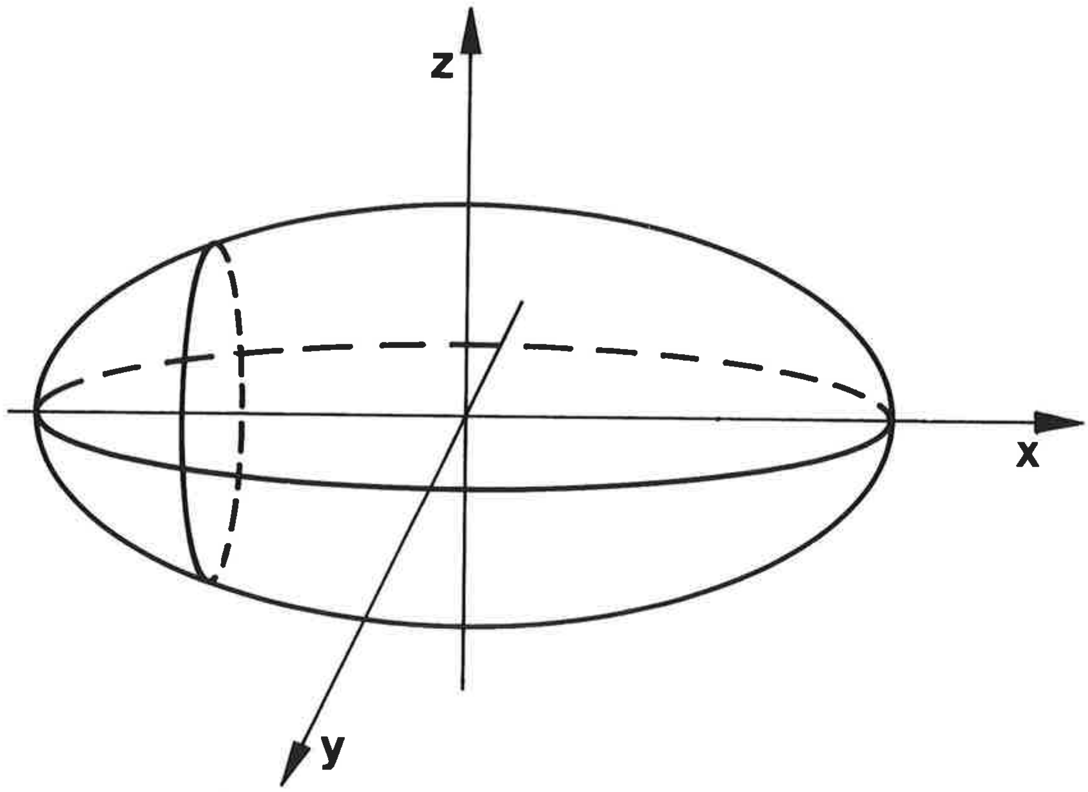
z
x
y

As before, without loss of generality $a,b>0$ and define $k=\frac{a}{b}$.

From the previous analysis slices parallel to the y-z plane produce a series of circular sections where

$$f(t) = \text{Total area of circular sections}$$

$$= \frac{\pi b^2 tn(n+1)(6a-t(2n+1))}{3a^2}$$

where the number of slices are $n<\frac{2a}{t}\leq n+1$ and t is the slice thickness.

For axial slices let n' equal the number of slices and the angle between slices is $\frac{4\pi}{n'}$. Now as the spherioid is an ellipsoid of rotation about the x-axis each axial slice will have the same area, being that of the ellipse

$$\frac{x^2}{a^2} + \frac{y^2}{b^2} = 1$$

where Area $=\pi ab$

Thus, total Area $=n'\pi ab$

but each section has two faces

thus Area $=2\pi abn'$.

In determining the most efficient method of sectioning we are only interested in comparing the number of slices used in each method. Now given a number of slices parallel to the y-z plane, say n, there is a range of slice thickness t that generate that number of slices. Hence there is a range of total slice area associated with a given number of slices. However, we only need consider the maximum area attained in the range.

Given n slices in the y-z plane, slice thickness t has the range

$$n < \frac{2a}{t} \leqslant n+1$$

that is $$t < \frac{2a}{n} \text{ and } t \geqslant \frac{2a}{n+1}$$

so $$\frac{2a}{n+1} \leqslant t < \frac{2a}{n}$$

Now f(t) is strictly decreasing hence it is a maximum when $t = \frac{2a}{n+1}$

$$\begin{aligned} \text{Area} &= \text{Maximum } f(t) \text{ for a given } n \\ &= f\left(\frac{2a}{(n+1)}\right) \end{aligned}$$

$$= \frac{\pi b^2}{3a^2} \frac{2a}{(n+1)} n(n+1)(6a- \frac{2a}{(n+1)} (2n+1))$$

$$= \frac{2\pi b^2 n}{3a} 2a(3-\frac{(2n+1)}{n+1}$$

$$= \frac{4}{3} \pi b^2 \frac{n(3n+3-2n-1)}{n+1}$$

$$= \frac{4}{3} \pi b^2 \frac{n(n+2)}{(n+1)}$$

Hence maximum area for slices parallel to the y-z plane is

$$= \frac{4}{3} \pi b^2 n\frac{(n+2)}{n+1}$$

Now, find the minimum number of slices n, that will generate a larger area than that generated by a given number of slices n'. That is, find the minimum number of slices parallel to the y-z plane that will generate a larger area than that generated by a given number of axial slices.

Find the minimum integer $n \geqslant 1$ such that

$$\frac{4\pi b^2}{3} \frac{n(n+2)}{(n+1)} > 2\pi abn'$$

for a given integer $n' > 1$.

$$\frac{4\pi b^2}{3} n\frac{(n+2)}{(n+1)} > 2\pi abn'$$

$$4\pi b^2 n(n+2) > 6\pi ab(n+1)n'$$

$$2b^2 n(n+2) > 3a(n+1)n'$$

$$2n^2 + 4n > \frac{3a}{b}(n+1)n'$$

as $k = \frac{a}{b}$ then

$$2n^2 + 4n > 3kn'(n+1)$$

$$2n^2 + 4n - 3kn'(n+1) > 0$$

$$2n^2 + 4n - 3kn'n - 3kn' > 0$$

$$2n^2 + (4-3kn')n - 3kn' > 0 \qquad (4)$$

This is an integer relationship so to solve it consider the analogus real equation

$h(x) = 2x^2+(4-3kn')x-3kn'$

Now $h(x)$ is a parabola with the solution to $h(x) = 0$ being

$$x = \frac{3kn'-4\pm\sqrt{(4-3kn')^2-4.2(-3kn')}}{4}$$

$$= \frac{3}{4}kn'-1\pm\frac{1}{4}\sqrt{16+9k^2(n')^2}$$

put $\quad x_1 = \frac{3}{4}kn'-1+\frac{1}{4}\sqrt{16+9k^2(n')^2}$

and $\quad x_2 = \frac{3}{4}kn'-1-\frac{1}{4}\sqrt{16+9k^2(n')^2}$

Now int (x) = the integer part of x

Consider $n = \text{int}(x_1+1)$ as a solution to equation (4) so that $n>1$

Therefore, given $n' \geq 1$ the mimimum $n \geq 1$ for

$$\frac{4\pi b^2}{3} \frac{n(n+2)}{(n+1)} > 2\pi abn'$$

is the positive solution of the quadratic in n

$$n = \text{int}\left(\frac{3kn'}{4} + \frac{1}{4}\sqrt{16+9k^2(n')^2}\right).$$

4.4 Discussion

The three modes of sectioning that have been considered are parallel to the long axis, short axis and axial slices at different degrees of rotation to the long axis. The mathematical analysis has considered ellipsoids of rotation with varying major to minor axis ratios (k) greater than one. That is spherical prolate ellipsoids. Consideration of the results of the analysis show that for the class of spheroids where $k>1$, rotational axial slices provide a larger cavity area for analysis than parallel short axis slices per slice (Fig. 4.3). Furthermore, if $k>2$, slices parallel to the short axis, of a given thickness,

Figure 4.3 A plot of the number of parallel minor axis slices of an ellipsoid of rotation with major to minor axis ratio, k, required to generate equal area to slices through the major axis.

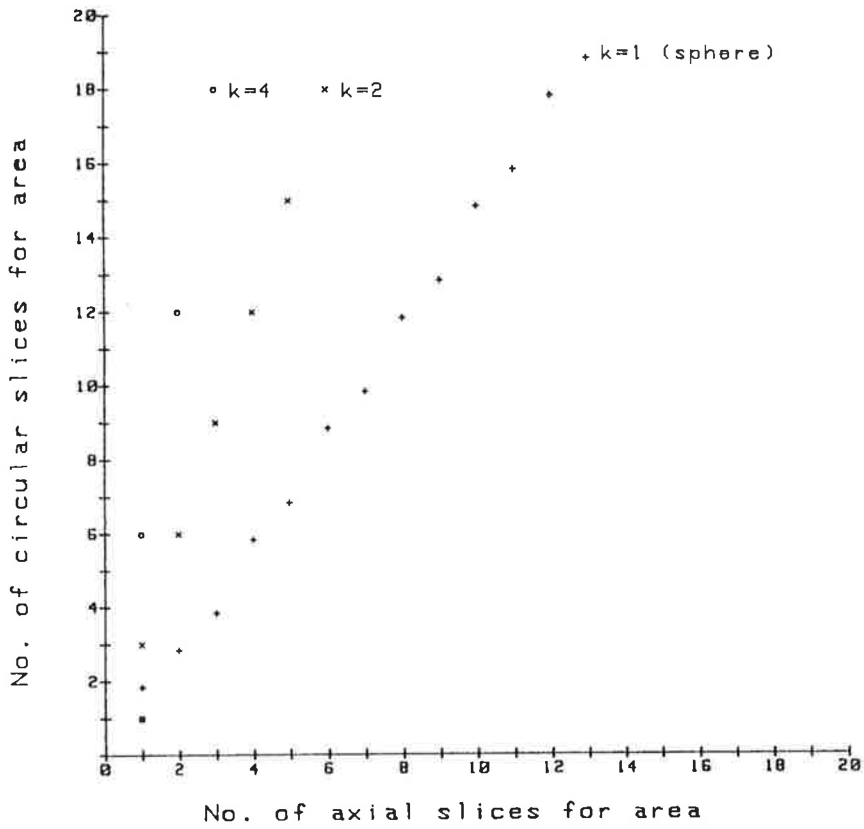

k=1 (sphere)
k=4
k=2
No. of circular slices for area
No. of axial slices for area
0
2
4
6
8
10
12
14
16
18
20

provide a greater area of ventricular cavity for analysis than slices parallel to the long axis which are of the same thickness (Fig. 4.4). It is apparent therefore that the most efficient method of slicing in terms of section area for a prolate ellipsoid is by axial slices through the major axis.

The implication for ultrasonic tomography of the left ventricle is that optimal views in terms of maximum spatial information per view and hence maximum information from multiple views is achieved by recording apical long axis views. The multiple views can be obtained by transducer rotation about the ventricle long axis. The obvious condition for this to be true is that sectioning of the ventricle is of finite thickness. This of course is in fact the case with ultrasound tomography.

This analysis then provides the theoretical basis for a 3-D left ventricular composite reconstruction method. The method is based on the spatial orientation of multiple 2-D echocardiographic images recorded at the cardiac apex.

Figure 4.4 A plot of the area generated from an ellipsoid of rotation with major to minor axis ratio, k, sliced parallel to the minor and major axes. The difference between the two areas is also plotted.

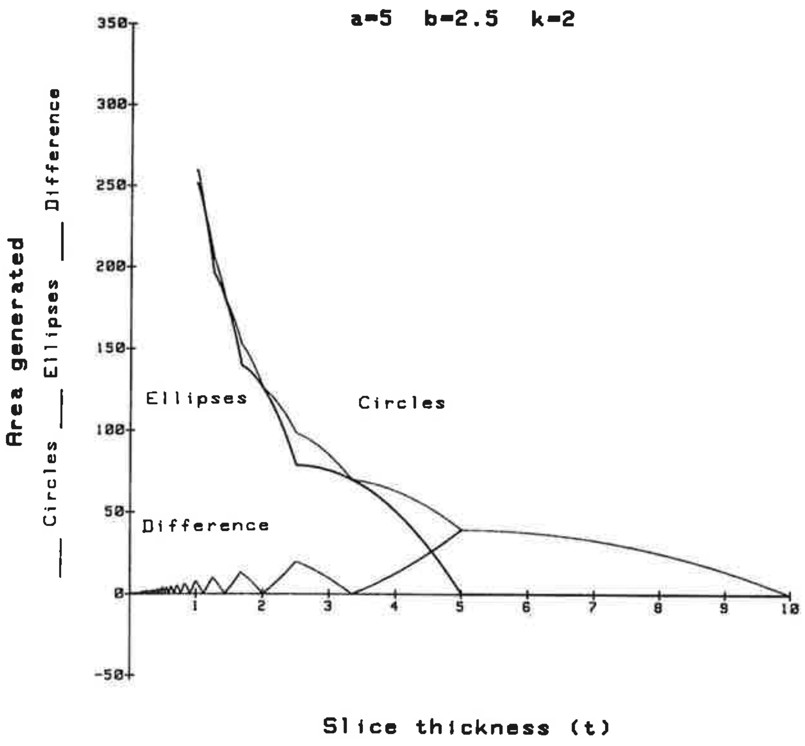

a=5 b=2.5 k=2
350
300
250
200
150
100
50
0
-50
1
2
3
4
5
6
7
8
9
10
Area generated
Circles Ellipses Difference
Ellipses
Circles
Difference
Slice thickness (t)

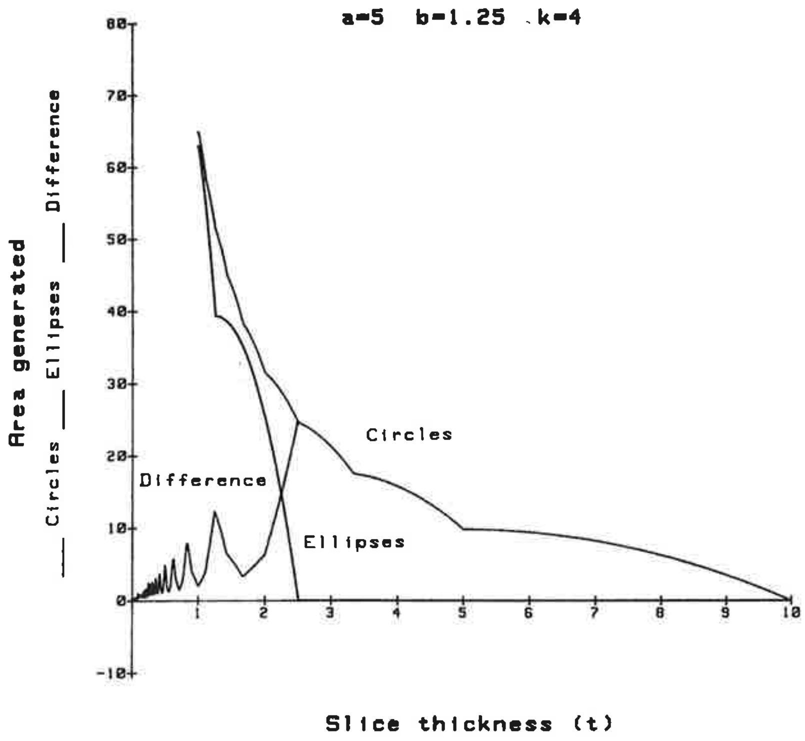

a=5 b=1.25 k=4
80
70
60
50
40
30
20
10
0
-10
1
2
3
4
5
6
7
8
9
10
Area generated
Circles Ellipses Difference
Circles
Difference
Ellipses
Slice thickness (t)

4.5 References

Dekker DL, Pizial RL, Dong E (1974)
A system for ultrasonically imaging the human heart in three dimensions.
Computers and Biomedical Research. 7: 544-553

Eiho S, Kuwahara M, Asada N, Sasayama S, Takahashi M, Kawai C (1981)
Reconstruction of 3-D images of pulsating left ventricle from two dimensional sector scan echocardiograms of apical long axis views.
Computers in Cariodogy IEEE. 19-24

Geiser EA, Ariet M, Conetta DA, Lupkiewicz SM, Christie LG, Conti CR (1982)
Dynamic three dimensional echocardiagraphic reconstruction of the intact human left ventricle: Technique and intial observations in patients.
Am. Heart Journal. 103: 1056-1065

Geiser EA, Lupkiewicz SM, Christie LG, Ariet M, Conetta DA, Conti CR (1980)

A framework for the three dimensional time varying reconstruction of the human left ventricle; Sources of error and estimation of their magnitude.
Computers and Biomedical Research. 13: 225-241

Ghosh A, Nanda NC, Maurer G (1982)
Three dimensional reconstruction of echocardiographic images using the rotation method.
Ultrasound in Med. and Biol. 8: 655-661

Greenleaf JF (1982)
Three dimensional imaging in ultrasound.
J. or Medical Systems. 6: 579-589

Matsumoto M, Inoue M, Tamura S, Tanaka K, Abe H (1981)
Three dimensional echocardiography for spatial visualisation and volume calculation of cardiac structures.
J. of Clinical Ultrasound. 9: 157-165

Matsumoto M, Matsuo H, Kitabatabe A, Inoue M, Hamanaka Y, Tamura S, Tanaka K, AbeH (1977)

Three dimensional echocardiograms and two dimensional echocardiographic images at desired planes by a computerised system.
Ultrasound in Med. and Biol. 3: 163-178

Moritz WE, Pearlman AS, McCabe DH, Medema DK, Ainsworth ME, Boles MS (1983)
An ultrasonic technique for imaging the ventricle in three dimensions and calculating its volume.
IEEE Transaction Biomedical Engineering 30: 482-492

Nixon JV, Saffer SI, Lipscomb K, Blomquist CG (1983)
Three dimensional echoventriculography.
Am. Heart Journal. 106: 435-442

Pao YC(1980)
Geometric modelling of the human left ventricle.
J. Biochemical Engineering. 102: 274-275

Sawada H, Fujii J, Kato K, Onoe M, Kuno Y (1983)
Three dimensional reconstruction of the left ventricle from multiple cross sectional echocardiagrams: Value for measuring left ventricular volume.

Br. Heart Journal. 50: 438-442

Sinak LJ, Hoffman EA, Schwartz, RS, Smith HC, Holmes DR, Bove AA, Robb RA, Harris LD, Ritman EL (1985)
Three dimensional cardiac anatomy and function in heart disease in adults: Initial results with the dynamic spatial reconstructor.
Mayo Clinic Proc. 60: 383-392

Smith RP (1976)
A technique for generating three dimensional images from ultrasonography.
J. or Clinical Ultrasound. 4: 49-51

Sjolander S, Matts E, Jang G C (1982)
A computer model of the left ventricular epicardial surface for quantification of jeopardized myocardium.
Computer Programmes in Biomedicine. 14: 127-132

Skorton DJ, Chandran KB, Nikravesh PE, Pandian NG, Kerber RE (1981)

Three dimensional finite element reconstruction from two dimensional echocardiograms for estimation of myocardial elastic properties.
Computers in cardiology IEEE. 383-386

Stickels KR, Wann LS (1984)
An analysis of three dimensional reconstructive echocardiography.
Ultrasound in Med. and Biol. 10: 575-580

Tamura S, Nakoro S, Matsumoto M, Shimazu T, Fujiwara M, Matsuyama T, Hanrath P (1985)
Three dimensional reconstruction of echocardiograms based on orthogonal sections.
Pattern Recognition. 18: 115-124

Wyatt HL, Heng MK, Meerbaum S, Gueret P, Hesterness J, Dula E, Corday E (1980)
Cross-sectional echocardiography.
II Analysis of mathematic models for quantifying volume of the formalin - fixed left ventricle.
Circulation. 61: 1119-1125

Yettram AL, Vinson CA (1979)
Geometric modelling of the human left ventricle.
J. Biomechanical Engineering. 101: 221-223

Yettram AL, Vinson CA, Gibson DG (1982)
Computer modeling of the human left ventricle.
Transactions of the ASME.
J. Biomechanical Engineering. 104: 148-152

Zanuttini D, Nicolosi GL, Marino P, Burelli C, Grattoni E, Cervesato E, Targa S (1981)
A framework for three dimensional time varying reconstruction of the human left ventricle from cardiac catheterisation and 2D ultrasound techniques.
Frontiers of Engineering in Health Care IEEE 277-280

CHAPTER 5

CARDIAC IMAGES

5.1 Introduction

This section describes the experimental, clinical procedures and algorithms used for the ventricular composite reconstruction evaluation and subsequent application. The reconstruction is used to measure the 3-D geometry of known geometric shapes, postmortem hearts and the left ventricle of patients. A technique of spatially orientating multiple 2-D echocardiographic views of the left ventricle taken by axial rotation of the ultrasonic transducer placed at the apex of the heart will be applied. This technique is preferred to those which utilise various parasternal short axis views of the left ventricle. We have demonstrated that the apical views maximise the area of left ventricular cavity available for qualitative and quantitative analysis per tomographic slice. Furthermore, the number of short axis views required to provide an equivalent total area for assessment as multiple axial apical views increases rapidly and may not be practical to achieve. This ultrasonic technique for the study of 3-D cardiac geometry is preferable to nuclear and x-ray alternatives because of its low cost, absence of known harmful effects to both patient and operator, hence its repeatability and manageability.

5.2 Geometric Shapes

A number of analytic geometries were selected for study to test the spatial reconstruction methodology and the computerised algorithms. Planar drawings of symmetrical geometric shapes, rectangular and prolate ellipses of various arbitrary long axis to minor axis ratio were selected. A cylindrical and five ellipsoidal vessels were reconstructed from the planar views. Dimensions of these shapes were chosen so that they had volumes within the physiological range usually encountered for the human left ventricle. Volume estimates of these vessels were compared to the true volumes calculated from formulae. Volume estimates were made from computer generated transverse minor axis slices with trapezoidal and polar integration scheme, and the application of Pappus' Theorem (Section 5.11)

5.3 In Vitro Studies

In vitro studies were performed on postmortem hearts. A comparison of volume estimated by the 3-D reconstruction technique was made with the absolute volume determined by filling the left ventricle to the mitral and aortic valve with fluid. On dissection the autopsy hearts were thoroughly flushed to remove blood clots that may have remained in the right and left ventricles and atria. The atria were then cut to access the tricuspid and mitral orifices so the left and right ventricles could be firmly packed with formalin soaked surgical gauze. Subsequently, the heart was fixed by immersion in 10 percent neutral buffed formalin at room temperature. After three days the gauze was removed leaving a firm fixed heart which maintained its packed shape.

The left and right ventricles were then filled with a solution of 20% alcohol, which has a temperature invariant ultrasound transmission velocity of 1540m/sec, the assumed ultrasound velocity in normal tissue. The filled hearts were placed in polyethylene plastic bags containing the alcohol solution. The bag was hot-wire sealed after all air was expelled. This procedure provided a postmortem heart suspended in an ultrasonically transparent bladder (Fig 5.1).

The ultrasonic transducer was positioned at the cardiac apex and the necessary tomographic apical views for 3-D reconstruction recorded on video tape. On completion the heart was then removed from the bladder and the volume of the left ventricle measured directly by filling the ventricle to the level of the aortic and mitral valves. After this consecutive hearts were sectioned along the various tomographic planes which corresponded to the recorded apical views and photographed (Fig 5.2).

5.4 In vivo Studies

In vivo studies were performed on normal volunteers and patients referred for cardiac investigation on clinical grounds. A proportion of patients with cardiac pathology underwent biplane ventriculography. Results from the invasive case studies were used as reference values to evaluate the 3-D reconstruction and its description of left ventricular geometry. Within 24 hours of

Figure 5.1 A formalin fixed post mortem heart in an air tight plastic bladder filled with 20% alcohol which is transparent to ultrasound.


50197
F83
0 1 2 3 cms 6 7 8

4 Chamber-View

Figure 5.2 Postmortem hearts cut in the four apical planes used in the composit three dimensional left ventricular reconstruction.

45 Anticlockwise View

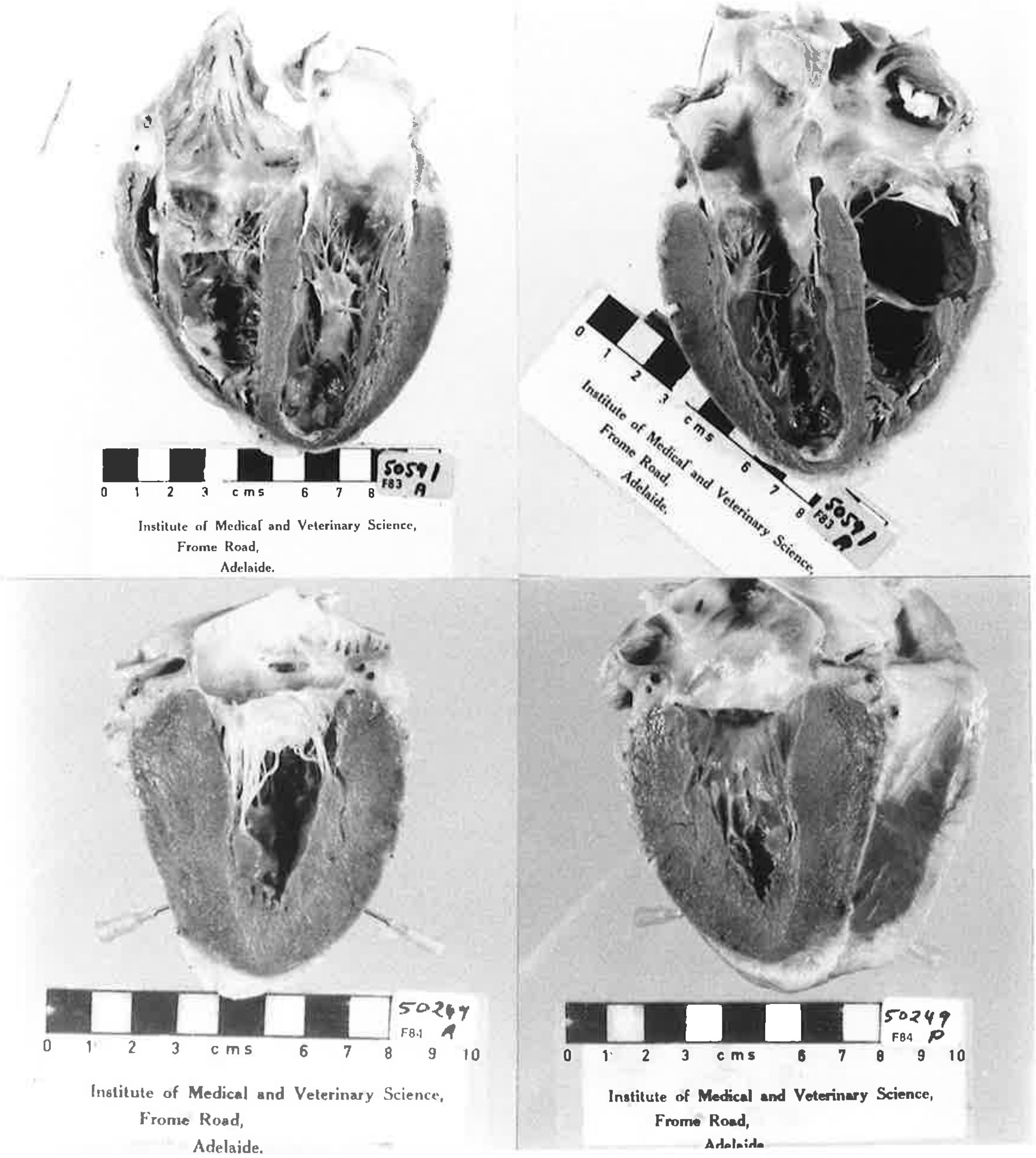
0 1 2 3 cms 6 7 8
50591
F83 A
Institute of Medical and Veterinary Science,
Frome Road,
Adelaide.
0 1 2 3 cms 6 7 8
50591
F83 A
Institute of Medical and Veterinary Science,
Frome Road,
Adelaide.
0 1 2 3 cms 6 7 8 9 10
50247
F84 A
Institute of Medical and Veterinary Science,
Frome Road,
Adelaide.
0 1 2 3 cms 6 7 8 9 10
50249
F84 P
Institute of Medical and Veterinary Science,
Frome Road,

2 Chamber View

Figure 5.2 continued

45 Clockwise View


0 1 2 3 cms 6 7 8
50593
F83
Institute of Medical and Veterinary Science,
Frome Road,
Adelaide.
0 1 2 3 cms 6 7 8
50593
F83
Institute of Medical and Veterinary Science,
Frome Road,
Adelaide.
0 1 2 3 cms 6 7 8 9 10
50623
F83 A
0 1 2 3 cms 6 7 8
50623
F83 P
Institute of Medical and Veterinary Science,

catheterisation 2-D echocardiograms were recorded on video tape. For echocardiography the patient lay recumbent or turned on the left lateral decubitus position.

A method of reconstruction from planar 2-D apical echocardiographic views obtained at 45^{o} axial rotational intervals was used in this study. The analysis presented in the previous Chapter has shown that four axial slices have an area equivalent to 12 short axis slices for a major to minor axis ratio of 2. Geiser et at (1982) used only five cross sections for 3-D reconstruction but suggested that even three of four cross sections may be sufficient for accurate volume estimations in non infarcted hearts. A postmortem study involving casts of canine hearts has demonstrated that short axis slices one centimeter apart are sufficient to provide accurate data for 3-D reconstruction (Janicki, Weber, Cochman et al, 1981). As a general rule that would require about eight to ten short axis views from an average mature heart. Obtaining five cross sections used by Geiser et al (1982) proved difficult at times. Satisfactory windows through the chest wall are not always available and obstruction by ribs and lungs are often unavoidable. Hence cross sections may not be parallel or perpendicular to the long axis and even incomplete.

Another factor of importance to be considered in relation to sufficient data for adequate 3-D reconstruction is image quality. The factors involved in image quality are primarily related to the physical mechanisms of ultrasound tissue interactions. In imaging the interactions of interest are the transmission and reflective properties of tissue which produce velocity changes and time lags in the transmitted and received ultrasound pulses. Ultrasound tomography then reconstructs the spatial distrubution of the ultrasound velocity from measured transmission times of ultrasound pulses that have travelled along different pathways through a cross section of the heart under study. This is the complex field of ultrasonic image instrumentation which has been briefly introduced earlier in this thesis. This study will focus on a discussion of the impact of ultrasonic image resolution in the context 2-D echocardiographic devices which are currently available for use in the cardiac clinic. The significance of resolution on the accuracy of data acquisition and subsequent computations is discussed. The impact on the localisation of boundaries and calculation of various estimates and descriptions of cardiac function will be considered in detail in a later section. Therefore, apart from the consideration of resolution the use of planar 2-D apical echocardiographic views obtained at 45^{o} axial rotation intervals is optimal, as pointed out earlier in consideration of the geometry of the left ventricle and its accessibility for imaging by ultrasound. The latter because of anatomical constraints imposed by the nature of the various tissue, bone and air interactions with ultrasound.

5.5 Anatomical Definition of Apical Views

The ultrasonic transducer is placed at the apex of the heart to record four anatomically defined apical views obtained at 45^{o} axial rotational intervals (Fig 5.3). Anatomical orientation is made with central reference to the apical four chamber view as the standard anatomical planar section.

Figure 5.3 Echocardiographic images of a patient study which demonstrate the four apical views used in the composite three dimensional left ventricular reconstruction.

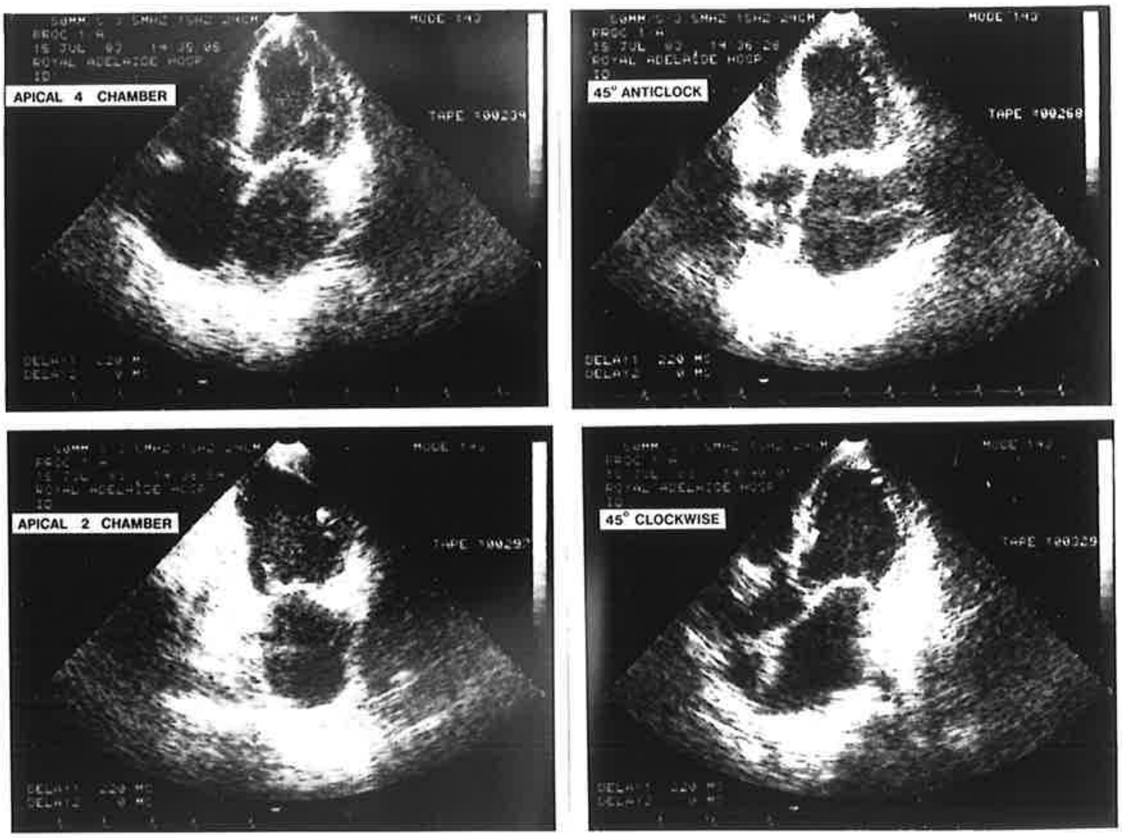
APICAL 4 CHAMBER
45° ANTICLOCK
APICAL 2 CHAMBER
45° CLOCKWISE

a) Four Chamber View

The four chamber view involves positioning the ultrasound sector beam to observe the heart from apex to base along the acute margin of the right ventricle and the obtuse margin of the left ventricle, continuing the plane of section through both atria (Edwards, Tajik, Seward,1981).

b) Two Chamber View

The ultrasound sector plane is positioned perpendicular to the four chamber view with anticlockwise rotation , such that it passes from the left ventricular apex to the left atrium. Both the anterior and posterior mitral leaflets are included in this view with the exclusion of the aortic valve, ventricular septum and right ventricular outflow tract (Edwards, Tajik, Seward, 1981).

c) Intermediate 45^{o} Anticlockwise

The four chamber view is first obtained. The rotation of the transducer through 45^{o} anticlockwise presents the left ventricle and left atrium in a plane parallel to the mitral valve commissure. Consequently only a single (anterior) mitral valve cusp is viewed during part of the cardiac cycle (diastole). The left ventricle may appear "waisted" by (partial) inclusion of both papillary muscles and the margins of right-sided chambers remain visible.

d) Intermediate 45° Clockwise

The four chamber view is again first obtained. Rotation of the transducer through 45° presents essentially a mirror image of the standard apical long axis view (Edwards, Tajik, Seward, 1981, Feigenbaum, 1976). That is, a view passing from the left ventricular apex through the outflow tract (ventricular septum and anterior mitral leaflet) and into the ascending aorta. The left atrium and right ventricular outflow tract (infundibulum), are also included in this planar section.

These four apical views section the ventricle in four complementary planes each separated by approximately 45° of angular rotation about the long axis of the left ventricle. The common long axis is defined as a line joining the most apical endocardial point to the centre of the mitral valve annulus. This left ventricular axis was chosen because it corresponds to that axis generated by centres of gravity of left ventricular cross sectional slices. Janicki et at (1981) have shown that in this case the left ventricular axis begins at the left ventricular apex, runs through the middle of the chamber, and exists at a point which is approximately centred in the mid portion of the anterior cusp of the mitral valve.

5.6 Experimental Procedure.

In the patient studies the patient lay recumbent or turned on to the left lateral decubitus position. The transducer, of the phased array type, was placed at the apex of the heart found by palpation to record four anatomically defined apical views. The transducer placed at the apical pulse is moved laterally if necessary to locate the apex immediately under the transducer. The ultrasound plane is then moved ventrally and dorsally to locate the largest left ventricular cross section which includes the mitral valve (Kantrowitz, Schnittger, Schwarzkopf et al, 1983). Anatomical orientation was made with central reference to the apical four chamber view as the standard anatomical planar section. The 2-D echocardiograms were recorded on video tape (Fig. 5.4). At least 10 cardiac cycles of the necessary apical views for 3-D reconstruction were obtained. The patient was

Figure 5.4 A block diagram of the experimental procedure used in the composite three dimensional left ventricular reconstruction of patients studied.

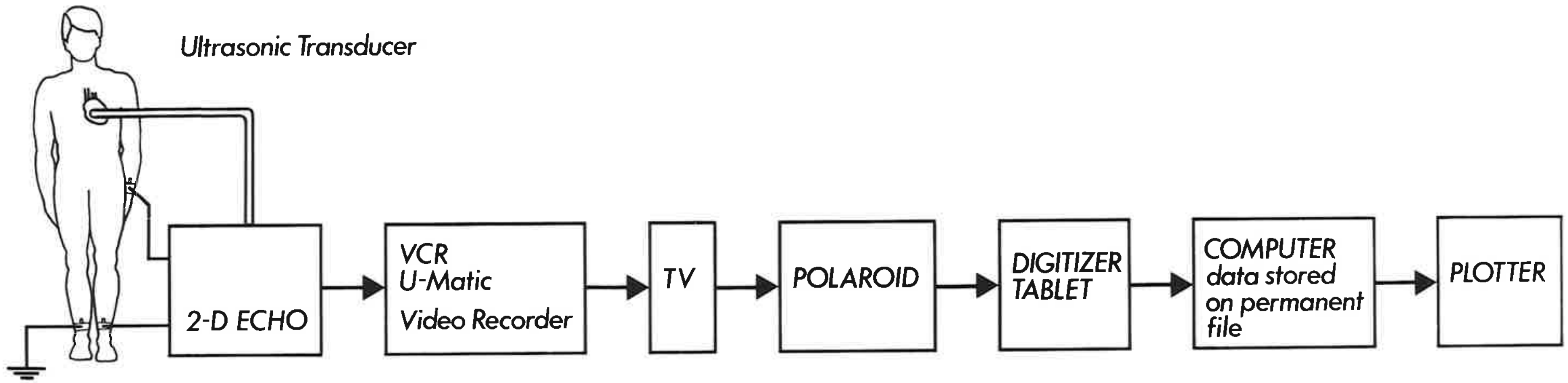

BLOCK DIAGRAM OF 3-D RECONSTRUCTION PROCEDURE dismissed on completion of the ultrasonic examination and video record. This procedure generally took no longer than 30 minutes.

Television viewing of the video record allowed for selection of a target cardiac cycle in each view prior to electrocardiogram gated frames being obtained at end diastole and end systole. It was important that the video recorder had both forward and reverse control together with fast, slow and freeze frame modes. A hard copy of the gated frames was then obtained by a thermal stripchart recorder or in some instances by a polaroid photograph. From the echocardiograms the ventricular endocardial boundaries were delineated with the large trabeculations traced to their base by an experienced echocardiographer. This procedure excludes the papillary muscles from the ventricular volume if they appear in a tomographic view. This resulted in smoothed endocardial outlines which were then digitised. This raw data was stored permanently on computer tape and hence available on demand by the computer. The planar data was spatially transformed to generate a 3-D reconstruction of the left ventricle and plotted in the required projection to view. Facility was also available to generate a continuous video display of projected views (see video tape). Besides the qualitative enhancement of being able to view the left ventricle in three dimensions the reconstruction was used to generate various segments to optimise quantitative analysis. Analysis of ventricular geometry together with its global and regional function was then undertaken.

The same procedures for digitisation, 3-D reconstruction and volume estimation were applied to postmortem hearts and symmetrical geometric figures. The ultrasonic imaging technique for the postmortem hearts was as described for the in vivo studies. However, the transducer in this instance was placed at the apex of the formalin fixed heart through the ultrasonically transparent bladder.

5.7 Image Digitisation

The hard copy of the gated frames which included end diastole and end systole had, as stated earlier, the ventricular endocardial boundaries delineated with the large trabeculation traced to their base. This resulted in smoothed endocardial outlines.

Before digitisation of these outlines could proceed it was necessary to construct the left ventricular major axis which is defined as the line that passes through the centre of the mitral valve and ventricular apex. Not only is this axis used for axial rotation of the ultrasonic transduce during image acquisition but it is now required for realignment of the four complementary planar apical views. This construction for realignment is shown in the figure below (Fig.5.5). The origin for digitisation is set at the apex of the ventricle and the outline traced in an anticlockwise direction back to the origin. This is done using a 9874 Hewlett-Packard digitiser tablet interfaced to a 200 series 9817 Hewlett-Packard scientific computer with a mass storage device. The data is collected sequentially for each view in the following order; the four chamber view (0^{o} view), the intermediate 45^{o} anticlockwise view (45^{o} view), the two chamber view (90^{o} view) and the intermediate clockwise view (-45^{o} view). Furthermore, the major axis is rotated about the origin at the apex so that the mid point of the mitral valve lies on the negative z axis of the x-z Cartesian co-ordinate system. That is all the

Figure 5.5 A schematic diagram of the smoothed left ventricular cavity obtained by drawing the ventricular boundary to the base of the trabeculae together with the axes used for rotation and realignment of the individual views in the composite three dimensional left ventricular reconstruction is shown.

DIASTOLE

A.

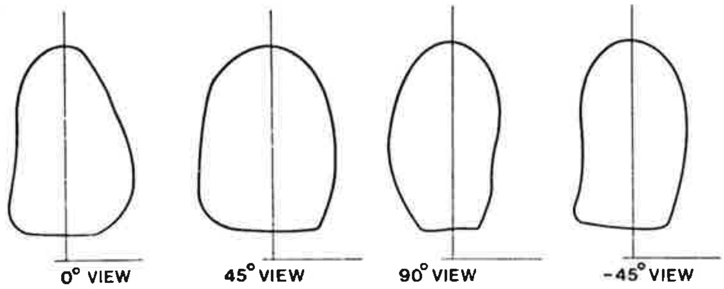

SYSTOLE

A.

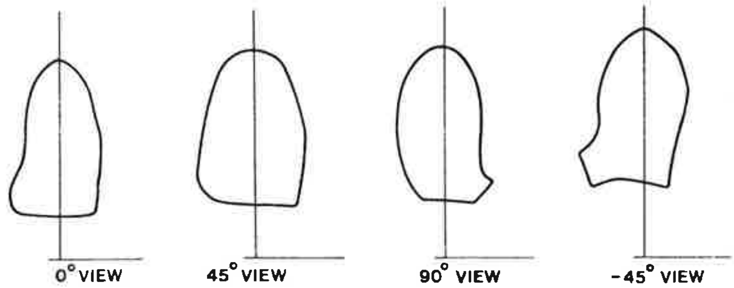

digitised data points (x,z) undergo a two dimensional matrix transformation such that the x co-ordinate of the centre of the mitral valve is zero. The data is therefore distributed in the third and fourth quadants of the Cartesian co-ordinate system, where z co-ordinates are negative ($z<0$) and x co-ordinates are negative then positive in the third and fourth quadrants respectively. Fundamentally there are two ways of specifying the position of these points in space either by absolute or relative co-ordinates. In relative co-ordinates the position of a point is defined by giving the displacement of the point with respect to the previous point. We have chosen to use absolute co-ordinates which are defined with respect to the origin.

5.8 Homogeneous Co-ordinates.

In homogeneous co-ordinates an n dimensional space is represented by n+1 dimensions, that is three dimensional data where the position of a point is given by (x,y,z) is represented by four co-ordinates (hx, hy, hz h) where h is an arbitrary number. The advantage of homogeneous co-ordinates is the ability to accurately represent specified co-ordinate positions in a computer with a limited word length. The largest integer number that can be specified by a full computer word is 2^{n-1} -1. where n is the number of bits in the word. For a 16-bit minicomputer this is 32767. If each of the co-ordinate positions were less than 32767, then h would be equal to 1 and the co-ordinate positions represented directly. If however the co-ordinates are larger than 32767, say, x=60000, then we can let h=½, and the co-ordinates of the point are then defined as (3000, ½y, ½z, ½) all acceptable numbers for the 16-bit computer. Hence a point in three dimensional space (x,y,z) is represented by a four dimensional position vector (x,y,z,1) or (hx,hy,hz,h).

The generalised 4x4 transformation matrix for three dimensional homogeneous co-ordinates is

$$t= \begin{bmatrix} a & b & c & p \\ d & e & f & q \\ h & i & j & r \\ l & m & n & s \end{bmatrix}$$

This 4x4 transformation matrix can be partitioned into four separate sections

$$T = \left[\begin{array}{c|c} 3x3 & \begin{matrix}3\\x\\1\end{matrix} \\ \hline 1x3 & 1x1 \end{array}\right]$$

The 3x3 matrix produces a linear transforamtion in the form of scaling, shearing and rotation. The 1x3 row matrix produces a translation and the 3x1 column matrix produces a perspective transformation. The final single element produces overall scaling.

5.9 Spatial Reconstruciton

Digitised data is stored on computer file with all the planar views on the x-z plane aligned along the ventricular major axis which lies on the z axis. Hence 3-D spatial alignment of the views simply requires rotation about the z axis. In the previous section we noted that the 3x3 component matrix of T produced a combination of scaling, shearing and rotation. However, as stated above we only required a rotation about the z axis. If the determinant of the 3x3 component matrix is 1, then it produces a pure rotation about the origin. In a rotation about the z axis, the z co-ordinates do not change. Thus the transformation matrix T will have zeros in the third row and third column except for unity on the main diagonal

$$T=\begin{bmatrix} \cos\theta & \sin\theta & 0 & 0 \\ -\sin\theta & \cos\theta & 0 & 0 \\ 0 & 0 & 1 & 0 \\ 0 & 0 & 0 & 1 \end{bmatrix}$$

Therefore the particular rotational angles for the spatial reconstruction applied to the stored data were obviously 0° for the reference four chamber view, 45° for the intermediate anticlockwise view, 90° for the two chamber view and -45° for the intermediate clockwise view. In computer memory we now have the left ventricle as a 3-D body but we are not yet in a position to be able to view the structure.

5.10 Display Geometry

Geometric theorems are available for both perspective and affine geometry. In affine geometry parallellism between lines and ratios between parallel lines is a feature of the geometry. These are common to Euclidean geometry which is the basis of standard drawing and sketching techniques. The theorems of affine geometry are identical to those for Euclidean geometry which is the standard method for graphical representation. On the other hand perspective views are often used by artists and architects because they give more realistic pictures. In perspective geometry no two lines are parallel. However, this is seldom used in technical work. We have decided therefore to project the 3-D composite reconstruction of the left ventricle which is stored in computer memeory, by an affine transformation.

The affine transformation selected is that which has a zero value for its determinant hence producing an axonometric projection. An axonometric projection is formed when the centre of the projection is at infinity. To mathematically form the projection, a 4x4 transformation matrix is used to produce the affine transformation on a set of co-ordinate points. The points are then projected onto a plane from a centre of projection at infinity. An axonometric projection from three dimensional space onto a plane z=n can be obtained by the following

$$[x\ y\ z\ 1]\begin{bmatrix}1 & 0 & 0 & 0\\ 0 & 1 & 0 & 0\\ 0 & 0 & 0 & 0\\ 0 & 0 & n & 1\end{bmatrix} = [x\ y\ n\ 1]$$

This transformation represents a translation in the z direction by the amount n given by the transformation

$$T' = \begin{bmatrix}1 & 0 & 0 & 0\\ 0 & 1 & 0 & 0\\ 0 & 0 & 1 & 0\\ 0 & 0 & n & 1\end{bmatrix}$$

followed by a projection from infinity onto the now z=0 plane given by the transformation

$$T'' = \begin{bmatrix}1 & 0 & 0 & 0\\ 0 & 1 & 0 & 0\\ 0 & 0 & 0 & 0\\ 0 & 0 & 0 & 1\end{bmatrix}$$

The concatenation of T' and T'' will give the transformation T=T"T' where

$$T = \begin{bmatrix} 1 & 0 & 0 & 0 \\ 0 & 1 & 0 & 0 \\ 0 & 0 & 0 & 0 \\ 0 & 0 & n & 1 \end{bmatrix}$$

The effect of the translation is to move the z=0 plane to some other position in the object. Projection onto the z=0 plane then corresponds to projection onto the z=n plane.

Combined rotations followed by projection from infinity is the basis for generating axonometric projections. In particular we will consider a rotation about the y-axis followed by a rotation about the x-axis. It is important to note that since rotations are caused by matrix multiplication, three dimensional rotations are non-commutative.

That is the order of multiplication will affect the final result. The transformation matrix for rotation about the y-axis is

$$T_y = \begin{bmatrix} \cos\phi & 0 & -\sin\phi & 0 \\ 0 & 1 & 0 & 0 \\ \sin\phi & 0 & \cos\phi & 0 \\ 0 & 0 & 0 & 0 \end{bmatrix}$$

for rotation about the x-axis is

$$T_x = \begin{bmatrix} 1 & 0 & 0 & 0 \\ 0 & \cos\theta & \sin\theta & 0 \\ 0 & -\sin\theta & \cos\theta & 0 \\ 0 & 0 & 0 & 0 \end{bmatrix}$$

Therefore, concatenation $T=T_yT_x$ is

$$T = \begin{bmatrix} \cos\phi & \sin\phi\sin\theta & -\sin\phi\cos\theta & 0 \\ 0 & \cos\theta & \sin\theta & 0 \\ \sin\phi & -\cos\phi\sin\theta & \cos\phi\cos\theta & 0 \\ 0 & 0 & 0 & 0 \end{bmatrix}$$

By use of this transformation matrix the transformed co-ordinates are

$$[X\ Y\ Z\ H] = [x\ y\ z\ 1]\ T$$

The most common axonometric projection is that in which all the three transformed axes are equally shortened. Such a projection is called isometric.

This requires that the ratio between parallel lines be maintained hence the relationship between the axial unit vectors.

The unit vector on the x-axis, [1 0 0 1] transforms to

$$[X\ Y\ Z\ H] = [\cos\phi\ \ \sin\phi\sin\theta\ \ -\sin\phi\cos\theta\ 1]$$

y-axis, [0 1 0 1] transforms to

$$[X\ Y\ Z\ H] = [0\ \ \cos\theta\ \ \sin\theta\ \ 1]$$

z-axis, [0 0 1 1] transforms to

$$[X\ Y\ Z\ H] = [\sin\phi\ \ -\cos\phi\sin\theta\ \ \cos\phi\cos\theta\ \ 1]$$

For a projection onto the z=0 plane the z co-ordinate is neglected.

Therefore, the magnitude of the transformed x-axis is

$$\sqrt{\cos^2\phi + \sin^2\phi\sin^2\theta}$$

Y-axis is $\sqrt{\cos^2\theta}$

z-axis is

$$\sqrt{\sin^2\phi + \cos^2\phi\cos^2\theta}$$

Now for an isometric projection, all three transformed axes are equally shortened. This requires that both

$$\cos^2\phi + \sin^2\phi\sin^2\theta = \cos^2\theta$$

and

$$\sin^2\phi + \cos^2\phi\sin^2\theta = \cos^2\theta$$

Using the identities $\cos^2\phi = 1-\sin^2\phi$ and

$\cos^2\theta = 1-\sin^2\theta$ it follows that

$$\sin^2\theta = \frac{\sin^2\theta}{1-\sin^2\theta} \quad \text{and}$$

$$\sin^2\theta = \frac{1-2\sin^2\theta}{1-\sin^2\theta}$$

From

$$\frac{\sin^2\theta}{1-\sin^2\theta} = \frac{1-2\sin^2\theta}{1-\sin^2\theta}$$

$$\sin^2\theta = \frac{1}{3}$$

$$\sin\theta = \frac{1}{\sqrt{3}}$$

Therefore $\theta = 35.3^{\circ}$

Then
$$\sin^2\phi = \frac{\sin^2\theta}{1-\sin^2\theta}$$

$$= \frac{1/3}{1-1/3}$$

$$= \frac{1}{2}$$

$$\sin\phi = \frac{1}{\sqrt{2}}$$

Therefore $\phi = 45^{\circ}$

Using the angular valves for an isometric projection the transformation matrix becomes

$$T = \begin{bmatrix} 0.707107 & 0.408248 & -0.577353 & 0 \\ 0 & 0.816597 & 0.577345 & 0 \\ 0.707107 & -0.408248 & 0.577353 & 0 \\ 0 & 0 & 0 & 0 \end{bmatrix}$$

A projection onto a zero plane perpendicular to any of the three orthogonal axes results when the corresponding column in the 4x4 transformation matrix contains all zeros. For example, a projection onto the z=0 plane will result when the following matrix is used

$$T = \begin{bmatrix} 1 & 0 & 0 & 0 \\ 0 & 1 & 0 & 0 \\ 0 & 0 & 0 & 0 \\ 0 & 0 & 0 & 1 \end{bmatrix}$$

x=0 plane

$$T = \begin{bmatrix} 0 & 0 & 0 & 0 \\ 0 & 1 & 0 & 0 \\ 0 & 0 & 1 & 0 \\ 0 & 0 & 0 & 1 \end{bmatrix}$$

y=0 plane

$$T = \begin{bmatrix} 1 & 0 & 0 & 0 \\ 0 & 0 & 0 & 0 \\ 0 & 0 & 1 & 0 \\ 0 & 0 & 0 & 1 \end{bmatrix}$$

5.11 Volume Algorithms

A number of studies have been carried out that determine left ventricular volume using various tomographic views from echocardiography. These studies have compared the echocardiographic estimates to invasive angiographic estimates. There are numerous algorithms that have been used based on both one and two dimensional data from echocardiography (Kronik, Slany, Mosslacher, 1979; Folland, Parisi, Moynihan et al, 1979 Wyatt, Heng, Meerbaum et al, 1980). Algorithms used in angiographic studies have also been extensively analysed (Davila, Sanmarco, 1966). In this thesis I have selected algorithms that are applicable to both angiography and echocardiography so that comparisons minimise unequal algorithm biases.

5.11.1 Ellipsoid Methods

The generally accepted reference method for left ventricular volume estimation is the biplane method proposed by Dodge and Sandler (1960). In this method the left ventricle is assumed to be an ellipsoid whose volume is:

$$V = \frac{4}{3} \pi abc$$

where V= volume; a= one half the length of the major axis; and b,c= one half the lengths of the minor axes. To determine a volume these axes must be estimated. Angiography provides projections of the left ventricle onto flat x-ray film and unless a given axis lies parallel to the x-ray film, it cannot be measured directly but a projection of the axis onto the film is measured. From a projection area and measured maximum axis one can determine the minor axis of an ellipse whose area is equivalent to the projection. The area of an ellipse is:

$$A = \Pi \frac{L}{2} \frac{D}{2}$$

where L and D are the major and minor axes.

rearranging $$D = \frac{4A}{\Pi L}$$

This calculation can be performed for each projection. Now the volume for the ventricle can be estimated by.

$$V = \frac{4}{3} \Pi \frac{L}{2} \frac{D_1}{2} \frac{D_2}{2}$$

$$= \frac{\Pi}{6} L D_1 D_2$$

where L is the longest axis of either projection and D_1, D_2 are the minor axes of each projection. In the case of a single plane only being available D_1 is assumed equal to D_2 so the ventricle becomes an ellipsoid of rotation or a prolate ellipsoid. Now the volume is:

$$V = \frac{4}{3}\,\pi\,\frac{L}{2}\,\frac{D^2}{4}$$

where $$D = \frac{4A}{\pi L}$$

so $$V = \frac{4}{3}\,\pi\,\frac{L}{2}\left(\frac{4A}{\pi L}\right)^2$$

$$= \frac{8A^2}{3\pi L}$$

5.11.2 Trapezoidal and Polar Methods

The use of multiple cross-sectional images (more than two) to reconstruct the left ventricle and estimate its volume provides the scope for the calculation of volume estimates independent of any assumptions about organ shape. The simplest of such methods is the use of parallel sections.

But it is difficult to obtain the parallel sections of the left ventricle by ultrasound directly when obstacles such as bones or air are present as discussed earlier. Instead, an apical view, which provided the maximum areal information of all the tomographic views available is used. Subsequently, the computerised spatial information was processed to provide computer generated parallel sections. Hence two methods were selected for volume estimation from the parallel slices. A trapezoidal integration system using a Cartesion co-ordinate system and a polar integration scheme using Polar co-ordinates.

Segmentation of the ventricle into parallel slices along the major axis, passing through the apex to the centre of the mitral valve, produces irregular octagonal cross-sections of the ventricle if the boundary points of the segments are linearly interpolated. The area of an irregular octagon, with origin of a Cartesian co-ordinate system at the centre of the polygon, can be calculated using the trapezoidal rule. The expression derived below is not restricted to octagons but is generally applicable to any polygon whose centre lies on the z-axis.

The area of the octagon is the sum of the absolute area of the interval areas. A generalised example of an interval is shown in figure 5.6, labelled A_1 and A_2.

Area

$$A_1 = LxW$$

$$= (Y_i - Y_0)\ ((X_{i+1} - X_i)^2 + (Z_{i+1} - Z_i)^2)^{\frac{1}{2}}$$

because $Y_o = 0$

$$A_1 = Y_i((X_{i+1} - X_i)^2 + (Z_{i+1} - Z_i)^2)^{\frac{1}{2}}$$

Area

$$A_2 = \tfrac{1}{2} \times W \times H$$

$$= \tfrac{1}{2}\ ((X_{i+1} - X_i)^2 + (Z_{i+1} - Z_i)^2)^{\frac{1}{2}}(Y_{i+1} - Y_i)$$

Interval area

$$= A_1 + A_2$$

$$= Y_i((X_{i+1} - X_i)^2 + (Z_{i+1} - Z_i)^2)^{\frac{1}{2}}$$

$$+ \tfrac{1}{2}((X_{i+1} - X_i)^2 + (Z_{i+1} - Z_i)^2)^{\frac{1}{2}}(Y_{i+1} - Y_i)$$

$$= ((X_{i+1} - X_i)^2 + (Z_{i+1} - Z_i)^2)^{\frac{1}{2}}(Y_i + \tfrac{1}{2}(Y_{i+1} - Y_i))$$

$$= \tfrac{1}{2}((X_{i+1} - X_i)^2 + (Z_{i+1} - Z)^2)^{\frac{1}{2}}(Y_{i+1} + Y_i)$$

Figure 5.6 Diagram used in the trapezoidal rule formulation.

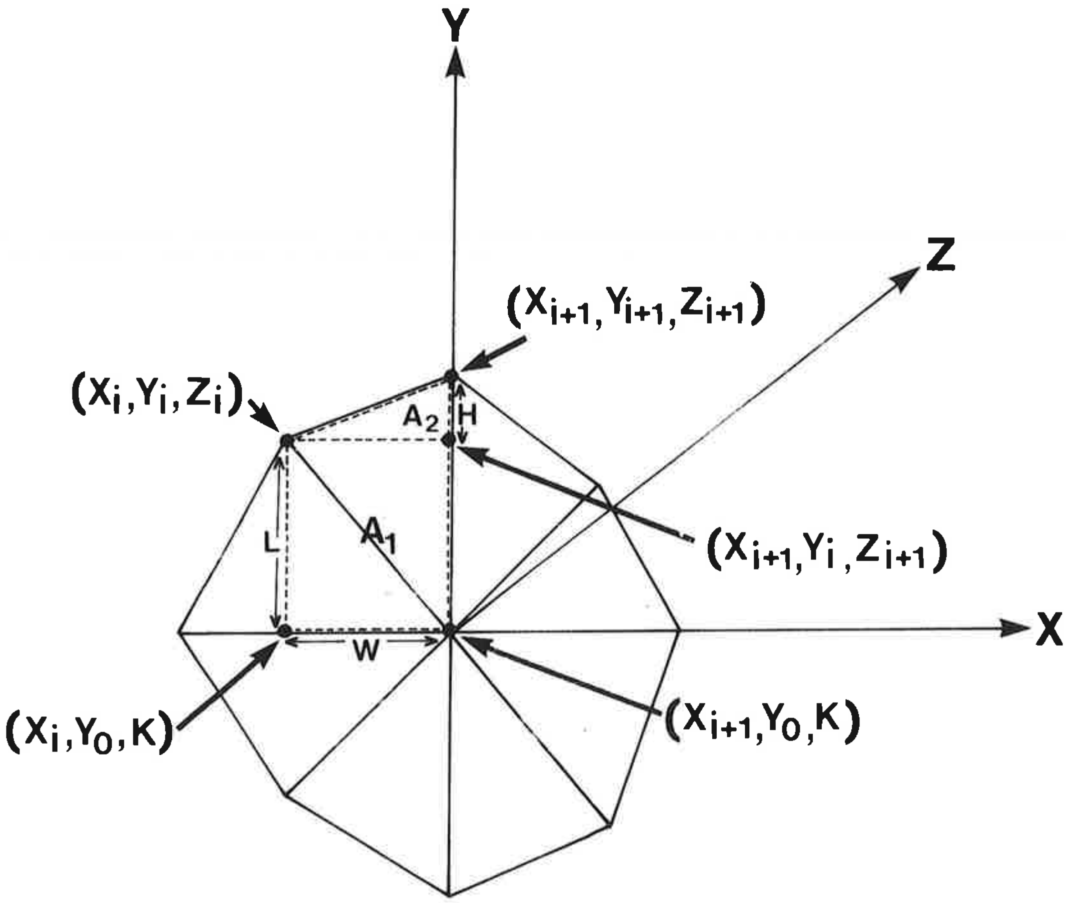

Y
Z
X
(Xi+1, Yi+1, Zi+1)
(Xi, Yi, Zi)
A2
H
A1
L
W
(Xi+1, Yi, Zi+1)
(Xi, Y0, K)
(Xi+1, Y0, K)

Area of the octagon

$$= \sum_{i=1}^{8} |\tfrac{1}{2}((X_{i+1} - X_i)^2 + (Z_{i+1} - Z_i)^2)^{\frac{1}{2}}(Y_{i+1} + Y_i)|$$

Volume of the ventricle

$$= \sum_{j=1}^{J} \sum_{i=1}^{I} |\tfrac{1}{2}((X_{i+1} - X_i)^2 + (Z_{i+1} - Z_i)^2)^{\frac{1}{2}}(Y_{i+1} + Y_i)| \times T_j$$

where

J = the number of slice segments

I = the number of sides of the polygon (sectors),

T = slice thickness.

Alternatively the area of the segment cross-section can be determined by using polar co-ordinates. Take the origin of the polar co-ordinate system as the point through which the major axis of the ventricle passes (Fig. 5.7).

The area of a sector

$$= \tfrac{1}{2} r^2 \Delta\theta$$

Hence the area of the sector

$$OCD = \tfrac{1}{2} r_i^2 \Delta\theta_{i+1}$$

the area of the sector

$$OBA = \tfrac{1}{2} r_{i+1}^2 \Delta\theta_{i+1}$$

Figure 5.7 Diagram used in the polar integration formulation

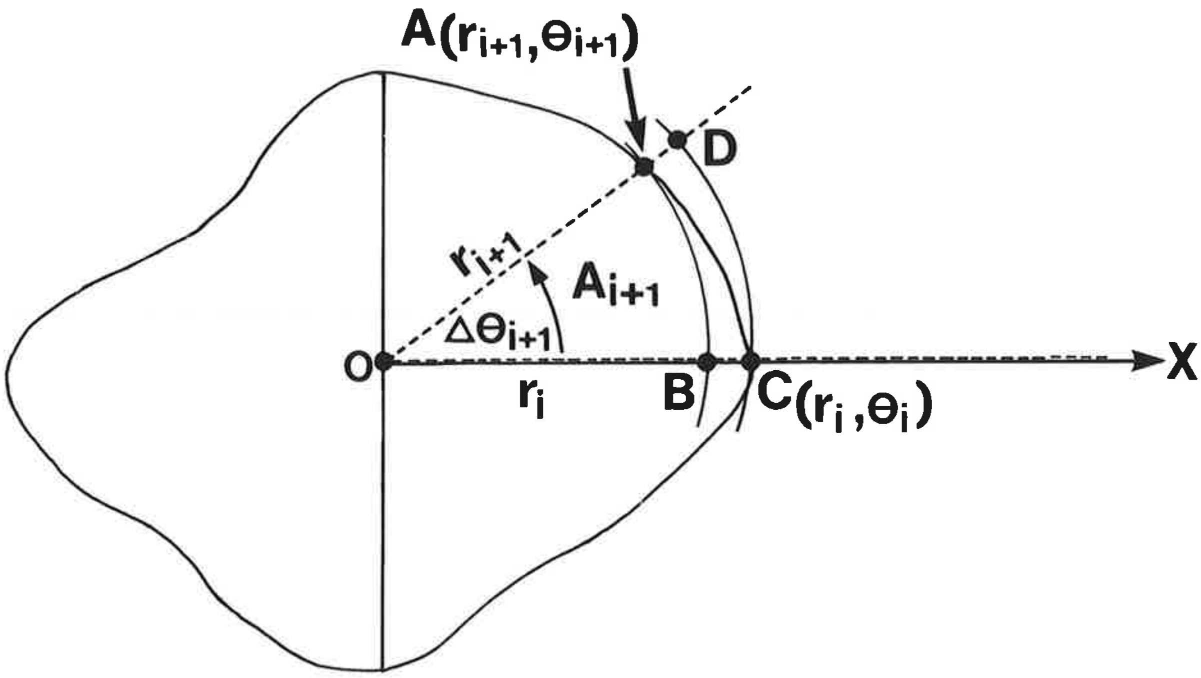

A(r_{i+1},θ_{i+1})
D
r_{i+1}
A_{i+1}
$\Delta\theta_{i+1}$
O
r_i
B
C(r_i,θ_i)
X

Thus $\frac{1}{2}r_{i+1}^2 \, \Delta\theta_{i+1} < A_{i+1} < \frac{1}{2}r_i^2 \, \Delta\theta_{i+1}$

From the intermediate value theorem

$$A_{i+1} = \tfrac{1}{2}(f(\theta))^2 \Delta\theta_{i+1}$$

Hence the area of the whole region of the segment

$$A = \sum_{i=1}^{n} \tfrac{1}{2}(f(\theta))^2 \Delta\theta_i$$

$$= \sum_{i=1}^{n} \tfrac{1}{2}r_i^2 \, \Delta\theta_i$$

For a cross sectional segment of eight sectors

$$A = \frac{1}{2}\left[r_1^2 \frac{\Pi}{4} + r_2^2 \frac{\Pi}{4} + \ldots + r_7^2 \frac{\Pi}{4} + r_8^2 \frac{\Pi}{4}\right]$$

$$= \frac{\Pi}{8}\left[r_1^2 + r_2^2 + \ldots + r_7^2 + r_8^2\right]$$

$$= \frac{\Pi}{8} \sum_{i=1}^{8} r_i^2$$

Volume of the ventricle

$$= \frac{\Pi}{8} \sum_{j=1}^{j=J} \sum_{i=1}^{i=I} r_i^2 \times T_j$$

where J = the number of slice segments,

I = the number of sectors,

T = slice thickness

5.11.3 Pappus' Theorem

There are a variety of methods which exist for estimating the volume of a solid. For reasons which will become apparent in the analysis of regional geometry a technique which employs the Theorem of Pappus will be developed. The theorem states that the volume (V) of a surface of revolution is equal to the product of the area (A) of the region to be rotated, the angle (θ) of rotation about the axis and the centre of mass ($\bar{c}$) of the solid of revolution. That is $V=A\theta\bar{c}$, assuming constant density. In this particular case the surface being generated will be that from the rotation about a vertical axis of a triangular region. One vertex will be on the vertical axis and the other two on the surface.

The co-ordinate system we have selected to develop this approach is the Cartesian system where the z-axis is identified as the vertical axis and the x and y axis form the horizontal plane. For the formulation of the volume estimate let us consider a triangular plane region in the xz plane.

Now our region is of constant density so the centre of mass of a region R is the point $(\bar{x},\bar{z})$ where

$$\bar{x} = \frac{\iint_R x \; dx \; dz}{\iint_R dx \; dz \; dz} \quad \text{and} \quad \bar{z} = \frac{\iint_R z \; dx \; dz}{\iint_R dx \; dz}$$

However, we define the centre of mass of the volume to be that point on the x axis whose x co-ordinate is $\bar{x}$ provided we rotate the region about the z-axis. In other words we can disregard the $\bar{z}$ co-ordinate when rotating about the z-axis.

Consider a triangular region of the form shown in figure 5.8. Setting $x_1 = 0$ in the formula for $\bar{x}$ we obtain $\iint_R x \; dx \; dz$

$$= \frac{X_2^3}{3}\left[\frac{(Z_2 - Z_1)}{X_2} - \frac{(Z_3 - Z_1)}{X_3}\right] + \frac{(X_3^3 - X_2^3)}{3}\left[\frac{(Z_3 - Z_2)}{(X_3 - X_2)}\right.$$

$$\left. - \frac{(Z_3 - Z_1)}{X_3}\right] - \frac{(X_3^2 - X_2^2)}{2}\left[X_2 \frac{(Z_3 - Z_2)}{(X_3 - X_2)} + (Z_1 - Z_2)\right]$$

Figure 5.8 Diagram used in the formulation of Pappus' Theorem

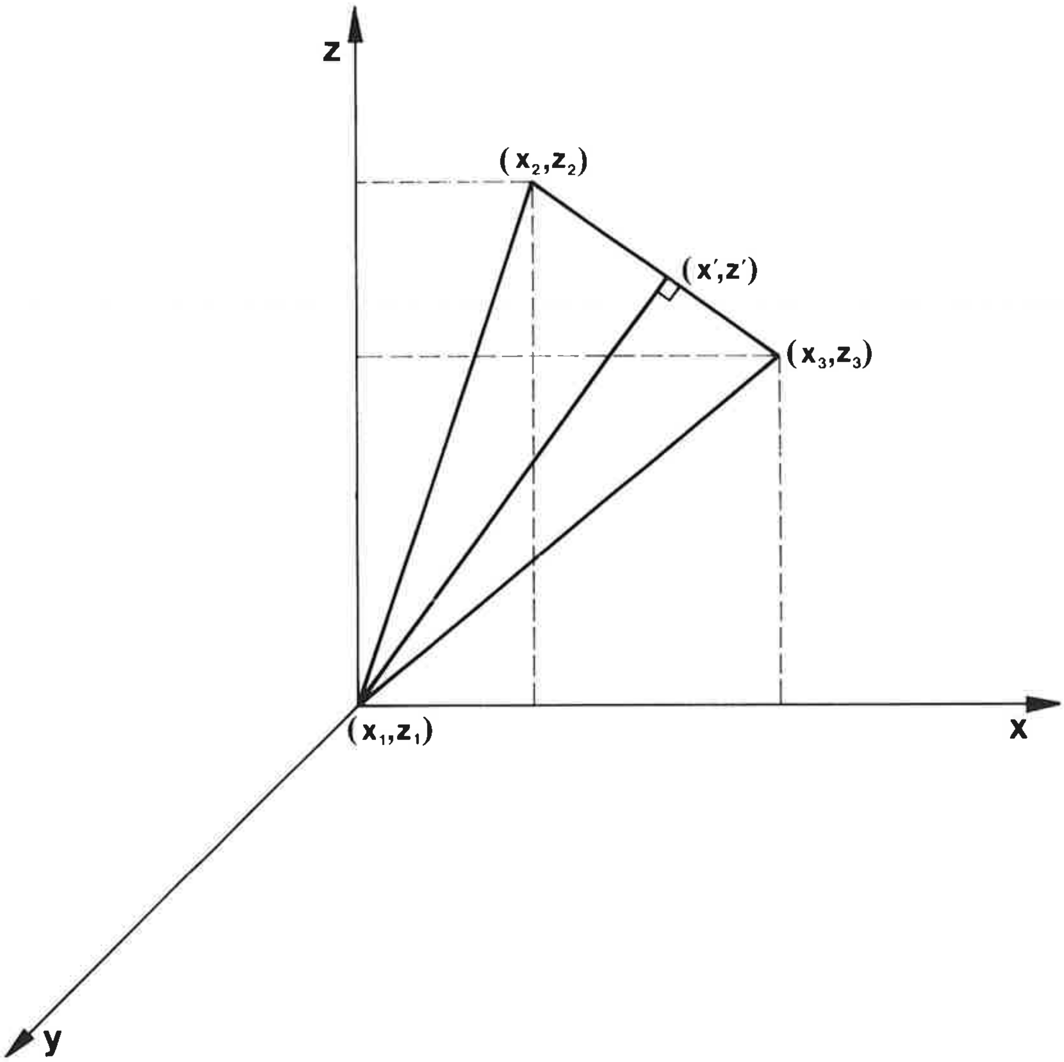
z
(x_2, z_2)
(x', z')
(x_3, z_3)
(x_1, z_1)
x
y

and

$$\iint_R dx\ dz$$

$$= \frac{X_2^2}{2}\left[\frac{(Z_2-Z_1)}{X_2}-\frac{(Z_3-Z_1)}{X_3}\right]+\frac{(X_3^2-X_2^2)}{2}\left[\frac{(Z_3-Z_2)}{(X_3-X_2)}-\frac{(Z_3-Z_1)}{X_3}\right]$$

$$- (X_3-X_2)\left[X_2\frac{(Z_3-\ Z_2)}{X_3-X_2}+(Y_1-Y_2)\right]$$

where

$$\bar{x} = \frac{\iint_R x\ dx\ dz}{\iint_R dx\ dz}$$

The area of a triangle is equal to the product of one half times the base (B) and height (H), that is:

$$\text{Area} = \tfrac{1}{2}\, B \times H$$

If we take (X',Z') as the point that the perpendicular height of the triangle intersects the base (Fig. 5.8) then the area, if the apex of the triangle lies at the origin is

$$\text{Area} = \tfrac{1}{2}\sqrt{[(X')^2+(Z')^2] \quad [(X_2-X_3)^2+(Z_2-Z_3)^2]}$$

The volume then of a triangular region, with apex at the origin, rotated through an angle of θ is

$$V = \tfrac{1}{2}\sqrt{[(X')^2+(Z')^2] \quad [(X_2-X_3)^2+(Z_2-Z_3)^2]}\ .\bar{x}\quad .\theta$$

5.12 Geometric Analysis

The detailed analysis of left ventricular geometry requires an adequate 3-D spatial description of the cavity. The methodology used in this thesis will allow the evaluation of a number of techniques for the description of global and segmental geometry together with the geometric changes which occur between diastole and systole. Keep in mind that ventricular ejection is not only a function of the extent of wall contraction but the particular shape which undergoes contraction. This applies not only in global but also in regional terms when asynergy of the ventricle is occurring or in the presence of congenital abnormalities which may influence details of ventricular shape. Therefore, any effective geometric analysis of the left ventricle which seeks to detail ventricular function and performance must include not only a description of the global geometry and the changes which occur at end systole with respect to end diastole but also a regional description. The latter is important for the evaluation of impaired segmental functioning of the ventricle which may be masked by a global assessment as well as the need to identify the location and extent of any regional abnormalities. This in turn will enable the impact of the myocardial contraction abnormality to be assessed in the context of overall ventricular performance. That is a detailed global and regional geometrical analysis would be of value for the understanding of cardiac function and performance and hence aid the Clinician in both diagnosis and prognosis.

As was discussed earlier the geometric analysis that has been carried out to date consists of single or biplane images which are either radiographic projections or tomographic slices. None of the methods have attempted a comprehensive analysis of ventricular geometry dealing with the issues we have introduced above. In this preliminary study we have selected a number of measures which we will consider at a regional and global level. In addition cross sectional descriptions as well as longitudinal descriptions of the venticle will be considered to determine the advantages of each. A study will be made of the endocardial surface area and segmental volume changes which occur between end diastole and end systole.

To estimate the endocardial surface area the ventricle is sliced perpendicular to the long axis. Each slice is divided into eight sectors (Figure 5.9). The surface area of each sector is the length of one curved boundary(s) times the slice thickness (t), that is

Sector Area $= s \times t$

where the arc length $s = r\theta$

if $\theta = \frac{\Pi}{4}$ (45^{o}) $\quad S = \frac{r\Pi}{4}$

The endocardial surface area of a slice thickness (t), is

$$\text{Slice Surface Area} = \sum_{i=1}^{8} r_i \times \frac{\Pi}{4} \times t$$

$$= \frac{\Pi}{4} t \sum_{i=1}^{8} r_i$$

Hence the total endocardial surface area of the ventricle is

$$\text{Total Surface Area} = \frac{\Pi}{4} t \sum_{j=1}^{n} \sum_{i=1}^{8} r_{ij}$$

where $\quad j$ = the number of slice segments,
$\quad\quad\quad i$ = the number of sectors.

In order to characterise the shape of the left ventricle a number of indices were defined using the measures referred to above. The mean value and coefficient of variation of each parameter was

Figure 5.9 Composite three dimensional left ventricular reconstruction, computer generated parallel short axis slices with eight sectors per slice.

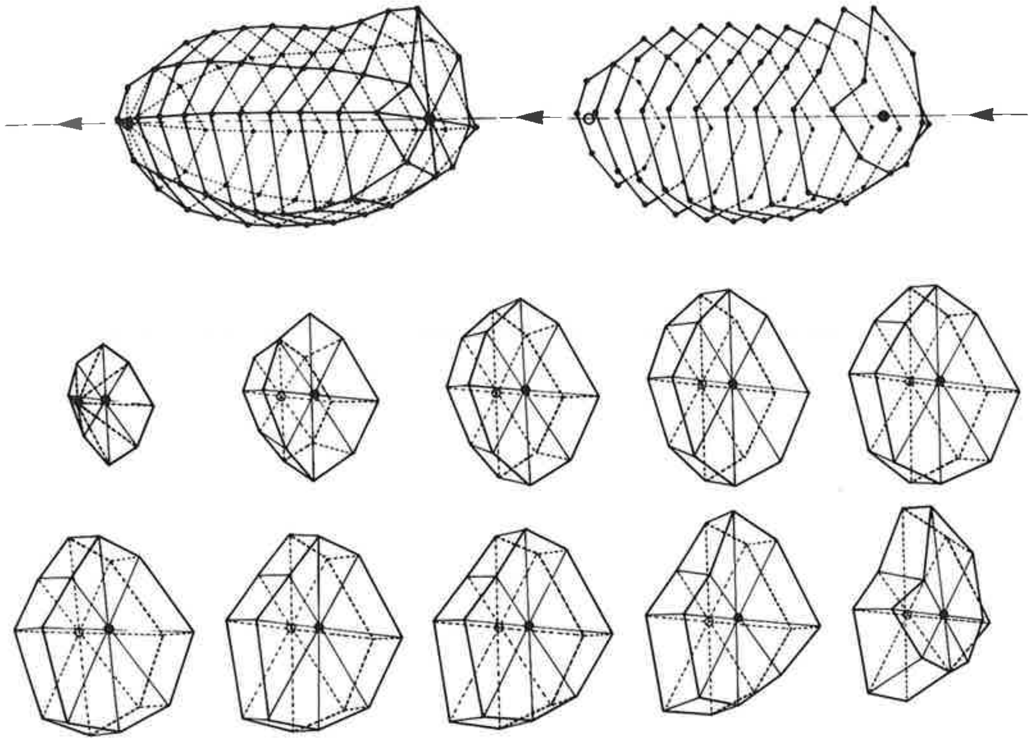

calculated for each slice perpendicular to the major axis and each sector from base to ventricular apex. The mean value (E) and the coefficient of variation (CV) of each parameter (P) was calculated by the following equations

$$E = \sum_{i=1}^{N} \frac{P_i}{N}$$

where N is the number of slices or sectors,

$$CV = \frac{\sqrt{\dfrac{\sum_{i=1}^{N} (E-P_i)^2}{N - 1}}}{E}$$

5.13 References

Davila JC, Sanmarco ME (1966)
An analysis of the fit of mathematical models applicable to the measurement of left ventricular volume.
Am. J. Cardiol. 18: 31-43

Dodge HT, Sandler H, Ballew DW, Lord JD (1960)
The use of biplane angiocardiography for the measurement of left ventricular volume in man.
Am. Heart J. 60: 766-776

Folland ED, Parisi AF, Moynihan PF, Jones MS, Feldman CL, Tow DE (1979)
Assessment of left ventricular ejection fraction and volumes by real time two dimensional echocardiography: A comparison of cineangiographic and radionuclide techniques.
Circulation. 60: 760-766

Geiser EA, Ariet M, Conetta DA, Lupkiewicz SM, Christie LG, Conti CR (1982)
Dynamic three dimensional echocardiographic reconstruction of the intact human left ventricle: Technique and initial observations in patients.
Am. Heart J. 103: 1056-1065

Janicki JS, Weber KT, Gochman RF, Shroff S, Geheb FJ (1981)
Three dimensional myocardial and ventricular shape: A surface representation.
Am. J. Physoil. 241: H1-H11

Kronik G, Slany J, Mosslacher H (1979)
Comparative value of eight M-mode echocardiographic formulas for determining left ventricular stroke volume. A correlative study with thermodilution and left ventricular single-plane cineangiography.
Circulation. 60: 1308-1316

Wyatt HL, Heng MK, Meerbaum S, Gueret P, Hesteness J, Dula E, Corday E (1980)
Cross-sectional echocardiography II Analysis of mathematic models for quantifying volume of the formalin fixed left ventricle.
Circulation. 61: 1119-1125

CHAPTER 6

THREE DIMENSIONAL CARDIAC GEOMETRY ANALYSIS AND INTERPRETATION

6.1 Introduction

A number of experiments have been carried out to evaluate the techniques described in Chapter 5. Analytical geometrics are used to determine the accuracy of the defined algorithms and the error attributable to digitization of an outline. A study of post mortem hearts was carried out to assess the techniques on the left ventricle which could be optimally imaged and whose fluid filled volume could be measured. Patients studies are carried out on 56 cases consisting of normal and pathological groups some of which underwent cardiac catheterisation. Detailed analysis of the left ventricle at end diastole and end systole will be presented. Together with comparative studies of volume estimates and a detailed global and regional geometric analysis of the 3D spatially reconstructed left ventricle will be presented.

Display modes of the data analysis from the 3-D spatial geometry will be presented to aid in the interpretation of regional wall abnormalities which occur in the presence of asynergy or other pathology. The presentation of complex structural information to the clinician to be subjected to the pattern recognition capability of the brain is important. The quantitative calculations used to describe the ventricle are discussed and correlated.

6.2 Analytical Shapes

Six symmetrical analytical shapes, one cylinder and five prolate ellipsoids of varying aspect ratio k (major axis/minor axis) were reconstructed mathematically from four planar views. The arbitrarily chosen aspect ratio of the shapes varied from 2.33 to 1.41. Volumes for these shapes were calculated using the following formulae for an ellipsoid $V = \frac{4\pi}{3} abc$

where a, b and c are half axis lengths

and for a cylinder $V = \pi r^2 l$

where r is the radius and l the length of the cylinder.

Dimensions of these shapes were chosen so that they had volumes within the physiological range usually encountered for the human left ventricle.

Three algorithms were selected to compute the volume of the shapes. These are the trapezoidal rule, Pappus' theorem and polar co-ordinate integration as described in Chapter 5. For each of these methods the shapes were computationally sectioned up to two hundred slices. The percentage error between the true volume and the calculated volume was determined for each increase in slice.

That is

$$\text{Percentage error}_s = \frac{\text{Calculated Volume}_s}{\text{True Volume}} \times 100$$

where s is the number of computed slices.

The percentage error versus the number of slices plotted for each algorithm is shown in figure 6.1. The significant feature to note is that the percentage error for a given number of slices is independent of the aspect ratio k but dependent on which of the three algorithms is used.

Surface Area

Figure 6.1 Systematic percentage error of each integration method is independent of the major to minor axis ratio, k, for both volume and surface area estimates.

Volume

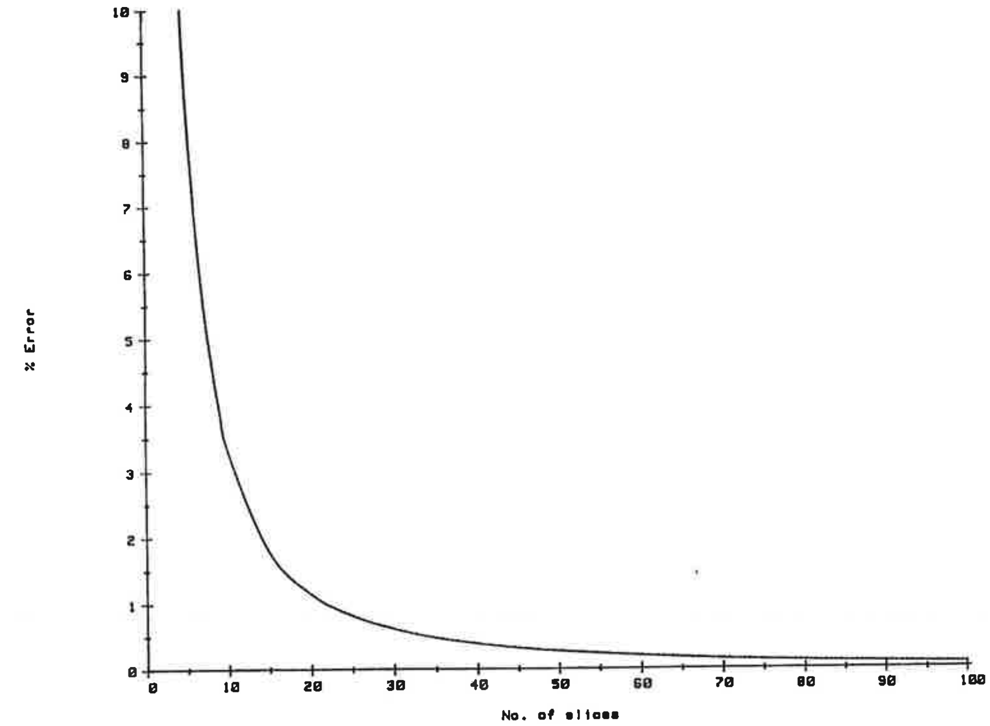

% Error
No. of slices

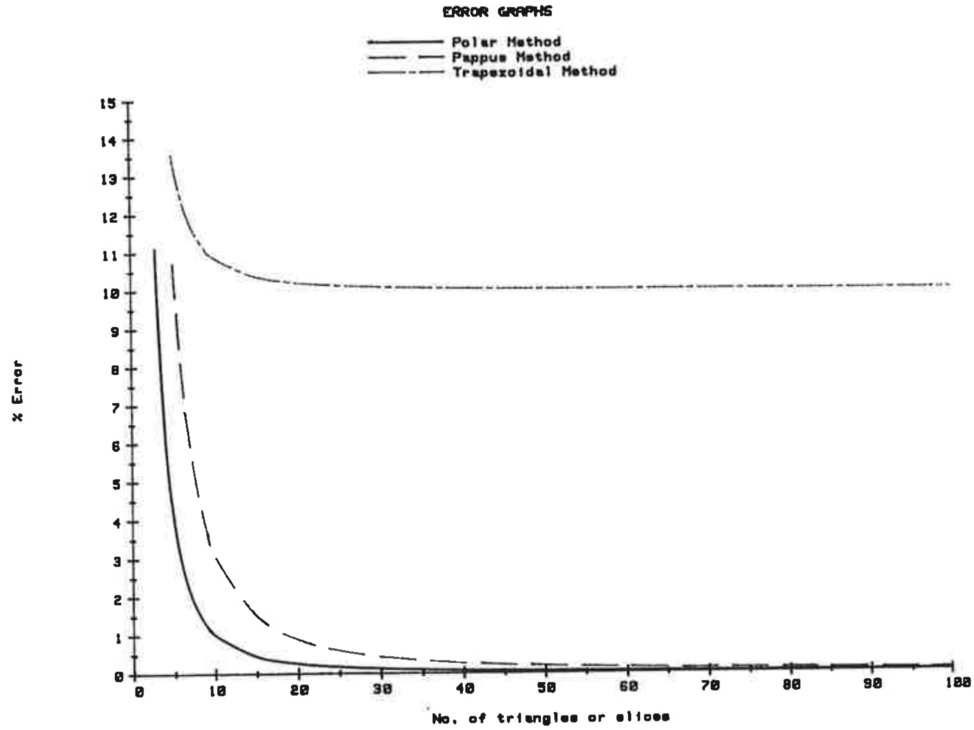

ERROR GRAPHS
Polar Method
Pappus Method
Trapezoidal Method
% Error
No. of triangles or slices

In consideration of the three dimensional resolution capabilities of ultrasound tomographic imaging devices as discussed in Chapter 3 and the studies that have been carried out to determine the number of slices required for accurate volume estimation of the left ventricle (Janicki, Weber, Gochman et al, 1981) and of organs (Zilles, Schleicher, Pehleman 1982) it was decided to closely study the volume estimates from five and ten short axis slices. The computed volumes using five and ten slices for each of the algorithms are shown in table 6.1 together with the true calculated volume. It can be seen that the percentage error for each method with five or ten slices remains constant independent of the aspect ratio k (Fig. 6.1). It is apparent that the polar integration using ten computationally generated slices gives the best result with a percentage error of 1%. Provided that the number of slices remains constant then the application of Pappus' theorem and the trapezoidal integration scheme follow in order of minimum percentage error 3.1% and 10.9% respectively (Table 6.2). The error in the computations then introduces a bias in the

MATHEMATICAL ANALYSIS

Volume (ml)

Integrated Method		Trapezoidal		Pappus		Polar		Calculated Volume
Number of Slices		5	10	5	10	5	10	
Ellipse	K							
	2.33	83.7	86.3	86.4	93.8	92.9	95.8	96.8
	1.96	117.7	121.4	121.6	132.0	130.7	134.8	136.2
	1.71	154.9	159.7	160.0	173.7	172.0	177.4	179.2
	1.52	197.1	203.3	203.6	221.0	219.0	225.8	228.1
	1.41	228.1	235.3	235.7	255.8	253.4	261.3	264.0
Cylinder	2.00	176.9	176.9	196.4	196.4	196.4	196.4	196.4

Table 6.1 Calculated volume of ellipsoids and cylinder by various algorithms for five and ten parallel short axis slices.

MATHEMATICAL ANALYSIS

Volume Error (%)

Integration Method	Trapezoidal		Pappus		Polar	
Number of Slices	5	10	5	10	5	10
Systematic Error (%)	13.6	10.9	10.7	3.1	4.0	1.0

Random Error = 0.

Table 6.2 Percentage error in calculated volume estimates with respect to the true volume. No random error is generated by the application of various algorithms on given numerical data.

volume estimates resulting in volume under estimates of a fixed percentage. The magnitude of the percentage depends on the number of slices.

Next an outline of the shapes were placed on the digitizer tablet and traced with the cursor. The boundary coordinate data was stored on computer file and used to reconstruct the ellipsoid as described in Chapter 5. Then using the three algorithms the volume was calculated for both five and ten slices. The volume estimates are shown in table 6.3. the ratio (r) of

$$\frac{\text{volume estimate}}{\text{true volume}} \quad \text{is used}$$

as a measure of method accuracy. We have determined that this ratio is constant for computational slicing of the ellipsoid shapes for each algorithm using five and ten slices. These will be used as reference values. The ratio for the volume estimates using the digitised boundaries are tabulated in table 6.4. The percentage error (E) of the volume estimate is defined as

DIGITISED DATA ANALYSIS

Volume (ml)

Integrated Method		Trapezoidal		Pappus		Polar		Calculated Volume
Number of Slices		5	10	5	10	5	10	
Ellipse	K							
	2.33	85.9	87.7	91.4	93.3	95.6	97.6	96.8
	1.96	119.6	121.4	125.8	127.6	133.2	135.1	136.2
	1.71	156.7	159.4	165.0	167.8	174.4	177.4	179.2
	1.52	197.6	202.4	211.5	216.5	220.0	225.2	228.1
	1.41	239.3	244.3	256.7	262.1	266.3	271.9	264.0
Cylinder	2.00	174.7	174.3	177.8	177.7	194.1	194.0	196.4

Table 6.3 Calculated volume estimates of ellipsoids and cylinder from digitised boundary data.

Volume Estimate/Calculated Volume

Integration Method		Trapezoidal		Pappus		Polar	
Number of Slices		5	10	5	10	5	10
Reference Value		0.864	0.891	0.893	0.969	0.960	0.990
Ellipse	K						
	2.33	0.887	0.960	0.944	0.963	0.988	1.008
	1.96	0.878	0.891	0.924	0.937	0.978	0.992
	1.71	0.874	0.890	0.930	0.946	0.973	0.990
	1.52	0.866	0.887	0.928	0.949	0.965	0.987
	1.41	0.907	0.926	0.973	0.993	1.009	1.030
Cylinder	2.00	0.890	0.887	0.905	0.905	0.988	0.988
Mean		0.884	0.898	0.935	0.949	0.984	0.999
SEM		0.006	0.006	0.009	0.012	0.006	0.007

Table 6.4 Ratio of calculated volume estimates from digitised boundary data to calculated volume from a given data set. Ratio < 1 shows the estimate from digitised data smaller than the calculated volume from given data. Ratio > 1 shows the reverse.

SEM - Standard Error of the Mean.

$$E = (1 - r) \times 100\%.$$

The percentage tracing error (TE) is defined as

$$TE = (E_{ref} - E_s)\%$$

where E_{ref} is the percentage error of mathematical analysis E_s is the average percentage error for the sample of the digitized boundary data analyses for s slices. This is the random error associated with boundary digitisation. The absolute percentage error (AE) is defined as

$$AE = (TE + E_{ref})\%$$

The absolute percentage error includes the systematic bias inherent in the algorithms together with the random error associated with boundary digitisation. It is important to note that because of the random nature of the tracing error this maybe either positive or negative. When it is positive this may over compensate or partly compensate for the negative bias of the algorithm. In some instances r may be greater than one or larger than the reference r value for a particular algorithm (Table 6.4). The addition of tracing error does not alter the trend established by the theoretical slicing and the application of the three algorithms, that is polar integration, Pappus' theorem and the trapezoidal scheme show increasing error for the volume estimate (Table 6.5). Furthermore, the tracing error is generally less in magnitude than the reference error (bias) of the estimate derived from the theoretical analysis (Table 6.2 and 6.5). The absolute error shown in table 6.5 is the sum of the algorithm error (reference) plus the tracing error. It is therefore obvious that the digitisation process gives reproducible results and error smaller than the algorithm based error. Hence volume estimates are less than 1.2% $\pm$ 0.5% (mean$\pm$ SEM) in error if ten slices are used with the polar integration algorithm and digitised boundary data points. Pappus' theorem can also be used to provide volume estimates less than 5.1% $\pm$ 1.2% in error. Table 6.6 shows a comparison of these methods of volume estimation.

Surface area for the ellipsoid shapes cannot be calculated directly therefore each ellipsoid was mathematically sliced into 200 slices. The surface

DIGITISED DATA ANALYSIS

Volume Error (%)

Integration Method		Trapezoidal		Pappus		Polar	
Number of Slices		5	10	5	10	5	10
Ellipse	K						
	2.33	11.3	9.4	5.6	3.6	1.2	-0.8
	1.96	12.2	10.9	7.6	6.3	2.2	0.8
	1.71	12.5	11.0	7.9	6.4	2.7	1.0
	1.52	13.4	11.3	7.3	5.1	3.5	1.3
	1.41	9.3	7.4	2.7	0.7	-2.4	-3.0
Systematic Error		11.7	10.0	6.2	4.4	1.4	-0.1
Random Error		1.6	1.6	2.2	2.4	2.3	1.8
Cylinder							
	2.0	11.0	11.0	9.5	9.5	1.2	1.2

Table 6.5 Using various algorithms, the percentage error of calculated volume estimates from digitised boundary data with respect to the calculated volume from given data is tabulated.

ERROR OF VOLUME ESTIMATES (%)

Integration Method	Trapezoidal		Pappus		Polar	
Number of Slices	5	10	5	10	5	10
Reference Value (%)	13.6	10.9	10.7	3.1	4.0	1.0
			Tracing Error			
	-2.0	-0.7	-4.2	2.0	-2.4	-0.9
			Absolute Error			
	11.6	10.2	6.5	5.1	1.6	0.1

Table 6.6 The percentage error which relates to tracing by digitiser and the absolute error which consists of both tracing and algorithm error.

area was calculated as described in Chapter 5 and used as the surface area reference value. This estimate was less than 0.1% in error when compared to the results from the numerical solution of the elliptic surface integral equations (Fig. 6.1). The mathematical analysis of a theoretical five and ten slice application of the polar integration scheme followed by the analysis of the digitised boundary point data is shown in table 6.7 and 6.8, table 6.9 lists the r values from the digitised data analysis. The tracing error is of the order 0.1% independent of slice number and the absolute error is 3.2% and 9.2% for ten and five slices respectively (Table 6.10 and 6.11).

As a result of this analysis the polar integration scheme using ten slices was the method of choice for both total volume and surface area estimations. For regional analysis using volume elements of pyrimidal shape the method of choice was the application of Pappus' theorem to ten slices. Sector volumes were analysed using polar integration.

MATHEMATICAL ANALYSIS

Surface Area (cm^2)

Integration Method		Polar		Calculated Surface
Number of Slices		5	10	
Ellipse	K			
	2.33	96.2	102.6	106.1
	1.96	114.1	121.7	125.8
	1.71	130.8	139.5	144.3
	1.52	147.6	157.5	162.8
	1.41	158.8	169.4	175.1
Cylinder	2.00	157.1	157.1	157.1

Table 6.7 Calculated surface area of ellipsoids and cylinder by various algorithms for five and ten parallel short axis slices.

DIGITISED DATA ANALYSIS

Surface Area (cm^2)

Integration Method		Polar		Calculated Surface
Number of Slices		5	10	
Ellipse	K			
	2.33	95.9	102.2	106.1
	1.96	112.3	119.8	125.8
	1.71	129.2	137.8	144.3
	1.52	148.1	158.0	162.8
	1.41	162.1	172.9	175.1
Cylinder	2.00	166.2	166.2	157.1

Table 6.8 Calculated surface area estimates of ellipsiods and cylinder from digitised boundary data.

Surface Estimate/Calculated Surface

Integration Method		Polar	
Number of Slices		5	10
Reference Value		0.907	0.967
Ellipse	K		
	2.33	0.904	0.964
	1.96	0.893	0.952
	1.71	0.895	0.955
	1.52	0.910	0.971
	1.41	0.926	0.987
Cylinder	2.00	1.058	1.058
Mean		0.931	0.981
SEM		0.026	0.016

Table 6.9 Ratio of calculated surface area estimates from digitised boundary data to calculated surface area from a given data set. Ratio < 1 shows the estimate from digitised data smaller than the calculated surface area from given data. Ratio > 1 shows the reverse.

SEM - Standard Error of the Mean.

DIGITISED DATA ANALYSIS

Surface Area Error (%)

Integration Method		Polar	
Number of Slices		5	10
Ellipse	K		
	2.33	9.6	3.6
	1.96	10.7	4.8
	1.71	10.5	4.5
	1.52	9.0	2.9
	1.41	7.4	1.3
Systematic Error		9.4	3.4
Random Error		1.3	1.4
Cylinder			
	2.00	-5.8	-5.8

Table 6.10 The percentage error of calculated surface area estimates from digitised boundary data with respect to the calculated surface area from given data is tabulated.

ERROR OF SURFACE ESTIMATES (%)

Integration Method	Polar	
Number of Slices	5	10
Reference Value (%)	9.3	3.3
	Tracing Error	
	-0.1	-0.1
	Absolute Error	
	9.2	3.2

Table 6.11 The percentage error which relates to tracing by digitiser and the absolute error which consists of both tracing and algorithm error.

6.3 In Vitro Studies

A study of post mortem hearts was carried out to assess the 3D reconstruction technique and the volume estimates of the left ventricle. With the formalin fixed heart in an ultrasonically transparent bladder as described in Chapter 5 the left ventricle was optimally imaged. The four anatomically defined apical views were recorded on video tape for analysis.

Three dimensional echo reconstruction studies were carried out on 23 hearts, 18 of which were from males and 5 from females. The left ventricular fluid filled volume was measured in 18 cases, 13 of which were males and 5 females. Fluid volumes of the left ventricle were not obtained from 5 male cases becauses of constraints imposed by the conditions prevailing in the post mortem room at the time. The 23 cases had a mean age 38.3 $\pm$ 4.5 years, body weight 71.7 $\pm$ 2.9 kg, height 173.2 $\pm$ 2.1 cm, body surface area 1.84 $\pm$ 0.04m^2 and heart weight 342.4 $\pm$ 18.7 gm, all of which were not significantly different to the corresponding values of the 18 cases with measured left ventricular fluid filled volumes. Hence this subgroup was anthropometrically respresentative of the total sample (Table 6.12). The hearts used in the study were all normal except for one where the patient suffered a myocardial infarction. The causes of death are listed in table 6.13.

The excised post mortem hearts were prepared according to the protocal described in Chapter 5. The ultrasonic transducer was positioned at the cardiac apex through the ultrasoncially transparent bladder. The four anatomically defined tomographic apical views were recorded on video tape for later analysis. The four views used in the 3D spatial reconstruction, the four chamber view together with views at 45^{o} anticlockwise and clockwise transducer rotation with respect to its four chamber position and the two chamber view were digitised and stored oncomputer file as described in Chapter 5.

A volume estimate was determined from each of the views using the single plane area-length algorithm

$$\text{Volume (V)} = \frac{8A^2}{3\pi L}$$

Where A is the area of the ventricular outline and

ANTHROPMETRIC DATA OF POSTMORTEM HEARTS

Case No	Sex	Age (yrs)	Height (cm)	Body Weight (kg)	Heart Weight (gm)	BSA (m^2)
50116/F83	M	55	178	72	480	1.88
50118/F83	M	40	184	81	375	2.04
50121/F83	F	60	165	65	390	1.72
50148/F83	M	51	190	106	600	2.34
50197/F83	M	63	186	72	305	1.96
50314/F83	M	16	178	58	290	1.72
50451/F83	M	19	178	83	410	2.02
50509/F83	F	21	152	58	200	1.54
50548/F83	M	17	173	80	350	1.92
50591/F83	M	32	160	63	265	1.66
50593/F83	F	27	160	61	245	1.63
50595/F83	M	21	185	86	340	2.10
50596/F83	F	88	158	61	275	1.62
50623/F83	M	52	182	87	360	2.08
50038/F84	M	59	165	47	260	1.50
50114/F84	F	20	170	86	360	1.98
50140/F84	M	17	168	58	280	1.60
50172/F84	M	21	175	88	370	2.04
50194/F84	M	20	183	75	370	1.96
50195/F84	M	18	178	56	280	1.70
50509/F84	M	51	173	69	270	1.80
50249/F84	M	38	164	75	330	1.80
Mean		38.3	173.2	71.7	342.4	1.84
SEM		4.5	2.1	2.9	18.7	0.04

Table 6.12 Mean and standard error of the mean for the anthropometric data of 22 postmortem hearts.
BSA is body surface area.

POSTMORTEM HEARTS

Case No.	Cause of Death
50116/F83	Bronchopneumonia
50118/F83	Tumour
50121/F83	Exsanguination
50148/F83	Myocardial infarction
50197/F83	Tumour
50314/F83	Cerebral oedema
50451/F83	Head injury
50509/G83	Exsanguination
50548/F83	Exsanguination
50591/F83	Cerebella vascular accident
50593/F83	Bronchopneumonia
50595/F83	Shock and haemorrhage
50596/F83	Peritonitis
50623/F83	Shock and haemorrhage
50038/F83	Status epilepticus
50050/F83	Haemoptysis - Hodkins disease
50114/F84	Head injury
50140/F84	Head injury
50172/F84	Head injury
50194/F84	Haemothorax
50195/F84	Tumour
50209/F84	Tumour
50249/F84	Exsanguination

Table 6.13 The cause of death for the 22 postmortem cases.

L the long axis of the ventricle defined as the distance from the apex to the centre of the mitral valve. The area of each ventricular view was computed, using a trapezoidal scheme, from at least 500 digitised endocardial boundary points. In addition the area of the ventricular image was determined by superimposing an ellipse of best fit (Figure 6.2). For each case then the four volume estimates were used to calculate a mean volume. These data are tabulated in table 6.14 and 6.15. A comparison of each of the four volumes to the measured fluid volume was done by regression analysis and calculation of the percentage differences (mean and standard deviation) between the fluid volume and the echocardiographic measurements expressed as a percent of fluid volume. The resulting regression equations of the form y=m x + b showed variation in the value of both the constant (b) and regression coefficient (m) (Table 6.16). For the ellipse of best fit and the traced area, b ranges from -1.753 to 5.658 and -1.092 to 14.491, m ranges from 0.620 to 0.826 and 0.523 to 0.881 respectively. All regressions were statistically significant (P <0.01). The average volume estimate derived from the four apical views

End Diastolic Views

Figure 6.2 End diastolic and end systolic echocardiographic apical views used in the composite three dimensional left ventricular reconstruction. The traced area boundary and the ellipse of best fit are shown in each apical view.

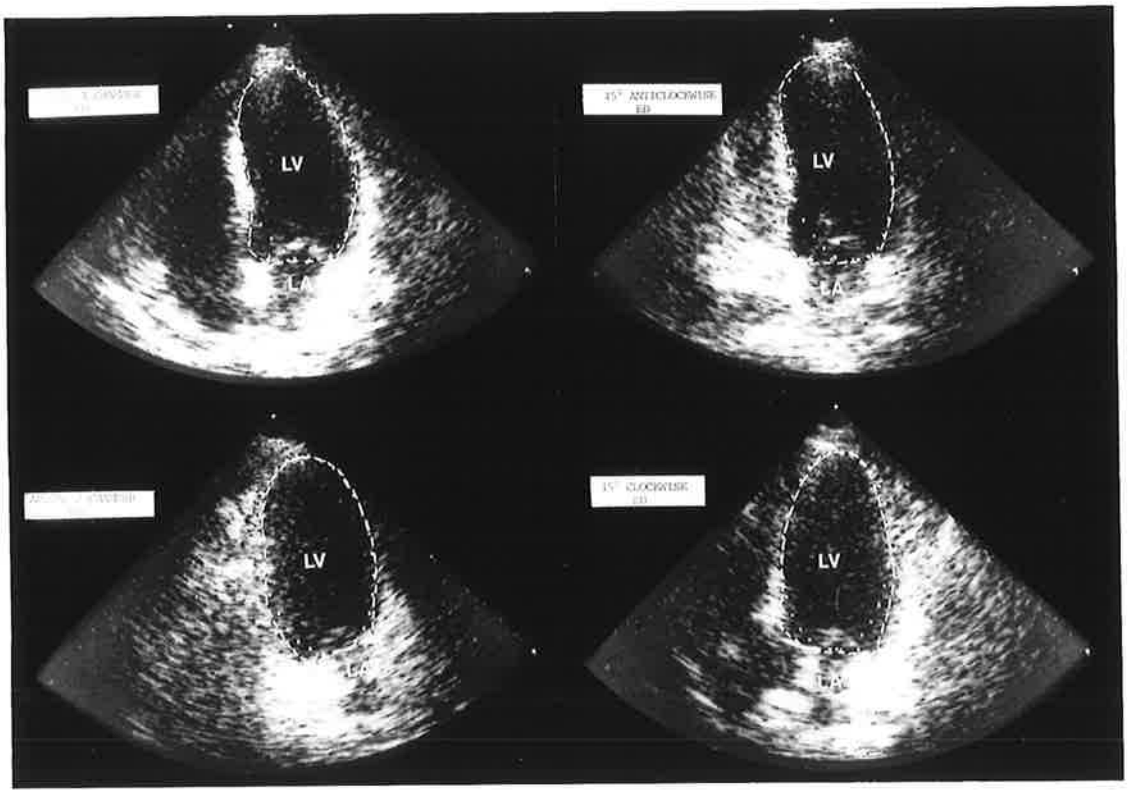

15° ANTICLOCKWISE
ED
LV
LA
15° CLOCKWISE
ED
LV
LA
LV
LV

End Systolic Views

Figure 6.2 continued

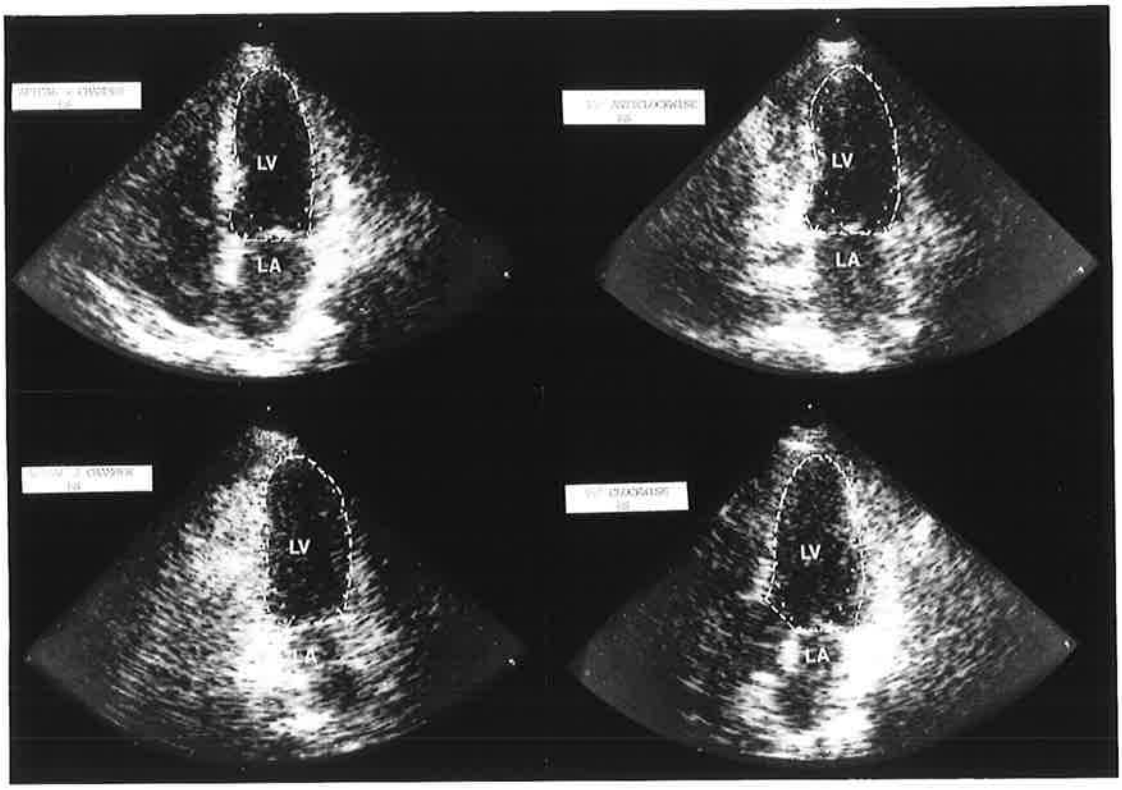
LV
LA
LV
LA
LV
LA
LV
LA

POSTMORTEM HEARTS

TRACED AREA LENGTH ($V = .85A^2/L$)

VOLUME (ml)

Case No.	0° View	45° View	90° View	-45° View
50116/F83	31.0	28.0	44.0	51.0
50121/F83	40.0	30.0	42.0	36.0
50197/F83	45.0	28.1	21.6	52.2
50314/F83	28.0	23.0	22.0	25.0
50451/F83	52.0	38.0	45.0	63.0
50509/F83	23.5	20.0	23.4	27.8
50548/F83	51.8	40.0	43.7	53.4
50591/F83	65.8	43.6	39.4	36.5
50593/F83	32.8	36.3	32.6	46.5
50595/F83	83.3	71.3	68.1	64.0
50596/F83	26.3	25.7	22.6	24.6
50623/F83	48.5	55.0	49.4	50.2
50038/F84	38.3	40.2	25.6	35.4
50050/F84	32.4	51.9	38.4	51.4
50114/F84	67.0	55.0	72.1	71.1
50140/F84	34.4	33.1	26.1	31.6
50172/F84	20.1	26.2	16.4	33.3
50209/F84	36.2	29.3	42.7	31.6
Mean	42.0	37.5	37.5	43.6
SEM	4.0	3.2	3.7	3.4

Table 6.14 The traced area length volume estimate of left ventricular volume from each echographic apical view. Mean and standard error of the mean for the sample is calculated for each apical view.

POSTMORTEM HEARTS

SINGLE PLANE ELLIPSE ($V=.85A^2/L$)

VOLUME (ml)

Case No.	0° View	45° View	90° View	-45° View
50116/F83	18.0	14.5	33.0	27.0
50121/F83	32.8	31.5	33.5	32.5
50197/F83	47.6	25.9	26.5	46.8
50314/F83	28.9	21.1	22.2	22.7
50451/F83	46.5	36.5	40.4	50.6
50509/F83	22.2	19.2	21.3	29.6
50548/F83	45.1	41.4	38.1	48.1
50591/F83	45.2	31.6	33.5	43.5
50593/F83	29.4	31.5	32.4	35.9
50595/F83	88.5	61.8	64.2	66.2
50596/F83	21.5	20.3	16.4	21.7
50623/F83	39.4	58.8	56.1	51.6
50038/F84	40.0	37.8	31.7	36.4
50050/F84	31.4	42.3	34.0	48.0
50114/F84	59.8	53.9	65.4	70.3
50140/F84	31.6	26.0	25.5	28.7
50172/F84	15.1	15.0	11.5	11.5
50209/F84	28.1	21.7	36.8	27.6
Mean	37.3	32.8	34.6	38.8
SEM	4.1	3.4	3.5	3.7

Table 6.15 The ellipse of best fit area length volume estimate of left ventricular volume from each echographic apical view. Mean and standard error of the mean for the sample is calculated for each apical view.

POST MORTEM HEARTS

Comparison of Methods for Estimating
Left Ventricular Volume

Method	Regression Equation	Correlation Coefficient	SEE (ml)	Δ%D± SD
Liquid Volume vs				
Traced Area length				
4 Chamber	y = 7.30 + 0.79x	0.739	11.7	3.2 ± 23.6
45 Anticlockwise	y =14.49 + 0.52x	0.608	11.1	11.5 ± 28.2
2 Chamber	y =-1.09 + 0.88x	0.899	7.0	15.1 ± 16.1
45 Clockwise	y =12.91 + 0.70x	0.776	9.2	-2.7 ± 25.8
Liquid Volume vs				
Single Plane Ellipse				
4 Chamber	y = 5.66 + 0.72x	0.654	13.5	14.3 ± 24.8
45 Anticlockwise	y = 5.55 + 0.62x	0.680	10.9	25.1 ± 24.4
2 Chamber	y = 1.75 + 0.83x	0.883	7.2	22.1 ± 15.8
45 Clockwise	y = 5.44 + 0.76x	0.770	10.2	10.7 ± 25.0
Liquid Volume vs				
Average of Area Length	y = 8.32 + 0.73x	0.840	7.6	6.5 ± 17.5
Liquid Volume vs				
Average of Single Plane	y = 3.71 + 0.73x	0.789	9.2	17.8 ± 19.3
Liquid Volume vs				
Polar Integration	y = 7.63 + 0.80x	0.900	6.3	2.1 ± 15.6

Table 6.16 The liquid volume of isolated postmortem hearts compared to echographic estimates. SEE is the standard error of estimate, Δ%D± SD is the mean percentage difference ± standard deviation related to filling volumes of the postmortem hearts.

for each area method gave significant regressions ($P < 0.01$)on the fluid volume estimate (Table 6.16). These regressions illustrate the fluctuations in geometry of the left ventricle which influence the volume estimates. The polar coordinate integration of the ventricular volume using the 3D spatial reconstruction was also significant ($P < 0.01$) when regressed on the fluid volume (Table 6.16) (Fig. 6.3).

The percentage differences with respect to the fluid volume and their standard deviation represent the systematic and random errors respectively (Altman, Bland, 1983) associated will the application of the echocardiographic method to each left ventricular apical view. Hence for the ellipse of best fit volume estimates the bias (systematic error) is significantly different to zero for all views except the 45° clockwise view. However, all views tended to provide estimates less than the measured fluid volume (Table 6.16). For the traced area estimates only the two chamber view showed a statistically significant bias though again the trend in the four views was that they

Figure 6.3 A plot of the average of the single plane volume estimates from the traced area and ellipse of best fit together with the composite three dimensional estimate versus the fluid filled volume measure of the left ventricle in the post mortem study.

o ·—·—·— Traced Area
Δ — — — — Ellipse of Best Fit
● ———— Three Dimensional Reconstruction

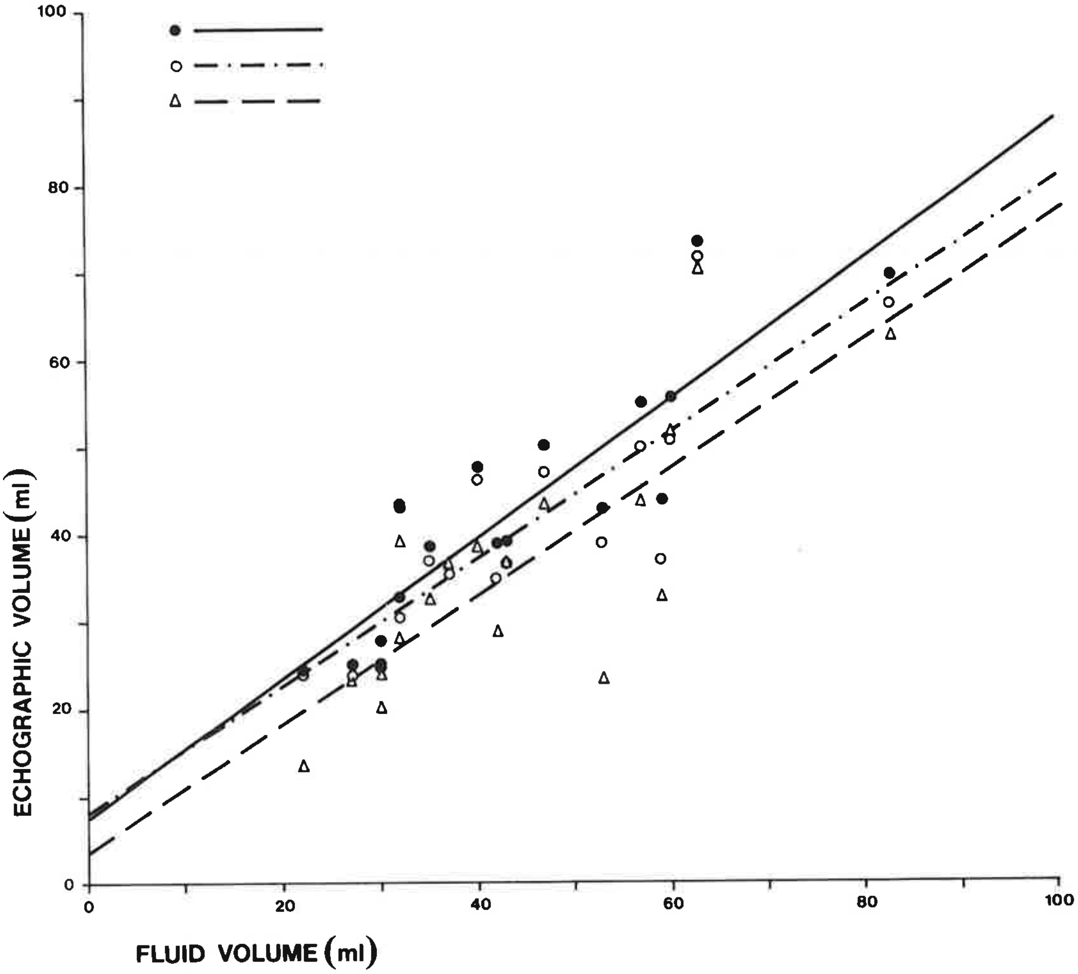
100
80
60
40
20
0
ECHOGRAPHIC VOLUME (ml)
0
20
40
60
80
100
FLUID VOLUME (ml)

under estimated the measured fluid volume (Table 6.16). The random error as expressed by the standard deviation showed no statistical differences between the two methods, ellipse of best fit and traced area, and within the four apical views for each method (Table 6.16).

The multiple comparison of the systematic errors within each method was done using a one way analysis of variance and the Newman - Keul method (Snedecor, Cochran, 1967) which tests for mean differences sequentially. For the ellipse of best fit and the traced area method respectively both the four chamber and 45^o clockwise views have a bias which is less than for the 45^o anti clockwise and four chamber view. However the bias for the traced area method is less than that of the ellipse of best fit for each corresponding apical view (Table 6.16).

An analysis of covariance (Snedecor, Cochran, 1967) was used to compare regression analyses. This analysis allows the question of whether or not the regression lines are the same to be addressed.

If not, how they differ, whether they differ fundamentally in their residual mean squares which suggests the sample used in the regression are heterogeneous. At this point the analysis would be complete and perhaps reasons for the heterogenicity sought by further study. On the other hand the samples may be homogeneous which allows for further analysis of the relationships. With linear regressions of the form $y = m x + b$ the regression coefficients and constants b can be compared. Either or both may be shown statistically different. In this study residual variances have been shown to be homogeneous unless stated otherwise.

Comparison of the four traced and the four ellipse of best fit area length regressions on the measured fluid volume within each method shows the residual variances to be homogeneous and subsequent analysis of the slopes and intercepts shows them to be statistically no different at the critical value. However, for the traced area length method comparison between the two chamber view and the 45^{o} anticlockwise view the regression coefficients have a marginal P value of $p<0.07$.

The averaged area length volume estimates and the polar integration estimates were analysed. Analysis found the regression lines identical. The regression constants or the y-intercepts for the two methods are 8.3ml for the traced area and 3.7ml for the ellipse of best fit (Table 6.16). The polar integration estimates compared to the four view average of the area length regressions showed no statistical difference. However, the polar regression compared to single plane estimate showed statistically significant differences for some views. For instance the 45^{o} anticlockwise view has a y-intercept statistically different to the polar integration estimates ($p < 0.01$). The systematic error of the averaged volume estimates and polar integration with respect to the fluid volume is only significant for the ellipse of best fit average. However, the three echographic estimates under estimate the fluid volume (table 6.16). Performing a multiple comparison of the systematic errors indicates that the polar integration has the smallest bias while the ellipse of best fit has the largest. The random error on the other hand is the same for each of the echographic methods (Table 6.16).

The post mortem hearts are a normal sample set except one which suffered a myocardial infarction. In addition the hearts were packed with surgical gauze during fixation and so the ultrasonic tomographic investigation was performed on a relatively symmetrical ventricle in which the trabeculations had been compressed into the endocardial wall during fixation (Figure 6.4).

This led to a relatively symmetrical and ellipsoidal shaped ventricle which may have resulted in the smaller intercept for the fluid volume regression on the ellipse of best fit estimates compared to the traced area-length estimates (Table 6.16).

Hence, the ventricles were not particularly asymmetrical though the extent of the geometric fluctuation is described later in this section. Despite the fact that the random error is the same for each echocardiographic method, the differences in y-intercept and slope are statistically demonstrable in some instances and so reveals the presence of underlying geometric fluctuation not taken into account by symmetrical single plane

Figure 6.4 A postmortem heart cut in the 4 chamber apical view shows the compressed trabeculations as a result of the gauze packing during fixation. The resultant ventricular cavity is smoothed in comparison to the invivo ventricle.


0 1 2 3 cms 6 7 8
50591
F83 A
Institute of Medical and Veterinary Science,
Frome Road,
Adelaide.

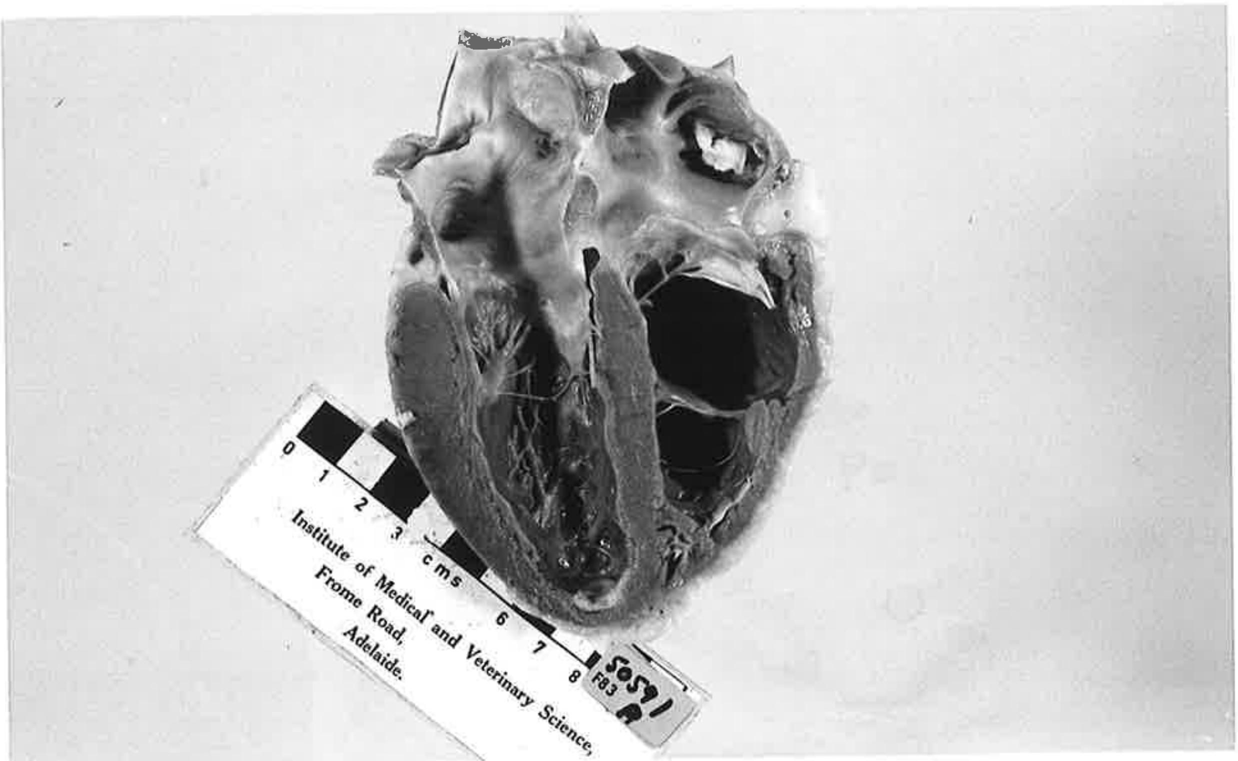
0 1 2 3 cms 6 7 8
50591
F83 A
Institute of Medical and Veterinary Science,
Frome Road,
Adelaide.

estimates. The polar integration method minimises assumptions of symmetry and is the most reliable. The bias in volume estimates is primarily a feature of the ultrasonic imaging of the left ventricular endocardium and the boundary delineation to the base of the large trabeculations. This procedure however excluded the papillary muscles from the ventricular volume if they appear in a tomographic view. This technique of delineation does not make it possible to estimate the ventricular volume contained within the trabeculations and the continuous endocardium. It therefore excludes a pseudo random volume element from the estimate which cannot be easily corrected. The intra trabecular volume is a principal factor involved in the underestimation of ventricular volumes using ultrasonic tomography. Polar integration is an optimal scheme for volume estimation though compared to the average of the traced area length method the regression is not significantly different. The trend is a decrease in the systematic error, a fall in the standard error of estimate (SEE) and an improvement in the correlation coefficient (r) to 0.9 (Table 6.16).

Further comparisons of individual volume estimates from the four apical views were made. In this instance with the estimate from polar integration of the spatially reconstructed left ventricle. These regression comparisons listed in table 6.17 are all statistically significant ($p<0.01$) and again show variation in the volume estimates from different rotational apical views. The traced and ellipse of best fit single plane area length volume estimates have the four chamber view regressions statistically different in both y-interecept and slope ($p<0.01$) compared to the 45^{o} anticlockwise view. The other views lie between the extremes represented by these two views. The average of the volume estimates regressed on the polar integration estimate are statistically different in both slope ($p<0.01$) and intercept ($p<0.01$) (Table 6.17). The average volume estimates from the traced area length method regressed on the polar integration estimation has a regression equation closest to the identity equation for the estimates of $y=x$. The ellipse of best fit is not the optimal method for estimating the area of a long axis view of the left

POSTMORTEM HEARTS

Comparison of Methods for Estimating
Left Ventricular Volume

Method	Regression Equation	Correlation Coefficient	SEE (ml)	Δ%D ± SD
Polar Integration vs				
Traced Area length				
4 Chamber	y =10.81 + 0.76x	0.964	5.4	2.8 ± 15.6
45 Anticlockwise	y = 4.72 + 1.04x	0.931	7.4	11.6 ± 16.2
2 Chamber	y = 8.81 + 0.91x	0.966	5.3	14.0 ± 13.5
45 Clockwise	y = 8.27 + 0.81x	0.944	6.7	-3.0 ± 17.6
Polar Integration				
Single Plane Ellipse				
4 Chamber	y =14.37 + 0.78x	0.916	8.2	14.1 ± 20.0
45 Anticlockwise	y = 7.39 + 1.11x	0.884	9.3	24.3 ± 17.1
2 Chamber	y = 7.17 + 1.10x	0.939	7.0	19.4 ± 10.1
45 Clockwise	y = 4.79 + 1.04x	0.915	8.2	8.3 ± 14.8
Polar Integration vs				
Average of Area Length	y = 4.84 + 0.94x	0.994	2.2	6.1 ± 4.0
Polar Integration				
Average of Single Plane	y = 4.92 + 1.09x	0.962	5.6	17.1 ± 12.7

Table 6.17 The three dimensional echographic volume estimate of isolated postmortem hearts compared to area length echographic estimates. SEE is the standard error of estimate, Δ%D±SD is the mean percentage difference ±

ventricle. Particularly in instances when the ventricular shape deviated from the idealised ellipsoidal shape.

For the ellipse of best fit estimates the bias is significantly different to zero for all views and all views provide estimates less than the polar integration estimate (Table 6.17). For the traced area estimates the 45 deg anticlockwise view and the two chamber view had systematic errors that were signficiant though the trend again was that the polar estimate was larger (Table 6.17). The random error on the other hand was the same for methods and views (Table 6.17).

The multiple comparison of the systematic errors shows the smallest bias for the four chamber and 45^{o} clockwise view (Table 6.17). However, the bias for the traced area method is less than that of the ellipse of best fit for each corresponding apical view (Table 6.17).

The systematic error of the averaged volume estimates with respect to the polar integration is significant in both instances and they under estimate the polar estimate (Table 6.17). Furthermore the traced area bias and random error is less than that of the ellipse of best fit (Table 6.17).

To identify and estimate sources of variability associated with echographic methods and with ventricular geometry a variance components model using one way analysis of variance was formulated and used (Sokal, Rohlf, 1981). A one way analysis of variance using a Model II approach was applied to the volume data from the various methods and to the four single plane area length estimates reflecting the fluctuation in ventricular geometry. This model enables the component of patient variance and method or geometric fluctuation variance to be estimated, as well as its percentage contribution to the variation. Application of this analysis procedure to volume estimates by the four echocardiographic complementary apical views showed that 27% and 17% of the variance of single plane estimates can be attibuted to fluctuations in ventricular geometry. This is for the traced area and ellipse of best fit method respectively. The paired Student t-test showed the average sample volume estimates which ranged from 43.6ml to 37.5ml for the traced area method and 38.8 ml to 32.8 ml for the ellipse of best fit method, to be significantly different, $p<0.025$ and $p<0.005$ respectively. In each instance the 45^{o} clockwise apical view and the 45^{o} anticlockwise apical view gave the maximum and minimum estimates respectively. This analysis supports the need to use multiple spatial images of the left ventricle to adequately estimate chamber volume and to adequately describe ventricular geometric which has been shown to fluctuate significantly ($p<0.01$). The impact of the geometric fluctuation on volume estimates can only be reduced by the use of multiple spatial images. This approach will enhance the ability to discriminate between pathologicial patient groups or to more effectively monitor a patients progress following treatment. The improved discrimination being a consequence of the reduced variance in the volume estimates caused by geometric fluctuations.

The Model II analysis applied to the three echocardiographic methods of volume estimation, the average of the four traced area and four ellipse of best fit area-length methods and the polar integration method, demonstrated that the proportion of variance associated with the methods was 5%. Note that the area-length estimates are an average of the four individual estimates and that the use of multiple view methods of volume estimation has reduced the proportion of the variance which is method dependant. Keep in mind that different methods, because of the views selected for the estimation, are inherently limited by geometric fluctuations in their volume estimations. The previous analysis could have been considered an analysis of geometry. The 5% proportion of variance attributable to the methods is a marked reduction on the 27% and 17% of the previous analysis. Nevertheless, using the Newman - Keul method (Snedecor, Cochran, 1967) the area length estimates (35.9ml and 39.1ml) are statistically less than the polar estimate (42.9ml) ($p<0.01$). However, the polar estimates are not statisically different to the fluid volume estimates.

Multiple tomographic apical images used to spatially reconstruct the left ventricle provide volume estimates which are not statistically different to directly measured chamber fluid volumes. The reconstruction then more effectively describes the spatial geometric fluctuations inherent in the ventricular chamber because of the correspondence in volume estimation.

6.4 In Vivo Studies.

Fifty six adult patients, 37 males and 19 females, were investigated by 2D echocardiography. The sample consisted of two principal groups one normal and one pathological. There were 22 normal patients, 12 males and 10 females, and 34 abnormal patients, 25 male and 9 females, with heterogeneous cardiac pathologies. The pathological group was further subdivided into a group that underwent left ventricular investigation by cardiac catherisation. Hence, 20 abnormal patients, 15 males and 5 females were catherised. The remaining, 14 patients, 10 males and 4 females, underwent 2D echocardiographic investigation. The 56 patients had a mean age 41.6 $\pm$ 3.6 years, body weight 64.8 $\pm$ 3.4 kg, height

164.7 $\pm$ 3.0 cm and body surface area 1.71 $\pm$ 0.06m^2 all of which were not significantly different to the corresponding values of the three subgroups, normal (A), pathological - catheterised (B), pathological - not catherised (C) (Table 6.18). Hence, the subgroups were anthropometrically similar .

The normal patients consisted of healthy volunteers or patients referred for cardiographic investigation but assessed as being normal. The 20 catheterised patients that underwent biplane left ventricular angiography were a group with hetergeneous pathologies which consisted of ischemic heart disease, aortic and mitral incompetence and/or stenosis though one patient was assessed as normal (Table 6.19). This group was also studied echocardiographically and represented 75% of 27 consecutive patients undergoing biplane left ventricular argiography in this laboratory. The remaining 25% were excluded because of poor quality angiography and/or echocardiography for quantitative assessment. A further 14 patients with various pathologies were examined echocardiographically (Table 6.20).

ANTHROPOMETRIC DATA

Patient Groups	Number	Age (Yrs)	Height (cm)	Weight (kg)	BSA (m^2)
Normal (A)	22	33.7 $\pm$ 4.4	162.2 $\pm$ 4.4	68.1 $\pm$ 3.9	1.66 $\pm$ 0.07
Catheterised (B)	20	45.2 $\pm$ 3.6	165.7 $\pm$ 2.4	66.5 $\pm$ 5.0	1.71 $\pm$ 0.06
Not Catheterised (C)	14	54.3 $\pm$ 9.1	158.8 $\pm$ 4.0	58.0 $\pm$ 4.2	1.58 $\pm$ 0.08
B+C	34	49.5 $\pm$ 3.3	165.8 $\pm$ 2.1	65.9 $\pm$ 3.3	1.73 $\pm$ 0.05
A+B+C	56	41.6 $\pm$ 3.6	164.7 $\pm$ 3.0	64.8 $\pm$ 3.4	1.71 $\pm$ 0.06

Table 6.18 Mean and standard error of the mean for the anthropometric data of the patient study groups.
BSA is body surface area.

CATHETERISED PATIENT GROUP

Patient Number	Sex	Age (yrs)	LVEDP (mmHg)	Aortic BP (mmHg)	Asynergy	Diagnosis
1	M	54	24	120/60		IHD
2	M	20	12	75/45		VSD/AI
3	M	20	7	90/45		AI
4	F	43	15	110/70		MS
5	M	59	7	83/30	inferior aneurysm	IHD
6	M	58	8	145/80	antero-septal aneurysm	IHD
7	M	63	14	110/70		MI
8	M	61	10	97/64		MI/AS
9	M	63	12	130/75	posterior hypokinesis	IHD
10	M	52	12	120/70	infero-posterior aneurysm	IHD
11	M	62	22	160/80	antero-opical hypokinesis	IHD
12	M	44	20	120/75		AS/AI
13	M	43	20	140/80	apical-septal hypokinesis	IHD
14	F	67	14	160/80		Normal
15	M	50	15	140/90	antero-apical & lateral hypokinesis	IHD
16	M	55	6	160/70		AI
17	M	40	28	108/55		AS/AI
18	F	48	20	110/60		IHD/LVH
19	M	22	3	120/50		AI
20	F	51	24	110/55	infero-posterior apical hypokinesis	IHD

Table 6.19 Some haemodynamic data and the diagnosis of 20 patients that were investigated by cardiac catheterisation.

IHD - Ischemic Heart Disease
VSD - Ventricular Septal Defect
AI - Aortic Incompetence
MS - Mitral Stenosis
MI - Mitral Incompetence
AS - Aortic Stenosis
LVH - Left Ventricular Hypertrophy

NON CATHETERISED PATIENTS

Patient Number	Sex	Age (yrs)	Cuff BP (mmHg)	Asynergy	Diagnosis
21	M	25	150/70		AI
22	M	80	130/80		AS
23	M	65	130/80		MS
24	M	69	120/90		MI
25	M	20			AI
26	M	55	100/60	global LV impairment & inco-ordinate	AV replacement LV dysfunction
27	M	61			MI
28	F	19			MS
29	M	64	80/60		HOCM
30	F	54		postero-lateral akinesis	IHD
31	M	22			AI
32	F	24	120/70		MI/MS
33	M	59	130/90	inferior akinesis	IHD
34	F	72	170/100	inferior hypokinesis	IHD

Table 6.20 The diagnosis of 14 patients that were investigated by echocardiography because of clinical indications.

AI - Aortic Incompetence
AS - Aortic Stenosis
MS - Mitral Stenosis
MI - Mitral Incompetence
AV - Aortic Valve
LV - Left Ventricle
HOCM - Hypotrophic Cardio Myopathy
IHD - Ischemic Heart Disease

A Hewlett-Packard 77020A ultrasound imaging system was used for the non-invasive image data acquisition. A series of left ventricular apical views were recorded on video tape at various rotational degrees by transducer rotation, for use in three dimensional reconstruction of the left ventricle. This method was applied to 56 adult patients all in sinus rhythm, 20 of which underwent biplane left ventricular cardiac catheterisation. Each catheterised patient had 30^{o} right anterior oblique and 60^{o} left anterior oblique projections of the left ventricle recorded on cine film at 60 frames per second. Within 24 hours of catheterisation two dimensional echocardiograms were recorded on video tape. All patients were studied echographically in the supine or the left lateral decubitus position.

Using the methodology described in Chapter 5 the ventricular outline was traced on a digitizer tablet to accurately determine the ventricular slice area. Together then with the area of a superimposed ellipse of best fit over the ventricular tomogram, the volume was calculated by the single plane area - length algorithm,

$$V = \frac{8\ A^2}{3\Pi\ L}$$

where A is the area of the ventricular outline

L is the longest axis of the ventricle defined as the distance from the apex to the centre of the mitral value,

for each of the apical views use in the composit 3D reconstruction. The four complementary volume estimates were used to calculate an average value. In addition volume estimates were calculated for all patients by the polar integration method applied to the 3D spatial reconstruction of the ventricle. The algorithm used,

$$\text{Volume (v)} = \frac{\Pi}{8}\ H \sum_{j=i}^{10} \sum_{i=i}^{8} r_i^2$$

where r_i is the radius of a sector.

i is the number of sectors

j is the number of slice seg ments.

H is the slice thickness,

was described in Chapter 5. Finally, the volume estimates from the biplane left ventricular angiograms were calculated by the Dodge and Sandler (1960) biplane algorithm for an ellipsoidal ventricular model. The algorithm is

$$V = \frac{\pi}{6} L D_1 D_2$$

where L is the largest axis of either projection and

D1, D2, the minor axes of each projection, described in Chapter 5.

In the clinical setting invasive and non invasive "standards" for comparative left ventricular volume estimation were chosen. In the case of echocardiographic assessment, volume estimation by the 3D spatial reconstruction polar integration algorithm, was selected as optimal. The theoretical basis, geometrical and in vitro analysis presented thus far provide the rational for this selection. On the other hand it is generally accepted by consensus in the literature that the invasive biplane technique proposed by Dodge and Sandler (1960) is an appropriate comparative standard. Furthermore, biplane oblique left ventriculography has been validated as a method of assessing true left ventricular volume (Wynne, Green, Mann et al, 1978).

Volume for each patient was estimated at end diastole and end systole in a give cardiac cycle. End diastole was defined as the onset of the QRS complex or the largest left ventricular cavity and end systole the end of the T wave or smallest left ventricular cavity. This criteria was applied to both the echocardographic and ventriculographic studies. The images were manually traced and processed as described in Chapter 5.

The comparison of each of the area-length and superimposed ellipse of best fit volume estimates to the polar integration estimate was performed by regression analysis. This was undertaken for each subgroup of the 57 patients studied. That is 22 normals, 20 pathological patients that underwent biplane left ventriculogrpahy and 14 pathological patients investigated echographically. The resulting linear regression equations of the form y = mx + b showed variation in the value of both the regression constant (b) and coefficient (m) (Table 6.21 - 6.26) For the normal group, the ellipse of best fit and traced area, b ranges from 23.51 to 44.73 and 24.84 to 46.01, m ranges from 0.74 to 0.99 and 0.64 to 0.83 respectively at end diastole. At end systole, b ranges from 10.55 to 29.55 and 10.00 to 24.21, m ranges from 0.75 to 1.18 and 0.72 to 0.96 respectively. All the regressions were statistically significant ($P<0.005$). For the pathological group of patients that were catheterised, the ellipse of best fit and traced area regressions at end diastole, b ranges from 36.46 to 71.11 and 25.05 to 74.91, m ranges from 0.72 to 0.95 and 0.62 to 0.96 respectively. At end systole, b ranges from 27.38 to 52.31 and 20.08 to 52.64, m ranges from 0.73 to 1.00 and 0.60 to 0.92 respectively. All the regressions were statistically significant ($P<0.005$) except the end systole single plane traced area-length estimates at 45^{o} anticlockwise transducer rotation from the four chamber reference view ($P<0.05$). For the pathological group of patients not catheterised, again for the ellipse of best fit and the traced

NORMAL PATIENTS

Comparison of Echographic Methods for
Determining Left Ventricular Volume in Vivo

Method	Regression Equation	Correlation Coefficient	SEE (ml)	Δ%D$\pm$ SD
	End Diastolic Volume			
Polar Integration vs Traced Area length				
4 Chamber	y =39.81 + 0.69x	0.788	14.4	4.6 $\pm$ 13.3
45 Anticlockwise	y =46.01 + 0.64x	0.840	12.7	6.0 $\pm$ 12.8
2 Chamber	y =32.30 + 0.81x	0.827	13.2	10.6 $\pm$ 11.4
45 Clockwise	y =24.84 + 0.83x	0.671	17.4	3.5 $\pm$ 14.1
Polar Integration vs Single Plane Ellipse				
4 Chamber	y =44.73 + 0.74x	0.735	15.9	15.9 $\pm$ 12.7
45 Anticlockwise	y =35.18 + 0.83x	0.919	9.2	16.5 $\pm$ 10.1
2 Chamber	y =33.65 + 0.89x	0.823	13.3	19.8 $\pm$ 10.7
45 Clockwise	y =23.51 + 0.99x	0.774	14.8	18.9 $\pm$ 10.4
Polar Integration vs Average of Area Length	y = 2.44 + 1.04x	0.937	7.97	5.7 $\pm$ 5.5
Polar Integration vs Average of Single Plane	y =13.23 + 1.08x	0.918	9.10	17.8 $\pm$ 6.3

Table 6.21 The three dimensional echographic volume estimate of normal in vivo hearts compared to area length echographic estimates at end diastole. SEE is the standard error of estimate, Δ%D$\pm$ SD is the mean percentage difference $\pm$ standard deviation related to the three dimensional echographic volume estimate.

NORMAL PATIENTS

Comparison of Echographic Methods for
Determining Left Ventricular Volume in Vivo

Method	Regression Equation	Correlation Coefficient	SEE (ml)	Δ%D± SD
	End Systolic Volume			
Polar Integration vs Traced Area length				
4 Chamber	y =10.59 + 0.96x	0.827	8.2	14.2 ± 14.6
45 Anticlockwise	y =18.51 + 0.79x	0.869	7.2	14.9 ± 13.0
2 Chamber	y =24.21 + 0.72x	0.769	9.3	19.0 ± 16.8
45 Clockwise	y =10.01 + 0.80x	0.812	8.5	-2.8 ± 16.0
Polar Integration vs Single Plane Ellipse				
4 Chamber	y =10.55 + 1.18x	0.765	9.4	29.8 ± 13.3
45 Anticlockwise	y =19.78 + 0.92x	0.840	7.9	29.4 ± 12.3
2 Chamber	y =29.55 + 0.75x	0.697	10.2	34.9 ± 14.8
45 Clockwise	y =12.17 + 1.04x	0.810	8.5	22.6 ± 11.9
Polar Integration vs Average of Area Length	y = 0.91 + 1.11x	0.959	4.04	10.7 ± 5.3
Polar Integration vs Average of Single Plane	y = 5.22 + 1.28x	0.924	5.44	29.1 ± 6.9

Table 6.22 The three dimensional echographic volume estimate of normal in vivo hearts compared to area length echographic estimates at end systole. SEE is the standard error of estimate, Δ%D±SD is the mean percentage difference ± standard deviation related to the three dimensional echographic volume estimate.

PATHOLOGICAL PATIENTS (CATHETERISED)

Comparison of Echographic Methods for
Determining Left Ventricular Volume in Vivo

Method	Regression Equation	Correlation Coefficient	SEE (ml)	Δ%D± SD
	End Diastolic Volume			
Polar Integration vs Traced Area length				
4 Chamber	y =25.05 + 0.88x	0.926	24.7	4.4 ± 14.6
45 Anticlockwise	y =74.91 + 0.62x	0.694	47.1	7.0 ± 21.7
2 Chamber	y =25.65 + 0.96x	0.948	20.9	12.0 ± 11.0
45 Clockwise	y =26.25 + 0.89x	0.937	22.8	4.6 ± 12.7
Polar Integration vs Single Plane Ellipse				
4 Chamber	y =38.76 + 0.90x	0.937	22.9	16.4 ± 13.9
45 Anticlockwise	y =71.11 + 0.72x	0.761	42.4	19.6 ± 17.1
2 Chamber	y =42.31 + 0.92x	0.951	20.3	21.4 ± 11.6
45 Clockwise	y =36.46 + 0.95x	0.958	18.8	19.3 ± 10.3
Polar Volume vs Average of Area Length	y = 6.51 + 1.03	0.987	10.2	6.7 ± 5.7
Polar Integration vs Average of Single Plane	y =25.00 + 1.03x	0.989	9.5	18.5 ± 5.9

Table 6.23 The three dimensional echographic volume estimate of catheterised in vivo hearts compared to area length echographic estimates at end diastole. SEE is the standard error of estimate, Δ%D±SD is the mean percentage difference ± standard deviation related to the three dimensional echographic volume estimate.

PATHOLOGICAL PATIENTS (CATHETERISED)

Comparison of Echographic Methods for
Determining Left Ventricular Volume in Vivo

Method	Regression Equation	Correlation Coefficient	SEE (ml)	Δ%D$\pm$ SD
	End Systolic Volume			
Polar Volume vs Traced Area length				
4 Chamber	y =24.56 + 0.81x	0.859	22.8	7.3 $\pm$ 19.6
45 Anticlockwise	y =52.64 + 0.60x	0.547	37.2	10.0 $\pm$ 16.6
2 Chamber	y =21.69 + 0.92x	0.937	15.6	15.4 $\pm$ 13.5
45 Clockwise	y =20.08 + 0.84x	0.881	21.0	3.3 $\pm$ 18.3
Polar Volume vs Single Plane Ellipse				
4 Chamber	y =29.10 + 0.93x	0.876	21.5	26.0 $\pm$ 20.1
45 Anticlockwise	y =52.31 + 0.73x	0.623	34.8	28.5 $\pm$ 13.5
2 Chamber	y =31.94 + 0.95x	0.941	15.0	29.9 + 14.4
45 Clockwise	y =27.38 + 1.00x	0.908	18.6	28.0 $\pm$ 16.0
Polar Volume vs Average of Area Length	y = 3.06 + 1.07x	0.973	10.0	9.4 $\pm$ 6.1
Polar Integration vs Average of Single Plane	y =18.78 + 1.11x	0.962	11.8	27.8 $\pm$ 9.2

Table 6.24 The three dimensional echographic volume estimate of catheterised in vivo hearts compared to area length echographic estimates at end systole. SEE is the standard error of estimate, Δ%D$\pm$SD is the mean percentage difference $\pm$ standard deviation related to the three dimensional echographic volume estimate.

PATHOLOGICAL PATIENTS (NOT CATHETERISED)

Comparison of Echographic Methods for
Determining Left Ventricular Volume in Vivo

Method	Regression Equation	Correlation Coefficient	SEE (ml)	Δ%D ± SD
	End Diastolic Volume			
Polar Integration vs Traced Area length				
4 Chamber	y = 6.51 + 1.01x	0.964	22.1	4.7 ± 14.9
45 Anticlockwise	y = 7.53 + 1.03x	0.943	27.6	4.3 ± 18.6
2 Chamber	y =25.89 + 0.87x	0.975	18.6	6.0 ± 11.8
45 Clockwise	y =17.19 + 0.96x	0.954	24.8	6.1 ± 18.9
Polar Integration vs Single Plane Ellipse				
4 Chamber	y =19.06 + 1.13x	0.943	27.5	20.5 ± 14.2
45 Anticlockwise	y =23.78 + 1.07x	0.935	29.3	21.8 ± 12.9
2 Chamber	y =31.50 + 0.99x	0.982	15.6	20.3 ± 10.1
45 Clockwise	y =36.11 + 1.01x	0.925	31.4	23.5 ± 18.2
Polar Integration vs Average of Area Length	y = 4.63 + 1.03x	0.996	27.3	7.3 ± 3.5
Polar Integration vs Average of Single Plane	y =16.51 + 1.13x	0.984	14.0	21.4 ± 5.9

Table 6.25 The three dimensional echographic volume estimate of non catheterised patient hearts compared to area length echographic estimates at end diastole. SEE is the standard error of estimate, Δ%D± SD is the mean percentage difference ± standard deviation related to the three dimensional echographic volume estimate.

PATHOLOGICAL PATIENTS (NOT CATHETERISED)

Comparison of Echographic Methods for
Determining Left Ventricular Volume in Vivo

Method	Regression Equation	Correlation Coefficient	SEE (ml)	Δ%D ± SD
	End Systolic Volume			
Polar Integration vs Traced Area length				
4 Chamber	y =-5.66 + 1.39x	0.879	37.4	10.8 ± 12.3
45 Anticlockwise	y = 2.54 + 1.46x	0.851	41.3	23.1 ± 13.5
2 Chamber	y = 8.89 + 1.20x	0.887	36.3	9.4 ± 16.4
45 Clockwise	y =21.52 + 0.93x	0.820	44.9	-1.3 ± 16.7
Polar Integration vs Single Plane Ellipse				
4 Chamber	y =11.29 + 1.40x	0.820	44.9	24.7 ± 13.9
45 anticlockwise	y = 7.30 + 1.69x	0.900	34.2	37.1 ± 9.0
2 Chamber	y =18.44 + 1.39x	0.874	38.1	30.7 ± 15.4
45 Clockwise	y =23.95 + 1.28x	0.894	35.2	31.6 ± 13.0
Polar Integration vs Average of Area Length	y =-4.39 + 1.25x	0.951	23.3	10.5 ± 5.4
Polar Integration vs Average of Single Plane	y =11.66 + 1.50x	0.894	33.7	31.5 ± 8.3

Table 6.26 The three dimensional echographic volume estimate of non catheterised patient hearts compared to area length echographic estimates at end systole. SEE is the standard error of estimate, Δ%D ± SD is the mean percentage difference ± standard deviation related to the three dimensional echographic volume estimate.

area regressions at end diastole b ranges from 19.06 to 36.11 and 6.51 to 25.89, m ranges from 0.99 to 1.13 and 0.87 to 1.03 respectively. At end systole, b ranges from 7.30 to 23.95 and -5.66 to 21.52, m ranges from 1.28 to 1.69 and 0.93 to 1.46 respectively. All the regressions were statistically significant ($P<0.005$).

Consideration of the polar integration volume estimate as the echographic "standard" allows the estimation of systematic and random error of the ellipse of best fit and traced area methods of volume measurement in each of the patient groups. That is the normal, non-catherterised and catherised patient groups.

The ellipse of best fit has systematic errors significantly greater then zero ($P<0.001$) for both end diastole and end systole in all patient groups (Table 6.21 - 6.26). However, the traced area single plane method has systematic errors significantly greater than zero for a variety of views depending on whether the view is at end diastole or end systole as well as the patient group (Table 6.21 - 6.26). For instance the end diastolic estimates of the non catheterised patient group have no systematic error with respect to the 3D polar integration estimate. On the other hand end systole in the normal patient group has a significant bias for all views except the 45^{o} clockwise view.

By a one way analysis of variance none of the views at end diastole show a statistical difference in the magnitude of the bias for each patient group irrespective of the single plane method used. For end systole, by the ellipse of best fit method, the two chamber view and the 45^{o} anticlockwise view have the largest bias in the normal and non catheterised patient groups respectively. The catherterised group shows no statistical difference in the magnitude of the bias. By the traced area method the 45^{o} clockwise view has the smallest bias for both the normal and pathological patient groups while the 45^{o} anticlockwise view has the largest bias for the non catherised group and the 2 chamber view for the other groups.

Comparison of bias between end diastole and end systole for the normal patient group, end systolic bias is greater than that for end diastole ($P<0.01$) for all views irrespective of the single plane method. However, with the traced area method for the other two patient groups there was no statistical difference in the bias between end diastole and end systole except for the 45^{o} anticlockwise view in the non catheterised group. End systolic bias was greater than end diastolic ($P<0.01$). On the other hand for the ellipse of best fit method, the two patient groups had bias significantly greater for end systole than end diastole ($P<0.01$) except for the four chamber view of the non catheterised group.

The random error estimates between views for each method show no statistical difference. This is also the case between end diastole and end systole. In addition the random error is the same between each patient group.

The average volume estimates derived from the four apical views for each single plane area method gave significant regressions ($P<0.001$) on the 3D reconstruction polar integration estimate (Table 6.21-6.26) for the three patient groups at both end diastole and end systole. These regressions take into account the fluctuations in geometry of the left ventricle which influence the volume estimates. Residual variance analysis of the traced area and ellipse of best fit regressions indicates that they are homogenous except for the non catheterised pathological group where end diastolic volumes are found to have heterogenious residual variances ($P<0.025$) (Table 6.27). Further analysis of convariance shows that for all the groups at end diastole and end systole the traced area regressions are statistically different to the ellipse of best fit.

In particular the traced area - length estimates are better than the ellipse of best fit although the slopes are not statistically different the intercepts are closer to zero and less than the ellipse of best fit intercepts ($P<0.001$) (Table 6.27). End diastolic volume regressions for the non catheterised pathological group however showed heterogeneous residual variance, therefore both slope and intercept are statistically different

ANALYSIS OF COVARIANCE

Echocardiographic Methods

Patient Groups

	Normal	Pathological (Catheterised)	Pathological (Not Catheterised)
End Diastolic Volume (EDV)			
ALX4 VS PI10	$Y = 2.44 + 1.04x$	$Y = 6.51 + 1.03x$	$Y = 4.63 \pm 1.03x$
SPEX4 VS PI10	$Y = 13.23 + 1.08x$	$Y = 25.0 + 1.03x$	$Y = 16.51 \pm 1.13x$
End Systolic Volume (ESV)			
ALX4 VS PI10	$Y = 0.91 + 1.11x$	$Y = 3.06 + 1.07x$	$Y = 4.39 \pm 1.25x$
SPEX4 VS PI10	$Y = 5.22 + 1.28x$	$Y = 18.78 + 1.11x$	$Y = 11.66 \pm 1.50x$
Residual Variances			
EDV	N.S.	N.S.	P<0.025
ESV	N.S.	N.S.	N.S.
Slope			
EDV	N.S.	N.S.	-
ESV	N.S.	N.S.	N.S.
Intercept			
EDV	P<0.001 (ALX4<SPEX4)	P<0.001 (ALX4<SPEX4)	-
ESV	P<0.001 (ALX4<SPEX4)	P<0.001 (ALX4<SPEX4)	P<0.001 (ALX4<SPEX4)

Table 6.27 Analysis of covariance on between echographic method regressions.

PI10 - Three dimensional echographic volume estimate
ALX4 - Average of four traced single plane area length echographic volume estimates
SPX4 - Average of four ellipse of best fit single plane area length echographic volume estimates
EDV - End diastolic volume
ESV - End systolic volume

($P<0.025$). The systematic error for the averaged traced area and averaged ellipse of best fit is statistically significant ($P<0.001$) and the error for the traced area method is significantly less than for the ellipse of best fit ($P<0.001$) in all patient groups. The random error on the other hand is the same for both methods and end systole at end diastole in all patient groups. Therefore, the traced area length volume estimates averaged over the four rotational apical views provides the best volume estimates compared to the 3D reconstruction polar integration technique.

Consideration of the traced area length regression only on the polar integration estimates for the three patient groups reveals that the normal group compared to both pathological groups and comparison between the two pathological groups have homogeneous residued variance for end diastole but heterogeneous variance ($P<0.001$) for end systole (Table 6.28). This is, because the polar integration method makes no particular assumption about ventricular geometry and the traced area length method assumes the chamber to be an ellipsoid of rotation, as a general rule end

ANALYSIS OF COVARIANCE

ECHOCARDIOGRAPHIC METHOD (AL X 4 VS PI10)

PATIENT GROUPS

	Normal (N)	Pathological (Catheterised) (C)	Pathological (Not Catherised) (NC)
EDV	y = 2.44 + 1.04x	y = 6.51 + 1.03x	y = 4.63 + 1.03x
ESV	y = 0.91 + 1.11x	y = 3.06 + 1.07x	y = 4.39 + 1.25x

Residual Variances

Comparison of Patient Groups

	N cf C	N cf C	C cf NC
EDV	N.S.	N.S.	N.S.
ESV	P<0.005	P<0.001	P<0.005

EDV

Slope	P<0.001 N>C	P<0.05 N>NC	N.S.
Intercept	P<0.005 N<C	P<0.025 N<NC	P<0.05 N<C

ESV

Heterogeneous residual variance therefore slope and intercepts are different.

Table 6.28 Analysis of covariance on between end diastolic and end systole echographic method regressions.

cf - compared with.
EDV - End diastolic volume
ESV - End systolic volume

diastolic volumes tend to be ellipsoidal in shape, so the traced area length may be applicable though accuracy of the estimates fluctuate. On the other hand end systolic left ventricular chamber geometry is fundamentally diverse between patient groups. Again because the 3D reconstruction polar integration technique makes minimal assumptions about chamber geometry in contrast to the traced area length method, if the left ventricle takes up a chamber shape that does not transform to an approximate ellipsoid this discrepency reveals itself in heterogeneous residual variance. Analysing end diastolic volumes more closely reveals that the slope of the regressions is statistically greater for the normal patient group than for the two pathological groups $P<0.001$ and $P<0.05$ for the catheterised and non catheterised group respectively. There is no difference between the two pathological groups themselves. The y-intercept is smallest for the normal group compared to the two pathological groups and the non catheterised group has a smaller intercept value than the catherised group (Table 6.28).

To further confirm these results an analysis of each of the apical view traced area length volume estimates regressed on the polar integration shows that for end systole the residual variances are heterogeneous for all the apical views in the comparison of normals to pathological groups and between the pathological groups except for the 45^{o} anticlockwise transducer rotation from the four chamber reference view (Table 6.29) for the latter comparison. The end diastolic comparisons have an equal number of views showing heterogeneous and homogeneous residual variances (Table 6.29).

The catheterised group of patients allowed the biplane volume estimates, at both end diastole and systole, to be made using the Dodge and Sandler (1960) technique applied to oblique ventriculographic projections (Wynne, Green, Mann et al, 1978). These estimates were used as an independent standard against which to evaluate the performance of the 3D reconstruction polar integration technique. Regression of traced area - length estimates on both polar integration and ventriculographic estimates were compared. Comparison of the residual variances shows them to

ANALYSIS OF COVARIANCE

ECHOCARDIOGRAPHIC METHOD (AL View VS PI10)

Polar Integration VS
Traced Area Length

	Normal (N)	Pathological (Catheterised) (C)	Pathological (Not Catheterised) (NC)

Residual Variances
Comparison of Patient Groups

	N cf C	N cf NC	C cf NC
End Diastolic Volume			
4 Chamber	P<0.025	P<0.05	N.S.
45 Anticlockwise	P<0.005	P<0.005	P<0.05
2 Chamber	P<0.025	N.S.	N.S
45 Clockwise	N.S.	N.S.	N.S.
End Systolic Volume			
4 Chamber	P<0.005	P<0.001	P<0.05
45 Anticlockwise	P<0.001	P<0.001	N.S.
2 Chamber	P<0.025	P<0.001	P<0.005
45 Clockwise	P<0.005	P<0.001	P<0.005

Table 6.29 Analysis of covariance between patient groups for method regressions.

be heterogenous for both end diastole (P<0.001) and end systole (P<0.005). The implication is that the polar integration and ventriculography are estimating volumes from fundamentally different images together with different ventricular models. The polar integration technique utilised multiple tomographic apical left ventricular views and makes minimal assumptions about ventricular chamber geometry. On the other hand biplane ventriculography utilises projections, onto two dimensions, of the left ventricular chamber following the injection of a radio opaque dye into the chamber. These projections are then assumed to represent orthogonal views of an ellipsoidal chamber. It is interesting to note that comparison of the regression of traced area - length averaged estimates on ventriculographic estimates for end diastole and end systole also shows hetergeneity of residual variance which reflect a change in fundamental shape of the left ventricular projections. However, comparison of the regression of traced area-length estimates on the polar integration estimates shows homogeneous residual variances with no statistical difference in scope or intercept. The tomographic views then do not change in fundamental shape for the catheterised pathological group while the normal group and the non catherised pathological group have heterogeneous variances. These results highlight the problems of comparative studies between models based on different imaging modes and different assumptions of left ventricular chamber geometry (Table 6.30). Nevertheless regression of polar integration estimates on the ventriculographic estimates are statistically significant ($P<0.005$).

The invasive cineangiographic "standard" was used to evaluate the echographic volume estimates for systematic and random errors. The four apical views used to estimate left ventricular volume by the traced area single plane method have statistically significant bias for end diastole, $P<0.025$ and $P<0.005$ for the four chamber, 45^{o} clockwise and 45 deg anticlockwise, two chamber views respectively. For end systole, only the 45^{o} clockwise view has a significant bias ($P<0.025$). The random error is the same for all views in both end diastole and end systole. However, compared to the traced area with the polar integration reference the random error is significantly larger

PATHOLOGICAL PATIENTS (CATHETERISED)

Comparison of Angiographic and Echographic Methods for Determining Left Ventricular Volume in Vivo

	Regression Equation	Correlation Coefficient	SEE (ml)	$\Delta\%D \pm SD$
		End Diastolic Volume		
ANGIO VS ALX4	Y =46.48 + 0.90x	0.772	46.4	17.8 ± 18.1
PI10 VS ALX4	Y = 6.51 + 1.03x	0.987	10.2	6.7 ± 5.7
ANGIO VS PI10	Y =50.76 + 0.81x	0.728	50.1	8.7 ± 26.1
		End Systolic Volume		
ANGIO VS ALX4	Y = 6.51 + 0.79x	0.754	27.9	-30.4 ± 56.2
PI10 VS ALX4	Y = 3.06 + 1.07x	0.973	10.0	9.4 ± 6.1
ANGIO VS PI10	Y = 7.80 + 0.70x	0.738	28.6	-38.9 ± 63.2

Table 6.30 Angiographic volume estimate of catheterised in vivo hearts compared to echographic estimates at end diastole and end systale. SEE is the standard error of estimate, $\Delta\%D \pm SD$ is the mean percentage difference ± standard deviation related to the three dimensional echographic volume estimate.

PI10 - Three dimensional echographic volume estimate

ALx4 - Average of four traced single plane area length echographic volume estimates

ANGIO - Invasive angiographic biplane volume estimate for the angiographic end systolic estimates ($P<0.005$) and the two chamber end diastolic view ($P<0.025$).

For the four view average the bias is significant at both end diastole and end systole $P<0.001$ and $P<0.05$ respectively. The random error is greatest for end systole ($P<0.025$). Also, the systematic and random errors are greatest in magnitude for the angiographic compared to the polar estimates ($P<0.05$ and $P<0.025$ respectively for end diastole and $P<0.001$ and $P<0.005$ respectively for end systole).

Finally for angiographic versus polar integration the systematic error is significant for end systole ($P<0.01$) and signficiantly different between end diastole and end systole ($P<0.001$). However, the end systolic bias is negative indicating that the echographic estimates of ventricular volume in this instance is greater than the invasive estimate. The end diastolic estimate showed no significant bias in its volume estimate. The random error is signficiantly larger for end systole ($P<0.025$) (Table 6.30).

Again, to identify and estimate sources of variability associated with ventricular geometry a variance components model using one way analysis of variance was formulated and used (Sokal, Rohlf, 1981). A one way analysis of variance components model using a Model II approach was applied to the four single plane traced area-length estimates. This model enables the component of patient variance and geometric fluctuation variance to be estimated, as well as its percentage contribution to the variation. Application of this analysis procedure to the traced area-length volume estimates from each of the four echocardiographic complementary apical views showed significant geometric changes among the complementary views and between the patient groups ($P<0.005$) (Table 6.31). It is noteworthy that the largest percentage of variance attributable to changes in ventricular chamber geometry occurs in the normal patient group for both end diastole and end systole than for the catheterised group and least for the non catheterised group respectively. However, the magnitude of the geometric variance is greatest for the catheterised group and least for the normal group (Table 6.31). Comparisons of the variance

MODEL II ANALYSIS OF VARIANCE

	Normal	Pathological (Catheterised)	Pathological (Not Catheterised)
		Proportion of Variance (%)	
EDV	42	23	10
ESV	47	30	14
		Magnitude of Variance	
EDV	260.0	1045.8	613.3
ESV	107.9	590.3	421.6

Patient Groups

Table 6.31 Analysis of variance showing the proportion of variance attributable to fluctuations in ventricular geometry and the magnitude of the variance.

EDV - End diastolic volume

ESV - End systolic volume

magnitudes using the variance F-test shows that the two pathological groups have statistically significant larger variances than the normal group for both end diastole and end systole with $P<0.005$ except for the non catheterised group at end diastole where $P<0.05$. There is no statistically significant difference in the magnitude of the variance attributable to geometric changes between the two pathological groups, though the proportions are about half.

6.5 Left Ventricular Geometry.

As discussed earlier the geometric analysis that has been carried out to date has been performed on either single or biplane images. None of the methods have attempted a comprehensive analysis of ventricular geometry. In this section a detailed analysis of ventricular geometry will consider regional and global shape descriptions. A study will be made of the endocardial surface area and segmental volume for end diastole and end systole. In the first instance an analysis of five arbitrary ellipsoids will be presented followed by the description of a normal population sample consisting of 22 patients. Then the left ventricular geometry of 13 patients with ischemic heart disease will be examined.

6.5.1 Geometric Shapes

i) Surface area.

The surface area of ellipsoid shapes cannot be calculated directly so each ellipsoid was mathematically sliced into 200 slices. The surface area was calculated as described in Chapter 5 and used as the reference value.

In order to regionally describe the surface area of ellipsoidal vessels the mean value and coefficient of variation of the surface elements was calculated (Section 5.12). This was done for each short axis slice perpendicular to the major axis and each sector the length of the major axis (Figure 6.5). Two descriptive plots were made, one of the percentage surface area of the area elements versus the slice number and one of coefficient of variation of the surface area element for varying k respectively. For the case where sectors the

Figure 6.5 An ellipsoid of rotation with arbitrary major to minor axis ratio, k, which shows the computerised segmentation into long axis sectors and short axis slices. Sector and pentahedral volume elements for volume estimation are illustrated.

MP - Mid point
CC - Centre of Contraction at 1/3 the long axis

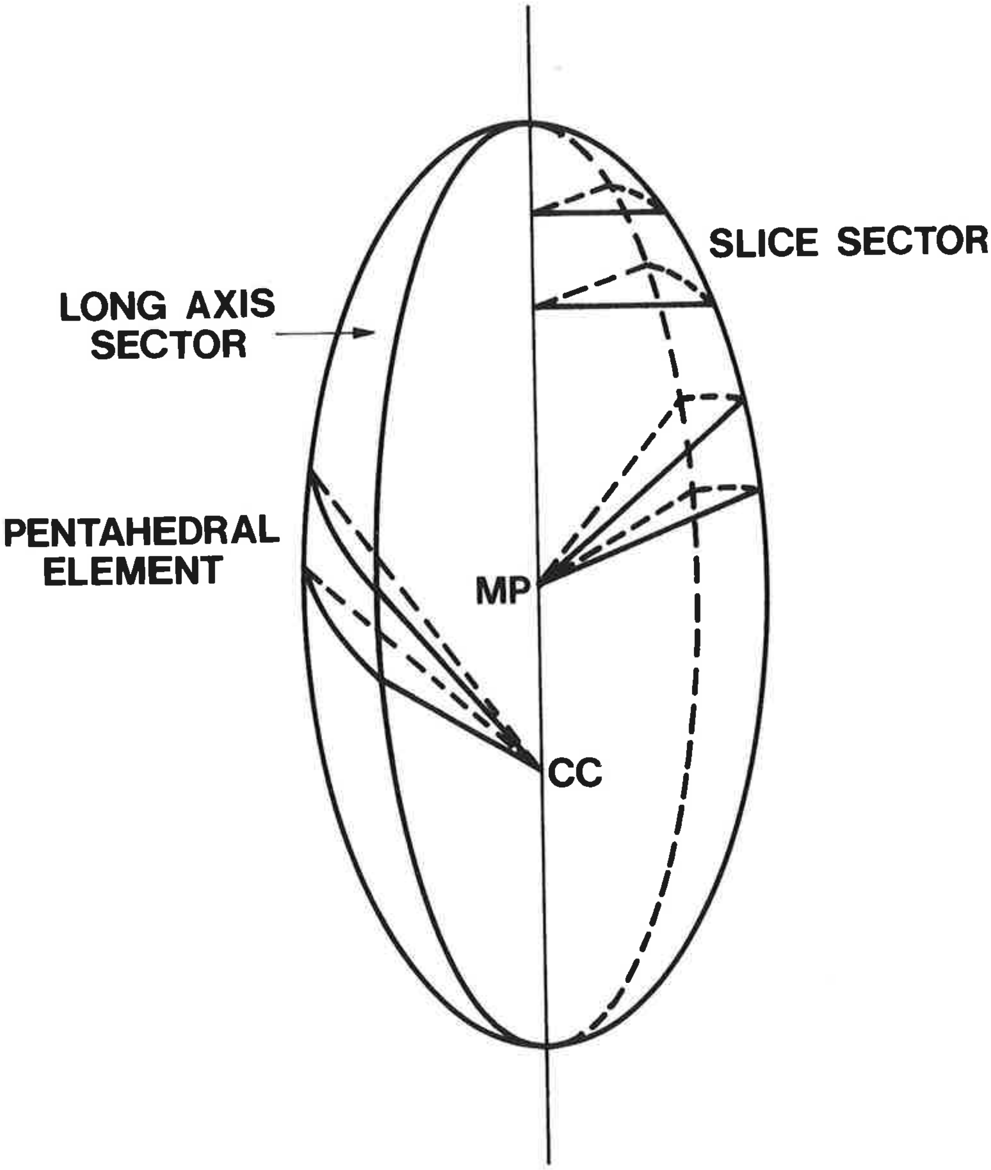

SLICE SECTOR
LONG AXIS
SECTOR
PENTAHEDRAL
ELEMENT
MP
CC

length of the major axis are taken the percentage surface area is a constant 12.5% in this instance where the ellipsoid is divided into eight equal sectors. Therefore, the coefficient of variation around the major axis is zero. The percentage area of short axis slices perpendicular to the major axis is characteristic of the general ellipsoid (Figure 6.6). Similarly the coefficient of variation asymptotes to a characteristic value. For ten slices the characteristic value is 40%.

ii) Volume.

The polar integration technique, applied to short axis slices perpendicular to the major axis and Pappus' Theorem, applied to the long axis centre and 1/3 along the major axis from the apex (the centre of contraction for the left ventricle) were used to calculate the percentage volume of elements from ellipsoids of varying k.

In each plot of percentage volume versus slice number or segment number the curves are characteristic of the ellipsoid vessel shape. The polar integration of slice volumes and Pappus'

Figure 6.6 The percentage surface area at ten levels of ellipsoids of arbitrary major to minor axis ratio, k, with respect to total surface area. This curve is characteristic of ellipsoid shapes and independent of ellipsoid magnitude.

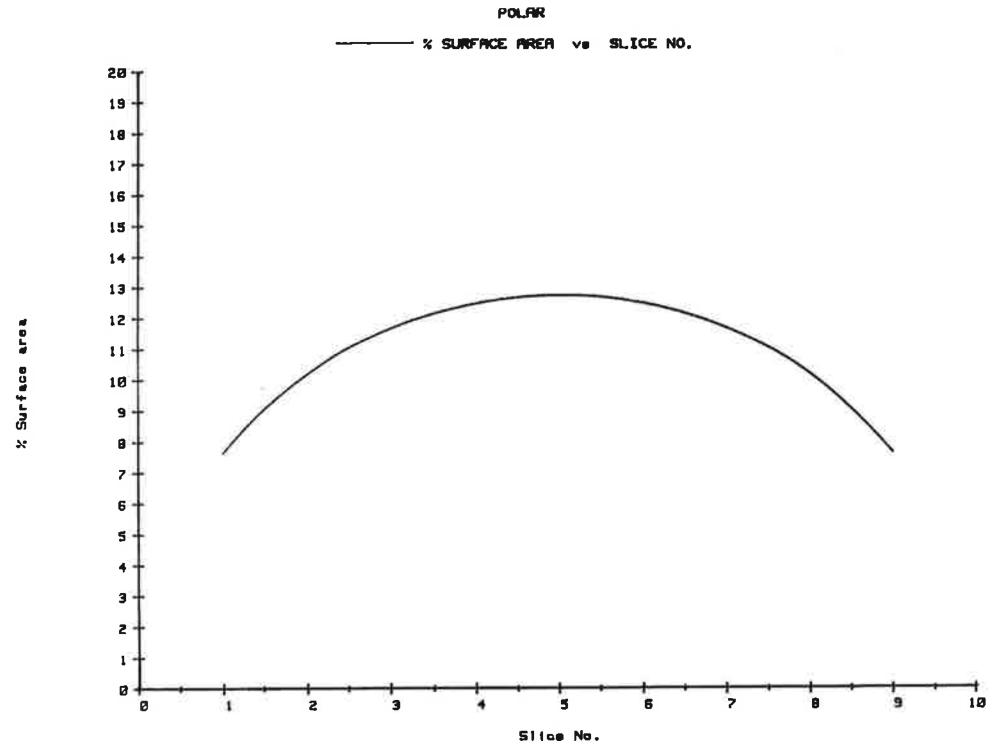

POLAR
% SURFACE AREA vs SLICE NO.
% Surface area
Slice No.

Theorem applied from the mid point of the long axis both present symmetrical characteristic plots as against the plot where Pappus' Theorem was applied 1/3 along the major axis from the apex (Fig. 6.7). The coefficient of variation asymptotes to a characteristic value for each analysis independent of the k value for the ellipsoid. For ten slices (eight sectors) the characteristic values for the polar integration and Pappus integrations at the mid point and at the centre of contraction are 50%, 3.8%, 21.2% respectively.

For the case where sectors the length of the major axis are taken the percentage volumes obtained by the three respective methods are constants. The volumes are a fixed 12.5% because in this instance the ellipsoid is divided into eight equal sectors. Therefore, the coefficient of variation around the major axis is zero.

This analysis provides the basis for a detailed study of global and regional geometry and geometric changes of the left ventricle. The characteristic plots and reference values for ellipsoids with arbitrary values of k or fixed

Figure 6.7 The percentage volume for ten levels of parallel short axis slices, eight contiguous pentahedral volume elements with the apex at the long axis mid point (0,0) and at the left ventricular centre of contraction (o,A/3). The percentage is with respect to total volume of ellipsoids with arbitrary major to minor axis ratios, k. The curves are characteristic of ellipsoid shapes and independent of ellipsoid magnitude.

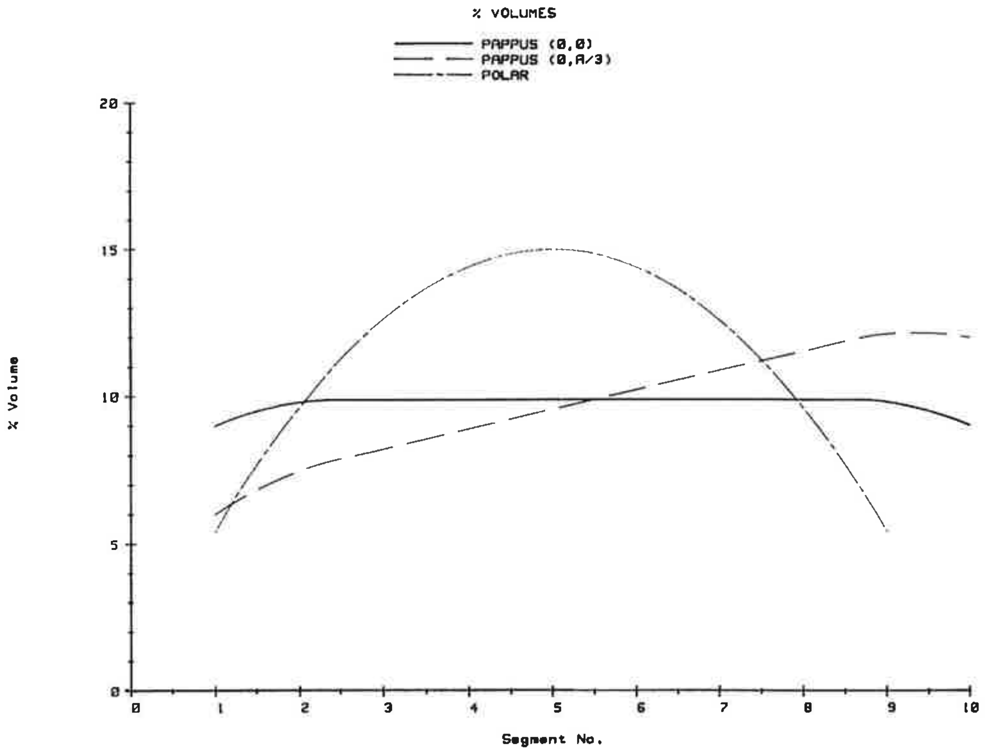

% VOLUMES
PAPPUS (0,0)
PAPPUS (0,A/3)
POLAR
% Volume
Segment No.
20
15
10
5
0
0
1
2
3
4
5
6
7
8
9
10

values of k will be used in a comparative study between 22 normal patients and 13 patients with ischemic heart disease.

6.5.2 In Vivo Study

The analysis of left ventricular patient data was carried out using the long axis sector and short axis slice procedure. The long axis analysis divides the ventricle into eight equally spaced sectors 45^{o} each, around the long axis which passes through the centre of the mitral valve oriface and ventricular apex. The short axis analysis segments the ventricle into ten equally spaced slices perpendicular to the ventricular long axis. Therefore, each long axis sector is divided into ten equally spaced slices and each slice is divided into eight equally spaced sectors. Hence the ventricle is divided into 80 symmetrically disposed elements (Fig. 6.8).

The elemental volume and surface area are plotted for each of the segmentation modes of the ventricle, short axis slices and both long axis mid point and centre of contraction point as

Figure 6.8 The computerised segmentation of the composite three dimensional left ventricular reconstruction at both end diastole and end systole. Long axis sectors and short axis slices are illustrated.

DIASTOLIC

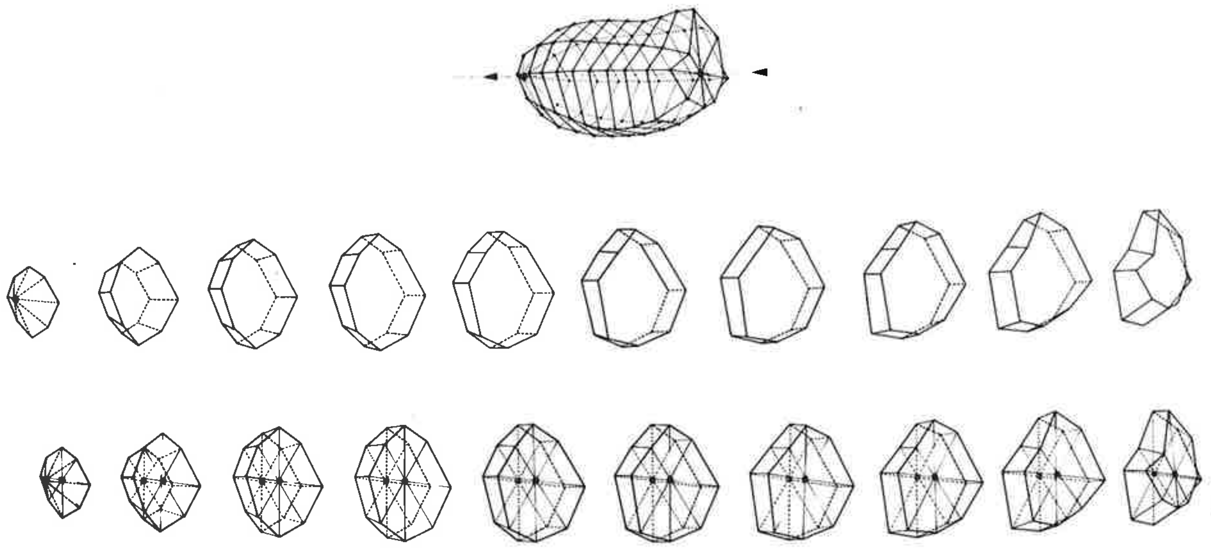

SYSTOLIC

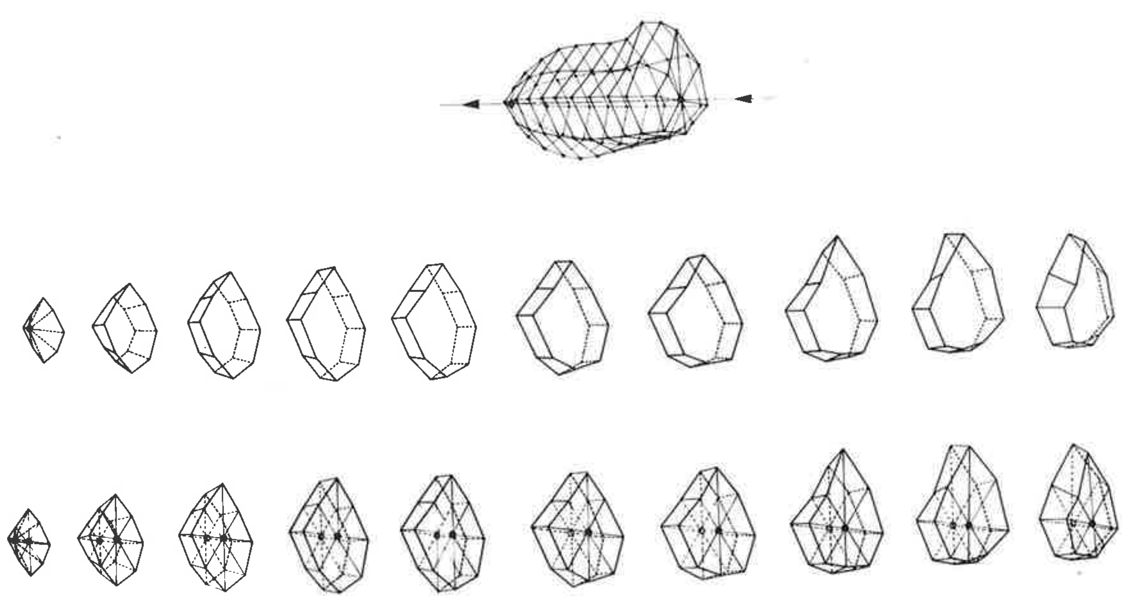

defined by Ingels (1980). The volume and surface area measures are normalised with respect to the total ventricular volume or surface area.

The analysis of 22 normal patients and 13 patients with ischemic heart disease was carried out. The data from the 22 normal patients was pooled to define the average trends in volume and surface area elements of the normal left ventricle. The 13 ischemic patients were individually analysed and compared to the normal patients behaviour.

i) Normal Patients

The long axis analysis of the left ventricle was first performed on the eight equally spaced sectors where each sector consisted of ten slices along the major axis. The average elemental volume and surface area for each segmentation mode was calculated for the eight sectors. The composite plot for the three segmentation modes of the volume elements is shown in figures 6.9. The surface area plot is shown in figure 6.10. The normalized volume and surface elements are expressed as a percentage.

Figure 6.9 The percentage left ventricular volume of eight long axis sectors with respect to total volume at end diastole and end systole respectively from a sample of 22 normal patients. The 95% confidence interval of both the mean values and sample are plotted.

Slice Number	
1	Medial
2	Posterio-Medial
3	Posterior
4	Postero-Lateral
5	Lateral
6	Antero-Lateral
7	Anterior
8	Antero-Medial

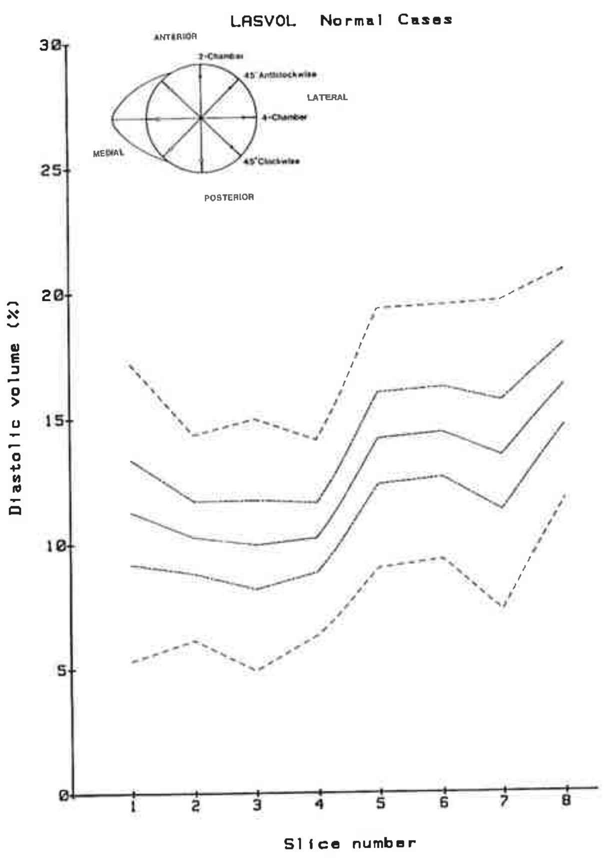
LASVOL Normal Cases
ANTERIOR
2-Chamber
45° Anticlockwise
LATERAL
4-Chamber
MEDIAL
45° Clockwise
POSTERIOR
Diastolic volume (%)
Slice number

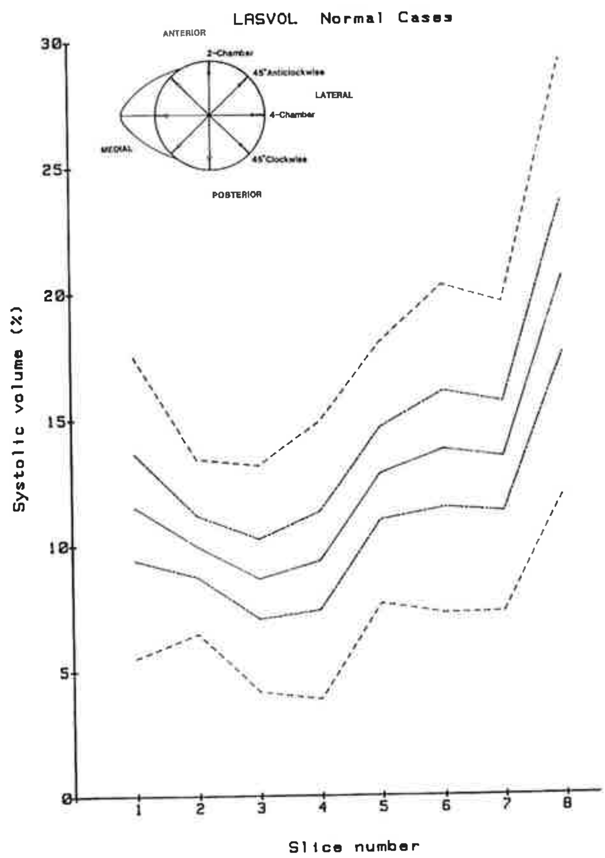
LASVOL Normal Cases
ANTERIOR
2-Chamber
45° Anticlockwise
LATERAL
4-Chamber
MEDIAL
45° Clockwise
POSTERIOR
Systolic volume (%)
Slice number

Figure 6.10 The percentage left ventricular myocardial surface area of eight long axis sectors with respect to total surface area at end diastole and end systole respectively from a sample of 22 normal patients. The 95% confidence interval of both the mean values and the sample are plotted.

Slice Number	
1	Medial
2	Postero-Medial
3	Posterior
4	Postero-Lateral
5	Lateral
6	Antero-Lateral
7	Anterior
8	Antero-Medial

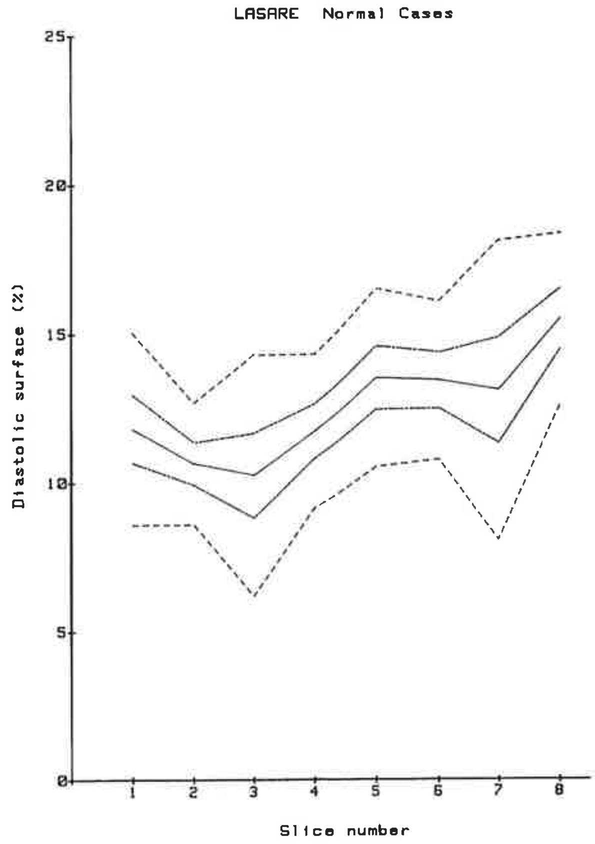
LASARE Normal Cases
Diastolic surface (%)
Slice number
0
5
10
15
20
25
1
2
3
4
5
6
7
8

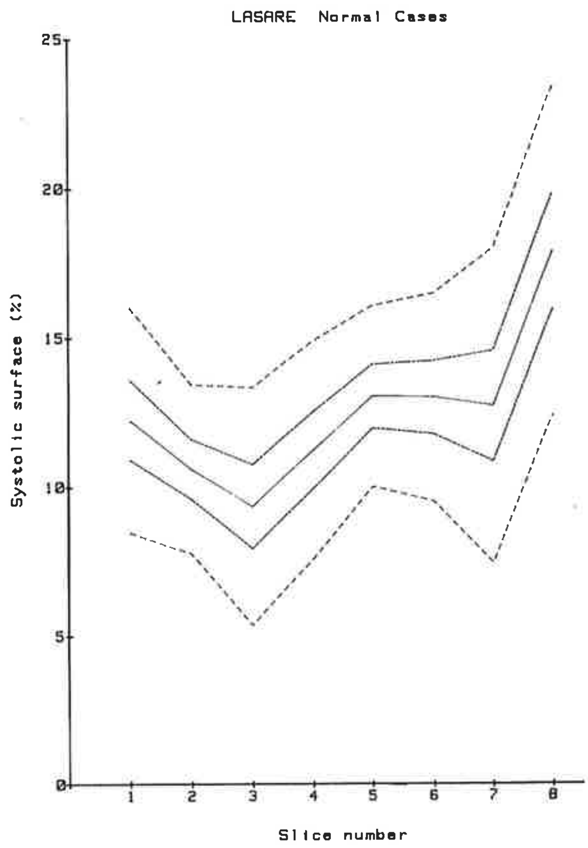
LASARE Normal Cases
Systolic surface (%)
Slice number
0
5
10
15
20
25
1
2
3
4
5
6
7
8

From the ellipsoid analysis, recall that the long axis analysis in that instance resulted in constant values for each parameter across the eight sectors. This was a consequence of the uniformity in shape. Hence any deviation from a constant value reflects a lack of uniformity in shape. In particular if elemental volume or elemental surface area percentage deviate from 12.5% the ventricular shape deviates from that of an ellipsoid. These plots indicate that the left ventricle of the normal heart has an inherent asymmetry both at end diastole and end systole. This is reflected in the percentage volume of the sectors medial, postero-medial, posterior and postero-lateral being less than 12.5% and the lateral, antero-lateral, anterior and antero-medial sectors being being greater than 12.5% (Fig. 6.9). This also demonstrates the relatively uniform distribution of regional contraction. That is each sector, the length of the long axis, contracts uniformly so that the relative volume proportion they represent is not statistically different between end diastole and end systole except for the antero-medial section where the volume proportion is signficiantly increased ($P<0.005$) over end diastole. However, the trend is that the volume proportion contained by the medial and anterior sectors is numerically identical between end diastole and end systole. The postero-medial, posterior, postero-lateral, lateral and antero-lateral sectors all decrease their volume proportion at end systole. The antero-medial sector contains the left ventricular out flow tract hence it is not surprising that during and at end systole the volume proportion of this sector has increased significantly. Similar trends are observed for the change in the percentage surface area of each sector for the left ventricle (Figure 6.10).

Again, from the ellipsoid analysis the short axis analysis has generated characteristic curves for percentage surface area, percentage volume for slice segments and pentahedral sectors from both the long axis mid point and the centre of contraction (Fig. 6.11 and 6.12). The short axis analysis was performed along the major axis which was sliced into ten segments perpendicular to the axis or quasi conical segments. Each slice segment or quasi conical segments consisted of eight

Figure 6.11 The percentage left ventricular myocardial surface area of ten short axis slices with respect to total surface area at end diastole and end systole respectively from a sample of 22 normal patients. The 95% confidence interval of both the mean values and the sample are plotted.

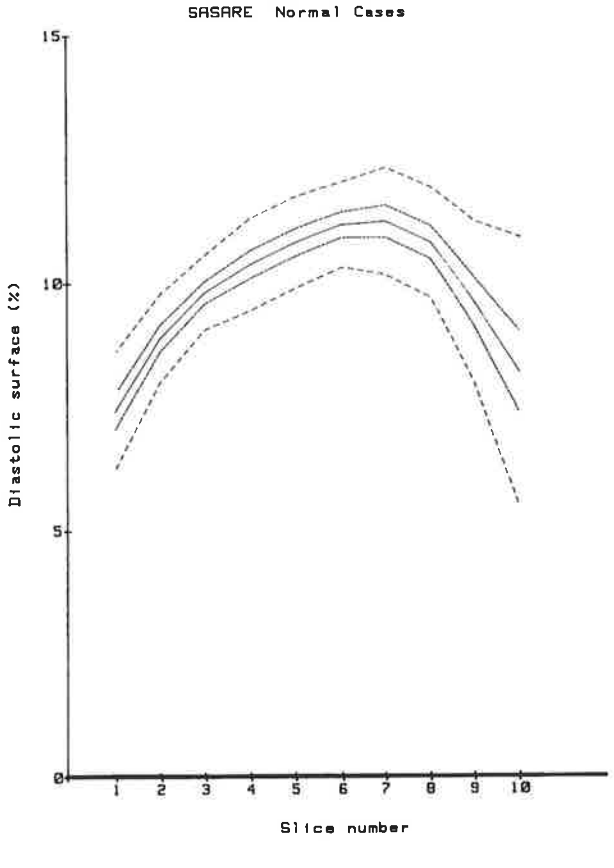
SASARE Normal Cases
Diastolic surface (%)
15
10
5
0
1 2 3 4 5 6 7 8 9 10
Slice number

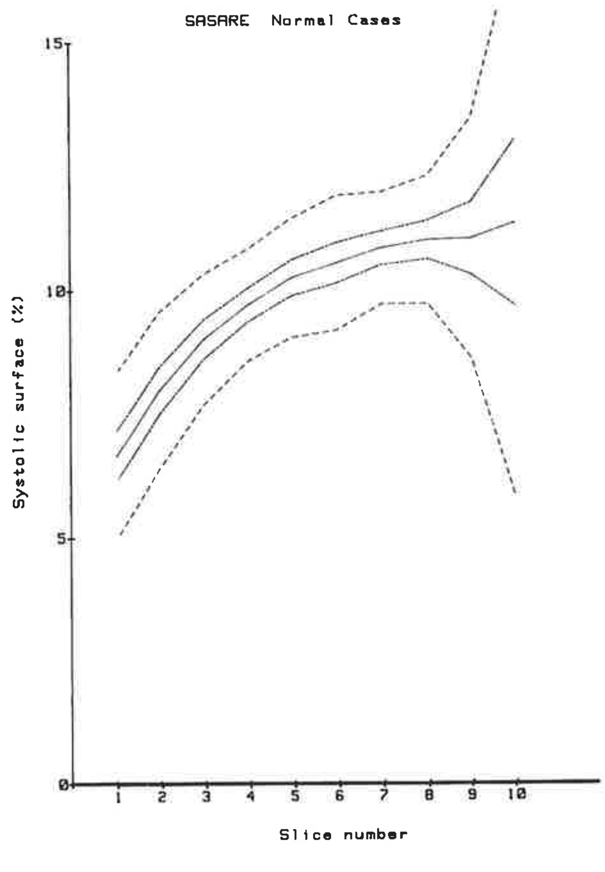
SASARE Normal Cases
Systolic surface (%)
15
10
5
0
1 2 3 4 5 6 7 8 9 10
Slice number

Figure 6.12a The percentage left ventricular volume of ten short axis slices with respect to total volume at end diastole and end systole respectively from a sample of 22 normal patients. The 95% confidence interval of both the mean values and sample are plotted.

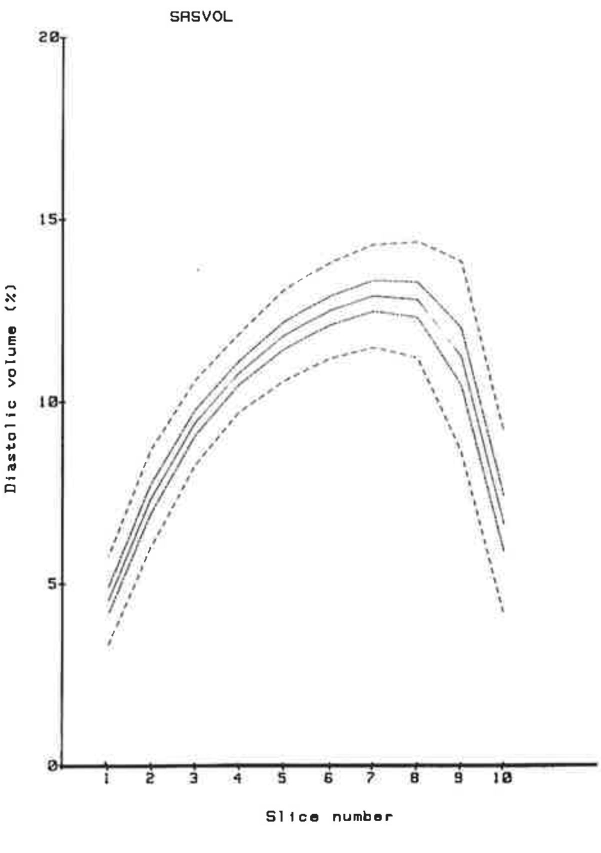
SASVOL
Diastolic volume (%)
20
15
10
5
0
1 2 3 4 5 6 7 8 9 10
Slice number

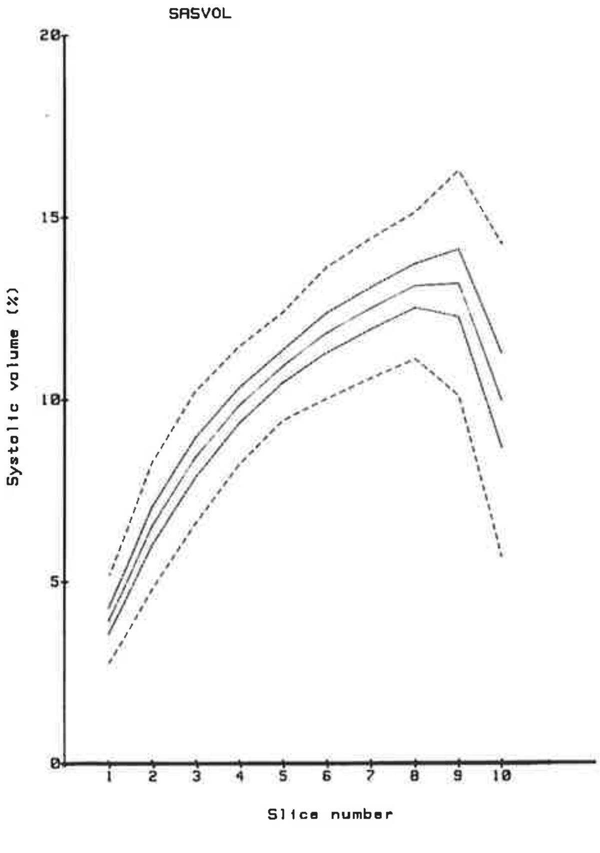
SASVOL
Systolic volume (%)
20
15
10
5
0
1 2 3 4 5 6 7 8 9 10
Slice number

Figure 6.12b The percentage left ventricular volume at ten levels of eight contiguous pentahedral volume elements with the apex at the long axis mid point. The percentage is with respect to the total volume at end diastole and end systole respectively from a sample of 22 normal patients. The 95% confidence interval of both the mean values and sample are plotted.

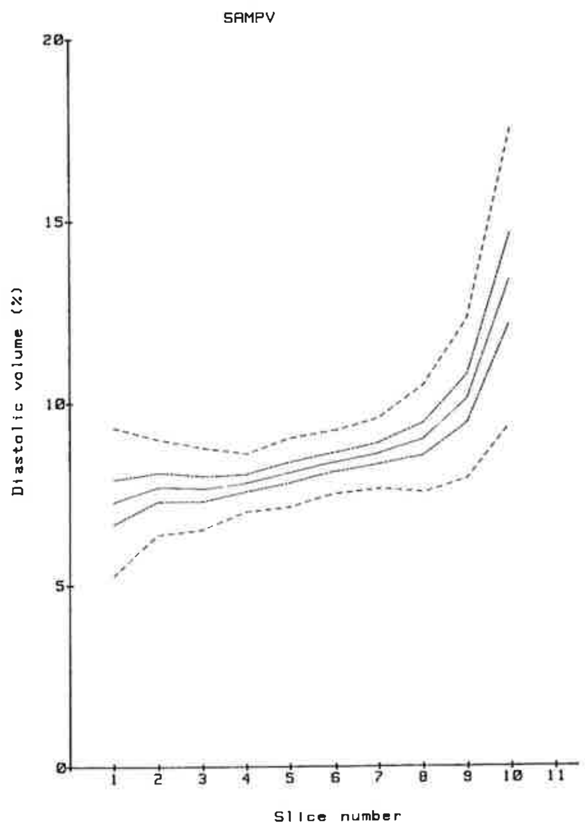
SAMPV
20
15
10
5
0
Diastolic volume (%)
1 2 3 4 5 6 7 8 9 10 11
Slice number

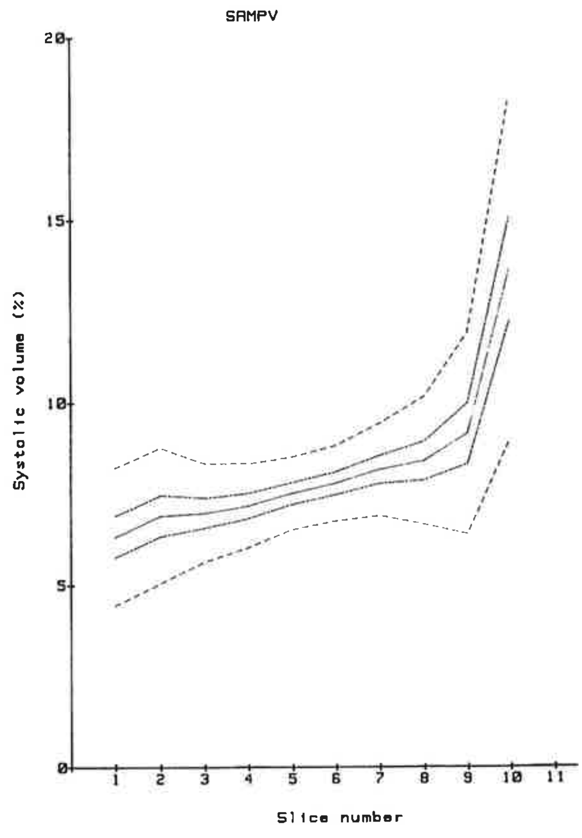
SAMPV
20
15
10
5
0
Systolic volume (%)
1 2 3 4 5 6 7 8 9 10 11
Slice number

Figure 6.12c The percentage left ventricular volume at ten levels of eight contiguous pentahedral volume elements with the apex at the left ventricular centre of contraction. The percentage is with respect to the total volume at end diastole and end systole respectively from a sample of 22 normal patients. The 95% confidence interval of both the mean values and sample are plotted.

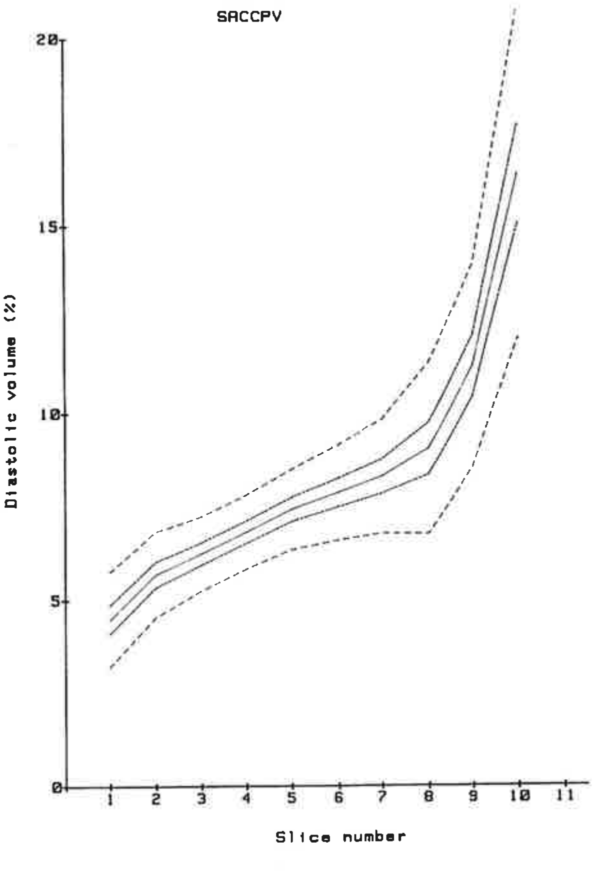
SACCPV
Diastolic volume (%)
Slice number
0
5
10
15
20
1
2
3
4
5
6
7
8
9
10
11

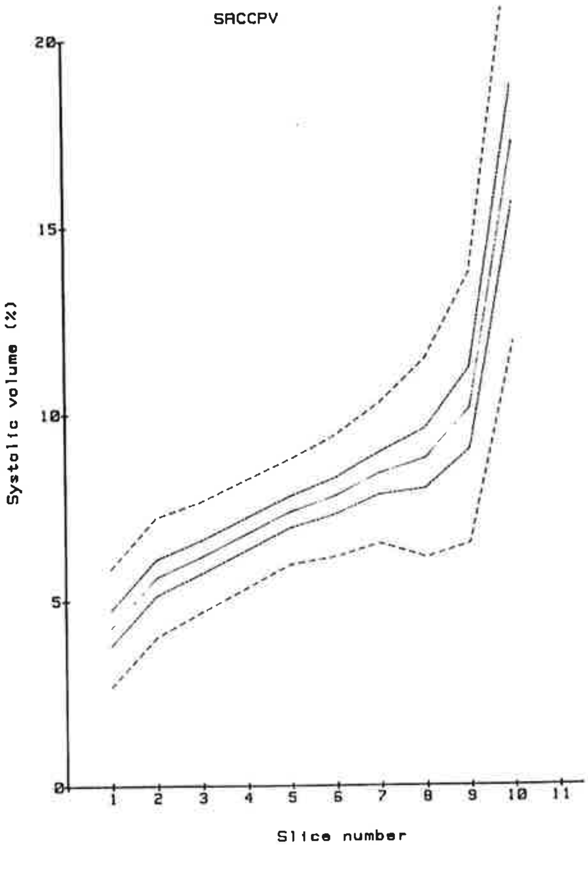
SACCPV
Systolic volume (%)
Slice number
0
5
10
15
20
1
2
3
4
5
6
7
8
9
10
11

sectors or pentahedral sectors respectively. The features to note about this analysis is that the curves are symmetrical and relatively smooth. The slice segment analysis for surface elements is independent of k (major to minor axis ratio). The slice segment analysis and pentahedral segment analysis for volume elements is independant of k but the shape of the curves is dependent on the vessel segmentation scheme.

Surface analysis of the 22 normal patients reflects the assymmetric nature of the left ventricle in a plane orthogoral to the long axis study. At slice segment number one we start with the minimum surface of the ventricular apex. Then progress through to the maximum surface just below the basal region of the ventricle but above the papillary muscle at slice segment number eight. For end diastole at the base, with the mitral and aortic valves, there is again a reduction in myocardial surface area. On the other hand for end systole there is a slight increase in basal myocardial surface over the surface at the eight slice segment.

The comparison of percentage surface area between end diastole and end systole shows that for slice segments one to seven end diastole is greater than end systole ($P<0.01$). For slices eight and nine there is no statistical difference. However, for slices ten the myocardial percentage surface area is increased ($P<0.005$). The mitral valve orifice area remains relatively constant during the cardiac cycle hence at end systole the area proportion of the total ventricular surface area increases significant over that at end diastole.

Percentage volume of slice segments perpendicular to the long axis for end diastole is a minimum at the apex (slice one) through to a maximum at slice eight just below the basal region of the ventricle but above the papillary muscle. The percentage volume then decreases to the base of the ventricle. On the other hand the end systolic percentage volume for each segment is continuously increasing from the apex through to the base of the ventricle (Fig. 6.12).

The comparison between end diastole and end systole shows that segments one to seven for end diastole have a larger percentage volume than at end systole ($P<0.01$). Segments eight and nine show no difference but for segment ten end systole is greater than end diastole ($P<0.005$).

From the centre of the long axis, eight pentahedral volume sectors were selected at each of ten equally spaced intervals along the axis. The percentage volume at each segment was a minimum at the apex and gradually increased up to the eight then steeply increased to the tenth segment. This is similar for both end diastole and end systole though for the latter the volume percentage rises steeply from the ninth segment.

Comparison between end diastole and end systole at each level shows end diastolic percentage volumes to be significantly greater than those at end systolic ($P<0.01$) except for that with respect to the tenth level which shows no statistical difference (Fig. 6.12).

Finally, the pentahedral volume elements with the apex at the left ventricular centre of contraction 2/3 down the long axis from the mitral valve are taken for analysis. The minimum percentage volume occurs at the apex increasing steadily to level 8 then increasing rapidly to the base. The trend is the same for both end diastole and end systole.

Comparison of end diastolic and end systole volume percentage at each level shows no statistical difference between the two except for level 9 where end diastolic is greater than end systolic ($P<0.01$) (Fig. 6.12).

ii) Ischemic Heart Disease Patients.

The long axis analysis was performed on the 13 patients with ischemic heart disease. The inherent asymmetry described for the normal patients was not apparent in some of the ischemic patients for both surface and volume percentages (Fig. 6.13 and 6.14). Ventricular shape changes are detectable in regions of the myocardium in the direction of the long axis. The anatomical location of a shape charge and the patient in which it occured for

Figure 6.13 The percentage left ventricular myocardial surface area of eight long axis sectors with respect to total surface area at end diastole and end systole respectively from a sample of 13 patients with ischemic heart disease. The dash lines show the mean value and 95% confidence interval of the normal sample. The horizontal line marks the 12.5% level of the ellipsoid analysis.

Slice Number	
1	Medial
2	Posterio-Medial
3	Posterior
4	Postero-Lateral
5	Lateral
6	Antero-Lateral
7	Anterior
8	Antero-Medial

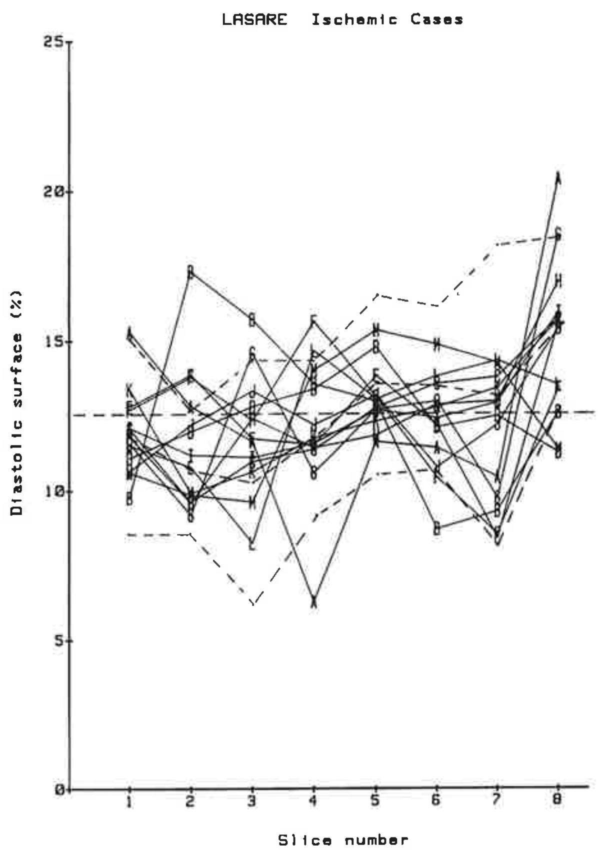

LASARE Ischemic Cases
Diastolic surface (%)
Slice number

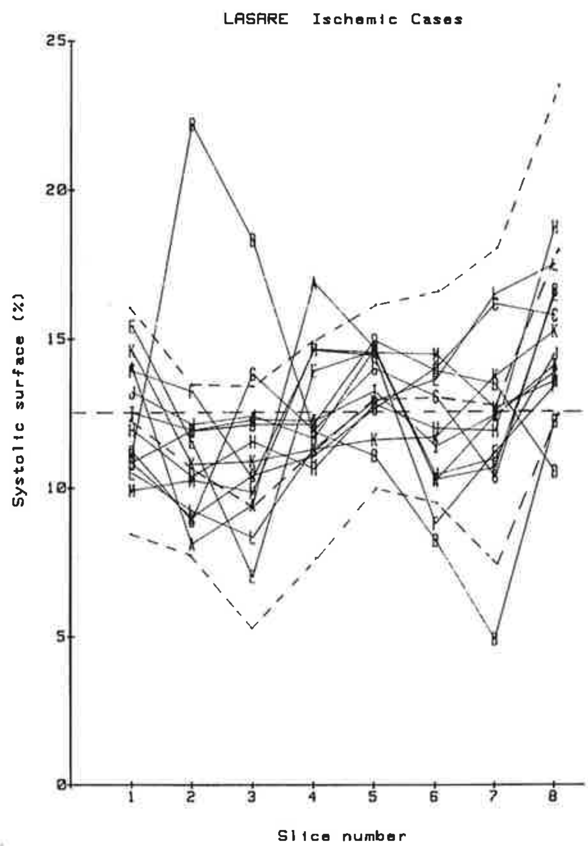

LASARE Ischemic Cases
Systolic surface (%)
Slice number

Figure 6.14 The percentage left ventricular volume of eight long axis sectors with respect to total volume at end diastole and end systole repectively from a sample of 13 patients with ischemic heart disease. The dash lines show the mean value and 95% confidence interval of the normal sample. The horizontal line marks the 12.5% level of the ellipsoid analysis.

Slice Number	
1	Medial
2	Posterio-Medial
3	Posterior
4	Postero-Lateral
5	Lateral
6	Antero-Lateral
7	Anterior
8	Antero-Medial

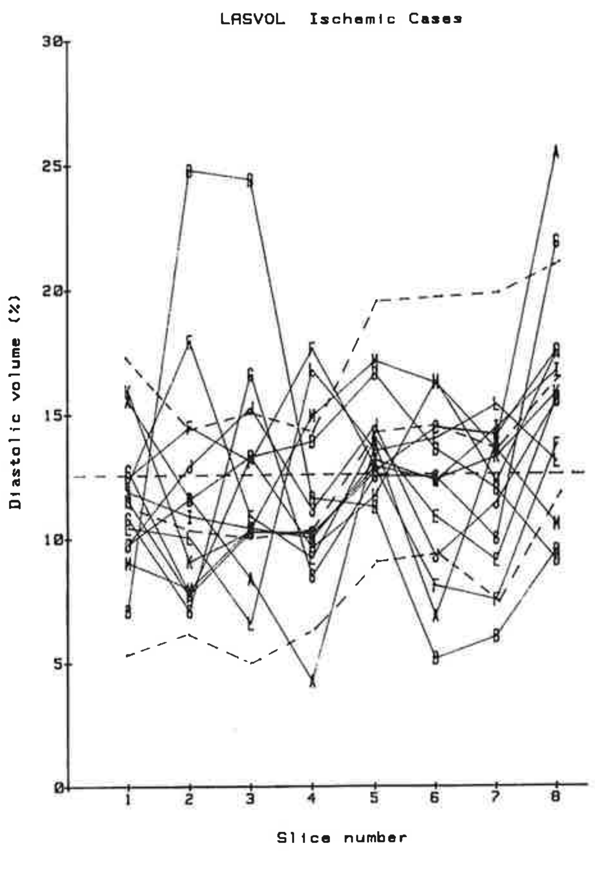
LASVOL Ischemic Cases
Diastolic volume (%)
Slice number

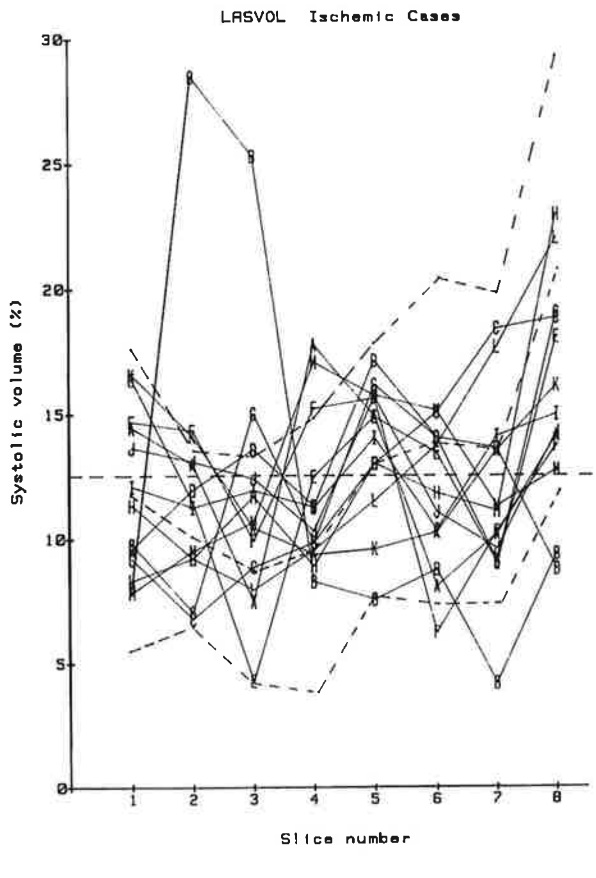
LASVOL Ischemic Cases
Systolic volume (%)
Slice number

either end diastole or end systole are tabulated in table 6.32 and 6.33. A greater proportion of volumetric shape changes occured in the medial, postero-medial, posterior and postero-lateral regions at both end diastole and end systole. In contrast, most of the charges in the antero-lateral and antero-medial regions are detected at end diastole. As a consequence 69% of patients have detectable volumetric shape charges at end diastole and 54% have detectable changes at end systole. Surface shape changes are similar to the volumetric changes at end diastole but there is an overall reduction in the detection of surface charges at end systole. Hence 62% of patients have detectable surface shape changes at end diastole and 38% have detectable changes at end systole.

Short axis analysis of left ventricular shape changes included percentage surface area and percentage volume changes for slice segments perpendicular to the long axis as well as pentahedral volume segments with the apex at the long axis mid point and the left ventricular centre of contraction (Fig 6.15 and 6.16). Most of the shape change in surface area occurs just above the

LONG AXIS SECTOR SURFACE AREA

	M	PM	P	PL	L	AL	A	AM
End Diastole	1	1	5	1		5		1
		5	13	11		11		9
		10		33				13
		11						34
End Systole		5	5	1		5	5	5
			13			11		9

Table 6.32 Patients with ischemic heart disease which show significant changes in left ventricular myocardial surface area in various long axis regions of the left ventricle.

M - Medial, P - Postero-Medial, P - Posterior,
PL - Postero - Lateral, L - Lateral, AL - Antero-Lateral,
A - Anterior, AM - Antero - Medial

LONG AXIS SECTOR VOLUME

	M	PM	P	PL	L	AL	A	AM
End Diastole		5	5	1		1	5	1
		10	13	11		5		5
		11	18	33		11		9
				34				13
								34
End Systole		5	5	1		11	5	5
		11	9	11				9
		20	13	34				

Table 6.33 Patients with ischemic heart disease which show significant changes in left ventricular sector volumes in various long axis sections of the left ventricle.

M - Medical, P Postero-Medial, P - Posterior,
PL - Postero - Lateral, L - Lateral, AL - Antero-Lateral,
A - Anterior, AM - Antero-Medial

Figure 6.15 The percentage left ventricular myocardial surface area of ten short axis slices with respect to total surface area at end diastole and end systole respectively from a sample of 13 patients with ischemic heart disease. The dash lines show the mean value and 95% confidence interval of the normal sample.

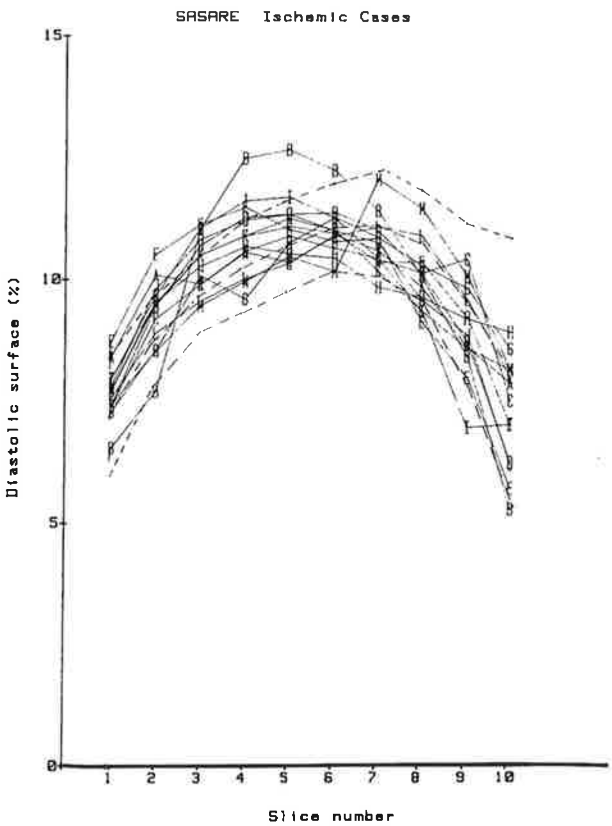
SASARE Ischemic Cases
Diastolic surface (%)
Slice number

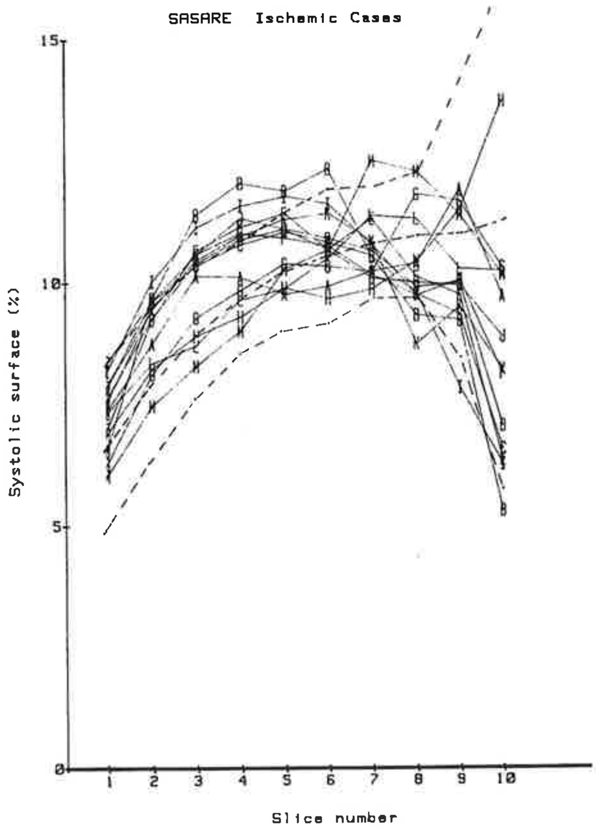
SASARE Ischemic Cases
Systolic surface (%)
Slice number

Figure 6.16a The percentage left ventricular volume of ten short axis slices with respect to total volume at end diastole and end systole respectivley from a sample of 13 patients with ischemic heart disease. The dash lines show the mean value and 95% confidence interval of the normal sample.

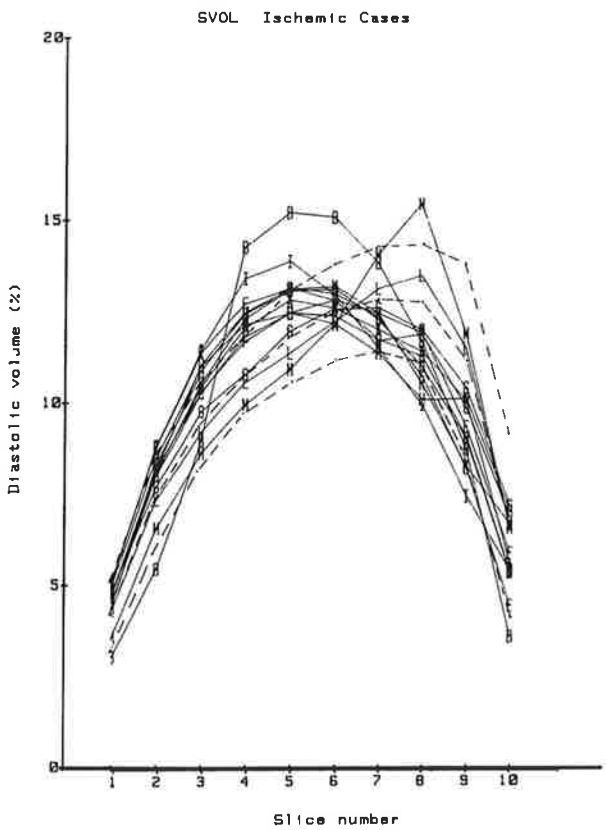
SVOL Ischemic Cases
Diastolic volume (%)
20
15
10
5
0
1 2 3 4 5 6 7 8 9 10
Slice number

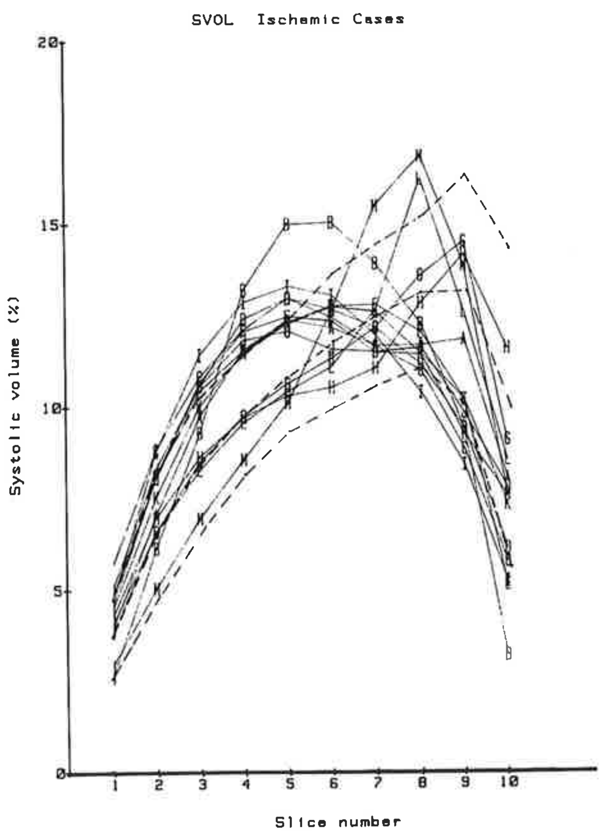
SVOL Ischemic Cases
Systolic volume (%)
20
15
10
5
0
1 2 3 4 5 6 7 8 9 10
Slice number

Figure 6.16b The percentage left ventricular volume at ten levels of eight contiguous pentahedral volume elements with the apex at the long axis mid point. The percentage is with respect to the total volume at end diastole and end systole respectively from a sample of 13 patients with ischemic heart disease. The dash lines show the mean value and 95% confidence interval of the normal sample.

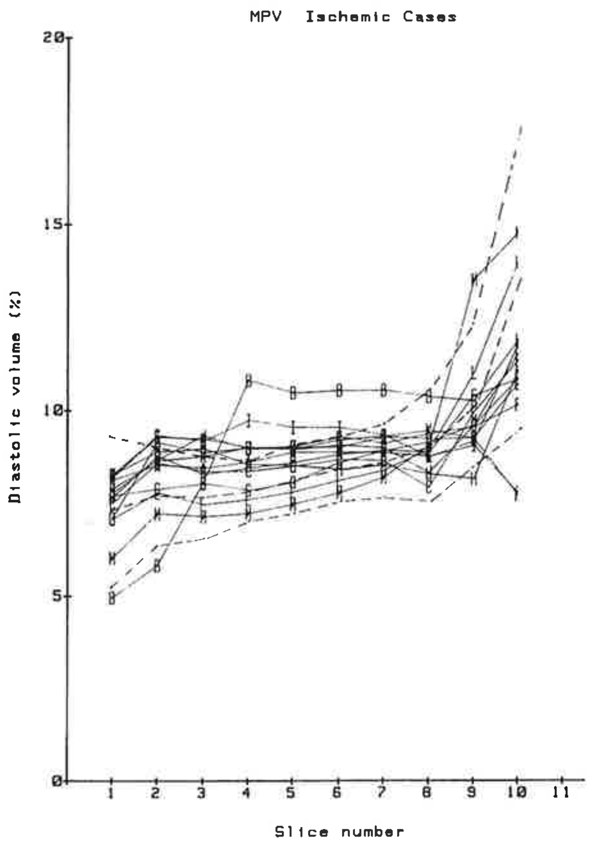
MPV Ischemic Cases
Diastolic volume (%)
Slice number
0
5
10
15
20
1
2
3
4
5
6
7
8
9
10
11

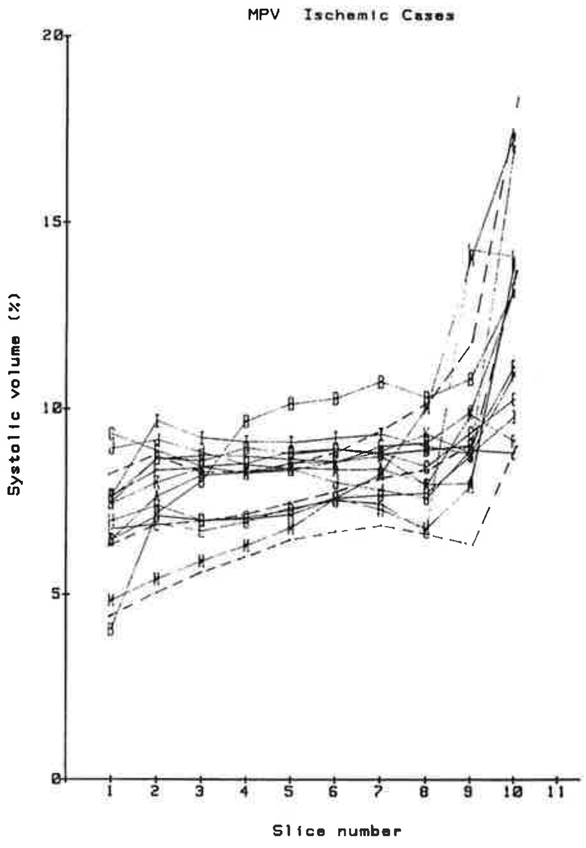
MPV Ischemic Cases
Systolic volume (%)
Slice number
0
5
10
15
20
1
2
3
4
5
6
7
8
9
10
11

Figure 6.16c The percentage left ventricular volume at ten levels of eight contiguous pentahedral volume elements with the apex at the left ventricular centre of contraction. The percentage is with respect to the total volume at end diastole and end systole respectively from a sample of 13 patients with ischemic heart disease. The dash lines show the mean value and 95% confidence interval of the normal sample.

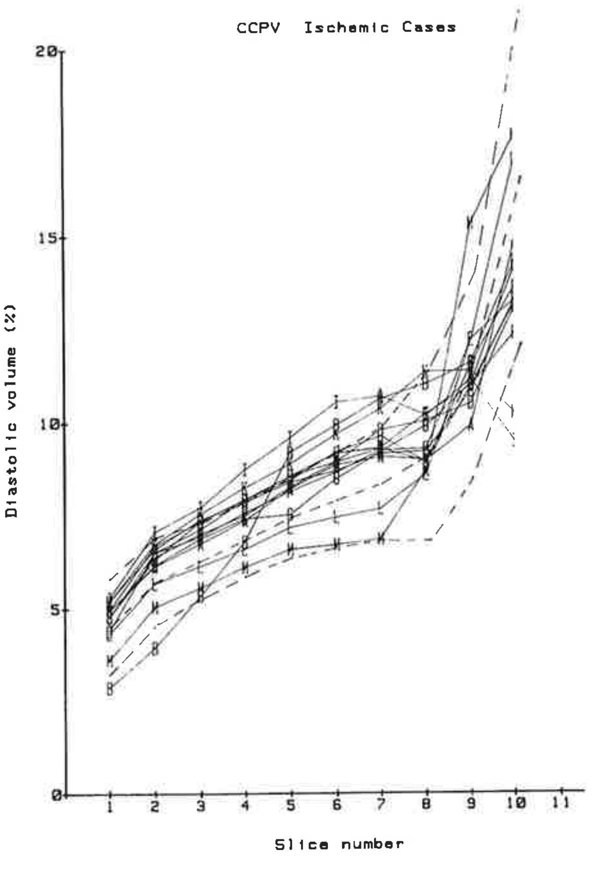
CCPV Ischemic Cases
Diastolic volume (%)
Slice number
0
5
10
15
20
1
2
3
4
5
6
7
8
9
10
11

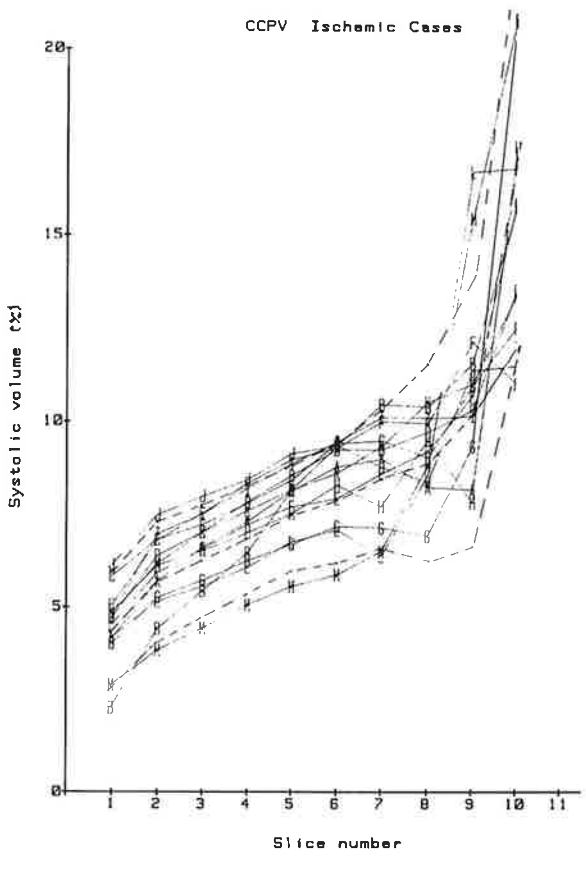
CCPV Ischemic Cases
Systolic volume (%)
Slice number
0
5
10
15
20
1
2
3
4
5
6
7
8
9
10
11

apex and below the mid level of the ventricle. Table 6.34 shows the patients and the locations in which surface changes have occurred. The basal region of the ventricular myocardium appears to undergo a minimum of surface change. Overall, 69% of the patients undergo detectable surface shape change at both end diastole and end systole.

Volume shape change of short axis slice segments tend to occur in the region toward the ventricular apex from the mid region of the ventricle. Similar to the surface changes. However there are also changes in the basal region of the ventricle (Table 6.35). The trends are similar for both end diastole and end systole. The volume percentage tends to be larger than normal in the apical to mid region where as in the basal region the volume percentage tends to be less than normal (Fig 6.16). Overall, 62% and 69% of the patients demonstrated detectable percentage volumetric shape change at end diastole and end systole respectively.

The percentage volume shape changes with respect to the long axis mid point occur principally in the region from the apex to the mid point with a few

SHORT AXIS SLICE SURFACE AREA

	Apex				Mid-Region					Base
Slice Number	1	2	3	4	5	6	7	8	9	10
End Diastole	10	1	5	5	5	5	30	10	15	5
		5	9	10	15	34		15		
		10	10	15				20		
		18	15	18						
			18							
End Systole	6	5	5	5	5	5	34	5	15	5
		6	6	9	10			20		
		15	9	10	15					
		18	10	11						
			11	15						
			15	18						
			18	20						
			20							

Table 6.34 Patients with ischemic heart disease which show significant changes in left ventricular myocardial surface area in parallel short axis slices along the length of the ventricle.

SHORT AXIS SLICE VOLUME

	Apex				Mid-Region				Base	
Slice Number	1	2	3	4	5	6	7	8	9	10
End Diastole		5	9	1	5	5	30	9		
		10	10	5	9			10		
		15	15	9	10			15		
			18	10	15			20		
			30	15	18			30		
				18	20					
				20						
				30						
End Systole	6	6	6	5	5	5	34	6	5	5
		15	9	6	6			15	6	10
			10	9	9			33	9	15
			11	10	11			34	11	
			15	11	15				15	
			18	15					18	
				18						

Table 6.35 Patients with ischemic heart disease which show significant changes in left ventriclar short axis slice volume along the length of the ventricle.

changes in the basal region (Table 6.36). This contrasts with the "bimodal" incidence of changes in the sliced segment analysis. The trends are similar for both end diastole and end systole. The volume element shape change most often is such that the percentage volume contained by the element is increased (Fig 6.16). Of the patients studied 62% and 77% demonstrated some detectable volumetric shape change at end of diastole and end systole respectively.

Shape changes with respect to the centre of contraction 1/3 up from the apex on the long axis occur above the apex to the mid region of the ventricle in end diastole. For end systole the changes seem to be evenly distributed along the ventricle (Table 6.37). Again shape changes tend to result in an increase of percentage volume over the normal population 95% confidence intervals (Fig 6.16). The analysis detects 69% and 46% of patients as undergoing volumetric shape change in end diastole and end systole respectively.

SHORT AXIS MIDPOINT VOLUME

	Apex			Mid-Range					Base	
Slice Number	1	2	3	4	5	6	7	8	9	10
End Diastole	5	5	9	5	5	5	5		30	18
		9	10	9	15	10			34	20
		10	15	10		15				
		15	18	15						
			20	18						
			30	20						
End Systole	5	6	6	5	5	5	5	5	33	18
	6	15	9	6	6	6			34	
	18	18	10	9	9	9				
			11	11	11	15				
			15	15	15					
			18	18						
			20							

Table 6.36 Patients with ischemic heart disease which show significant changes in tetrahedral volume elements with the apex taken at the left ventricular long axis mid point.

SHORT AXIS CENTRE OF CONTRACTION POINT VOLUME

	Apex			Mid-Range					Base	
Slice Number	1	2	3	4	5	6	7	8	9	10
End Diastole	5	5	9	6	5	5	5		34	15
		15	10	9	9	9	15			20
			11	10	10	15	20			
			15	11	15	18				
			20	15	20	20				
				20						
End Systole	5	18	18	11	11	34	5		33	11
	18	34	34	18	15		33		34	18
				34	18		34			
					34					

Table 6.37 Patients with ischenic heart disease which show significant changes in tetrahedral volume elements with the apex taken at the left ventricular centre of contraction point.

Table 6.38 contains a summary of the patients in which shape changes in at least one region were detected for each analysis. It is apparent that the short axis analysis of surface area and volume by slice segments or long axis mid point volumes provide the highest percentage detection of change. The latter method giving the best detection rate overall. However, the short axis analysis fails to detect any change in patient 13 whereas the long axis analysis, for both surface and volume, detects shape changes. If one takes only the short axis mid point volume analysis patient 1 also fails to demonstrate shape change but the long axis analysis again detects a change. Hence, by undertaking short and long axis analysis as complementary procedures the detection of change in the left ventricle for ischemic patients increases to 100%.

6.6 Qualitative Echocardiographic Assessment.

A comprehensive qualitative echocardiographic assessment of the left ventricular wall motion was performed by an experienced observer without knowledge of the results from the quantititive analysis. Although such a qualitative

DETECTED SHAPE CHANGES

Patient Number	SASARE ED	SASARE ES	SASVOL ED	SASVOL ES	SAMPV ED	SAMPV ES	SACCPV ED	SACCPV ES	LASARE ED	LASARE ES	LASVOL ED	LASVOL ES
1	*		*						*	*	*	*
5	*	*	*	*	*	*	*	*	*	*	*	*
6		*		*		*	*					
9	*	*	*	*	*	*	*		*	*	*	*
10	*	*	*	*	*	*	*		*		*	
11		*		*		*	*	*	*	*	*	*
13									*	*	*	*
15	*	*	*	*	*	*	*	*				
18	*	*	*	*	*	*	*	*			*	
20	*	*	*		*	*	*					*
30	*		*		*							
33				*		*		*	*		*	
34	*	*		*	*	*	*	*	*		*	*
Percentage	69%	69%	62%	69%	62%	77%	69%	46%	62%	38%	69%	54%

Table 6.38 The * marks the detection of at least one significant change in the parameter shown for the patient. The number of patients in which significant changes have been detected are shown as a percentage.

echocardiographic analysis cannot serve as absolute reference, it seemed appropriate to use for comparison. For the qualitative analysis the four complementary apical views were examined. In each apical view the segments that corresponded to the segments in the quantitive analysis were identified. This is the medial, postero-medial, posterior, postero-lateral, lateral, antero-lateral, anterior, antero-medial and the apical, mid-portion and basal regions of the left ventricle. Each segment was judged to be normal, hypokinetic, akinetic or dyskinetic. A score system then was used where localisation of a dyskinetic, akinetic, hypokinetic and normal region was given a score of -3, -2, -1 and 0 respectively. The 13 ischemic patients were studied in this manner. Table 6.39 shows the scores for patient 11 that was assessed. The scores were then summed along the ventricle and across the short axis levels.

To compare the qualitative assessment with the quantitative analysis the summed scores were plotted with respect to the long axis rotational anatomy and with respect to the apical, mid-region

REGIONAL WALL MOTION STUDY

Patient Name: No. 11

R.W.M. Score:	normal	hypokinetic	akinetic	dyskinetic
	0	-1	-2	-3

-4 Chamber View

	Lateral	Medial
Basal	0	0
Mid	0	-2
Apical	0	-2

45 Anticlockwise View

	Antero-Lateral	Postero-Medial
Basal	0	0
Mid	0	0
Apical	-1	-1

2 Chamber View

	Anterior	Posterior
Basal	0	-1
Mid	0	0
Apical	-1	-1

45 Clockwise View

	Antero-Medial	Postero-Lateral
Basal	0	0
Mid	-1	0
Apical	-1	-1

Table 6.39 Qualitiative assessment scores for patient No. 11.

and basal segment of the ventricle (Fig 6.17 and 6.18). From Figure 6.17, it is apparent that regional wall abnormalities are most common in the medial, postero-medial, posterior and postero-lateral regions of the left ventricle. It is this part of the left ventricle which has been quantitatively shown to contain the lower volume proportion of the total ventricular volume (Fig. 6.9) in normal patients. For the ischemic patients 62% and 54% underwent left ventricular shape change in these regions at end diastole and end systole respectively. In the remaining regions only 46% and 23% of the patients underwent changes at end diastole and end systole respectively (Table 6.33).

On the other hand figure 6.18 demonstrates that regional wall abnormalities are generally present throughout the length of the ventricle from the apex through to the base. This is still consistent with the observation above that medial and posterior regions tend to have more abnormalities in the patient sample studied. These regions extend from the apex to the base of the ventricle. However, the quantitive analysis shows a bimodal

Figure 6.17 Plot of qualitative scores from the long axis assessment of left ventricular performance.

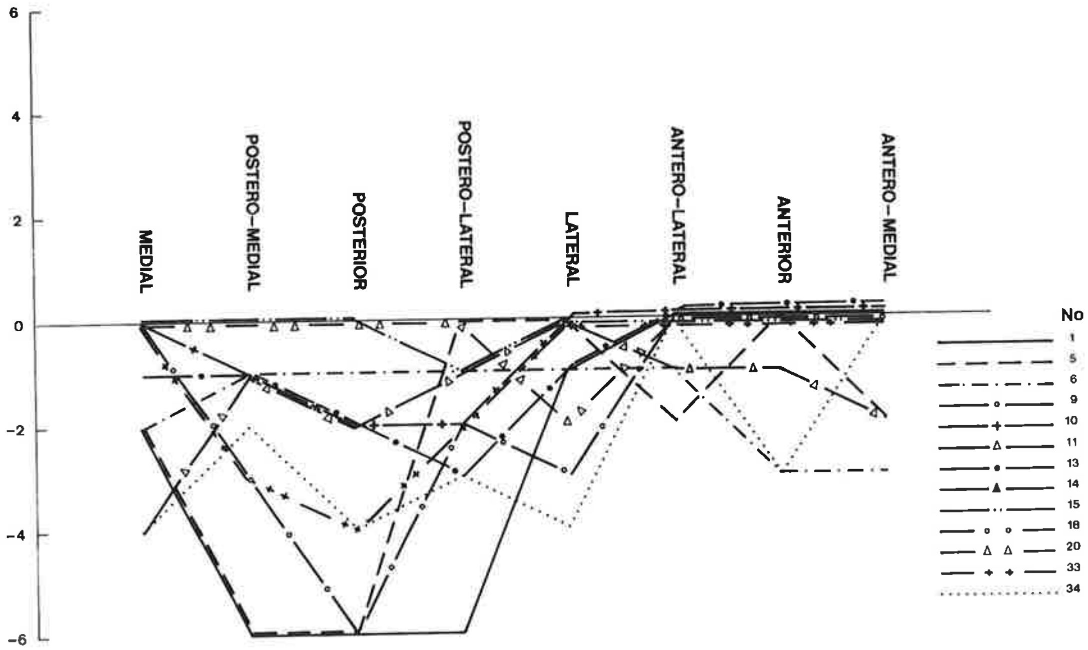

6
4
2
0
-2
-4
-6
MEDIAL
POSTERO-MEDIAL
POSTERIOR
POSTERO-LATERAL
LATERAL
ANTERO-LATERAL
ANTERIOR
ANTERO-MEDIAL
No
1
5
6
9
10
11
13
14
15
18
20
33
34

Figure 6.18 Plot of qualitative scores from the short axis assessment of left ventricular performance.

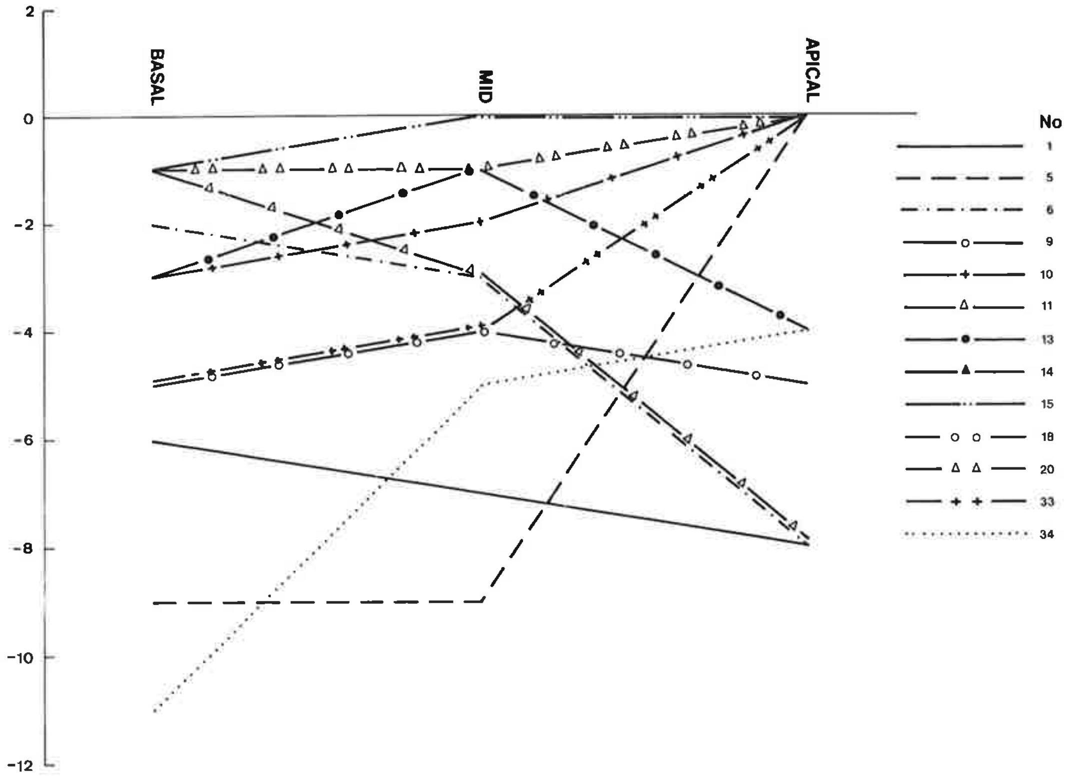

2
0
-2
-4
-6
-8
-10
-12
BASAL
MID
APICAL
No
1
5
6
9
10
11
13
14
15
18
20
33
34

nature in the patients detected with ventricular shape changes in short axis slice segments (Table 6.35). The general trend in ventricular shape change is consistent with the pattern of qualitative regional wall abnormality observed for the ischemic patients. However, the ten slice segmentation used in the quantitative analysis is much more sensitive than the apical, mid-portion and basal region subdivisions used for the qualitative assessment. The quantitive analysis further identifies that the shape changes in the apical to mid-portion of the ventricle lead to an increase in the volume proportion contained in these regions. The basal region however has a shape charge which leads to a decrease in the volume proportion. Relative ventricular enlargement then tends to occur in the apical to mid-portion region of the left ventricle.

6.7 Three Dimensional Display.

The computerised data processing for 3D graphical display has been described in Chapter 5. The implimentation of the procedures allows the display of a 3D wire-cage model of the reconstructed ventricle in various rotational views. In figure 6.19 are displayed reconstructed left ventricles. One is patient 26, male, with global left ventricular impairment who has undergone aortic valve replacement. The other is patient 5, male, with an inferior aneurysm. Displayed are both end diastolic and end systole reconstructed ventricles in isometric projections. It is apparent by inspection that patient 26 has generally maintained its ventricular shape more than patient 42. Indeed in patient 5, the aneursysm has been highlighted further at end diastole.

For patient 5, a series of 3-D reconstructions at various rotations have been produced and displayed in sequence to highlight the enhanced perception that can be obtained of cardiac geometry by qualitative pattern recognition skills. To enchance these perceptions a video record has also been made of the ventricular rotational views and is available for viewing.

Patient No. 26

Figure 6.19a Isometric projections of patient No. 26 and No. 5 at end diastole and end systole

Patient No. 5

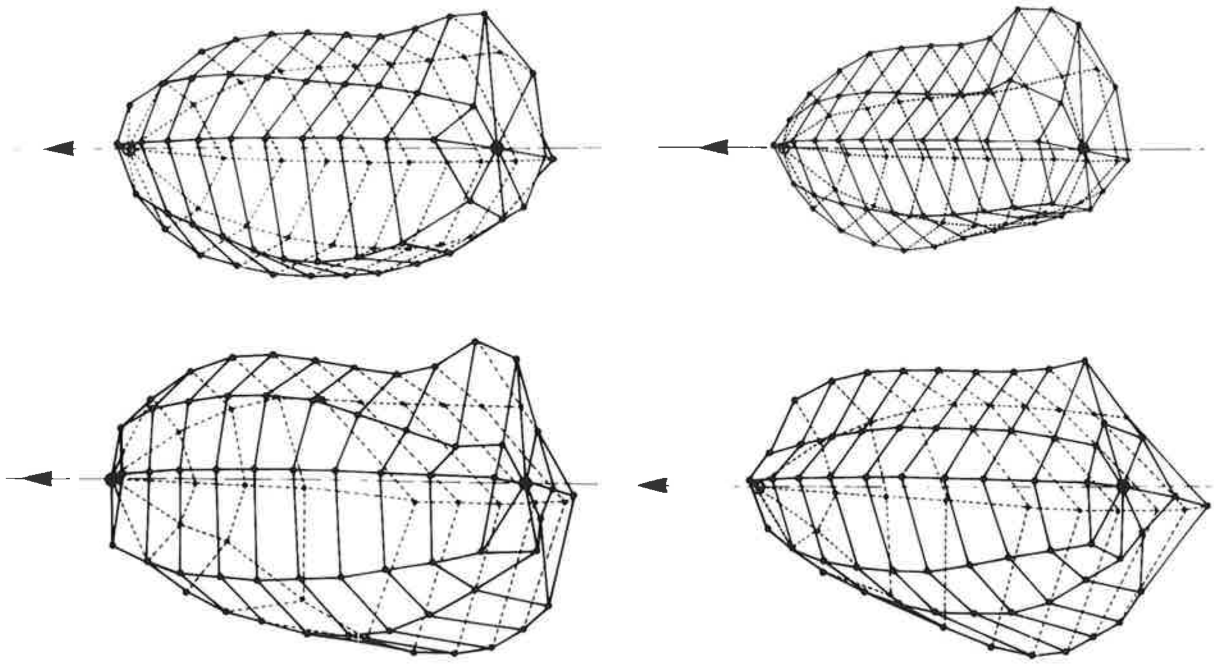

End Diastole

Figure 6.19b Detailed graphic output of patient No. 5 showing the left ventricle at end diastole and end systole in consecutive long axis and short axis rotational views.

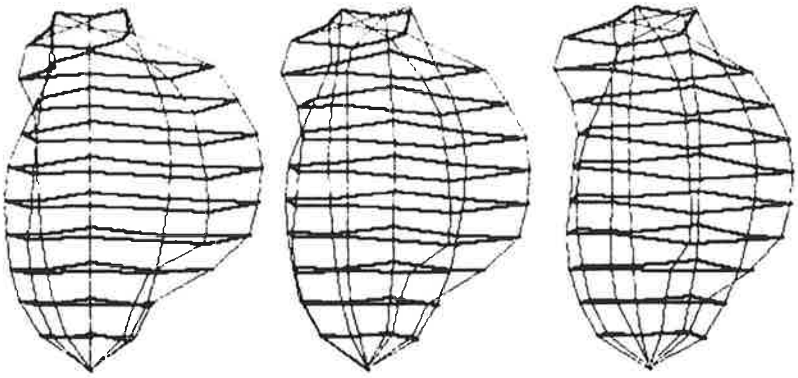

Angle= 360 degrees Angle= 345 degrees Angle= 330 degrees

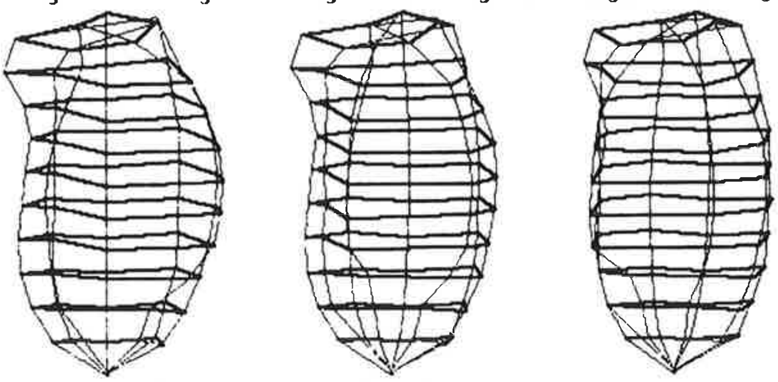

Angle= 315 degrees Angle= 300 degrees Angle= 285 degrees

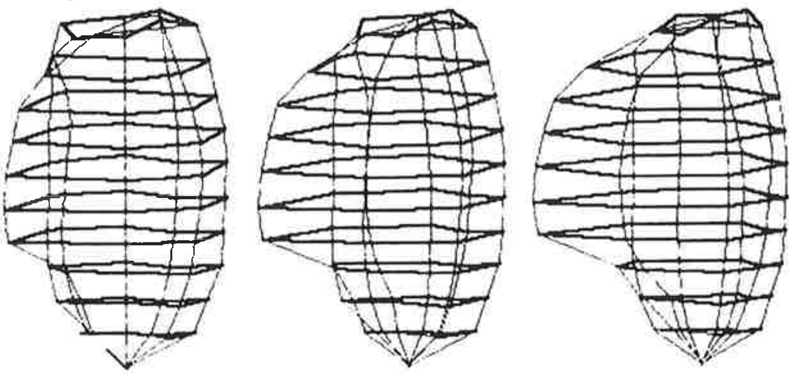

Angle= 270 degrees Angle= 255 degrees Angle= 240 degrees

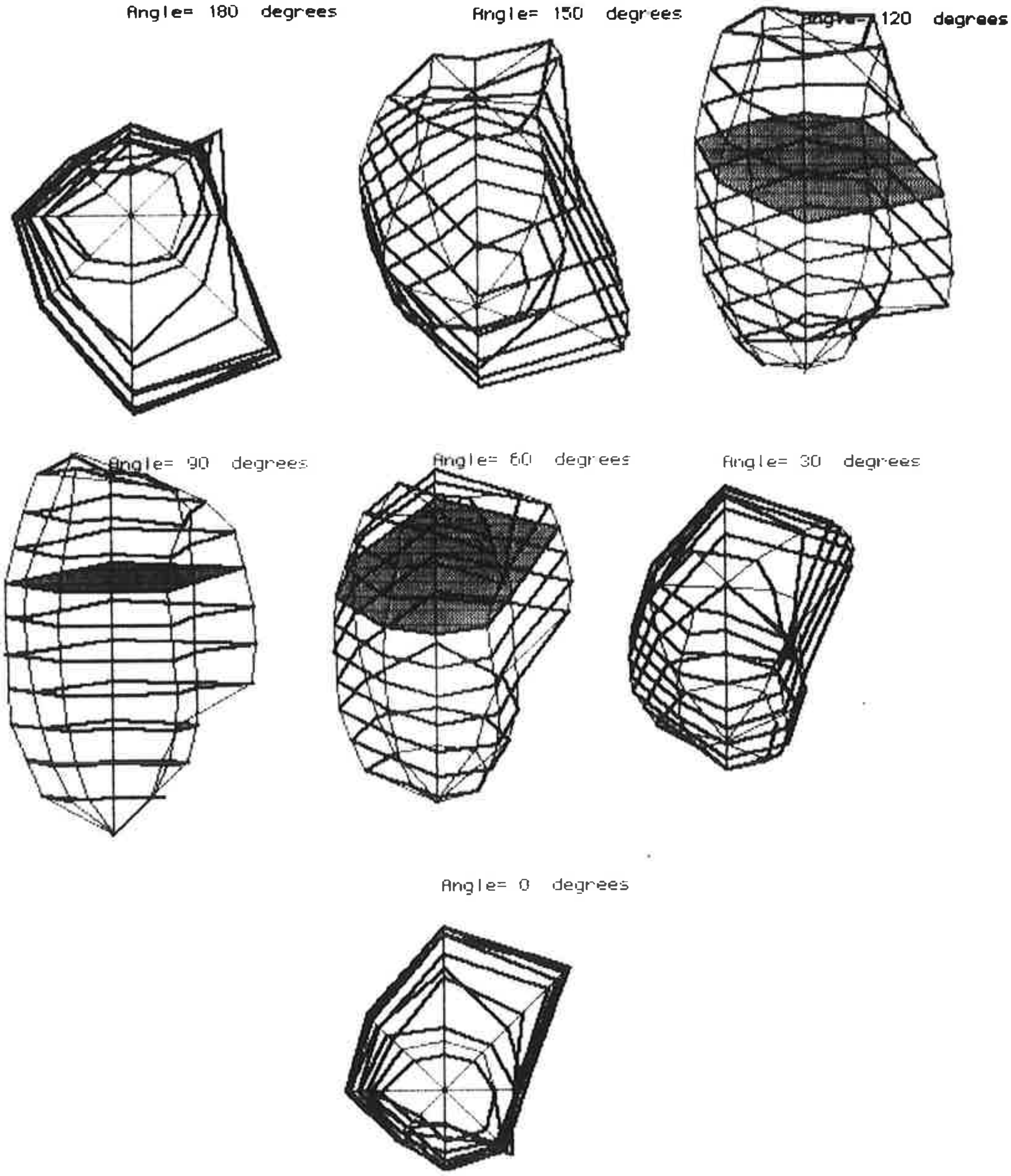

Angle= 180 degrees
Angle= 150 degrees
Angle= 120 degrees
Angle= 90 degrees
Angle= 60 degrees
Angle= 30 degrees
Angle= 0 degrees

End Systole

Figure 6.19b continued

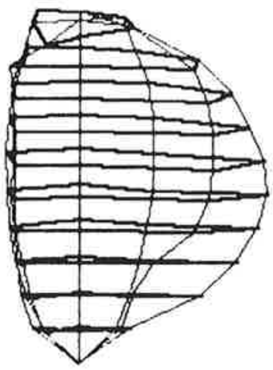
Angle= 360 degrees

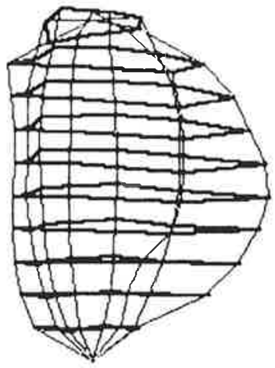
Angle= 345 degrees

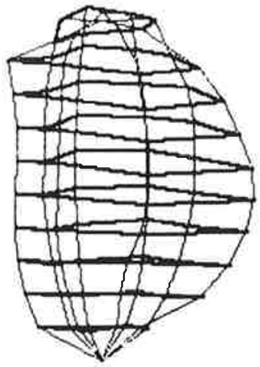
Angle= 330 degrees

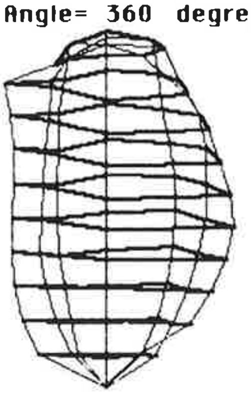
Angle= 315 degrees


Angle= 300 degrees


Angle= 285 degrees


Angle= 270 degrees

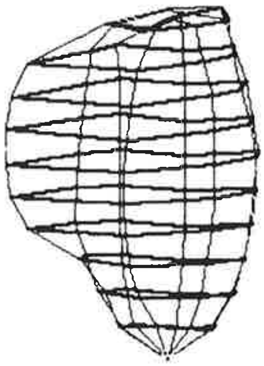
Angle= 255 degrees

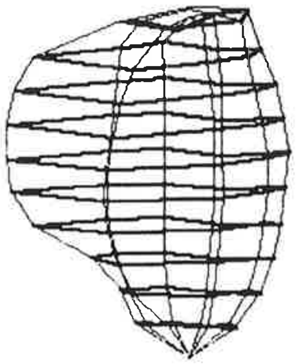
Angle= 240 degrees

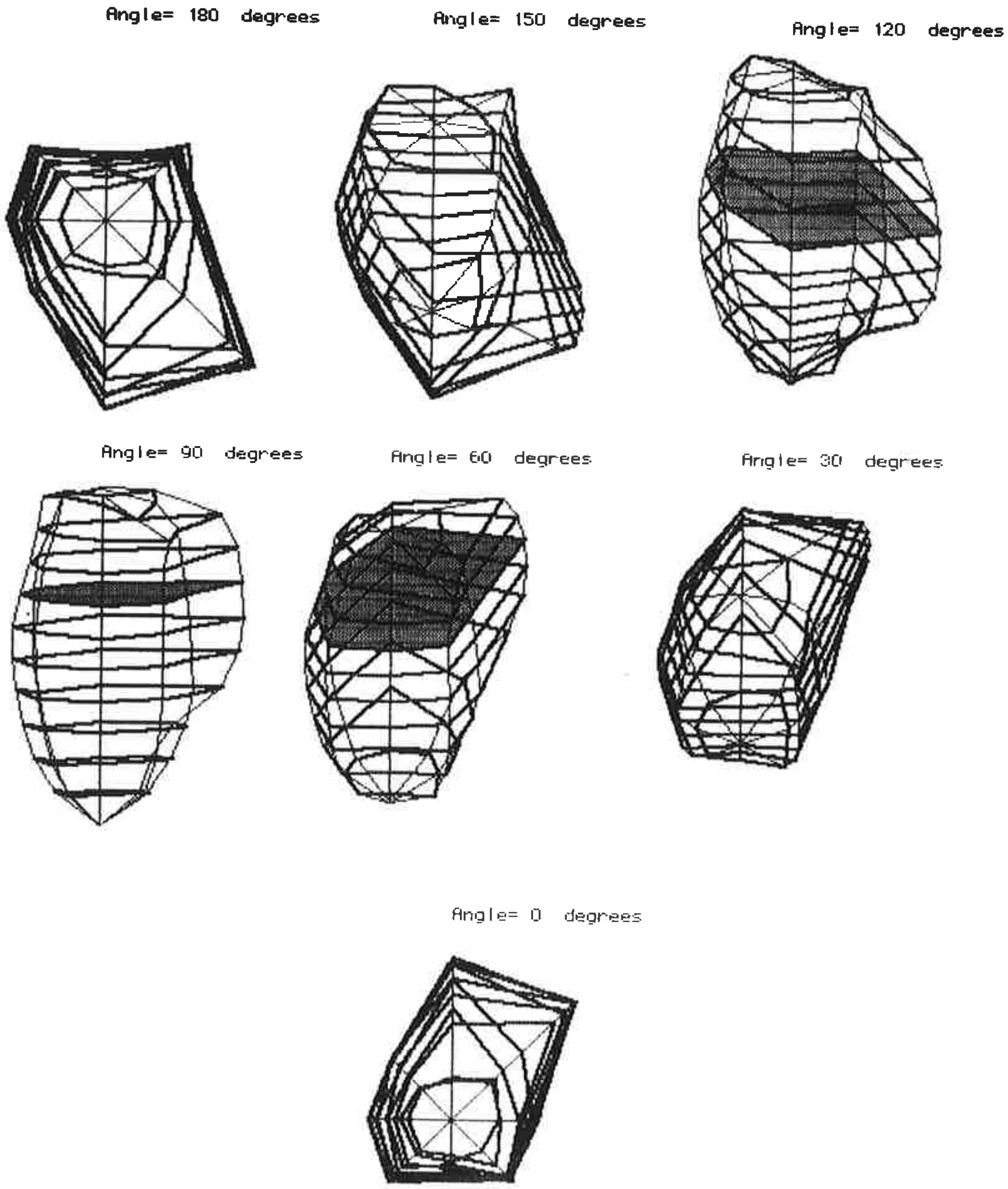
Angle= 180 degrees
Angle= 150 degrees
Angle= 120 degrees
Angle= 90 degrees
Angle= 60 degrees
Angle= 30 degrees
Angle= 0 degrees

6.8 References.

Altman DG, Bland JM (1983)
Measurement in medicine : the analysis of method comparison studies.
The Statistician. 32: 307-317.

Dodge HT. Sandler H, Ballew DW, Lord JD (1960)
The use of biplane angiocardiography for the measurement of left ventricular volume in man.
Am. Heart J. 60: 766-776.

Ingels NB, Daughters GT, Stinson EB, Alderman EL (1980)
Evaluation of methods for quantitating left ventricular segmental wall motion in man using myocardial markers as a standard.
Circulation. 61: 966-972.

Janicki JS, Weber KT, Cochman RF, Shroff S, Geheb FJ (1981)
Three dimensional myocardial and ventricular shape: A surface representation.
Am. J. Physiol. 241: H1-H11.

Snedecor GW, Cohran WG (1967)
Statistical Methods 6th Edition.
The Iowa state University Press, Ames, Iowa, U.S.A.

Sokal RR, Rohlf FJ (1981)
Biometry: The Principles and Practice of Statistics in Biological Research 2nd Edition.
W H Freeman and Company, N.Y.

Wynne J, Green LH, Mann T, Levin D, Grossman W (1978)
Estimation of left ventricular volumes in man from biplane cineangiograms filmed in oblique projections.
Am. J. Cardio. 41: 726-732.

Zilles K. Schleicher A, Pehlemann FW (1982)
How many sections must be measured in order to reconstruct the volume of a structure using serial sections?
Microscopica Acta 86: 339-346.

CHAPTER 7

GENERAL DISCUSSION AND CONCLUSIONS

7.1 Introduction

The primary goal of the study described in this thesis was to develop a method to generate 3D spatial reconstructions of the left ventricle in vivo. Then to use this method to determine left ventricular volume and describe left ventricular geometry at end diastole and end systole of normal and ischemic patients.

7.2 Discussion

The analysis of ellipsoid geometries in Chapter 4 showed that rotational slices about the long axis are the most efficient mode of sectioning to obtain the maximum area per slice. This analysis was necessary because of the limitations placed on tomographic imaging of the left ventricle by both ultrasonic imaging instrumentation and human anatomy. From the literature survey in Chapter 4 it is apparent that the basis for selecting tomographic views for 3D left ventricular geometry has been arbitrary, often based on anatomic impressions and observations that have not been objectively examined to evaluate the relative merits of various tomographic views. We have shown in Chapter 6 that the use of four rotational axial tomographic slices about the major axis of an ellipsoid provide very reliable volume estimates using a polar integration method. Also evaluated were volume estimation by the trapezoidal rule and Pappus' Theorem. For the ellipsoidal segmentation selected in this study the best estimates were by polar integration, Pappus' Theorem and the trapezoidal rule respectively. The limitation on accuracy of each method is the finite number of segments used to make the volume estimate. If the number of segments became infinite then each of the methods would give equally reliable volume estimates.

The question of the degree of subdivision of the 3D reconstructed chamber involves a compromise between conflicting considerations. Subdivision of the chamber into many regions offers an advantage of improved quantitation. However, unless the signal -to- noise ratio of the ultrasonic imaging mode is of sufficient quality the reproducibility of image boundaries over short distances will be poor with large variability. Moreover, as the number of subdivisions becomes very large they lose anatomic significance. Both these factors were carefully considered in the selection of the number of apical tomograph views for the 3D spatial reconstruction of the left ventricle at end diastole and end systole.

The results of left ventricular volume estimation by four anatomically defined apical echocardiographic views highlights the need for an effective and reliable reference method for volume measurement in vivo. In Chapter 6 the error analysis of the post mortem studies where fluid volume was directly measured shows that the 3D method developed has no significant systematic error or bias and all the error is randomly distributed. The principal component of the error could be attributed to the inadequate spatial resolution of ultrasonic transducers. The technical aspects of ultrasonic cardiac imaging were reviewed in Chapter 3. However, for in-vivo studies the biplane cineangiographic method discussed in Chapter 5 is generally accepted as the reference method for evaluation of alternatives.

Despite the common problems of boundary delineation for both the invasive and non invasive imaging modes the amount of spatial information on which to base any estimate is fundamental. The cineangiographic method provides two quasi-orthogonal projections which obscures any information which does not appear as a boundary phenomena. Viewing the video tape of patient 5 demonstrates explicitly the appearance and disappearance of an aneurysm on the projected boundary. Quite obviously at times the aneurysm is obscured by the overlying myocardium of the ventricular chamber. It is not unexpected then that the random error in volume estimates with respect to the cineangiographic estimates is increased, particularly for end diastolic volumes, compared to the post mortem study. The smaller size of the end systolic ventricle makes it more susceptible to larger relative errors. Nevertheless the 3D spatial reconstruction method is an improvement over the single plane and multiple plane methods discussed in Chapter 6. Particularly in situations where the invasive method fails to adequately project an aneurysm or some significant asynergy.

The results on shape variation at a global and regional level have not previously been reported. The global assessment of ventricular geometric fluctuation has been carried out by a one way analysis of variance Model II formulation. The results are rather unexpected in that the greatest percentage of volume variance attributable to geometry occurs for normal patients. However, the magnitude of the variance is a minimum in this instance which suggests that the pathological left ventricle most commonly enlarges. Undeniably then global shape changes do occur in heterogenous heart disease patient groups. Most of these changes it would appear are masked by compensation mechanisms which maintain ejection volumes at satisfactory levels. One can speculate that quantitation of global shape changes may provide a useful screening procedure to identify patients with the potential for debilitating heart disease. The complementary analysis of regional changes in myocardial surface and volume elements of the segmented ventricle isolated the regions in which changes tend to occur and in which direction with respect to normal patients. In the 13 patients with ischemic heart disease we have been able to demonstrate regional changes in geometry for all patients. These changes have not been described to date but are encompassed in such qualitative generalisations as left ventricular "ellipticalisation" and "sphericalisation". These crude descriptions are often used to characterise dimensional changes. The results of the regional analysis show that myocardial changes in ischemic heart disease lead to changes in ventricular shape and that the changes tend to be grouped. That is in the medial, posterior long axis region and from the mid-position toward the apex or basal region.

The graphical display of the 3D reconstruction of the left ventricle at end diastole and end systole provides the spatial information to enable a visualisation of the general shape characteristics of a patients ventricle. It also provides a view of any specific local features which deviate from normal shapes or the general shape of the particular ventricle. This complementary visual information together with the quantitative assessment of the ventricle enables a more thorough assessment of ventricular performance to be made by a clinician.

7.3 Recommendations for further study

The detailed geometric analysis of the left ventricle is still to be fully explored in vivo. A limiting factor to date has been the availability of suitable technology to pursue these studies. Echocardiography is an emerging technology which is providing a tool, albeit with limitations, to begin exploration of ventricular geometry in vivo. This study has made a preliminary evaluation of an echographic 3D reconstruction of the left ventricle using four anatomically defined apical views. Though some new information on ventricular shape has been presented, further questions need to be addressed to fully unravel the implications of the shape changes for cardiac function and performance.

Some of the questions that need to be addressed relate to the impact of shape changes on stroke volume and injection fraction. Whether particular regions or types of shape change are more significant in relation to pathology. Furthermore, whether shape changes are associated with particular histological and/or elastic changes in the myocardium.

7.4 Conclusion

This thesis has applied a relatively new technology, that of echocardiography, and attempted to optimise both the technical and anatomical constraints on effective cardiac imaging to study left ventricular geometry. A theoretical study of the various tomographic slices available for left ventricular imaging showed that rotational apical views about the long axis optimise the spatial data available for both qualitative and quantitative analysis. From four anatomically defined apical views a 3D reconstruction of the left ventricle was generated by computer. Polar integration, which minimised geometric assumptions about the left ventricle, gave reliable volume estimates for ellipsoidal vessels, post mortem human hearts and in vivo studies with respect to a cineangiographic reference.

Left ventricular shape analysis at end diastole and end systole has for the first time described global fluctuations and region variation in ventricular geometry. The proportion of global geometric fluctuation is greatest for normal patients but the magnitude of the fluctuation is greatest for the pathological groups. The regional surface and volume proportions for the segmented ventricle in a normal population were described. The changes which occurred in 13 patients with ischemic heart disease were then quantified and compared to the normal data. In all instances change in left ventricular shape was detected in at least one region. This confirms that ischemic heart disease is closely linked with ventricular shape change and that this change is closely linked with ventricular dysfunction.

A 3D spatial reconstruction can be performed in a clinical setting which enhances the qualitative evaluation of global and regional ventricular shape. This, in combination with quantitative data has the potential to improve patient assessment, and the understanding of cardiac function and performance.

APPENDIX

Acta Cardiologica, Vol. XXXIX, 1984, 6, pp. 409-436.

THREE DIMENSIONAL RECONSTRUCTION OF THE LEFT VENTRICLE FROM FOUR ANATOMICALLY DEFINED APICAL TWO-DIMENSIONAL ECHOCARDIOGRAPHIC VIEWS

Received for publication, January 3, 1984.

by

N.L. FAZZALARI (*), J.A. DAVIDSON (**), J. MAZUMDAR (***), L.J. MAHAR (**) and E. DENARDI (*)

Three dimensional reconstruction of the left ventricle from four anatomically defined apical two-dimensional echocardiographic views — *A method is described for three dimensional reconstruction of the left ventricle which uses four anatomically defined apical views. It is shown that the algorithms developed for reconstruction and volume estimation provide accurate results when applied to planar views with accurately defined boundaries. The linear regression equation was $y = -6.32 + 1.04x$, with $SEE = \pm 3.4$ ml, $r = 0.999$. For both "in vitro" and "in vivo" studies this method is found to be better than various geometrical models used to estimate volumes from two dimensional tomographic or projection views. The linear regression equation of in vitro fluid volume on volume estimate is $y = 8.44 + 0.68x$, with $SEE = \pm 4.9$ ml, $r = 0.988$. For pooled end diastolic and end systolic volumes (EDV and ESV) determined by three dimensional reconstruction (3-DR) and angiography the linear regression equation is $y = 54.50 + 0.50x$, with $SEE = \pm 33.5$ ml, $r = 0.670$. For stroke volume (SV), the regression equation is $y = 21.10 + 0.40x$, with $SEE = \pm 12.8$ ml, $r = 0.750$, and for ejection fraction (EF) it is $y = 1.10 + 0.70x$, with $SEE = \pm 7.8\%$, $r = 0.840$. In patients with ischemic heart disease, the method presented is shown to be better than existing methods of volume estimation. Three dimensional perspective images can be plotted in any orientation as a visual aid to the cardiologist. In vivo studies demonstrate the feasibility of 3-DR, from anatomically defined apical views, in the clinical setting.*

(*) Division of Tissue Pathology, Institute of Medical and Veterinary Science.
(**) Cardiovascular Investigational Unit, Royal Adelaide Hospital.
(***) Department of Applied Mathematics, University of Adelaide, South Australia.

KEY WORDS

Left ventricle
Volume
Three dimensional
Echocardiography
Ventriculography
Noninvasive techniques

Introduction

Assessment of left ventricular performance is a most important investigative procedure for the diagnosis and prognosis of heart disease. The information gained from such studies often determines the course of medical and/or surgical treatment. An important parameter of ventricular performance is a measure of ventricular volume during the cardiac cycle. From volume estimates at end diastole and end systole a number of derived numerical parameters can be calculated, such as stroke volume, ejection fraction, cardiac output and cardiac index (Feigenbaum, 1976). Both invasive and non-invasive methods are currently used to estimate LV volumes. Invasive cardiac catheterisation methodologies although accepted as reliable and effective, present obvious risks to the patient. Non-invasive echocardiographic methods present no known risk to the patient. No case of harmful effects of ultrasound in normal patient use has ever been documented. Hence, a principal advantage of echocardiography is its repeatability.

Modelling of the left ventricle for effective volume estimation has presented problems for both invasive and non-invasive investigative methodologies. The ventricular geometry does not conform to any single geometric shape nor is there constancy of shape during the cardiac cycle, particularly in various pathological states (Dumesnil & Shoucri, 1982). Consequently, models based on a particular geometric shape have involved invalid assumptions about left ventricular shape. Various geometric models better suit left ventricular shape at different phases of the cardiac cycle and in different pathological states. In invasive cardiac catheterisation the recognised comparative standard is the area-length method of Dodge & Sandler (1960). However, there are at least eight mathematical models applicable to ventriculograms for left ventricular volume estimations (Davila & Sanmarco, 1966). The non-invasive models developed initially utilised M-mode ultrasound which provides an "ice-pick" view of cardiac structures over time (Feigenbaum, 1976). This imaging mode provides minimal spatial information and hence resulted in the most simple of ventricular models. A major assumption is that the ventricular shape is that of a prolate ellipsoid with an aspect ratio of 2:1 for all stages of the cardiac cycle, irrespective of pathology. Nevertheless, M-mode echocardiography has provided useful information, supported empirically, where there is no left ventricular segmental wall motion abnormalities (Murray et al., 1972; Teichholz et al., 1976; Kronik et al., 1979).

Two dimensional echocardiography permits unique visualisation of the heart in vivo (Tajik et al., 1978) and provides spatial information in tomographic views previously unavailable. The availability of this spatial information has led to the development of more sophisticated models of the left ventricle, many of which still require some basic assumptions about shape and geometry (Folland et al., 1979; Alpert et al., 1979; Schiller et al., 1979; Silverman et al., 1980). The complexity of the models is often reflected in the difficulty of data acquisition and analysis. Despite the comparative limitations of biplane left ventricular angiography the more complex models reported to data have provided better volumetric comparisons (Mercier et al., 1982; Schnittger et al., 1982).

Few studies have been reported which obviate geometric assumptions, particularly with respect to symmetry. One model which attempts to minimise errors associated with assumptions of regular geometry assumes ventricular symmetry about the major axis for a stack of elliptical discs (Edelman, 1981). To overcome the limitations of geometric mathematical models it is necessary to consider the spatial arrangement of the ventricle in three dimensions. Two reports of three dimensional left ventricular reconstruction have employed different methods. One is a reconstruction from arbitrary parasternal short axis views (Geiser et al., 1982), and the other from apical views obtained by angular rotation of the transducer about the left ventricular long axis (Ghosh et al., 1982). This study is the first to present a method based on anatomically defined apical views. A preliminary analysis of the application of this method to (i) given geometrical shapes, (ii) post-mortem hearts, (iii) patients referred for investigation on clinical grounds, is presented.

Materials and methods

A Hewlett Packard two dimensional ultrasound imaging system 77020A with a phased array 3.5 MHg transducer and 90° sector angle was used for all image data acquisition at 30 frames per second. Apical views were recorded at various rotational degrees for use in three dimensional reconstruction of the heart.

1. *Geometric shapes*

In order to test the reconstruction methodology six planar drawings of symmetrical geometric shapes, one rectangle and five ellipses of various arbitrary aspect ratio (table I) were selected for reconstruction of a cylindrical and five ellipsoidal vessels. Dimensions for these shapes were chosen so that they had volumes within the physiological range usually encountered for the human left ventricle.

Table I. — *Three-dimensional volume estimates of various geometric figures having used four planar figures for the three dimensional reconstruction. Volume expressed in ml*

Geometry aspect ratio *Minor axis* / *Major axis*	*Trapezoidal rule*		*Polar integration*		*Calculated volume*
	5 slices	*10 slices*	*5 slices*	*10 slices*	
0.42	85.9	87.7	95.6	97.6	96.8
0.50	119.6	121.4	133.2	135.1	136.2
0.57	156.7	159.4	174.4	177.4	179.2
0.64	197.6	202.4	220.0	225.2	221.9
0.71	239.3	244.3	266.3	271.9	264.0
Cylinder	174.7	174.3	194.1	194.0	196.4
μ	162.3	164.9	180.6	183.5	182.4
SEM	22.4	22.9	24.9	25.4	24.4

2. *In vitro studies*

In vitro experiments were performed on seven post-mortem hearts. A comparison of volume estimates using the three dimensional reconstruction technique was made with the absolute volume determined by filling the left ventricle with fluid (table II). The post-mortem hearts were thoroughly flushed to remove blood clots that may have remained in the right and left ventricles and atria. The atria were subsequently cut to access the tricuspid and mitral orifices enabling the left and right ventricles to be packed with surgical gauze. Following packing, the heart was fixed in formalin. After three days the gauze was removed leaving a firm, fixed heart which maintained its packed shape. The left and right ventricles were filled with a solution of 20% alcohol, which has a temperature invariant ultrasound transmission velocity of 1540 $msec^{-1}$, the assumed normal tissue ultrasound velocity. The filled post-mortem hearts were placed in

Table II. — *Regression of reference parameters on the three dimensional reconstruction estimate*

Method used in parameter estimate		*Regression equation*	*Standard error of estimate*	*Pearson's correlation r*
Reconstructed vol. vs calculated vol. (ml)				
Trapezoidal	5 slices	$Y = -5.68+0.94x$	3.1	0.998
	10 slices	$Y = -5.68+0.94x$	3.1	0.998
Polar	5 slices	$Y = -6.32+1.04x$	3.4	0.998
	10 slices	$Y = -6.32+1.04x$	3.4	0.998
3-D echo vol. vs liquid vol. (ml)				
Trapezoidal	5 slices	$Y = 9.32+0.61x$	5.1	0.983
	10 slices	$Y = 7.90+0.61x$	4.4	0.987
Polar	5 slices	$Y = 8.77+0.69x$	5.3	0.986
	10 slices	$Y = 8.44+0.68x$	4.9	0.988
3-D echo ED and ES vol. vs angio vol. (ml)				
Trapezoidal	5 slices	$Y = 53.58+0.44x$	33.1	0.612
	10 slices	$Y = 51.60+0.45x$	31.7	0.620
Polar	5 slices	$Y = 56.90+0.51x$	34.5	0.652
	10 slices	$Y = 54.50+0.50x$	33.5	0.670
3-D echo stroke vol. vs angio stroke vol. (ml)				
Trapezoidal	5 slices	$Y = 23.87+0.26x$	11.1	0.674
	10 slices	$Y = 20.42+0.30x$	11.9	0.705
Polar	5 slices	$Y = 23.73+0.34x$	11.1	0.764
	10 slices	$Y = 21.10+0.40x$	12.8	0.750
3-D echo% EF vs angio% EF				
Trapezoidal	5 slices	$Y = 4.03+0.63x$	7.9	0.801
	10 slices	$Y = 1.62+0.68x$	8.5	0.805
Polar	5 slices	$Y = 2.66+0.67x$	7.3	0.840
	10 slices	$Y = 1.10+0.70x$	7.8	0.840

polyethylene plastic bags containing the alcohol solution. The bag was hot-wire sealed after all air was expelled. This procedure provided a post-mortem heart suspended in an ultrasonically transparent bladder. The ultrasonic transducer was positioned at the apex and the chosen apical views for three dimensional reconstruction recorded. Subsequently the volume of the left ventricle was measured directly by filling the left ventricle to the level of the aortic and mitral valves.

3. *In vivo studies*

The methodology was applied to eight patients in sinus rhythm who underwent cardiac catheterisation with biplane LV angiography. Each patient had biplane left ventricular angiograms recorded on cine film at 48 frames per second. End systolic and end diastolic volumes were then calculated according to the method of Dodge and Sandler (1960). Within 24 hours of catheterisation two dimensional echocardiograms were recorded on VHS video tape employing the necessary apical views for three dimensional reconstruction. The patient lay recumbent or turned on to the left lateral decubitus position.

A method of reconstruction from planar two dimensional apical echocardiographic views obtained at 45° rotational intervals was used in this study. The transducer was placed at the apex of the heart, found by palpation, to record four anatomically defined apical views. Anatomical orientation was made with central reference to the apical four chamber view as the standard anatomical planar section.

a) *Four chamber view*

The four chamber view (fig. 1a) involves positioning of the sector beam to observe the heart from apex to base along the acute margin of the right ventricle and the obtuse margin of the left ventricle, continuing the plane of section through both atria (Edwards et al., 1981).

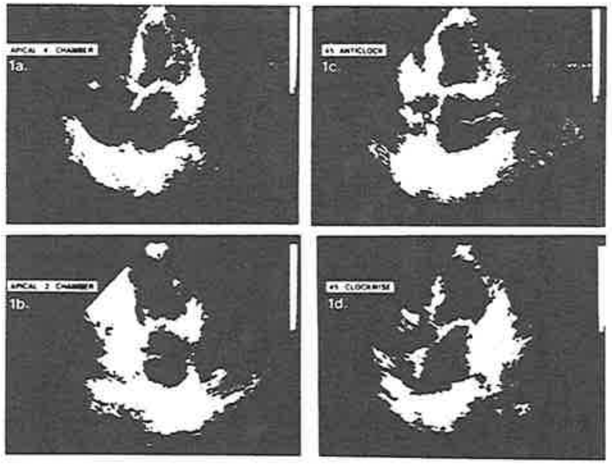

Fig. 1. — Echocardiographic apical views used in three dimensional reconstruction of the left ventricle. Anatomical definition is given in the text.

b) *Two chamber view*

The sector plane is positioned perpendicular to the four chamber view with anticlockwise rotation (fig. 1b), such that it passes from the left ventricular apex to the left atrium. Both the anterior and posterior mitral leaflets are included in this view with the exclusion of the aortic valve, ventricular septum and right ventricular outflow tract (Edwards et al., 1981).

c) *Intermediate* (45° anticlockwise)

The four chamber view is first obtained. Subsequent rotation of the transducer through 45° anticlockwise (fig. 1c) presents the left ventricle and left atrium in a plane parallel to the mitral valve commissure. Consequently only a single (anterior) mitral valve cusp is viewed during part of the cardiac cycle (diastole). The left ventricle may appear "waisted" by (partial) inclusion of both papillary muscles and the margins of right-sided chambers remain visible.

d) *Intermediate* (45° clockwise)

The four chamber view is again first obtained. Rotation of the transducer through 45° clockwise (fig. 1d) presents essentially a mirror image of the standard apical long axis view (Edwards et al., 1981; Feigenbaum, 1976) viz. a view passing from the left ventricular apex through the outflow tract (ventricular septum and anterior mitral leaflet) and into the ascending aorta. The left atrium and right ventricular outflow tract (infundibulum), are also included in this planar section.

These four apical views section the ventricle in four complementary planes each separated by approximately 45° of angular rotation about the long axis of the left ventricle. The common long axis was defined as a line joining the most apical endocardial point to the centre of the mitral valve annulus.

A hard copy of ECG gated frames at end diastole and end systole was obtained for each view from the video record. The ventricular endocardial boundaries were delineated by an experienced echocardiographist. These ventricular boundaries were subsequently digitised with an HP 9874A digitiser, and stored permanently on computer file and tape. This stored planar data was transformed to generate a three dimensional reconstruction of the left ventricle and plotted on an HP 9864A plotter in the required perspective. The reconstruction can be used to generate short axis segments at various levels along the major axis and to calculate the volume from a number of slices using both a trapezoidal rule and polar coordinate integration. The same procedures for digitisation, three dimensional reconstruction and volume estimation were applied to post-mortem hearts and symmetrical geometric figures.

Furthermore, from the orthogonal two chamber and four chamber views, the left ventricular volume was estimated by the area-length biplane technique (Silverman et al., 1980).

Results

1. *Analytical shapes*

Six symmetrical analytical shapes, one cylinder and five prolate ellipsoids of varying aspect ratio, were reconstructed mathematically from four identical planar views. The aspect ratio of the arbitrarily chosen ellipsoids

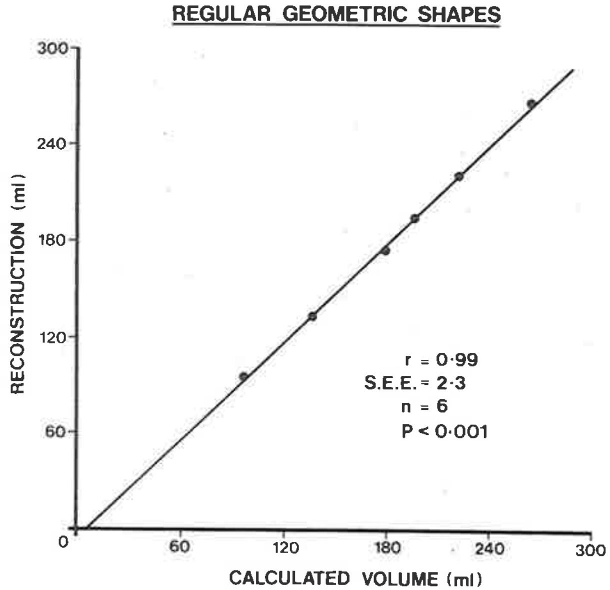

Fig. 2. — Regression of regular geometric shape calculated volumes on reconstructed volume estimates.

varied from 0.42 to 0.71. Using five and ten, computer generated, short axis views of the geometries the volumes calculated by the trapezoidal rule and using polar coordinates were not significantly different to the volumes calculated by analytical methods (table I). However, the absolute errors in volumes calculated by the trapezoidal rule and polar coordinates were significantly different both for the 5 and 10 slice segmentation ($P<0.0001$). The trapezoidal method underestimated volumes, on average, by about 20 ml, while polar coordinated integration estimated volumes, on average, within 3 ml of the calculated volumes. There was no significant difference in the volume estimates from 5 and 10 slices. Regressions of calculated volumes on estimated volumes for the trapezoidal method had a slope less than an identity value of 1 and a negative intercept (table II). Polar coordinate integration resulted in a slope greater than one and a negative intercept (table II, fig. 2).

2. *In vitro studies*

3-D echo reconstruction studies were carried out on 7 hearts taken at autopsy. Volume estimates by the trapezoidal rule and polar coordinates showed on average no significant difference compared to the fluid filled volume of the left ventricle (table II). Polar coordinate integration underestimated liquid volumes least. Regression analysis of liquid volume on estimated volume showed slopes less than the identity value of 1 and positive intercept (table II). The use of polar coordinates gave marginally better results than the trapezoidal rule though the difference was not statistically significant (fig. 3). This result was independent of whether 5 or 10 slice segments of the left ventricle were used.

3. *In vivo studies*

Eight patients, 7 males and 1 female, were studied by two dimensional echocardiography being 75% of all patients undergoing biplane left ventricular angiography in this laboratory. End diastolic volume, end systolic volume, stroke volume and ejection fraction for trapezoidal, polar coordinate integration and biplane ventriculography are tabulated in table IV. Comparing the averages of the pooled patient data, the end diastolic and end systolic volumes determined by trapezoidal volume integration are not significantly different to volume estimates by polar coordinate integration and by the Dodge-Sandler biplane angiographic technique. Nevertheless, the trapezoidal volumes underestimate the angiographic volumes by about 12 ml compared with polar integration which underestimates by

Table III. — *Clinical data and three dimensional volume estimates (ml) for seven in vitro studies of autopsy hearts*

Case number	Sex	Age yr.	BSA m^2	Heart wt. gm.	Trapezoidal rule 5 slices	Trapezoidal rule 10 slices	Polar integration 5 slices	Polar integration 10 slices	Liquid filled volume	Pathology
116	M	55	1.85	480	43	40	45	43	53	Moderate LV hypertrophy
118	M	40	2.02	375	73	74	82	83	116	Normal
121	F	60	1.70	390	42	40	45	44	59	Normal
148	M	51	2.34	600	99	96	111	108	141	Myocardial Infarction LV hypertrophy
197	M	63	1.96	305	33	33	39	39	43	Normal
314	M	16	1.74	290	26	25	29	28	30	Normal
451	M	19	2.01	410	51	50	55	55	57	Normal
μ		43.4	1.94	407	52.4	51.1	58	57.1	71.3	
SEM		7.3	0.08	40.2	9.6	9.5	10.8	10.7	15.5	

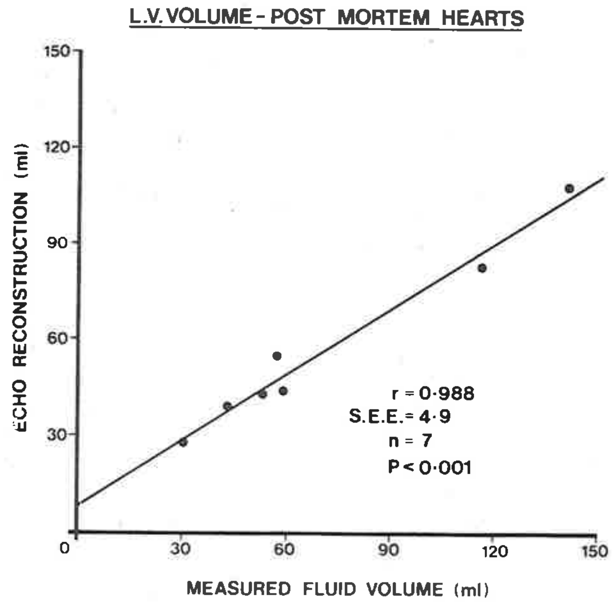

Fig. 3. — Regression of post-mortem hearts fluid volume measures on echographic three dimensional reconstruction estimates.

about 3 ml. This is consistent with our findings for analytical shapes.

Regression analysis of echocardiographic volume estimates versus angiographic estimates showed a slope less than 1 and a positive intercept for the method with the best correlation. This was obtained for the application of polar integration to 10 computer generated slices of the left ventricle (table II, fig. 4). Similarly, stroke volume showed no significant difference among the echographic methods though the trapezoidal stroke volume estimates were about 7 ml less than the polar estimates. Both methods produce estimates significantly less than the angiographic estimates ($P < 0.0001$). Regression analysis of angiographic stroke volume on echocardiographic estimate showed slopes less than 1 and positive intercept (table II, fig. 5).

Table IV. — *Clinical data and three dimensional parameter estimates for in vivo studies of the left ventricle together with catheterisation data*

Case no.	Sex	Age yr.	BSA (m^2)	Trapezoidal rule						Polar integration						Angio			LV Asynergy	Diagnosis
				5 slices			10 slices			5 slices			10 slices							
				EF %	SV (ml)	ED ES (ml)	EF %	SV (ml)	ED ES (ml)	EF %	SV (ml)	ED ES (ml)	EF %	SV (ml)	ED ES (ml)	EF %	SV (ml)	ED ES (ml)		
1	M	18	1.30	51	68	133 65	52	69	133 64	51	77	151 74	52	79	151 72	58	121	210 89	—	V.S.D.*
2	M	18	1.30	39	44	113 69	39	44	113 69	40	52	129 77	40	51	128 77	60	134	222 88	—	Post. op. A.I.
3	F	43	1.60	42	38	88 50	44	37	85 48	42	43	99 56	44	43	97 54	64	65	103 38	—	M.S.
4	M	54	1.80	39	44	120 76	40	48	120 72	41	56	137 81	41	57	137 80	47	89	188 99	Inferior akinesis	I.H.D.
5	M	62	1.90	30	47	155 108	31	49	157 108	33	57	173 116	34	60	175 115	56	85	153 68	Inf. post hypokinesis	I.H.D.
6	M	59	1.80	20	40	196 156	19	37	193 156	18	39	210 171	18	37	210 173	20	29	144 115	Inferior dyskinesis	I.H.D. M.R.
7	M	57	1.55	23	26	113 87	21	23	110 87	24	30	125 95	22	27	123 96	46	56	121 65	Ant-apical dyskinesis	I.H.D.
8	M	61	1.70	54	65	120 55	55	67	121 54	54	72	134 62	55	75	136 61	71	117	165 48	—	M.R. M.V.P.
	μ SEM	46.5 6.6	1.60 0.08	37.3 4.3	46.5 4.9	106.5 10.1	37.6 4.7	46.8 5.5	105.6 10.2	37.9 4.4	53.3 5.6	118.1 11.0	38.3 4.6	53.6 6.3	117.8 11.2	52.8 5.5	87.0 12.7	119.8 14.0		

V.S.D. ventricular septal defect.
* sinus of valsalva fenestration.
A.I. aortic incompetence.
I.H.D. ischaemic heart disease.
M.S. mitral stenosis.
M.R. mitral regurgitation.
M.V.P. mitral valve prolapse.

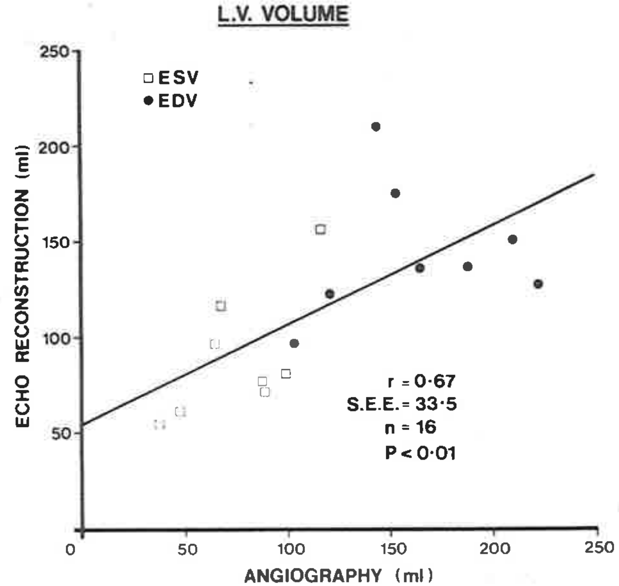

Fig. 4. — Regression of biplane left ventricular angiographic volume estimates on echographic three dimensional reconstruction estimates.

The pooled average of ejection fraction estimates ranged from 37.3% to 38.3% for the three dimensional echographic methods and hence showed no statistical difference.

These estimates were significantly lower than the corresponding angiographic estimates. Regression analysis of angiographic ejection fraction on echographic estimates again showed a slope less than the identity value of 1 and a positive intercept. Polar integration regressions showed the best correlation (table II, fig. 6).

The comparison of three dimensional echographic methods with the echographic biplane area length estimates shows quite clearly that the bias of the three dimensional technique is to increase the value of ventricular volume estimates (table V). Estimates of ejection fraction are not statistically different. Biplane echographic estimates compared to all angiograph-

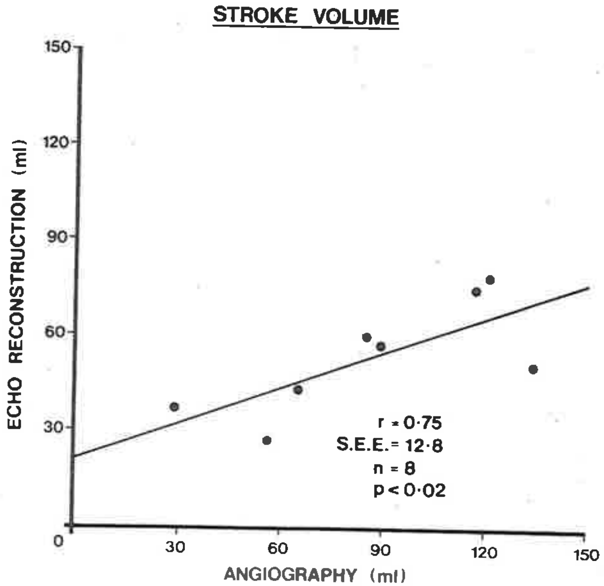

Fig. 5. — Regression of biplane left ventricular angiographic stroke volume estimates on echographic three dimensional reconstruction estimates.

ic values (table VI) show lower correlation coefficients and a larger standard error of estimate than the three dimensional data (table II).

Discussion

Previously published attempts of three dimensional reconstruction using echocardiography in which details of methodology have been documented use either parasternal short axis views (Geiser et al., 1982; Moritz et al., 1983), or apical views where the transducer has been rotated about the left ventricular long axis (Ghosh et al., 1983). With these methods a mechanical spatial registration arm is used to register the spatial coordinates of the two dimensional echo data. In this study we have used rotated apical views which we have anatomically defined obviating the need for the sophistication of a spatial registration arm. Considering that the

Table V. — *Regression of echo biplane estimates on the three dimensional reconstruction estimates*

Method used in parameter estimate		*Regression equation*	*Standard error of estimate*	*Pearson's correlation r*
3-D echo ED and ES vol. vs echo biplane vol. (ml)				
Trapezoidal	5 slices	Y = 21.22+0.86x	13.1	0.946
	10 slices	Y = 19.75+0.87x	12.8	0.949
Polar	5 slices	Y = 25.99+0.93x	14.3	0.946
	10 slices	Y = 23.93+0.95x	14.2	0.948
3-D echo stroke vol. vs echo biplane vol. (ml)				
Trapezoidal	5 slices	Y = 15.99+0.57x	7.3	0.853
	10 slices	Y = 12.48+0.63x	7.8	0.863
Polar	5 slices	Y = 17.09+0.66x	8.4	0.857
	10 slices	Y = 13.49+0.74x	8.7	0.871
3-D echo % EF vs echo biplane % EF				
Trapezoidal	5 slices	Y = −0.02+0.89x	3.0	0.977
	10 slices	Y = −0.05+0.97x	3.0	0.981
Polar	5 slices	Y = −0.02+0.91x	3.0	0.979
	10 slices	Y = −0.04+0.97x	2.0	0.987

Table VI. — *Regression of the angiographic estimates on the echo biplane estimates*

Regression equation	*Standard error of estimate*	*Pearson's correlation r*
Echo biplane ED and ES vol. vs angio vol. (ml)		
Y = 43.41 + 0.46x	36.3	0.581
Echo biplane SV vs angio SV (ml)		
Y = 25.97 + 0.32x	17.4	0.558
Echo biplane % EF vs angio % EF		
Y = 0.08 + 0.68x	8.0	0.795

quoted lateral resolution of most two dimensional echocardiographic equipment is of the order of 4-5 mm (Logan Sinclair et al., 1983), there is no value in operating at a level of precision better than the accuracy that can be achieved by current ultrasonic transducers. Lateral resolution and endocardial border definition are limiting features of the technique. Consequently the high level of precision conferred by spatial registration apparatus is considered unnecessary, particularly when four complementary apical echocardiographic tomographic orientations can be easily defined. Hence, we considered that four anatomically defined apical views are ade-

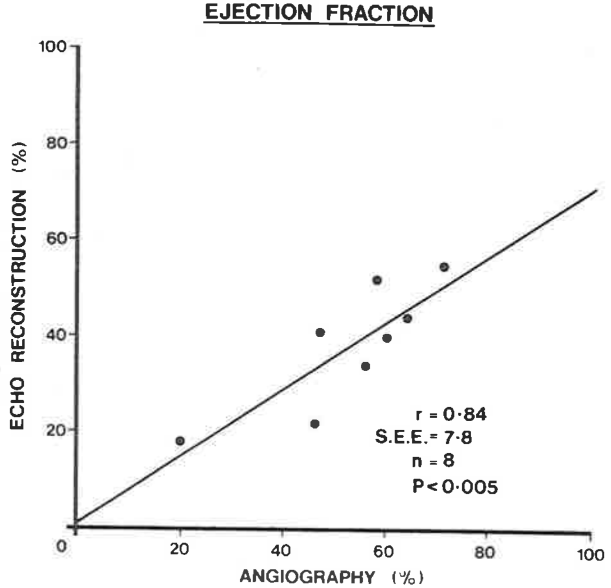

Fig. 6. — Regression of biplane left ventricular angiographic ejection fraction estimates on echographic three dimensional reconstruction estimates.

quate to evaluate our methodology for three dimensional left ventricular reconstruction.

Our approach is supported by the results presented on the analysis of analytical shapes where boundaries are well defined. These results show that the algorithms we have developed provide excellent estimates of volume for reconstructed three dimensional volumes. This implies that a number of factors degrade the boundary definition of the apical left ventricular views used in three dimensional reconstruction. Primarily, lateral resolution limits accurate delineation of the left ventricular boundary. Furthermore, transducer placement over the available echocardiographic window at the apex may result in tangential shortening of both long and short axes. This difficulty can be minimised with operator experience, though sometimes ribs can obscure optimal transducer placement. Additional factors, such as inner trabecular registration by ultrasound, act to

underestimate true left ventricular size (Schnittger et al., 1982). However, provided an optimal apical window can be found then simple transducer rotation normally provides all the necessary views. Parasternal short axis views recorded for three dimensional reconstruction require multiple windows through the ribs or complex correction algorithms for transducer tilt (Geiser et al., 1982; Moritz et al., 1983). In addition, lung tissue may present a greater obstruction in parasternal short axis views. The long-axis is often inadequately defined from parasternal long axis views due to truncation necessitating an apical view to obtain a satisfactory estimate. Consequently reconstructions from short axis views require multiple transducer placements to record sufficient three dimensional information. Apical rotational reconstruction requires the definition of only one appropriate transducer location to obtain the information required for 3-DR.

This study has demonstrated that our methodology applied to analytical geometries gives very reliable results (tables I and II). Further, the in vitro comparisons showed higher correlation coefficients and lower standard errors of estimates (tables II and III) than the corresponding values obtained by Wyatt et al. (1980) using various geometric ventricular models on formalin fixed canine left ventricles. In vivo reconstructions underestimated volumes compared to biplane angiography though not consistently (table IV). Four apical echocardiographic views were compared to two projected views for biplane angiography. Echocardiographic volume estimates were greater than angiographic estimates in cases of ischemic heart disease. Ejection fraction compared most favourably with angiographic estimates. Both correlation and standard error of the estimates were better than recently published results by Erbel et al. (1983). In addition, we have shown that volume estimates made by the 3-DR technique are an improvement over the area-length biplane technique that utilises the four chamber and two chamber echographic views, principally by giving higher estimates of ventricular volume.

Volume underestimation is a major feature of echocardiographic geometric techniques and is caused primarily by two technical factors. The point of maximum palpable apical impulse does not always provide the most optimal echocardiographic window. Hence, in an endeavour to optimize the image quality, and continuity of endocardial outline, transducer placement may not always coincide with the true apex position so that long axis foreshortening could occur. Consequently, the largest of four long axis measurements is utilised during reconstruction to minimize this potential error. Echo reflection from the innermost trabecular margins presents a reduced internal left ventricular boundary area. Angiographic measurement projects opacification to the outermost chamber boundaries.

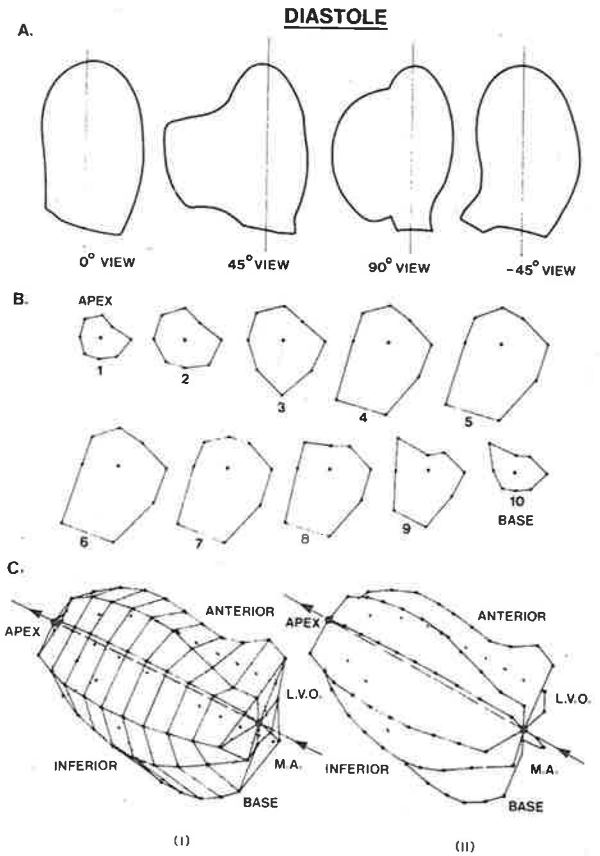

Fig. 7. — Diastolic and systolic three dimensional reconstruction of the left ventricle for cases with an infero-posterior aneurysm. A. Diastolic and systolic two dimensional echographic outlines of the four anatomically defined apical views used in 3-D reconstruction. B. Ten computer generated short axis slices of the left ventricle. Slices numbered 3 to 9 demonstrate the presence of the aneurysm. C. Two presentations of the 3-D reconstruction for the left ventricle with the infero-posterior aneurysm clearly identifiable.
M.A. — mitral annulus.
L.V.O. — left ventricular outflow tract.

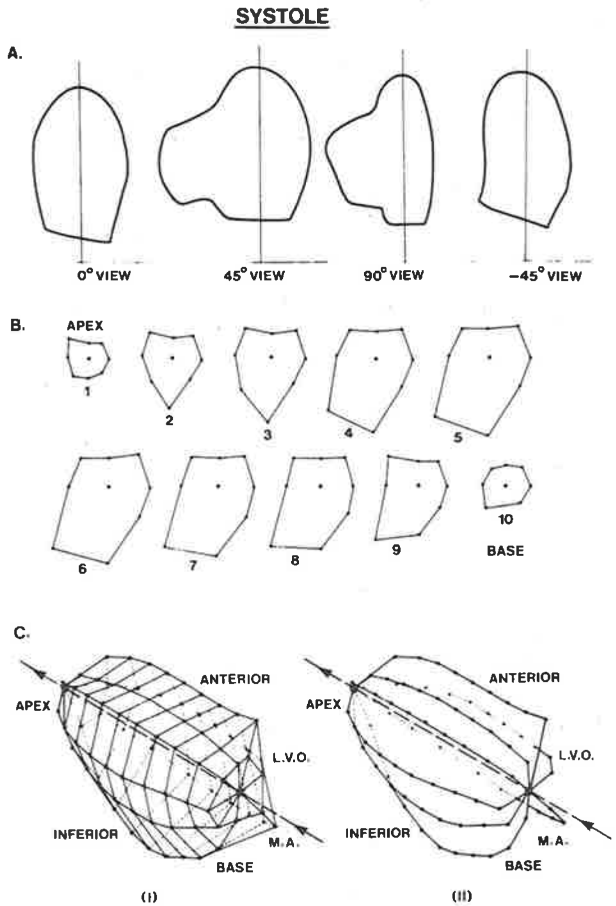

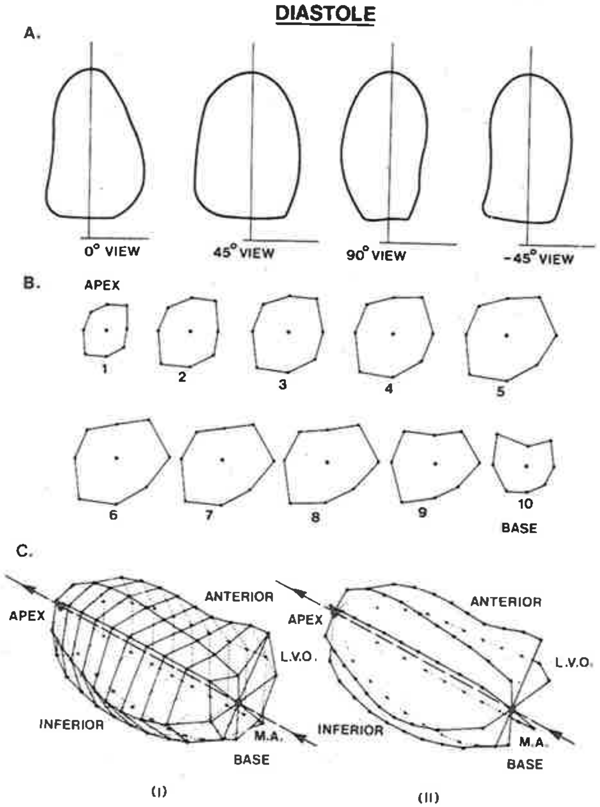

Fig. 8. — Diastolic and systolic three dimensional reconstruction of the left ventricle for case 2, which has no left ventricular asynergy. A. Diastolic and systolic two dimensional echographic outlines of the four anatomically defined apical views used in 3-D reconstruction. B. Ten computer generated short axis slices of the left ventricle. C. Two presentations of the 3-D reconstruction of the left ventricle.

M.A. — mitral annulus.
L.V.O. — left ventricular outflow tract.
μ — mean value.
SEM — standard error of the mean.

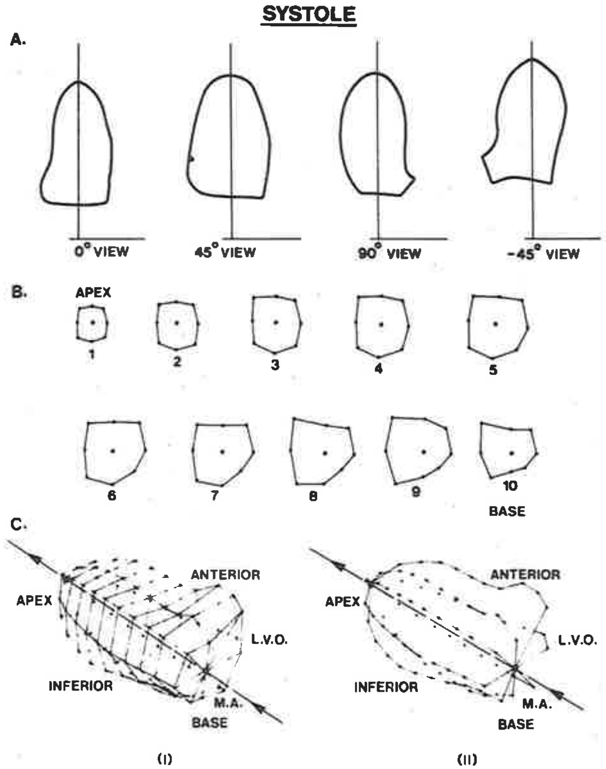

These variations will occur because of technical differences in the two imaging methods.

Composite three dimensional reconstruction of the left ventricle can provide readily accessible comprehensive global information about ventricular performance (fig. 7 and 8) without risk to the patient. Problems exist with volume estimation in general but patients with ischemic heart disease are specially difficult. In this group of patients, wall-motion abnormalities and aneurysms compound the problems of volume estimation from two dimensional tomographic or projected views. In case 6, composite echo reconstruction of the left ventricle (fig. 7) demonstrates a clearly defined aneurysm boundary. This case had an infero-posterior aneurysm which was clearly visible in two apical views and in one of these demonstrated paradoxical movement. Biplane angiography demonstrated the extent of the aneurysmal region less comprehensively than echo reconstruction by presenting only two projected orthogonal views. Therefore, volume estimates by echo reconstruction more closely reflect the true chamber volume.

Consequently, LV reconstruction makes an important contribution to the investigation of this difficult pathological group, with a realistic estimate of cardiac performance. LV reconstruction can also provide a visual presentation of shape irregularities and the ventricle can be viewed in any desired perspective.

In conclusion, a method is described for left ventricular three-dimensional reconstruction which uses four anatomically defined apical views. Our developed algorithms for reconstruction and volume estimation provide accurate results when applied to planar views with accurately defined boundaries. For the in vitro and in vivo studies this method is at least as good as various geometric models currently used to estimate volumes from two dimensional tomographic or projection views. In particular, ejection fraction estimates are better than the results of a simultaneous two dimensional echocardiography and ventriculography study recently published (Erbel et al., 1983). This method appears to have performed well in LV analysis in the traditionally difficult setting of ischemic heart disease. Further detailed clinical studies are in progress to assess in greater depth regional LV wall motion and the real clinical value of non-invasive left ventricular three dimensional reconstruction.

ACKNOWLEDGMENTS

The authors wish to thank the Pathologists in the Division of Tissue Pathology who cooperated in the collection of autopsy hearts. In addition, the assistance which was provided by Mr. P. Ritter, Technical Officer, and Mr. R. Bright, Technical Assistant, is greatly appreciated.

REFERENCES

ALPERT, B.S., BLOOM, K.R., GILDAY, D. & OLLEY, P.M. — The comparison between non-invasive and invasive methods of stroke volume determination in children. *Am. Heart J.*, 1979, *98*, 763.

DAVILA, J.C., SANMARCO, M.E. — An analysis of the fit of mathematical models applicable to the measurement of left ventricular volume. *Am. J. Cardiol.*, 1966, *18*, 31.

DODGE, H.R., SANDLER, H., BALLEW, D.W. & LORD, J.D. — The use of biplane angiocardiography for the measurement of left ventricular volume in man. *Am. Heart J.*, 1960, *60*, 766.

DUMESNIL, J.G., SHOUCRI, R.M. — Effect of the geometry of the left ventricle on the calculation of ejection fraction. *Circulation*, 1982, *65*, 91.

EDELMAN, S.K., ROWE, D.W., PECHACEK, L.N. & GARCIA, E. — Left ventricular volumes and ejection fraction derived from apical two dimensional echocardiography. *Bulletin of the Texas Heart Institute*, 1981, *8*, 344.

EDWARDS, W.D., TAJIK, A.J. & SEWARD, J.B. — Standardised nomenclature and anatomic basis for regional tomographic analysis of the heart. *Mayo Clin. Proc.*, 1981, *56*, 479.

ERBEL, R., SCHWEIZER, P., LUMBERTZ, H., HENN, G., MEYER, J., KREBS, W. & EFFERT, S. — Echoventriculography. A simultaneous analysis of two dimensional echocardiography and cineventriculography. *Circulation*, 1983, *67*, 205.

FEIGENBAUM, H. — *Echocardiography*. 2nd ed. Lea and Febiger, Philadelphia, 1976.

FOLLAND, E.D., PARISI, A.F., MOYNIHAN, P.F., JONES, M.S., FELDMAN, C.L. & TOW, D.E. — Assessment of left ventricular ejection fraction and volumes by real-time, two dimensional echocardiography. A comparison of cineangiographic and radionuclide techniques. *Circulation*, 1979, *60*, 760.

GEISER, E.A., ARIET, M., CONETTA, D.A., LUPKIEWIEZ, S.M., CHRISTIE, L.G. & CONTI, C.R. — Dynamic three dimensional echocardiographic reconstruction of the intact human left ventricle: Technique and initial observations in patients. *Am. Heart J.*, 1982, *103*, 1056.

GHOSH, A., NANDA, N.C. & MAURER, G. — Three dimensional reconstruction of echocardiographic images using the rotation method. *Ultrasound in Med. and Biol.*, 1982, *8*, 655.

KRONIK, G., SLANY, J. & MOSSLACHER, H. — Comparative value of eight M-mode echocardiographic formula for determining left ventricular stroke volume. A correlative study with thermodilution and left ventricular single-plane cineangiography. *Circulation*, 1979, *60*, 1308.

LOGAN SINCLAIR, R.B., OLDERSHAW, P.J. & GIBSON, D.G. — Computing in Echocardiography. *Progress in Cardiovascular Diseases*, 1983, *25*, 465.

MERCIER, J.C., DI SESSA, T.G., JARMAKANI, J.M., NAKANISKI, T., HIRAAISHI, S., ISABEL-JONES, J. & FRIEDMAN, W.F. — Two dimensional echocardiographic assessment of left ventricular volumes and ejection fraction in children. *Circulation*, 1982, *65*, 962.

MORITZ, W.E., PEARLMAN, A.S., McCABE, D.H., MEDEMA, D.K., AINSWORTH, M.E. & BOLES, M.S. — An ultrasonic technique for imaging the ventricle in three dimensions and calculating its volume. *IEEE transactions on Biomedical Engineering*, 1983, *BME-30*, 482.

MURRAY, J.A., JOHNSTON, W. & REID, J.M. — Echocardiographic determination of left ventricular dimensions, volumes and performance. *Am. J. Cardiol.*, 1972, *30*, 252.

SCHILLER, N.B., ACQUATELLA, H., PORTS, T.A., DREW, D., GOERKE, J., RINGERTZ, H., SILVERMAN, N.H., BRUNDAGE, B., BOTVINICK, E.H., BOSWELL, R., CARLSSON, E. & PARMLEY, W.W. — Left ventricular volume from paired biplane two dimensional echocardiography. *Circulation*, 1979, *60*, 547.

SCHNITTGER, I., FITZGERALD, P.J., DAUGHTERS, G.T., INGELS, N.B., KANTROWITZ, N.E., SCHWARZKOPF, A., MEAD, G.W. & POPP, R.L. — Limitations of comparing left ventricular volumes by two dimensional echocardiography, myocardial markers and cineangiography. *Am. J. Cardiol.*, 1982, *50*, 512.

SILVERMAN, N.H., PORTS, T.A., SNIDER, R.A., SCHILLER, N.B., CARLSSON, E. & HEILBRON, D.C. — Determination of left ventricular volume in children. Echocardiographic and angiographic comparisons. *Circulation*, 1980, *62*, 548.

TAJIK, A.J., SEWARD, J.B., HAGLER, D.J., MAIR, D.D. & LIE, J.T. — Two-dimensional real-time ultrasonic imaging of the heart and great vessels. *Mayo Clin. Proc.*, 1978, *53*, 271.

TEICHHOLZ, L.E., KREULEN, T., HERMAN, M.V. & GORLIN, R. — Problems in echocardiographic volume determinations: echocardiographic angiographic correlations in the presence or absence of asynergy. *Am. J. Cardiol.*, 1976, *37*, 7.

WYATT, H.L., HENG, M.K., MEERBAUM, S., GUERET, P., HESTENESS, J., DULA, E. & CORDAY, E. — Cross-sectional echocardiography. II. Analysis of mathematic models for quantifying volume of the formalin fixed left ventricle. *Circulation*, 1980, *61*, 1119.

Address for correspondence: N.L. Fazzalari, Division of Tissue Pathology, Institute of Medical and Veterinary Science, Adelaide 5000, Australia.

Appendix

Segmentation of the ventricle into parallel slices along the major axis, apex to the centre of the mitral valve, produces irregular octagonal cross-sections of the ventricle if the boundary points of the segments are linearly interpolated.

The area of an irregular octagon, with the origin of a cartesian coordinate system at the centre of the polygon, can be calculated using the trapezoidal rule.

The expression derived below is not restricted to octagons but is generally applicable to any polygon whose centre lies on the *z*-axis.

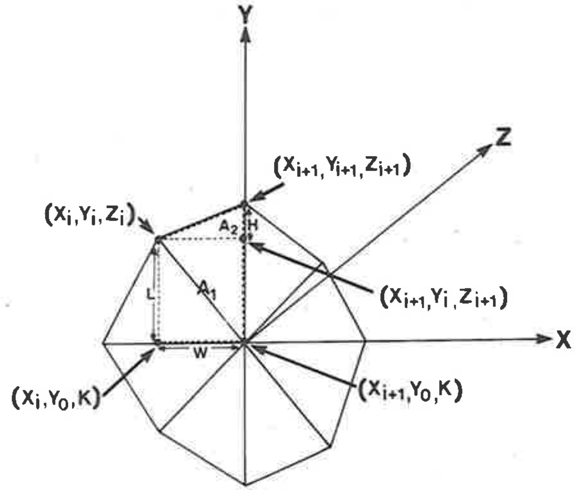

The area of the octagon is the sum of the absolute area of the interval areas. A generalised example of an interval is shown on the figure, labelled A_1 and A_2.

Area $A = L \times W$

$$= (y_i - y_0)((x_{i+1} - x_i)^2 + (z_{i+1} - z_i)^2)^{\frac{1}{2}}$$

because $y_0 = 0$

$$A_1 = y_i((x_{i+1} - x_i)^2 + (z_{i+1} - z_i)^2)^{\frac{1}{2}}$$

Area $A_2 = \frac{1}{2} \times W \times H$

$$= \tfrac{1}{2}((x_{i+1}-x_i)^2+(z_{i+1}-z_i)^2)^{\frac{1}{2}}(y_{i+1}-y_i)$$

Interval area $= A_1 + A_2$

$$= y_i((x_{i+1}-x_i)^2+(z_{i+1}-z_i)^2)^{\frac{1}{2}}$$
$$+ \tfrac{1}{2}((x_{i+1}-x_i)^2+(z_{i+1}-z_i)^2)^{\frac{1}{2}}(y_{i+1}-y_i)$$
$$= ((x_{i+1}-x_i)^2+(z_{i+1}-z_i)^2)^{\frac{1}{2}}(y_i+\tfrac{1}{2}(y_{i+1}-y_i))$$
$$= \tfrac{1}{2}((x_{i+1}-x_i)^2+(z_{i+1}-z_i)^2)^{\frac{1}{2}}(y_{i+1}+y_i)$$

Area of the octagon

$$= \sum_{i=1}^{8} \left| \tfrac{1}{2}((x_{i+1}-x_i)^2+(z_{i+1}-z_i)^2)^{\frac{1}{2}}(y_{i+1}+y_i) \right|$$

Volume of the ventricle

$$= \sum_{j=1}^{j=J} \sum_{i=1}^{i=I} \left| \tfrac{1}{2}((x_{i+1}-x_i)^2+(z_{i+1}-z_i)^2)^{\frac{1}{2}}(y_{i+1}+y_i) \right| \times T_j$$

where J = the number of segments,
I = the number of sides of polygon,
T = slice thickness.

Alternatively the area of the segment cross-section can be determined by using polar coordinates.

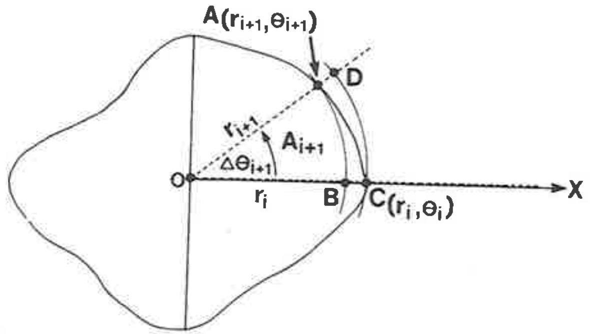

Take the origin of the polar coordinate system as the point through which the major axis of the ventricle passes.

The area of a sector $= \frac{1}{2}r^2\Delta\theta$

Hence the area of the sector

$$OCD = \tfrac{1}{2}r_i^2\Delta\theta_{i+1}$$

the area of the sector

$$OBA = \tfrac{1}{2}r_{i+1}^2\Delta\theta_{i+1}$$

Thus $\frac{1}{2}r_{i+1}^2\Delta\theta_{i+1} < A_{i+1} < \frac{1}{2}r_i^2\Delta\theta_{i+1}$

From the intermediate value theorem

$$A_{i+1} = \tfrac{1}{2}(f(\theta))^2\Delta\theta_{i+1}$$

Hence the area of the whole region of the segment

$$A = \sum_{i=1}^{n} \tfrac{1}{2}(f(\theta))^2\Delta\theta_i$$
$$= \sum_{i=1}^{n} \tfrac{1}{2}r_i^2\Delta\theta_i$$

For a cross sectional segment of eight sectors

$$A = \frac{1}{2}\left[r_1^2\frac{\pi}{4} + r_2^2\frac{\pi}{4} + \dots + r_7^2\frac{\pi}{4} + r_8^2\frac{\pi}{4}\right]$$

$$= \frac{\pi}{8}[r_1^2+r_2^2+\dots+r_7^2+r_8^2]$$

$$= \frac{\pi}{8}\sum_{i=1}^{8} r_i^2.$$

JCU
JOURNAL OF CLINICAL ULTRASOUND
A JOHN WILEY & SONS INC., PUBLICATION

EDITOR
Russell L. Deter, MD
Dept. of Ob/Gyn
Baylor College of Medicine
Texas Medical Center
Houston, Texas 77030
(713) 791-4025

May 21, 1986

N. L. Fazzalari
Institute of Medical and Veterinary Science
Box 14 Rundle Mall Post Office
Adelaide south Australia 5000
Australia

RE:(#819-RP)"A composite three dimensional echocardiographic technique for left ventricular volume estimation in children: Comparison with angiography and established echographic methods"

Dear Dr. Fazzalari:

I am pleased to inform you that the review of your manuscript has been completed, and your manuscript has been accepted for publication in the JOURNAL OF CLINICAL ULTRASOUND.

Acceptance of this manuscript by the JOURNAL is based upon the understanding that it will not be submitted to any other journal for publication.

Thank you for considering the JOURNAL OF CLINICAL ULTRASOUND for the publication of your work.

Sincerely,

Russell L Deter

Russell L. Deter, M.D.
General Editor
JOURNAL OF CLINICAL ULTRASOUND

RLD/mar

A COMPOSITE THREE DIMENSIONAL ECHOCARDIOGRAPHIC TECHNIQUE FOR LEFT VENTRICULAR VOLUME ESTIMATION IN CHILDREN: COMPARISON WITH ANGIOGRAPHY AND ESTABLISHED ECHOGRAPHIC METHODS

Running Title:

THREE DIMENSIONAL ECHOCARDIOGRAPHIC VOLUME ESTIMATION

* NICOLA L FAZZALARI

** ELTON GOLDBLATT

** A PHILLIP S ADAMS

* Institute of Medical and Veterinary Science
Adelaide South Australia Australia

** Adelaide Children's Hospital
Adelaide South Australia Australia

Address for reprints:

Mr N L Fazzalari
Institute of Medical and Veterinary Science
Box 14 Rundle Mall Post Office
Adelaide South Australia 5000
Australia

ABSTRACT

A composite three dimensional (3D) echographic left ventricular (LV) reconstruction to measure LV volumes was evaluated in 26 children. Four apical views, to minimise assumptions about LV shape, were used to obtain a "wire-cage" model of the LV in 3D. Numerical integration was used to make estimates of both end diastolic and end sytolic volumes. A comparison of volume estimates by echographic techniques with angiographic biplane estimates was performed. There is a negative bias in the echographic estimates ($P<0.005$) and a consistent trend, though not significant, which shows a decrease in this systematic error for the 3D method. One way analysis of variance confirms significant global geometric fluctuations. Hence 3D reconstruction can be performed in a clinical setting and the enhanced graphic representation of global LV geometry may contribute to improved patient management.

KEY WORDS

Left ventricular volume

Three dimensional volume

Congenital heart disease

Ventricular geometry

Left ventricle reconstruction

INTRODUCTION

Assessment of left ventricular (LV) performance in the evaluation of children with congenital heart disease is an important investigative procedure. The information obtained from such studies often determines the medical and/or surgical management. It is known that children with congenital heart disease who undergo surgical correction of defects such as aortic obstruction or coarctation and septal defects may have a successful operation, but there may be subsequent myocardial failure. Often this is because the LV does not have the capacity to provide the necessary output to sustain normal life. Hence accurate objective measures of ventricular volume would be of significant prognostic value. Therefore, an important parameter of ventricular performance is the measurement of ventricular volume during the cardiac cycle. From these volume estimations at end diastole and end systole, derived numerical parameters can be calculated, such as stroke volume (SV), ejection fraction, cardiac output and cardiac index[1]

Both invasive and non-invasive methods can be used to estimate LV volumes. Invasive cardiac catheterisation methods, although accepted as reliable and effective, present obvious risks to the patient, whereas no case of harmful effects of ultrasound in patient use has ever been documented. Hence, an important advantage of echocardiography is that it can be safely repeated.

Modelling of the LV for effective volume estimation has presented problems for both invasive and noninvasive investigative methods. The ventricular geometry does not conform to any single geometric shape nor is there constancy of shape during the cardiac cycle, particularly in various pathological states.(2) Consequently, models based on a particular geometric shape make invalid assumptions about the LV. Various geometric models better suit the LV at different phases of the cardiac cycle and in different pathological states. In invasive cardiac catheterisation the recognised comparative standard is the area-length method of Dodge and Sandler (1960)(3), though there is a number of mathematical models applicable to ventriculograms for LV volume estimations.(4) The noninvasive models developed initially utilised M-mode ultrasound which provides an "ice-pick" view of cardiac structure over time.(1). This imaging mode provides minimal spatial information and hence resulted in the most simplistic of ventricular models. A major assumption is that the ventricular shape is

that of a prolate ellipsoid with an aspect ratio of 2:1 for all stages of the cardiac cycle, irrespective of pathology. Nevertheless, M-mode echocardiography has provided useful information, supported empirically, where there is no LV segmental wall motion abnormalities.(5-7) Two dimensional echocardiography on the other hand permits unique visualisation of the heart in vivo(8), and provides spatial information in tomographic views previously unavailable. The availability of this spatial information has led to the development of more sophisticated models of the LV, many of which still require some basic assumptions about shape and geometry.(9-12) Few studies have been reported which obviate geometric assumptions, particularly with respect to symmetry.

To overcome the limitations of geometric mathematical models, it is necessary to consider the spatial arrangement of the ventricle in 3D. Three dimensional studies which have reported patient data involve reconstruction from arbitrary parasternal short axis views(13) and from apical views obtained by angular rotation of the transducer about the LV long axis.(14) Moreover, none of these studies has reported on children. A 3D LV reconstruction based on anatomically-defined apical views has been reported.(15) An analysis of the application of this method to given geometrical shapes, postmortem hearts and adult patients referred for investigation on clinical grounds was reported. Nevertheless, it is necessary to validate this composite 3D method for children because of differences between adults and children in the size of ventricles, incidence of abnormalities of cardiac geometry and types of cardiac problems. Moreover, the position of the heart in the chest in children does tend to be located more medially than is the case for adults. We, therefore, present here a study which comprises two parts. A comparison of LV volumes derived from a composite 3D reconstruction based on anatomically-defined apical views to those derived from cineangiography followed by a comparison of the composite LV volumes to estimates by classical single plane and biplane echographic techniques. This is presented to determine the value of the composite technique for predicting these variables in children.

PATIENTS AND METHODS

This study involved 26 patients, 12 of which were catheterised for invasive study and 14 without any invasive investigations. Hence, the two groups used were 12 patients, six males and six females, for the angiographic comparison and 26 patients, 13 males and

13 females, which included the 12 patients who were catheterised, for the comparison of echographic techniques. The 26 patients had a mean age 89.3 $\pm$ 11.5[a] months, body weight 24.0 $\pm$ 3.4 kg, height 120.3 $\pm$ 5.6 cm and body surface area 0.94 $\pm$ 0.08 m^2, all of which were not significantly different to the corresponding values of the 12 patients who comprised the catheterised subgroup. Hence the subgroup was anthropometrically representative of the total sample (Table 1).

The 12 catheterised patients all had some type of congenital heart disease that may have required surgery to correct. They were a group which required hemodynamic data for both diagnostic and prognostic evaluation. In addition, of the 14 patients investigated non-invasively eight had some form of congential heart disease, four were qualitatively normal following investigation and two were assessed because of secondary complications due to medication. Hence the total sample of 26 consisted of 20 children with congenital heart disease.

A Toshiba (SSH 10A) sector scanning echograph was used for non-invasive image data acquisition. A series of LV apical views were recorded at various rotational degrees for use in 3D reconstruction of the heart. This method was applied to 26 patients all in sinus rhythm, 12 of which underwent cardiac catheterisation with biplane LV angiography. Each catheterised patient had 30° right anterior oblique and 60° left anterior oblique projections of the LV recorded on the cine film at 60 frames per second while under general anaesthetic. The end systolic volume and end diastolic volume were then calculated according to the method of Dodge and Sandler (1960).[3] End systole and end diastole were defined as the smallest and largest frame of one cardiac cycle. Within 24 hours of catheterisation two dimensional echocardiograms were recorded on Sony U-Matic Video tape employing the necessary apical views for 3D reconstruction. The further 14 patients were studied solely echographically without any invasive investigation. Hence, in total, 26 patients were studied echographically in the supine or the left lateral decubitus position, 12 having undergone catheterisation.

A method of reconstruction from planar two dimensional apical echocardiographic views obtained at 45° rotational intervals was used in this study.[15] The transducer was placed at the apex of the heart, found by palpation, to record four anatomically-

defined apical views. The transducer was moved laterally if necessary to locate the apex immediately under the transducer. The ultrasound plane was then moved ventrally and dorsally to locate the longest LV cross section which included the mitral valve.

The four chamber and two chamber views are widely accepted as defined for routine cardiac imaging in a clinical environment.[16] Two additional intermediate rotational views between the four and two chamber are defined in reference to the four chamber image. A 45° anticlockwise rotation presents the LV and left atrium in a plane parallel to the mitral valve commissure. Consequently only the anterior mitral valve cusp is viewed during diastole. The LV may appear "waisted" by partial inclusion of both papillary muscles and the margins of right-sided chambers remain visible. In addition, a 45° clockwise rotation presents essentially a mirror image of the standard apical long axis view, that is, a view passing from the LV apex through the outflow tract and into the ascending aorta. The left atrium and right ventricular outflow tract are also included in this planar section (Fig. 1).

These four apical views section the ventricle in four complementary planes each separated by approximately

45° of angular rotation about the long axis of the LV. The common long axis defined as a line joining the most apical endocardial point to the centre of the mitral valve annulus was chosen as the axis of rotation.

A Polaroid (10 x 8 inch type 55) hard copy of ECG gated frames at end diastole and end systole was obtained for each view from the video record (Fig. 2). From the echocardiograms the ventricular endocardial boundaries were delineated with the large trabeculations traced to their bases. This resulted in smoothed endocardial outlines which were subsequently digitised with an HP 9874A digitiser, and stored permanently on computer file and tape. This stored planar data was transformed so that each of the four digitized apical views, representing end diastole and end systole, were aligned along the major axis, the apex and mid points of the mitral valve overlapping. The 3D spatial arrangement of the views then required rotation about this axis to generate a 3D reconstruction of the LV at both end diastole and end systole in each patient. The reconstruction was then plotted on an HP 9864A plotter in the desired perspective (Fig. 3). The data transformations required for the view alignment, spatial reconstruction and perspective

plots were all performed in computer memory by matrix manipulations which define rotation and projection goemetry[17].

The reconstruction was used to generate sections perpendicular to the long axis of thickness H at various levels along the axis to calculate the volume from the slices using polar coordinate integration.[15] Each slice was a cross-sectional segment divided into eight sectors with thickness H the value of which was dependent on the absolute length of the long axis (Fig. 3). The value of H was between 5 to 10 mm. The volume of each slice was calculated using the expression $V = \frac{\pi}{8} H \sum_{i=1}^{8} r_i^2$ where r is the radius of a sector. Sector geometry was selected to minimise the distance over which ventricular geometry remains unchanged. Hence the LV volume estimates at end diastole and systole are the sum of the respective slice volumes. In addition, volume estimations were made with each of the four complementary views using the classical method of area-length [12] for a prolate ellipsoid and the biplane [11] echographic technique using the apical two and four chamber views. The single plane area-length estimates were averaged.

The analysis of the data was carried out using parametric statistical methods. Comparisons of mean values and variance were carried out by the Student t-test and variance F-test respectively. Regression analyses were tested by analysis of variance. Statistical significance of a relationship was determined using the one-tail F-test. Regressions were compared using analysis of covariance to test for the relative sensitivity of various echographic methods compared to angiographic methods of volume estimation. The systematic and random errors associated with each method were determined and analysed according to the techniques described by Altman and Bland [18]. The multiple comparison of errors was done using the Newman-Keul method [19]. To identify and estimate sources of variability which may be associated with echographic methods and with ventricular geometry a variance components model using one way analysis of variance was formulated and used.[19]

RESULTS

End diastolic, end systolic and stroke volumes estimated by echographic techniques using single plane and biplane area length methods and the 3D method were less than the ventriculographic biplane estimates (Table 2). This systematic error or bias associated with each method is negative and

statistically differs from zero ($P<0.005$) (Table 4). The random error on the other hand, for each method, is not statistically different though the trend is that stroke volume estimates have a larger random error (Table 4). The systematic errors were compared using the Neuman - Keul method for multiple comparisons (19). This showed no statistical difference among the methods though the 3D method demonstrated a consistent trend of a decrease in the bias (Table 4). For the non-invasive echographic methods the systematic error associated with the area length and biplane methods again is negative but with respect to the 3D estimates. This error differs statistically from zero except for the biplane end systolic, volume estimate (Table 5). The random errors are not statistically different.

Regression analysis shows that the 3D volumes better predict ventriculographic biplane estimates than averaged echographic single plane and biplane area length methods. Comparison of residual mean squares from regression for the three methods using the two-tailed F-test showed no difference in variances (Table 6). Hence assuming homogeneity of residual variances, comparisons of slopes or regression coefficients for the methods showed the slope for 3D volume (0.73) greater than the echographic biplane volume (0.53), $p < 0.05$ (Fig. 4a). The average of four area-length single plane volume estimates showed no statistical difference. For stroke volume estimates the 3D method had the highest regression coefficient though not statistically greater than single plane and biplane estimates (Fig. 4b). Furthermore, comparison of non-invasive echographic methods showed that 3D volumes regressed on echographic area-length and biplane methods had significant relationships with the regression coefficient greater than one. The slope is significantly greater than one, $p < 0.001$ for regression both on echo biplane and single plane area length estimates (Figs 5 and 6). This is the case for ventricular volumes and stroke volumes.

A one way analysis of variance using a Model II approach [19] was applied to 26 patients who underwent the three methods of echographic volume estimation. The analysis demonstrated that the proportion of variance associated with the methods was of the order of 5%.

Application of the same analysis procedure to volume estimates using the single plane area-length method with each of the four complementary views showed that about 25% of the variance of single plane estimates can

be attributed to fluctuations in ventricular geometry. The paired Student t-test showed end diastolic and end systolic volume estimates which ranged from 28.4 ml to 36.4 ml and 14.6 ml to 19.1 ml respectively to be significantly different ($p < 0.025$). In each instance, the four chamber view gave the smallest volume estimate and 45° anticlockwise view and two chamber view gave the largest volume estimates for end diastole and end systole repectively.

DISCUSSION

Left ventricular volume estimates in children with congenital heart disease provide valuable information regarding ventricular function.[20] Hence, an effective non-invasive technique is of diagnostic and prognostic value. Segmental dysfunction or paradoxical septal motion has been shown to compromise volume determination in adults. [9,11] It has been demonstrated in an adult study that composite three dimensional LV reconstruction gives improved volume estimates, in particular, in instances with segmental abnormalities.[15] Except for septal motion abnormalities, segmental wall motion abnormalities are unusual in children. However, the diverse ventricular shapes and sizes seen with congenital heart defects are significant in the assessment of postoperative LV function.[21] Furthermore, the heart with a congenital defect is subject to different loading conditions than normal, highlighting the weaknesses in the assumptions of more simplistic methods.

The method used in this study has been applied to geometric shapes of known volume and to fluid-filled postmortem hearts and, in both instances, the method has been shown to be very reliable.[15] In evaluating the method clinically, however, it must be recognised that no effective "standard" exists though it is generally accepted by consensus that the invasive biplane technique proposed by Dodge and Sandler (1960)[3] is an appropriate comparative standard. Apart from the geometric assumptions about the LV there are also the problems caused by unavoidable changes in the patient's physiological state between the invasive and non-invasive examinations. For instance, differences which occur in time, level of anxiety, sedation, heart rate, state of arousal, and introduction of contrast material.[12]

The apparent underestimated echographic end diastolic volume, end systolic volume and stroke volume can be attributed to a number of factors. A major source of error is the scanner resolution which varies in each

of three dimensions. Range resolution is of the order 1.5 mm to 2 mm, azimuthal resolution 2 mm to 5 mm and resolution out of the image plane 3 mm to 7 mm. In combination these factors can contribute to substantial error. Skill and care are required by the echocardiographer in the selection of beam depth, again settings and placement of the image in the central field of view to minimise errors of resolution. Tangential cuts of the ventricle are also a problem and must be avoided to minimise the under-estimation of the long axis length and, hence, volume.[22,23] As described earlier this foreshortening of the long axis can be minimised by careful manipulation of the transducer by the echocardiographer. Another source of error may be the selection of the echographic frame used to trace the endocardial boundary for both end diastole and end systole. End systolic volume is a smaller absolute value than end diastolic volume, so an error in measurement caused by frame selection would lead to a greater percentage error than for end diastole. This error in frame selection can be due to the slow frame rate with respect to the heart rate. Consequently this would overestimate end systolic volume and underestimate end diastolic volume both of which would add to underestimate stroke volume. Angiographic studies also have particular problems which lead to inaccurate volume estimation. Injection of radio-opaque dye will alter the ventricular volume, hence, contractility, though this can be overcome if only the first two or three cardiac cycles after opacification are used for volume estimation.(24) Frame slection is also a problem as it is for echographic studies. Furthmore, angiographic outline of the LV includes some volume within the trabeculae carnae because they are surrounded by radio-opaque dye. The echographic outline probably represents the inner edge of trabeculae carnae due to the level of lateral resolution of the ultrasonic beam.(25) These factors, together with the effect of nonsimultaneous echographic and angiographic study, contribute to the discrepancy in volume estimates.(12) Despite these sources of error the method we have presented gives better results than the established echographic methods we have compared.

The end diastolic volume, end systolic volume and stroke volume estimates by the composite 3D reconstruction showed a consistent trend that the negative bias was less than the echographic biplane technique or the averaged single plane area-length method with respect to the angiographic volumes.

Furthermore, with respect to the 3D reconstruction the systematic error was significant except for the end systolic biplane estimate. The method appears to be more sensitive than for adults though it should not be overlooked that the adult study involved mainly patients with coronary artery disease, which had associated regional wall abnormalities. Regional wall abnormalities do not allow effective volume estimation by angiography if the abnormality cannot be projected. It seems that the absence of segmental wall motion abnormalities in the children studied has contributed to this improved sensitivity. This serves to highlight the problem of the need for an effective "standard" which is easy to use for the evaluation of echographic techniques for volume estimation. The study has shown that an algorithm using multiple long axis views is potentially superior to algorithms which use either a single plane or biplane apical views. Furthermore, the shape assumptions about ventricular geometry can be relaxed to the consideration of fixed sector geometry only over a small region of each ventricle. Each ventricle then being described by a set of sectors defined by the multiple long axis views. In our study we have used four views which provides eight slice sectors, but the method can be extended to any number of slice sectors as the number of long axis views is increased. If the number of sectors increases and their size decreases the method tends to become shape independent. Shape independent volume estimation methods are available [26] but generally require high point density and large numbers of multiple images. The challenge for echocardiography is to optimise image acquisition in the light of practical patient constraints and instrument engineering difficulties to adequately reconstruct in 3D the LV to improve volume estimation and assessment of cardiac performance.

The clinical significance of a variance component of a measure is judged by whether the measurement will reliably differentiate between persons. That is, the better measurement in this context will be that for which the patient variance component is dominant over the other variance component. We have demonstrated that multiple view echographic volume estimates are suitable for differentiating between patients. Furthermore, we have shown that geometric fluctuations in the left ventricle account for 25% of the variance in volume estimates in our heterogeneous sample of 26 patients. Single plane views for volume estimation are inadequate if abnormalities of card-

iac geometry lead to ventricular dysfunction. In particular, four chamber views give the lowest estimates of both EDV and ESV, while the two chamber view gives the highest estimate of ESV. The intermediate 45^{o} anticlockwise view from the four chamber gives the highest single plane estimate of EDV. Hence, 3D reconstruction of the LV provides volume estimates which take into account geometric fluctuation, which we have shown is a significant feature of the LV in children. This would appear to be the case in children with congenital heart disease.

A significant number of children who undergo corrective surgery for congenital defects are left with residual cardiac defects, despite optimum surgical results. Postoperative LV dysfunction occurs due to the inability of the LV to function in the systemic circuit. This can be caused by the muscular configuration of the abnormal LV or the absolute size of the LV is insufficient to provide the systemic demands. Furthermore, the LV shape may fail to provide the necessary ejection fraction increase with the stress of exercise. In normal subjects the ventricular ejection fraction has been shown to increase by 5% or more with stress of maximal exercise.[27] In patients with residual cardiac dysfunction after surgery the ejection fraction fails to increase or decreases. Hence the significant fluctuations in geometric shape, which we have demonstrated are important in addressing these problems. Our results suggest further clinical study to identify subgroups with particular geometrics and their relationship to efficiency of ejection. Studies of regional ejection fraction in relation to geometric shape would help in the prognostic assessment of patients being selected for surgery.

This technique allows the clinician to appreciate fully the global contraction of the heart and the extent and location of an abnormality. Further studies may provide evidence that the sensitivity of echocardiography is increased by the improved diagnostic potential. Nevertheless, the technique may contribute to alteration of the clinicians "index of suspicion" in favour of the patient by allowing him/her to make more informed decisions about treatment and progress.

We have demonstrated that echographic left ventricular 3D reconstruction, which uses four anatomically-defined apical views, can be carried out in a clinical setting on children with congenital heart disease. Further study of ventricular geometry fluctuation which we have described may contribute to

the development of new insights into left ventricular performance. Three dimensional volume estimates are greater than single plane and biplane echographic estimates and more sensitive in estimating biplane ventriculographic volumes.

REFERENCES

1 Feigenbaum H. Echocardiography. 2nd ed. Philadelphia: Lea and Feibiger, 1976.

2 Dumesnil JG, Shoucri RM. Effect of the geometry of the left ventricle on the calculation of ejection fraction. Circulation 65: 91, 1982.

3 Dodge HR, Sandler H, Ballew DW, Lord JD. The use of biplane angiocardiography for the measurement of left ventricular volume in man. Am Heart J 60: 766, 1960.

4 Davila JC, Sanmarco ME. An analysis of the fit of mathematical models applicable to the measurement of left ventricular volume. Am J Cardiol 18: 31, 1966.

5 Murray JA, Johnston W, Reid JM. Echocardiographic determination of left ventricular dimensions, volumes and performance. Am J Cardiol 30: 252, 1972.

6 Teichholz LE, Kreulen T, Herman MV, Gorlin R. Problems in echocardiographic volume determinations: echocardiographic angiographic correlations in the presence or absence of asynergy. Am J Cardiol 37: 7, 1976.

7 Kronik G, Slany J, Mosslacher H. Comparative value of eight M-mode echocardiographic formula for determining left ventricular stroke volume. A correlative study with thermo-dilution and left ventricular single-plane cineangiography. Circulation 60: 1308, 1979.

8 Tajik AJ, Seward JB, Hagler DJ, Mair DD, Lie JT. Two-dimensional real-time ultrasonic imaging of the heart and great vessels. Mayo Clin Proc 53: 271, 1978.

9 Folland ED, Parisi AF, Moynihan PF, Jones MS, Feldman CL, Tow DE. Assessment of left ventricular ejection fraction and volumes by real-time, two dimensional echocardiography. A comparison of cineangiographic and radionuclide techniques. Circulation 60: 760, 1979.

10 Alpert BS, Bloom KR, Gilday D, Olley PM. The comparison between non-invasive and invasive methods of stroke volume determination in children. Am Heart J 98: 763, 1979.

11 Schiller NB, Acquatella H, Ports TA, Drew D, Goerke J, Ringertz H, Silverman NH, Brundage B, Botvinick EH, Boswell R, Carlsson E, Parmley WW. Left ventricular volume from paired biplane two dimensional echocardiography. Circulation 60: 547, 1979.

12 Silverman NH, Ports TA, Snider RA, Schiller NB, Carlsson E, Heilbron DC. Determination of left ventriculr volume in children. Echocardiographic and angiographic comparisons. Circulation 62: 548, 1980.

13 Geiser EA, Ariet M, Conetta DA, Lupkiewiew SM, Christie LG, Conti CR. Dynamic three dimensional echocardiographic reconstruction of the intact human left ventricle: technique and initial observations in patients. Am Heart J 103: 1056, 1982.

14 Ghosh A, Nanda NC, Maurer G. Three dimensional reconstruction of echocardiographic images using the rotation method. Ultrasound in Med and Biol 8: 655, 1982.

15 Fazzalari NL, Davidson JA, Mazumdar J, Mahar LJ, DeNardi E. Three dimensional reconstruction of the left ventricle from four anatomically defined apical two-

dimensional echocardiographic views. Acta Cardiologica 6: 409, 1984.

16 Edwards WD, Tajik AJ, Seward JB. Standardised nomenclature and anatomic basis for regional tomographic analysis of the heart. Mayo Clin Proc 56: 479, 1981.

17 Roger DF, Adams JA. Mathematical elecments for computer graphics. McGraw-Hill, N.Y., 1976.

18 Altman DG, Bland JM. Measurement in medicine: the analysis of method comparison studies. The Statistician 32: 307, 1983.

19 Snedecor GW, Cochran WG. Statistical Methods. Iowa State University Press, Ames, 1967.

20 Parrish MD, Graham TP, Born ML, Jones JP. Radionuclide evaluation of right and left ventricular function in children: validation of methodology. Am J Cardiol 49: 1241, 1982.

21 Parrish MD, Thomas PG, Bender HW, Jones JP, Patton J, Partain CL. Radionuclide angiographic evaluation of right and left ventricular function during exercise after repair of transposition of the great arteries. Comparison with normal subjects and patients with congenitally corrected transposition. Circulation 67: 178, 1983.

22 Erbel R, Schweizer P, Lambertz H, Henn G, Meyer J, Krebs W, Effert S. Echoventriculography - a simultaneous analysis of two dimensional echocardiography and cineventriculography. Circulation 67: 205, 1983.

23 Barrett MJ, Jacobs L, Gomberg J, Horton L, Meister SG. Simultaneous contrast two-dimensional echocardiography and contrast ventriculography: discrepancies in left ventricular volume. Am J Cardiol 47: 453, 1981.

24 Carleton RA. Change in left ventricular volume during angiocardiography. Am J Cardiol 27: 460, 1971.

25 Schnittger I, Fitzgerald PJ, Daughters GT, Ingels NB, Kantrowitz NE, Schwarzkopf A, Mead CW, Popp RL. Limitations of comparing left ventricular volumes by two dimensional echocardiography, myocardial markers and cineangiography. Am J Cardiol 50: 512, 1982.

26 Deter RL, Harrist RB, Hadlock FP, Cortissoz CM, Batten GW. Longitudinal studies of fetal growth using volume parameters determined with ultrasound. J Clin Ultrasound 12: 313, 1984.

27 Kalff V, Kelly M, Jennings G, Lim Y, Anderson S, Korner P, Harper R, Pitt A. The radionuclide assessment of left ventricular function using graded exercise in normal subjects. Aust N Z J Med 10: 533, 1980.

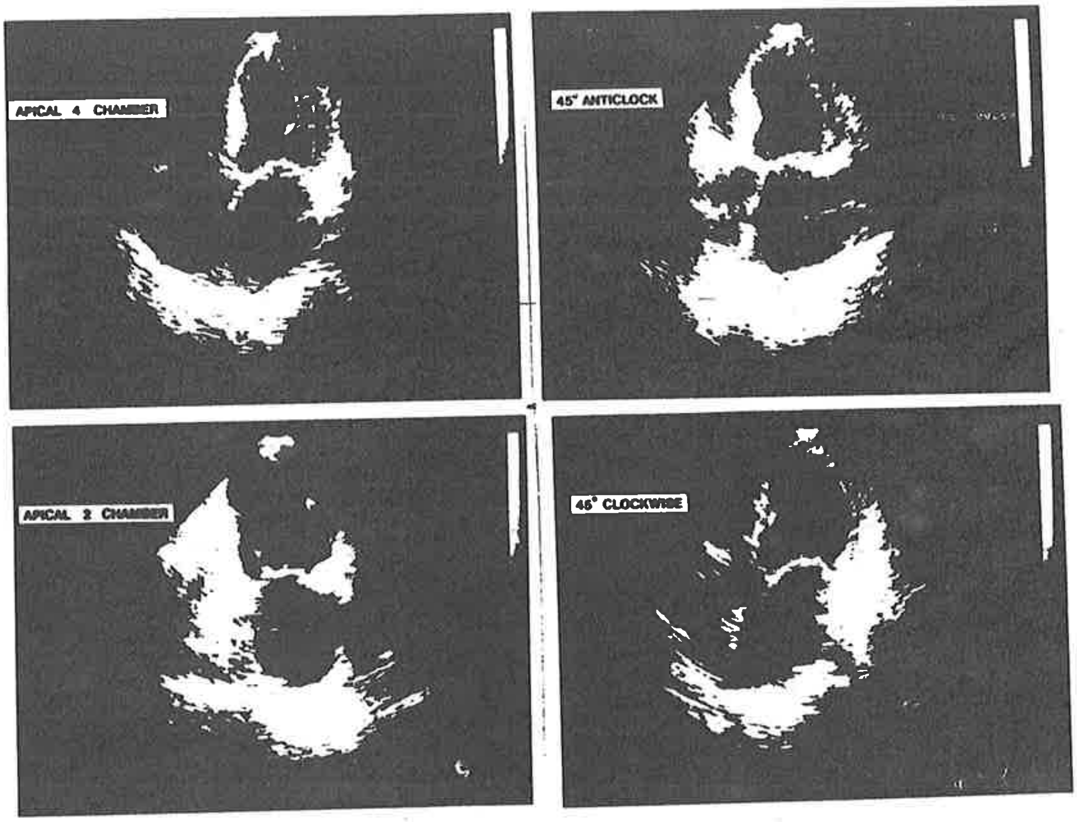

Figure 1 Echocardiographic apical views used in the three dimensional reconstruction of the left ventricle. Anatomical definition is given in the text.

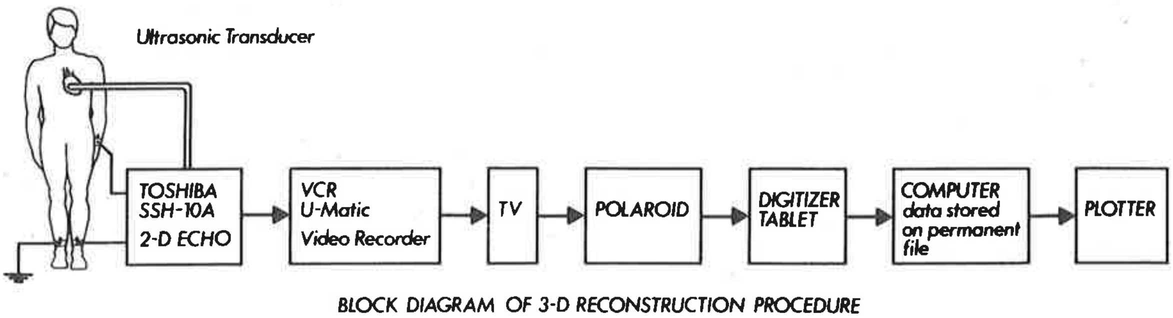

Figure 2 Outline of the composite three dimensional reconstruction procedure.

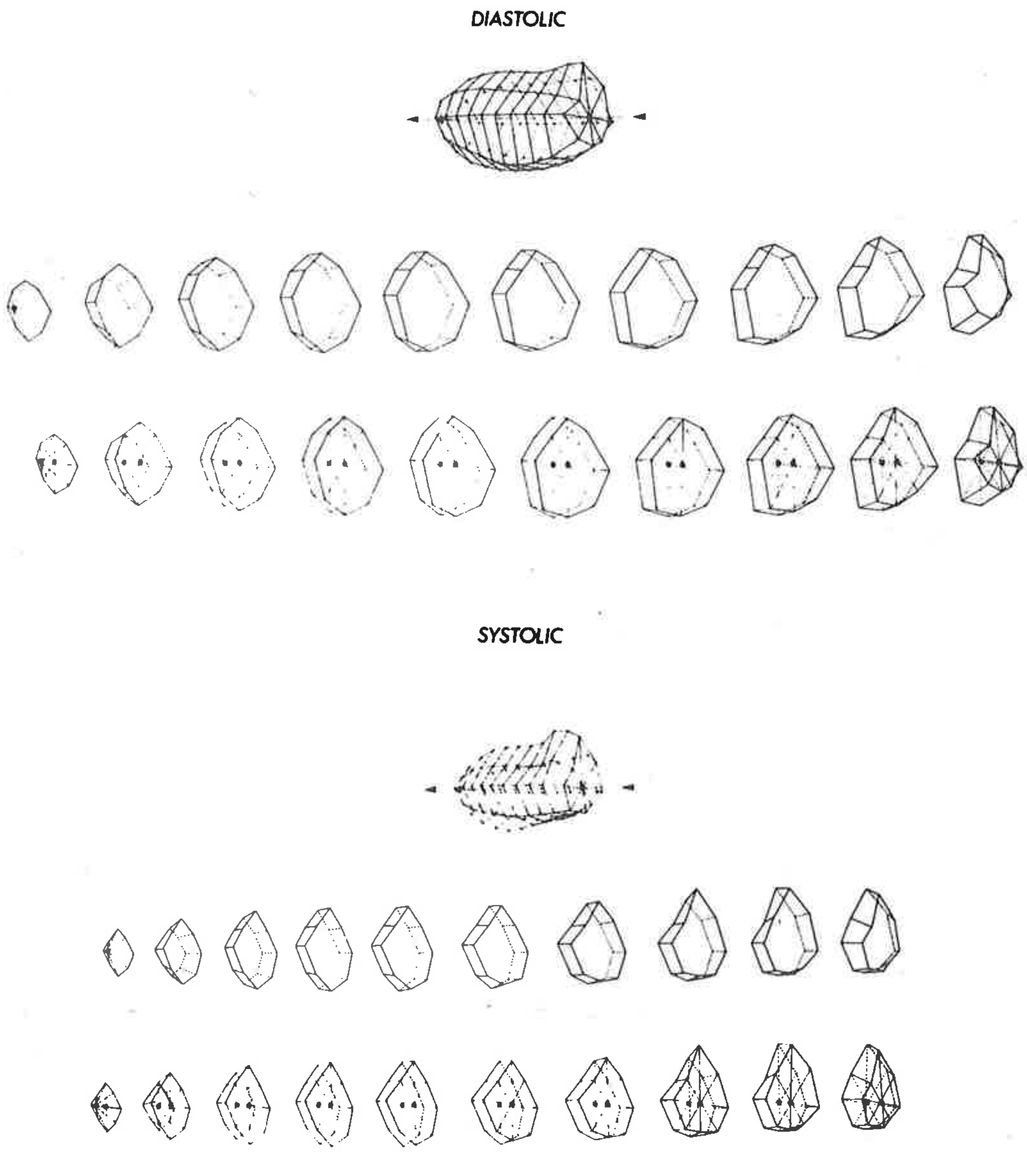

Figure 3 Diastolic and systolic composite three dimensional reconstruction. Displayed also are the computer generated sliced sections perpendicular to the long axis of the left ventricle used for volume estimation. The section thickness H depends on the long axis length which is divided into ten equal lengths. There are eight sectors and the sector radius is labelled r.

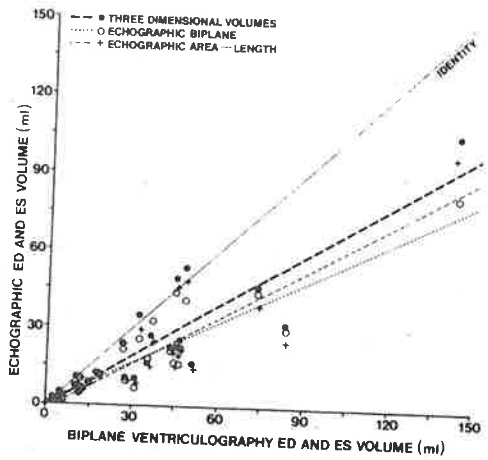

Figure 4a

Regression analysis of composite reconstruction, echographic biplane and area-length comparisons with biplane ventriculographic volume estimates.

i) Composite reconstruction r = 0.93, SEE = 8.51, n = 24, Y = -1.73 + 0.73 X.

ii) Echographic area-length r = 0.87, SEE 9.61, n = 24, Y = -1.25 + 0.59 X.

iii) Echographic biplane r = 0.89, SEE = 8.16, n = 24, Y = 0.97 + 0.53 X.

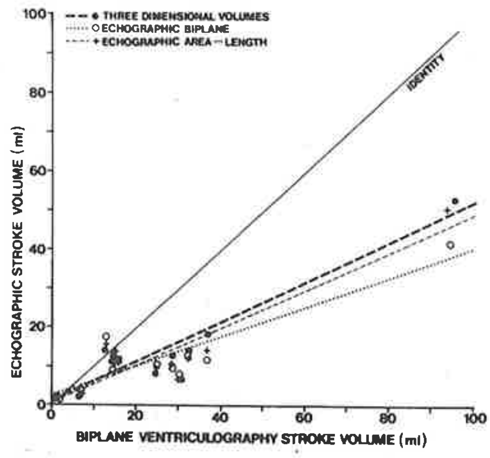

Figure 4b

Regression analysis of composite reconstruction, echographic biplane and area-length comparisons with biplane ventriculographic stroke volume estimates.

i) Composite reconstruction r = 0.94, SEE = 4.40, n = 12, Y = 1.01 + 0.51 X.

ii) Echographic area-length r = 0.92, SEE = 4.77, n = 12, Y = 1.04 + 0.47 X.

iii) Echographic biplane r = 0.90, SEE = 4.44, n = 12, Y = 2.61 + 0.38 X.

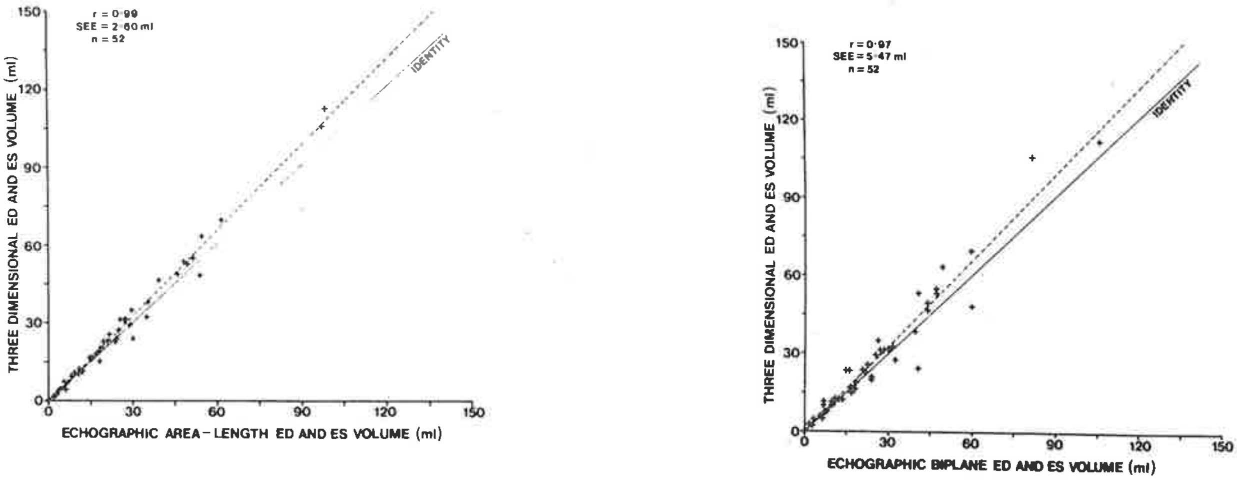

Figure 5 Composite reconstruction comparison with

(a) echographic area-length, Y = -0.09 + 1.09 X volume estimates.

(b) echographic biplane, Y = -0.60 + 1.10 X volume estimates.

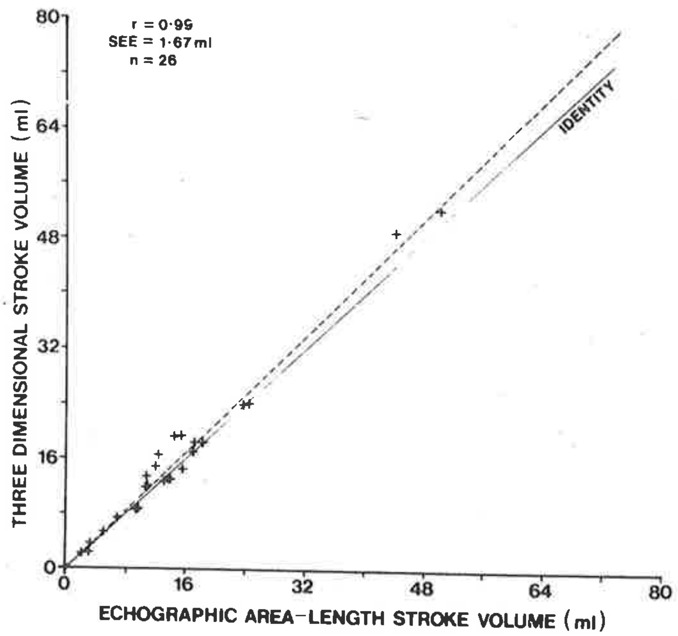

Figure 6 Composite reconstruction comparison with

(a) echographic area-length, Y = 0.09 + 1.06 X stroke volume.

(b) echographic biplane, Y = -0.73 + 1.25 X stroke volume.

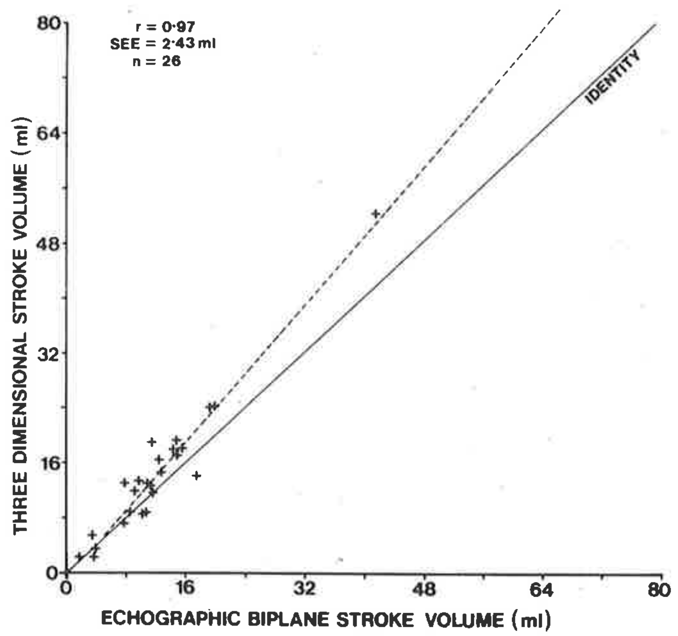

Table 1 Anthropometric patient data and diagnosis

CASE	SEX	AGE (mth)	HEIGHT (cm)	WEIGHT (kg)	BSA (m^2)	DIAGNOSIS
1	F	77	109.0	16.0	0.71	Normal
2	M	75	123.5	24.9	0.92	Normal
3	F	131	150.0	24.2	1.30	[a]ASD
4	F	37	90.0	13.0	0.56	Elastosis
5	F	44	95.0	13.7	0.60	[b]VSD
6	F	72	123.8	20.1	0.84	[c]Post VSD
7	F	96	108.0	14.3	0.63	[d]FT
8	F	96	108.0	14.3	0.63	FT
9	F	96	108.0	14.3	0.63	Post FT
10	M	30	97.3	14.4	0.62	Marfan
11	M	0.5	35.0	3.7	0.17	[e]AC
12	F	138	144.0	26.7	1.08	Normal
13	F	83	117.0	20.3	0.82	VSD
14	F	1	51.4	4.0	0.23	VSD
15	M	81	105.0	17.0	0.72	Post VSD [f](R-BBB)
16	F	84	117.0	18.7	0.80	Post VSD [g](C-BBB)
17	M	52	102.0	17.8	0.70	Post ASD
18	M	48	104.0	17.7	0.70	ASD
19	M	2	57.0	4.3	0.25	AC
20	M	180	138.0	44.7	1.28	[h]LV-Hyp [i](R-TX)
21	M	136	139.0	29.2	1.10	VSD
22	F	60	103.0	18.0	0.70	VSD
23	M	228	185.0	80.0	2.04	Osteosarcoma
24	M	154	145.0	34.8	1.20	[j]AO
25	M	187	176.0	65.2	1.80	[k]AI
26	M	132	143.5	32.0	1.14	ASD
MEAN		89.3	120.3	24.0	0.94	
STANDARD ERROR OF THE MEAN		11.5	5.6	3.4	0.08	

Table 1 continued

[a]ASD	Atrial septal defect
[b]VSD	Ventricular septal defect
[c]Post	Postoperative
[d]FT	Fallots tetrology
[e]AC	Aortic coarctation
[f]R-BBB	Right bundle branch block
[g]C-BBB	Complete bundle branch block
[h]LV-Hyp	Left ventricular hypertrophy
[i]R-TX	Renal transplant
[j]AO	Aortic obstruction
[k]AI	Aortic incompetence

Table 2 Left ventricular volume estimates by biplane ventriculography for 12 catheterised patients and the echographic non-invasive estimates

CASE NO	DIAGNOSIS	THREE DIMENSIONAL VOLUME (ml)			SINGLE PLANE AREA LENGTH (ml)			BIPLANE AREA LENGTH (ml)			BIPLANE VENTRICULOGRAPHY (ml)		
		EDV	ESV	SV	EDV	ESV	SV	EDV	ESV	SV	EDV	ESV	SV
3	[a]ASD	23.2	11.2	12.0	19.6	8.9	10.8	16.1	6.9	9.2	46.5	31.7	14.8
5	[b]VSD	25.8	12.4	13.4	21.8	11.0	10.8	22.4	12.6	9.8	47.4	19.0	28.4
6	VSD	49.3	35.0	14.3	46.2	29.6	15.7	43.8	26.2	17.6	45.8	33.0	12.8
7	[c]FT	17.0	9.6	7.4	15.3	8.4	6.9	17.2	9.4	7.8	45.4	15.5	29.9
11	[d]AC	4.6	2.3	2.3	3.7	1.7	2.1	3.4	1.6	1.8	5.5	3.8	1.7
13	VSD	16.4	7.6	8.8	15.3	5.6	9.7	18.2	7.5	10.7	36.3	11.4	24.9
18	ASD	22.9	11.1	11.8	20.8	9.9	10.9	21.6	9.9	11.7	44.6	28.9	15.7
19	AC	5.0	2.5	2.5	5.9	2.8	3.1	6.5	2.8	3.7	12.7	5.7	7.0
21	VSD	56.4	41.5	14.9	25.5	14.7	12.1	30.0	17.2	12.8	84.2	51.9	32.3
22	VSD	24.2	11.1	13.1	24.1	10.1	14.0	21.7	10.8	10.9	27.4	12.5	14.9
24	[e]AO	46.5	27.4	19.1	39.3	24.9	14.5	44.0	32.4	11.6	74.4	37.6	36.8
25	[f]AI	105.6	53.3	52.3	97.6	48.6	50.3	82.0	40.6	41.4	142.6	48.8	93.8
MEAN		**33.0**	**18.7**	**14.3**	**27.9**	**14.7**	**13.4**	**27.2**	**14.8**	**12.4**	**51.1**	**25.0**	**26.1**
STANDARD ERROR OF THE MEAN		**7.9**	**4.7**	**3.7**	**7.2**	**3.9**	**3.6**	**6.1**	**4.3**	**2.9**	**10.5**	**4.6**	**6.9**

[a]ASD Atrial septal defect
[b]VSD Ventricular septal defect
[c]FT Fallots tetrology
[d]AC Aortic coarctation
[e]AO Aortic obstruction
[f]AI Aortic incompetence

Table 3 Leftventricular volume estimates by composite three dimensional reconstruction and conventional echographic techniques for 26 patients

CASE NO	THREE DIMENSIONAL VOLUME (ml)			SINGLE PLANE AREA LENGTH (ml)			BIPLANE AREA LENGTH (ml)		
	EDV	ESV	SV	EDV	ESV	SV	EDV	ESV	SV
1	32.6	15.5	17.2	35.1	18.1	17.1	31.6	16.7	14.9
2	48.3	24.3	24.0	54.0	30.1	23.9	59.8	40.6	19.2
3	23.2	11.2	12.0	19.6	8.9	10.8	16.1	6.9	9.2
4	69.5	53.0	16.5	62.1	49.6	12.5	59.7	47.2	12.5
5	25.8	12.4	13.4	21.8	11.0	10.8	22.4	12.6	9.8
6	49.3	35.0	14.3	40.2	29.6	15.7	43.8	26.2	17.6
7	17.0	9.6	7.4	15.3	8.4	6.9	17.2 -	9.4	7.8
8	18.9	9.8	9.1	17.6	8.2	9.4	18.6	10.0	8.6
9	29.6	11.5	18.1	29.0	10.7	18.3	25.3	10.9	14.4
10	23.6	10.7	12.9	23.7	10.6	13.1	20.8	9.6	11.2
11	4.6	2.3	2.3	3.7	1.7	2.1	3.4	1.6	1.8
12	38.4	20.1	18.3	35.6	18.4	17.2	39.5	23.9	15.6
13	16.4	7.6	8.8	15.3	5.6	9.7	18.2	7.5	10.7
14	5.7	2.0	3.7	4.9	1.6	3.2	5.9	1.9	4.0
15	20.9	12.2	8.7	19.3	10.3	9.1	24.0	13.8	10.2
16	12.6	7.0	5.6	11.8	6.5	5.2	11.2	7.7	3.5
17	23.4	10.2	13.2	21.7	8.0	13.7	15.0	7.1	7.9
18	22.9	11.1	11.8	20.8	9.9	10.9	21.6	9.9	11.7
19	5.0	2.5	2.5	5.9	2.8	3.1	6.5	2.8	3.7
20	55.1	31.0	24.1	51.5	27.0	24.5	47.0	27.2	19.8
21	56.4	41.5	14.9	25.5	14.7	12.1	30.0	17.2	12.8
22	24.2	11.1	13.1	24.1	10.1	14.0	21.7	10.8	10.9
23	112.2	63.3	48.9	98.8	54.8	44.3	106.3	49.3	57.0
24	46.5	27.4	19.1	39.3	24.9	14.5	44.0	32.4	11.6
25	105.6	53.3	52.3	97.6	48.6	50.3	82.0	40.6	41.4
26	31.4	12.0	19.4	27.6	12.1	15.6	28.3	13.5	14.8
MEAN	35.4	19.6	15.8	31.8	17.0	14.9	31.5	17.6	13.9
STANDARD ERROR OF THE MEAN	5.3	3.2	2.3	4.8	2.9	2.2	4.7	2.7	2.3

Table 4 The systematic error and random error of the angiographic comparisons is tabulated as the mean percentage difference and its standard deviation respectively. All mean values are statistically less than zero (P<0.005).

Angiographic Comparisons

	3-D		Area Length		Biplane	
	Mean	SD	Mean	SD	Mean	SD
EDV	-36.8	21.7	-44.6	21.6	-45	18.1
ESV	-31.0	24.1	-43.0	23.5	-41	23.3
SV	-34.0	33.1	-37.0	34.4	-39	33.3

Table 5 The systematic error and random error of the 3D comparisons is tabulated as the mean percentage difference and its standard deviation respectively. All mean values are statistically less than zero except the biplane end systolic mean.

3-D Comparisons

	Area - Length		Biplane	
	Mean	SD	Mean	SD
EDV	- 8.8*	12.9	-6.2+	13.6
ESV	-11.2*	16.2	-4.9#	23.9
SV	- 4.3	11.5	-9.8+	21.5

* P < 0.005

\+ P < 0.02

P < 0.05

\# N.S.

Table 6 Residual mean squares of regression were compared by the variance F-test. No statistically significant differences were found.

Residual Mean Square of Regression

Echographic estiamate regressed on invasive estimate

	3D	Biplane Echo	Area Length
EDV + ESV	74.7	69.7	109.2
SV	21.5	21.6	27.3